UNIVERSIDAD NACIONAL AUTÓNOMA DE MÉXICO

PROGRAMA DE MAESTRÍA Y DOCTORADO EN CIENCIAS QUÍMICAS

"Aislamiento, semisíntesis, evaluación biológica (anti-inflamatoria, citotóxica y anti-*Helicobacter pylori*) y análisis de la relación entre la estructura y la bioactividad de los sesquiterpenos cadinanoides presentes en *Heterotheca inuloides* (árnica mexicana)."

T E S I S

PARA OPTAR POR EL GRADO DE

DOCTORA EN CIENCIAS

P R E S E N T A

M. en C. María Verónica Egas Ortuño

TUTOR: Dr. E. Guillermo Delgado Lamas

Instituto de Química, UNAM

Ciudad de México, Abril 2017

Agradecimientos

Al tutor de este proyecto de investigación: Dr. E. Guillermo Delgado Lamas.

A los miembros del comité tutor: Dra. María Isabel Aguilar, Dr. Gerardo Zepeda y Dr. E. Guillermo Delgado Lamas.

Al Dr. Eduardo Muñoz Blanco (Universidad de Córdoba), y al personal técnico del Instituto Maimónides de Investigación Biomédica de Córdoba: Estrella Millán y Juan A. Collado.

A los miembros del jurado de Tesis: Dr. Manuel Jiménez Estrada, Dr. Francisco Hernández Luis, Dr. Rafael Castillo Bocanegra, Dr. Gerardo Zepeda y Dr. Rogelio Pereda Miranda.

A la Universidad Nacional Autónoma de México y al Programa de Maestría y Doctorado en Ciencias Químicas. A la Dirección General de Asuntos del Personal Académico (PAPIIT IG200514). Al personal técnico: María Isabel Chávez, Beatriz Quiroz, Alejandra León, Rocío Patiño, Ángeles Peña, Elizabeth Huerta, Antonio Nieto, Luis Delgado-Chávez, José Luis Rodríguez-Chávez, Luis Velasco, Javier Pérez (Instituto de Química de la UNAM). Al CONACyT (número de becario 257805) y a la Asociación Universitaria Iberoamericana de Postgrado.

Jurado Asignado

Presidente: Dr. Manuel Jiménez Estrada

Vocal: Dr. Rafael Castillo Bocanegra

Vocal: Dr. Gerardo Zepeda

Vocal: Dr. Rogelio Pereda Miranda

Secretario: Dr. Francisco Hernández Luis

El presente trabajo fue realizado en el laboratorio 1-C del Instituto de Química de la UNAM, dirigido por el Dr. E. Guillermo Delgado Lamas, y en el Instituto Maimónides de Investigación Biomédica de Córdoba, España, dirigido por el Dr. Eduardo Muñoz Blanco.

Los resultados de esta investigación fueron presentados en el evento "The International Congress and Annual Meeting of the Society for Medicinal Plant and Natural Product Research" que se celebró en la ciudad de Budapest, Hugría, en agosto de **2015**, e integrados en dos publicaciones científicas:

- Egas, V.; Toscano, R.; Linares, E.; Bye, R.; Espinosa-García, F.; Delgado, G. *J. Nat. Prod*. **2015**, 78, 2634. **DOI**: 10.1021/acs.jnatprod.5b00571.
- Egas, V.; Millán, E.; Collado, J. A.; Ramírez-Apan, T.; Méndez-Cuesta, C. A.; Muñoz, E.; Delgado, G. *Bioorg. Med. Chem*. **2017**, **DOI**: http://dx.doi.org/10.1016/j.bmc.2017.03.069.

---------- ----------

Dr. E. Guillermo Delgado Lamas M en C. Verónica Egas Ortuño

TUTOR **ALUMNA**

A mi familia y amigos

Índice

RESUMEN

El estudio químico de la especie vegetal *Heterotheca inuloides* (árnica mexicana) permitió el aislamiento de metabolitos de tipo cadinano, algunos triterpenos, flavonoides y esteroles. De entre estas sustancias, cuatro representan nuevos productos naturales. Su estructura fue elucidada por medio del análisis de sus espectros de resonancia magnética nuclear y confirmada por cristalografía de rayos X. Su configuración absoluta se estableció aplicando métodos experimentales y teóricos. Algunos de los metabolitos de tipo cadinano poseen actividad antiinflamatoria moderada. El compuesto más activo mostró un 43.14 ± 8.09 % de inhibición del edema, a una dosis de 228 µg/oreja. Adicionalmente, se evaluó el efecto de estos compuestos sobre tres factores de transcripción involucrados en la inflamación y el cáncer. El principal constituyente en esta especie, el 7-hidroxi-3,4-dihidrocadaleno, mostró actividad anti-NF-κB y fue capaz de activar la ruta antioxidante del Nrf2. A partir de los productos naturales activos se preparó un grupo de derivados semisintéticos, que incluyen ésteres y carbamatos, de los cuales se evaluó su efecto sobre los factores de transcripción antes mencionados y su actividad antiproliferativa *in vitro* sobre líneas celulares de cáncer humano. Los derivados de tipo carbamato mostraron una potente actividad inhibitoria de la proliferación sobre células de adenocarcinoma colorectal. Uno de los derivados de tipo éster, mostró mayor potencia en la inhibición del NF-κB y activación del Nrf2 que el producto natural original. A través de experimentos de western blot y modelado molecular se propuso el mecanismo por el cual esta sustancia interfiere en la cascada de señalización del NF-κB. Adicionalmente, se determinó que los productos naturales mayoritarios aislados de *H. inuloides*, y algunos derivados de semisíntesis tienen una actividad mayor que uno de los fármacos de referencia (metronidazol) como inhibidores del crecimiento de *Helicobacter pylori*. Finalmente, en el presente trabajo se diseñó un método que permite la identificación de los sesquiterpenos de tipo cadinano aislados previamente, en extractos de distintas poblaciones de *H. inuloides*, aplicando cromatografía de líquidos de alta resolución.

ABSTRACT

Chemical research of the plant species *Heterotheca inuloides* led to the isolation of various metabolites, including cadinane type sesquiterpenes, triterpenes, flavonoids and sterols. Among these substances, four are new natural products. Their structures were elucidated on the basis of NMR data analysis and confirmed by X-ray crystallography. Their absolute configuration was established by experimental, theoretical and semi-empirical methods. Some of the cadinane metabolites exhibit moderate anti-inflammatory activity. The most active compound showed 43.14 ± 8.09 % of inhibition of edema at a dose of 228 µg/ear. Additionally, the effect of these compounds on three transcription factors involved in inflammation and cancer was evaluated.

The main constituent in this species, 7-hydroxy-3,4-dihydrocadalene, showed anti-NF-κB activity and activated the antioxidant Nrf2 pathway. Starting from the active natural products, a novel semi-synthetic derivative set was prepared, including esters and carbamates, and evaluated for their potential *in vitro* antiproliferative activity against human cancer cell lines. Carbamate derivatives were found to exhibit potent activity against human colorectal adenocarcinoma. An ester derivative was determined to be a more potent NF-κB inhibitor and Nrf2 activator than its parent natural product. Through western blot experiments and molecular simulations, the mechanism of inhibition of NF-κB pathway was proposed.

Additionally, it was established that the major natural products of *H. inuloides*, and some semi-synthetic derivatives, possess higher anti-*Helicobacter pylori* activity than the reference drug (metronidazole).

Finally, an HPLC method for the identification of previously isolated cadinane type sesquiterpenes, in extracts prepared from different populations of *H. inuloides*, was developed.

INTRODUCCIÓN

Heterotheca inuloides es una de las plantas más comúnmente utilizadas en la medicina tradicional mexicana, principalmente para el tratamiento de padecimientos relacionados con la inflamación.[1] Desde hace varias décadas, el estudio químico de esta especie ha sido motivado por el alto aprecio etnomédico que tiene esta planta, principalmente en las zonas del centro y sur del país.

Los sesquiterpenos de tipo cadinano han sido identificados como constituyentes característicos de la especie. A pesar de que estos compuestos han mostrado tener una actividad importante en diversos bioensayos, la configuración absoluta de la mayor parte de ellos aún no ha sido definida. El primer estudio concerniente a la configuración absoluta de derivados de cadinanos fue realizado por Ruzicka, quien también definió su esqueleto.[2] Durante mucho tiempo, los métodos de correlación química permitieron la asignación de la configuración absoluta de diversos productos naturales de tipo cadinano. Estas técnicas más adelante fueron complementadas por métodos quirópticos, resonancia magnética nuclear (RMN) y análisis por dispersión anómala de rayos-X. Con el advenimiento de estas nuevas herramientas, algunas asignaciones estereoquímicas fueron corregidas. Por ejemplo, las configuraciones absolutas de algunos cadinanos establecidas basándose únicamente en argumentos deducidos de experimentos de RMN, más adelante fueron corregidas a través de métodos cristalográficos.[3]

En el presente trabajo se aislaron diez sesquiterpenos de tipo cadinano, algunos flavonoides, triterpenos y esteroles, a partir del extracto acetónico preparado de las partes aéreas de la especie en estudio. De entre estas sustancias, cuatro representan productos naturales novedosos. La configuración absoluta de estos compuestos fue establecida por comparación de sus espectros de dicroísmo circular electrónico (DCE), experimentales y calculados, y fue confirmada a través del refinamiento del parámetro de Flack aplicando dispersión anómala de rayos-X. La actividad anti-inflamatoria de estas sustancias fue evaluada aplicando un modelo *in vivo*. Conjuntamente, estos diez productos naturales de tipo cadinano y 21 derivados semisintéticos, que incluyen ésteres y carbamatos, fueron evaluados sobre blancos moleculares involucrados en procesos de inflamación y

carcinogénesis. Sus efectos citotóxicos sobre seis líneas celulares de cáncer humano fueron evaluados por medio de expermientos *in vitro*, y estos resultados se correlacionaron con la capacidad inhibidora o activadora sobre los factores de transcripción NF-κB, STAT3 y Nrf2. Con el objetivo de entender cómo algunos de estos compuestos inhiben el factor de transcripción NF-κB, se hicieron estudios por western blot y modelado molecular sobre una de las proteínas involucradas en su vía de activación.

Este tipo de investigaciones aplicadas a productos naturales son importantes debido a que muchos de estos compuestos poseen actividad antiinflamatoria y, actualmente, la relación entre inflamación y el desarrollo de cáncer es ampliamente aceptada.[4] A pesar de que esta conexión puede ser compleja, las evidencias sugieren que los procesos inflamatorios crónicos predisponen la aparición de células cancerosas.[5] Más aún, las vías moleculares que vinculan la inflamación con el cáncer han sido descritas. Estas vías conocidas como intrínseca y extrínseca, convergen dando como resultado la activación de factores de transcripción, principalmente el factor nuclear-κB (NF-κB), el transductor de señales y activador de la transcripción 3 (STAT3), y el factor 1α inducido por hipoxia (HIF1α) en células tumorales.[6]

La activación del NF-κB en células inflamatorias conduce a la producción de factores que mejoran el crecimiento, supervivencia y vascularización de células cancerosas.[7] STAT3 es considerado uno de los blancos moleculares nuevos más prometedores en la terapia del cáncer. Su activación en células tumorales y en el micro-ambiente tumoral promueve la proliferación y la supervivencia celular y facilita el desarrollo de cáncer a través de la inflamación.[8] El factor de transcripción Nrf2 desempeña un papel protector al suprimir el estrés oxidante y, consecuentemente, el aparecimiento de cáncer. La activación del Nrf2 inhibe la inflamación y facilita la adaptación de las células, a través de la regulación de la reparación y degradación de macromoléculas que han sufrido algún daño.[9]

Este conocimiento facilita la investigación y desarrollo de sustancias que tengan efecto sobre los componentes inflamatorios del micro-ambiente de las células cancerosas. De hecho, varios estudios experimentales, epidemiológicos y clínicos, sugieren que los agentes antiinflamatorios pueden considerarse substancias prometedoras como agentes terapéuticos.[10,11]

Los productos naturales de tipo cadinano son un grupo representativo de substancias con efectos quimiopreventivos, como resultado de sus propiedades anti-inflamatorias.[12] Se ha demostrado que algunos productos naturales pueden ejercer un efecto regulador a un nivel transcripcional en las vías moleculares involucradas en inflamación y cáncer, por lo tanto, representan una fuente interesante de agentes potencialmente útiles en la prevención y terapia de estos padecimientos.[13]

A pesar de que las actividades biológicas de muchos productos naturales han sido ampliamente estudiadas, la identificación de los blancos moleculares involucrados en dichas propiedades, representa un reto que podría explicar el uso de varias especies en la medicina tradicional.

En esta investigación también se evaluó, la actividad inhibitoria del crecimiento de *Helicobacter pylori* (*H. pylori*) de los productos naturales mayoritarios aislados de *H. inuloides*, y algunos derivados de semisíntesis, en busca de sustancias que representen una fuente alterna al tratamiento de infecciones causadas por esta bacteria. Los resultados mostraron que los compuestos 7-hidroxi-3,4-dihidrocadaleno y 7-hidroxi-cadaleno, tienen una actividad mayor que la del metronidazol (fármaco de referencia), y esta actividad es comparable con la desarrollada por el fármaco claritromicina.

Literatura

(1) Comisión Nacional Forestal. *Plantas Medicinales de la Farmacia Viviente del CEFOFOR: Usos Terapéuticos Tradicionales y Dosificación* **2010,** 12.

(2) Herout, V.; Sykora, V. *Chem. & Ind*. **1958**, 130.

(3) Ding, L.; Pfoh, R.; Rühl, S.; Qin, S.; Laatsch, H. *J. Nat. Prod*. **2009**, 72, 99.

(4) Coussens, L. M.; Werb, Z. *Nature* **2002**, 420, 860.

(5) Mantovani, A.; *Nature*. **2005**, 435, 752.

(6) Mantovani, A.; Allavena, P.; Sica, A.; Balkwill, F.; *Nature* **2008**, 454, 436.

(7) Karin, M.; *Nature* **2006**, 441, 431.

(8)Yu, H.; Lee, H.; Herrmann, A.; Buettner, R.; Jove, R. *Nat. Rev. Cancer*. **2014**, 14, 736.

(9) Hayes, J. D.; Dikova-Kostova, A. T. *Trends Biochem Sci*. **2014**, 39, 199.

(10) Kashfi, K. *Adv Pharmacol*. **2009**, 57, 31.

(11) Thun, J. T.; Henley, S. J.; Patrono, C. *J. Natl. Cancer Inst.* **2002**, 94, 252.

(12) Bremner, P.; Heinrich, M. *J. Pharm. Pharmacol*. **2002**, 54, 453.

(13) Orlikova, B.; Legran, N.; Panning, J.; Dicato, M.; Diederich, M. *Cancer Treat Res*. **2014**, 159, 123.

ANTECEDENTES

1. Generalidades de *Heterotheca inuloides*

1.1 Distribución y hábitat

El género *Heterotheca* Cass. (Asteraceae: Astereae) incluye 24 especies de plantas herbáceas anuales y perennes, distribuidas en México, Estados Unidos y Canadá.[1] *H. inuloides* Cass es una planta endémica de México que posee la misma distribución geográfica que otras especies perenecientes al género, como *H. grandiflora* Nutt., *H. subaxilaris* (Lam.) Britton & Rusby, y *H. leptoglossa* DC.[2] Esta especie crece como maleza de forma silvestre en las regiones frías y templadas de México, a una altitud comprendida entre los 2000 y 3000 metros sobre el nivel del mar.[3]

1.2 Caracterización botánica

Es una planta herbácea perenne de altitud no mayor a 1 m. Posee hojas alternas, lanceoladas y pubescentes con márgenes dentados, e inflorescencias constituidas por varios discos en el centro, los cuales a su vez se encuentran rodeados por flores ligulares.[2]

En México, esta especie recibe los nombre comunes de árnica del país, árnica morada, árnica de peluche, árnica de untar, árnica hembra, hornilla y tabaco de las montañas, además de una serie de nombres prehispánicos. Fuera de México es frecuentemente conocida como árnica mexicana, nombre que deriva de sus similitudes morfológicas con la especie Europea *Arnica montana* L.[4,5]

Su clasificación botánica es la siguiente: familia Asteraceae (Compositae), tribu Astereae, subtribe Crisopsidinae.

1.3 Usos en la medicina tradicional

H. inuloides (árnica mexicana), es una especie con gran aprecio por su uso empírico en el tratamiento de inflamaciones. También, se ha descrito su uso para disminuir los síntomas asociados a contusiones, reumatismo y úlceras estomacales.[6] De forma general, las preparaciones obtenidas a partir de las partes aéreas (flores, hojas y ramas) se administran por vía tópica u oral.[7]

1.4 Composición química y actividad biológica

La investigación química de esta especie ha conducido al aislamiento e identificación de diferentes metabolitos, entre los cuales se encuentran triterpenos, esteroles, flavonoides, y sesquiterpenos de tipo cadinano.[8] Estos últimos se consideran constituyentes representativos del género *Heterotheca*, ya que son biosintetizados por otras especies pertenecientes a este género, tales como *H. latifolia*,[9,10] *H. grandiflora* [11,12] and *H. subaxillaris.*[13]

Los constituyentes de tipo cadinano que han sido aislados de *H. inuloides* se ilustran en la Figura 1. Estos metabolitos poseen una variedad de propiedades biológicas, entre las más importantes se encuentran las actividades antioxidante,[14,15] antiinflamatoria,[16,17] antinociceptiva,[18] inhibidora de la peroxidación lipídica,[19] citotóxica,[20] antimicrobiana [21] y antiparasitaria.[22]

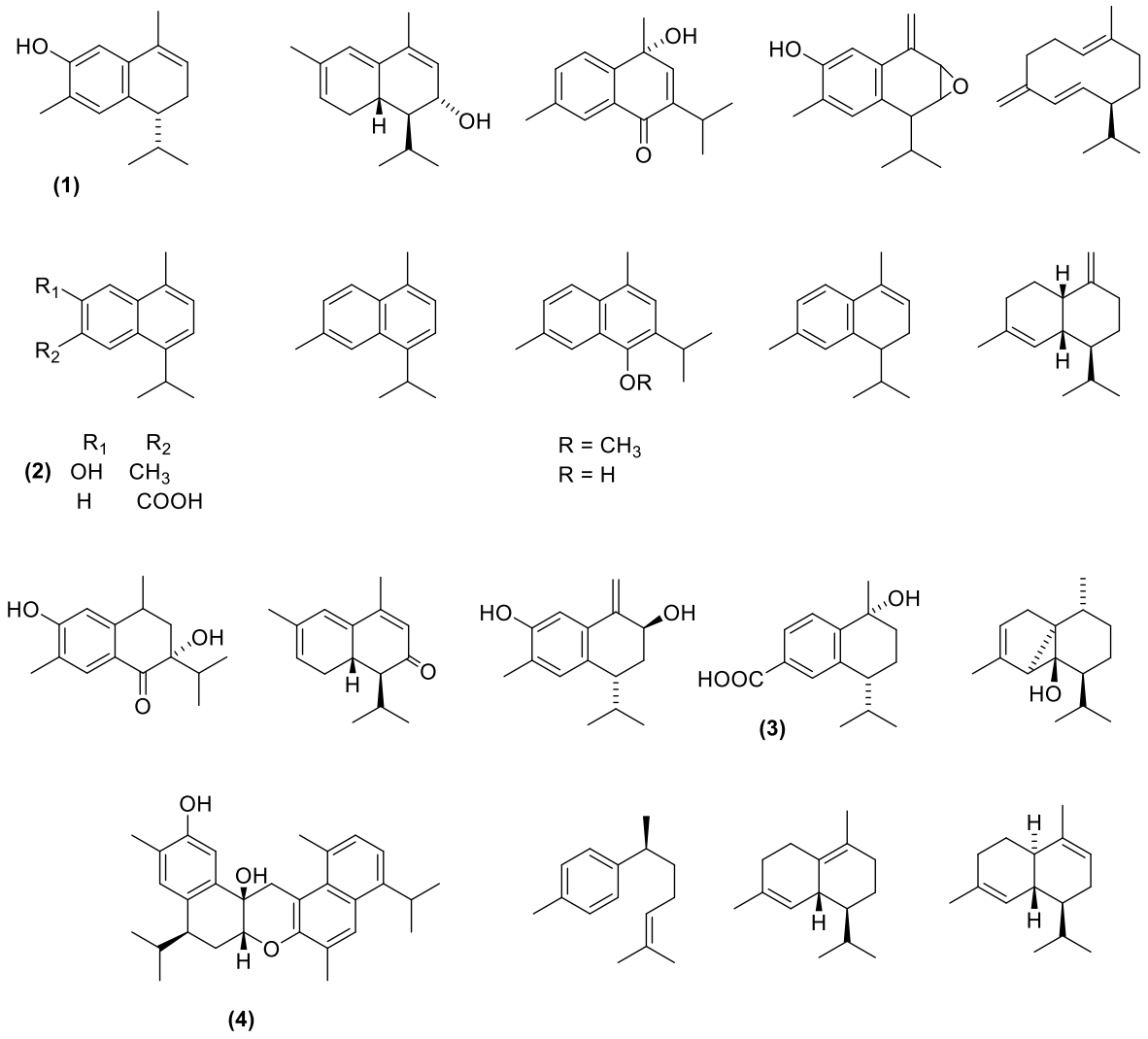

Figura 1. Productos naturales de tipo cadinano aislados de *H. inuloides*.

1.4.1 Actividad antiinflamatoria

Se ha observado que los extractos acetónico, metanólico y de diclorometano preparados a partir de *H. inuloides*, y algunos de los constituyentes de tipo cadinano aislados de esta especie, poseen actividad antiinflamatoria en modelos *in vivo* e *in vitro*. Los compuestos 7-hidroxi-3,4-dihidrocadaleno (**1**), 7-hidroxycadaleno (**2**), ácido-cadalen-15-oico (**3**) y dicadalenol (**4**) disminuyen el edema en oreja de ratón inducido por el acetato de tetradecanoilforbol (ATF), que se utiliza como una herramienta de investigación en

modelos de inflamación.[16] Se ha demostrado que las infusiones preparadas a partir de *H. inuloides*, y el metabolito 7-hidroxy-3,4-dihidrocadaleno (**1**), disminuyen la actividad de la enzima COX, la cual está directamente involucrada en el proceso de inflamación.[23,24]

1.4.2 Actividad citotóxica

Los sesquiterpenos de tipo cadinano 7-hidroxy-3,4-dihidrocadaleno (**1**) y 7-hidroxicadaleno (**2**) poseen actividad citotóxica sobre líneas celulares tumorales,[20] e inhiben la proliferación en líneas celulares de leucemia (K562), cáncer de colon (HCT-15) y mama (MCF-7).[25]

2. Inflamación y cáncer

La inflamación es una respuesta adaptativa desencadenada por estímulos y condiciones nocivas, como infecciones o lesiones tisulares. En general, se piensa que una respuesta inflamatoria controlada es beneficiosa (por ejemplo, al proporcionar protección contra infecciones), pero puede resultar perjudicial si no existe una regulación apropiada. La respuesta inflamatoria está coordinada por una amplia gama de mediadores que forman redes reguladoras complejas. Para entender su funcionamiento, resulta útil colocar estas señales en categorías funcionales y distinguir entre inductores y mediadores de la inflamación. Los inductores son las señales que inician la respuesta inflamatoria al activar sensores especializados, lo que provoca la producción de un conjunto de mediadores. Los mediadores, a su vez, alteran los estados funcionales de tejidos y órganos (que son los efectores de la inflamación) de tal forma que les permite adaptarse a las condiciones indicadas por el inductor particular de la inflamación. Por lo tanto, una "vía" inflamatoria genérica, consiste en inductores, sensores, mediadores y efectores, con cada componente determinando el tipo de respuesta inflamatoria.[26]

La existencia de una conexión entre inflamación y cáncer se sospechaba antes del descubrimiento del NF-κB y otros factores de transcripción. A pesar de que en el siglo XIX Virchow sugirió que la inflamación crónica puede dar origen a la aparición de células malignas, únicamente en años recientes la correlación entre inflamación y cáncer ha sido comprendida. Estudios epidemiológicos han identificado a las infecciones e inflamación crónica como los principales factores de riesgo para el desarrollo de varios tipos de cánceres. Conjuntamente, la inflamación y las infecciones están relacionadas con un 15-

20% de las muertes por cáncer. Por ejemplo, las infecciones crónicas producidas por los virus de la hepatitis B y C, son los principales factores de riesgo en el desarrollo de carcinoma hepatocelular, mientras que las infecciones con *Helicobacter pylori* están asociadas con la mayoría de los tipos de cáncer gástrico.[27] Se piensa que la colitis ulcerativa incrementa el riesgo de padecer cáncer colorectal, y la inflamación crónica producida al aspirar partículas irritantes presentes en el aire, o humo de tabaco, está muy probablemente relacionada con el desarrollo de cáncer de pulmón.[27]

2.1 Factores de transcripción

Los factores de transcripción son componentes celulares clave que controlan la expresión génica y su actividad determina el funcionamiento de las células y las respuestas de éstas al medio ambiente. Al garantizar la expresión correcta de genes específicos, el sistema regulatorio transcripcional juega un papel central en el control de varios procesos biológicos, incluyendo el ciclo celular, el mantenimiento del equilibrio metabólico y fisiológico intracelular y la diferenciación celular. En la actualidad se conoce que varias enfermedades surgen como consecuencia de un desequilibrio en este sistema regulador.[28]

2.1.1 NF-κB

El factor de transcripción nuclear kappa B (NF-κB, por sus siglas en inglés) regula varios procesos fisiológicos importantes, incluyendo la inflamación, la respuesta inmune, el crecimiento celular, la apoptosis, y la expresión de ciertos genes virales. Por lo tanto, la cascada de señalización de NF-κB proporciona una oportunidad para la intervención farmacológica, principalmente en situaciones de inflamación crónica o cáncer, en las cuales la vía está frecuentemente activa y desempeña un papel importante en el desarrollo de la enfermedad.[29]

La familia de proteínas conocidas como NF-κB está compuesta de dos subfamilias: las proteínas NF-κB y las proteínas Rel. Todas estas proteínas comparten el dominio llamado RHD (del inglés Rel homology domain). Como tales, las proteínas miembros de la subfamilia NF-κB no son capaces de activar la transcripción, excepto cuando forman dímeros con los miembros de la subfamilia Rel. La actividad del NF-κB se encuentra estrechamente regulada por la interacción con las proteínas inhibitorias IκB. En la mayoría

de las células, el NF-κB se encuentra en una forma latente e inactiva en el citoplasma, lo cual es una consecuencia de la unión con las proteínas inhibitorias IκB.[30]

La vía más importante que conducen a la activación del NF-κB se conoce como vía clásica. En esta vía los dímero de NF-κB, tales como p50/RelA, son mantenidos en el citoplasma por interacción con una molécula independiente de IκB. En muchos casos, la unión de un ligando a un receptor en la superficie celular (por ejemplo el receptor del factor de necrosis tumoral α), activa al complejo IKK, el cual a su vez fosforila dos serinas de la proteína IκB, conduciendo a su degradación y subsecuente liberación del dímero del NF-κB, el cual puede entonces entrar al núcleo y activar genes específicos (Figura 2).[30]

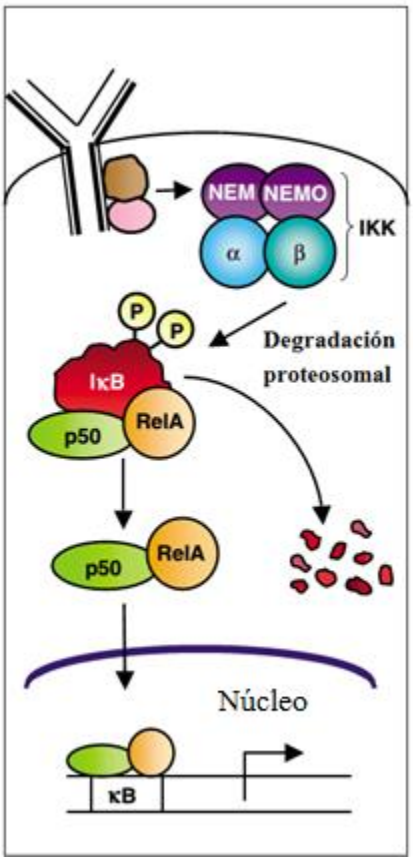

Figura 2. Vía clásica de activación del NF-κB (modificada de Gilmore[30]).

2.1.2 STAT3

Los factores de transcripción STAT (por sus siglas en inglés) funcionan en los niveles primarios de las vías de señalización de los receptores de citoquina y factores de crecimiento (Figura 3). En comparación con células y tejidos normales, STATs activos han sido detectados en una gran variedad de líneas celulares cancerosas humanas y en tumores primarios. Se ha demostrado que la activación persistente de STATs, en particular, STAT3 y STAT5, contribuyen al desarrollo de cáncer estimulando la proliferación celular y evitando la apoptosis. STATs participan en la oncogénesis a través de la regulación de genes que codifican para la producción de inhibidores de la apoptosis y reguladores del ciclo celular. Experimentos *in vivo* e *in vitro* han mostrado que la inhibición de las vías de señalización de STATs activas, disminuyen el crecimiento celular de tumores. Estos hallazgos proporcionan una nueva fuente de intervención terapéutica en el tratamiento del cáncer.[31,32]

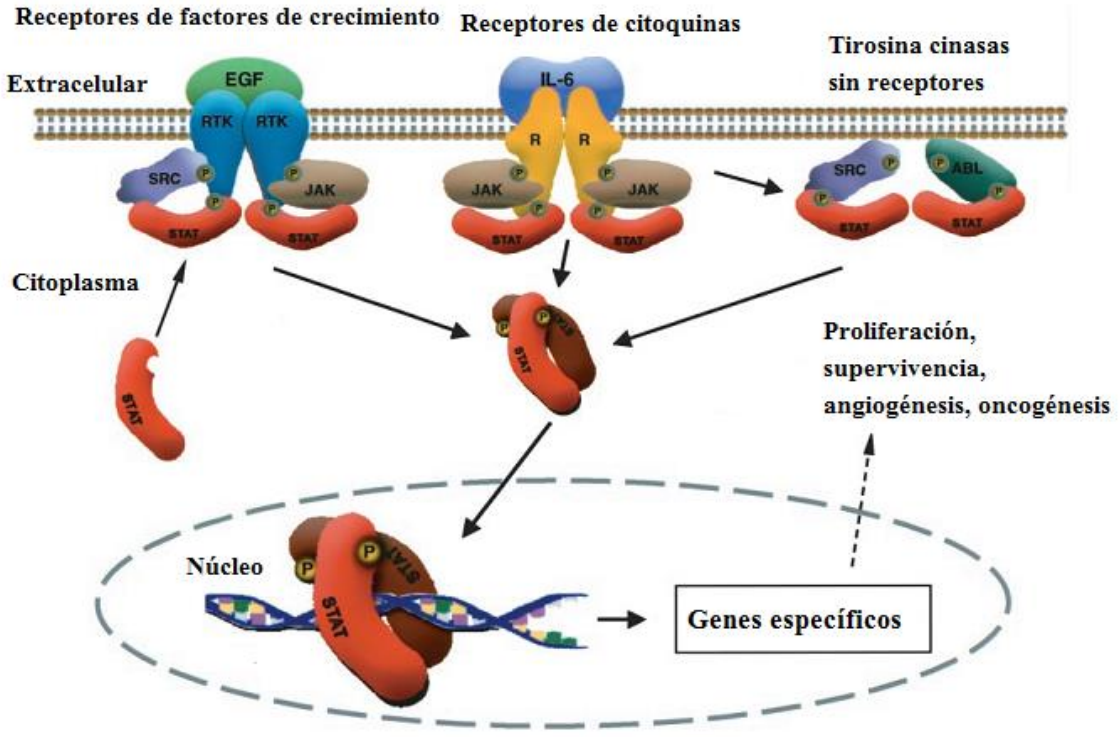

Figura 3. Vía de señalización del STAT (modificada de Buettner[31]).

2.1.3 Nrf2

El factor nuclear tipo 2 derivado de eritroide (Nrf2, por sus siglas en inglés) es un factor de transcripción que regula el estado redox celular y es controlado a través de una red compleja trancripcional/epigenética y postranslacional, que asegura que su actividad se incremente durante la perturbación redox, la inflamación, el estímulo de factores de crecimiento y los flujos de nutrientes y energía. De esta manera, es posible que exista una respuesta adaptativa ante diversas formas de estrés. Además de ser un mediador de la inducción de genes antioxidantes y desintoxicantes, el Nrf2 contribuye a la adaptación a través de la regulación de la reparación y la degradación de moléculas, y la modulación del metabolismo intermedio.[33] En las células, el Nrf2 puede ser activado por especies reactivas de oxígeno o por el factor de crecimiento de queratinocito, lo cual genera que el inhibidor citosólico Keap 1 lo libere, y de esta manera pueda penetrar al núcleo donde forma dímeros con las proteínas MAF y se liga a la secuencia ARE del ADN, activando así genes específicos (Figura 4).[34]

Varios estudios, acerca de compuestos que poseen efectos quimiopreventivos, sugieren que muchos de sus efectos benéficos al suprimir la carcinogénesis y otras enfermedades crónicas son consecuencia de la activación del factor de transcripción Nrf2.[35]

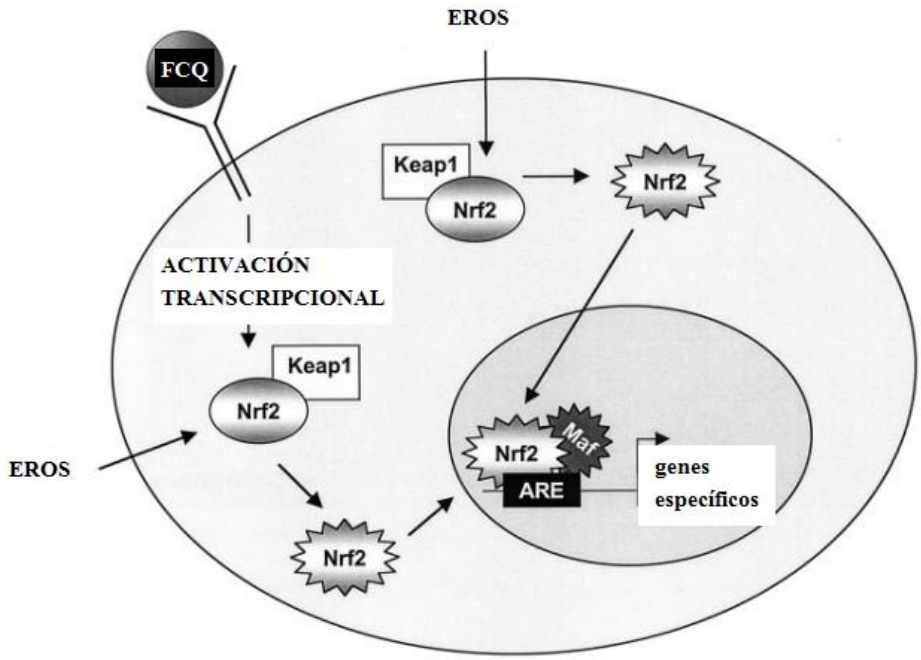

Figura 4. Vía de activación del Nrf2 (modificada de Braun[34]).

2.2 Agentes antiinflamatorios y anticancerígenos de origen natural

En la actualidad los productos naturales mantienen su importancia central en el descubrimiento de agentes anticancerígenos. Los metabolitos secundarios poseen bioactividades útiles dentro de los mecanismos de defensa, supervivencia o comunicación de los organismos productores. Por lo tanto, no resulta sorprendente que dichos compuestos bioactivos hayan llegado a desempeñar un papel importante en el desarrollo de nuevos fármacos. Sin embargo, el uso de productos naturales posee algunas limitaciones, ya que frecuentemente los organismos sintetizan cantidades mínimas de estas sustancias, y algunas de ellas pueden llegar a tener poca biodisponibilidad. Este último factor está determinado en gran medida por la polaridad. Sin embargo, los productos naturales pueden ser optimizados a través de la remoción, modificación o introducción de grupos funcionales. Estas sustancias también pueden ser útiles en el desarrollo de bibliotecas para el descubrimiento de nuevos análogos sintéticos activos.[36]

Existen actualmente aproximadamente 120 sustancias químicas utilizadas como agentes farmacológicos que derivan de plantas. Muchas de ellas se emplean como agentes anticancerígenos, ya sea sin haber modificado su estructura o como simples derivados de semisíntesis. Algunos ejemplos importantes incluyen al taxol, la vincristina, la vinblastina, y la doxorrubicina (nombre comercial adriamicina).[37]

Los productos naturales desempeñan un papel importante en la conservación de la salud humana, principalmente cuando se asocian con la prevención y el tratamiento de condiciones inflamatorias. En los últimos años se ha realizado un gran esfuerzo para investigar el mecanismo de acción, metabolismo, seguridad y efectos secundarios a largo plazo de estas sustancias, y es probable que en los próximos años, nuevos agentes antiinflamatorios derivados de productos naturales comiencen a ser comercializados como fármacos.[37]

Existe un gran número de investigaciones que reportan la actividad antiinflamatoria de distintos productos naturales; sin embargo, solamente algunos de ellos sobresalen, respecto a su potencia o disponibilidad. Estos compuestos naturales incluyen a la curcumina, partenólida, cucurbitacina, 1,8-cineol, lyprinol, bromelaina, y algunos flavonoides y saponinas.[38]

El entendimiento actual acerca de la cascada de señalización del NF-κB proporciona a los investigadores una oportunidad para la identificación de posibles blancos moleculares. En 2004, los primeros compuestos de origen natural descritos en la literatura como moduladores de este factor fueron el salicilato de sodio y el ácido acetil salicílico (aspirina). Tras este descubrimiento, una serie de nuevos productos naturales han demostrado tener una actividad inhibidora del NF-κB, lo cual hace aún más importante la identificación de blancos específicos dentro de la cascada, incluyendo la degradación del IκB, el complejo IKK, la translocación nuclear del NF-κB y la unión ADN-NF-κB.[39]

3. *Helicobacter pylori*

Helicobater pylori (*H. pylori*) es uno de los patógenos con mayor prevalencia en el mundo, afectando alrededor del 50% de población. Fue descrito por Warren y Marshall en 1983. Es un bacilo Gram-negativo que infecta la mucosa estomacal del ser humano, produciendo enfermedades en la parte superior del tracto gastrointestinal, tales como gastritis crónica, úlcera péptica y carcinoma gástrico. Algunos estudios han demostrado que el consumo de alimentos contaminados puede incrementar el riesgo de una infección por *H. pylori*. La ruta más frecuente de transmisión es de persona a persona.[40]

Existen varios esquemas para el tratamiento de infecciones causadas por *H. pylori*; sin embargo, aún no se ha definido un tratamiento óptimo, ya que no existe un único antibiótico capaz de erradicar a esta bacteria. Para erradicar la infección normalmente se usa una combinación de varios antibióticos. Los antibióticos más comúnmente empleados son la claritromicina, amoxicilina, metronidazol, tetraciclina, fluoroquinolonas y tinidazol. La efectividad de las terapias más comúnmente empleadas se ha visto comprometida por la rápida emergencia de cepas de *H. pylori* resistentes a antibióticos y por el poco apego al tratamiento por parte de los pacientes.[41]

Literatura

(14) Semple, J. C. *Botany* **2008**, *86*, 886.

(15) Nesom, G. L. *Phytologia* **1990**, *69*, 282.

(16) García-Sánchez, C.A.; Sánchez-González, A.; Villaseñor, J.L. *Acta Bot. Mex* **2014**, *106*, 97.

(17) Aguilar, A.; Camacho, J.R.; Chino, S.; Jácquez, P.; López, M.E. *Herbario Medicinal del Instituto Mexicano del Seguro Social. Información etnobotánica. IMSS* **1994**.

(18) Linares, E.; Flores, B.; Bye, R. Selección de Plantas Medicinales de México. 1st Ed. Editorial Limusa **1988**.

(19) Comisión Nacional Forestal. *Plantas Medicinales de la Farmacia Viviente del CEFOFOR: Usos Terapéuticos Tradicionales y Dosificación* **2010,** 12.

(20) González-Stuart, A.E. *Not. Sci. Biol*. **2010,** 2, 7.

(21) Rodríguez-Chávez, J.L.; Egas, V.; Linares, E.; Bye, R.; Hernández, T.; Espinosa-García, F. J.; Delgado, G.; *J Ethnopharmaco*l **2017**, *195*, 39.

(22) Bohlmann, F.; Gupta, R, K.; King, R, M.; Robinson, H. *Phytochemistry* **1982**, *21*, 2982.

(23) Bohlmann, F.; Wolfrum, C.; Jakupovic, J.; King, R, M.; Robinson, H. *Phytochemistry* **1985**, *24*, 1101.

(24) Bohlmann, F.; Zdero, C.; Robinson, H.; King, R, M. *Phytochemistry* **1979**, *18*, 1675.

(25) El-Dahmy, T.; Sarg, T.; Farrag, N, M.; Ateya, A, M.; Jakupovic, J.; Bohlman, F.; King, R. M. *Phytochemistry* **1986**, *25*, 1474.

(26) Bohlmann, F.; Zdero, C. *Phytochemistry* **1979**, *18*, 1185.

(27) Coballase-Urrutia, E.; Pedraza-Chaverri, J.; Camacho-Carranza, R.; Cárdenas Rodríguez, N.; Huerta-Gertrudis, B.; Medina-Campos, O.; Mendoza-Cruz, M.; Delgado-Lamas, G.; Espinoza-Aguirre, J. *Toxicology* **2010**, *276*, 41.

(28) Haraguchi, H.; Ishikawa, H.; Sanchez, Y.; Ogura, T.; Kubo, Y.; Kubo, I. *Bioorg. Med. Chem.* **1997**, *5*, 865.

(29) Delgado, G.; Olivares, M.; Chávez, M.; Ramírez-Apan, T.; Linares, E.; Bye, R.; Espinosa-García, F. *J. Nat. Prod*. **2001**, *64*, 861.

(30) Segura, L.; Freixa, B.; Ringbom, Th.; Vila, R.; Perera, P.; Adzet, T.; Bohlin, L.; Cañigueral, S. *Planta Med*. **2000**, *66*, 553.

(31) Rocha-Gonzáles, H.; Blaisdell-López, E.; Granados-Soto, V.; Navarrete, A. *Eur. J. Pharmacol.* **2010**, *649*, 154.

(32) Haraguchi, H.; Saito, T.; Ishikawa, H.; Sanchez, Y.; Ogura, T.; Kubo, I. *J. Pharm. Pharmacol*. **1996**, *48*, 441.

(33) Kubo, I.; Chaudhuri, S, K.; Kubo, Y.; Sanchez, Y.; Ogura, T.; Saito, T.; Ishkawa, H.; Haraguchi, H. *Planta Med*. **1996**, *62*, 427.

(34) Kubo, I.; Muroi, H.; Kubo, A.; Chaudhuri, S, K.; Sanchez, Y.; Ogura, T. *Planta Med*. **1994**, *60*, 218.

(35) Rodríguez-Chávez, J. L.; Rufino-González, Y.; Ponce-Macotela, M.; Delgado G. *Parasitology* **2015**, *142*, 576.

(36) Muñoz-Velázquez, E.E.; Rivas-Díaz, K.; Loarca-Piña, M.G.; Mendoza-Díaz, S.; Reynoso-Camacho, R.; Ramos-Gómez, M. *Rev. Mex. Cienc. Agríc.* **2012**, *3*, 481.

(37) Segura, L.; Freixa, B.; Ringbom, T.; Vila, R.; Perera, P.; Adzet, T.; Bohlin, L.; Cañigueral, S. *Planta Med* **2000**, *66*, 553.

(38) Rodríguez-Chávez, J.L.; Coballase-Urrutia, E.; Sicilia-Argumedo, G.; Ramírez-Apan, T.; Delgado, G. *J. Ethnopharmacol*. 2015, *175*, 256.

(39) Medzhitov, R. *Nature* **2008**, *454*, 428.

(40) Karin, M.; *Nature*. **2006**, *441*, 431.

(41) Vaquerizas, J. A.; Kummerfeld, S. K.; Teichman, S. A.; Luscombe, N. M. *Nature* **2009**, *10*, 252.

(42) Gilmore, T. D.; Herscovitch, M. *Oncogene* **2006**, *25*, 6887.

(43) Gilmore, T. D. *Oncogene* **2006**, *25*, 6680.

(44) Buettner, R.; Mora, L.; Jove, R. Clin Cancer Res **2002**, *8*, 945.

(45) Yu, H.; Lee, H.; Herrmann, A.; Buettner, R.; Jove, R. *Nat. Rev. Cancer*. **2014**, *14*, 736.

(46) Hayes, J. D.; Dikova-Kostova, A. T. *Trends Biochem Sci*. **2014**, *39*, 199.

(47) Braun S.; Hanselmann C.; Gassmann MG.; auf dem Keller U.; Born-Berclaz C.; Chan K.; Kan YW.; Werner S. *Mol Cell Biol* **2002**, 15, 5492.

(48) Sporn, M. B.; Liby, K. T. *Nat. Rev. Cancer*. **2012**, *12*, 564.

(49) Orlikova, B.; Legran, N.; Panning, J.; Dicato, M.; Diederich, M. *Cancer Treat Res*. **2014**, *159*, 123.

(50) Luqman, S.; Pezzuto, J. M. *Phytother*. *Res*. **2010**, *24*, 949.

(51) Yuan, G.; Wahlqvist, M.; He, G.; Yang, M.; Li, D. *Asia Pac. J. Clin. Nutr*. **2006**, *15*, 143.

(52) Bremner, P.; Heinrich, M. *J. Pharm. Pharmacol*. **2002**, *54*, 453.

(53) Thung, I.; Aramin, H.; Vavinskaya, S.; Gupta, S.; Park, J. Y.; Crowe, S. E.; Valasek, M. A. Aliment Pharmacol Ther **2016**, *43*, 514.

(54) Garza-Gonzáles, E.; Perez-Perez, G. I.; Maldonado-Garza, H. J.; Bosques-Padilla, F. J. *Gastroenterol*. **2014**, *20*, 1438.

OBJETIVOS

Objetivo general

Contribuir al conocimiento químico y biológico de los metabolitos secundarios bioactivos presentes en *H. inuloides*, y obtener a partir de los productos naturales de tipo cadinano, derivados químicos para realizar bioevaluaciones que permitan establecer las relaciones entre la estructura molecular y la actividad biológica.

Objetivos específicos

- Aislar y caracterizar estructuralmente los productos naturales presentes en *H. inuloides* a través de métodos cromatográficos, espectroscópicos y espectrométricos.
- Establecer la configuración absoluta de las sustancias aisladas por primera vez, haciendo uso de distintos métodos experimentales y teóricos.
- Evaluar la actividad antiinflamatoria de los metabolitos obtenidos en forma pura, aplicando el modelo de edema en oreja de ratón inducido por ATF.
- Preparar derivados semisintéticos a partir de los productos naturales bioactivos, por medio de reacciones simples en las cuales los grupos funcionales puedan ser manipulados para obtener estructuras adicionales.
- Evaluar la actividad inhibidora o activadora de los productos naturales y derivados sobre los factores de transcripción involucrados en la inflamación y el cáncer.
- Correlacionar los resultados de las actividades sobre los factores de transcripción con los efectos citotóxicos en líneas celulares de cáncer humano.
- Establecer un método por cromatografía líquida de alta resolución para determinar el perfil metabólico de los extractos acetónico de *H. inuloides*.
- Evaluar la actividad anti-*Helicobacter pylori in vitro* de algunos derivados semisintéticos obtenidos a partir de compuestos de tipo cadinano.

RESULTADOS

CAPÍTULO I

Sesquiterpenos de tipo cadinano aislados a partir de *Heterotheca inuloides*: configuración absoluta y actividad anti-inflamatoria

Egas, V.; Toscano, R.; Linares, E.; Bye, R.; Espinosa-García, F.; Delgado, G.

Journal of Natural Products 2015, 78, 2634-2641.

Resumen

A partir de las partes aéreas de *Heterotheca inuloides* se aislaron ocho sesquiterpenos de tipo cadinano (**1-8**), junto con algunos triterpenos, flavonoides y esteroles. La estructura de los compuestos nuevos (**1-4**) fue elucidada por medio del análisis de sus espectros de resonancia magnética nuclear, mono y bidimensionales. Las estructuras de los sesquiterpenos nuevos (**1-3**), y conocidos (**5-7**), fueron confirmadas por cristalografía de rayos X. La configuración absoluta de los metabolitos **2-5** fue establecida por comparación de sus espectros experimentales de dicroísmo circular electrónico con los calculados y confirmada por medio del refinamiento del parámetro de Flack usando dispersión anómalada de rayos X de los átomos de oxígeno y métodos de correlación química. La actividad antiinflamatoria de los compuestos de tipo cadinano fue evaluada aplicando el modelo de edema de inflamación en oreja de ratón inducido por ATF. Los resultados indican que algunos de estos metabolitos poseen actividad moderada. El compuesto **1** mostró un 43.14 ± 8.09 % de inhibición del edema a una dosis de 228 µg/oreja, lo cual indica una IC_{50} > 228 μg/oreja.

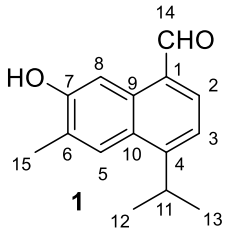
14
CHO
HO
1
2
3
4
5
6
7
8
9
10
11
12
13
15

1

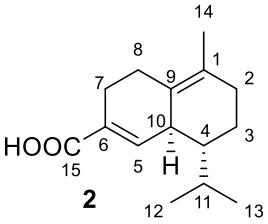
14
HOOC
H
1
2
3
4
5
6
7
8
9
10
11
12
13
15

2

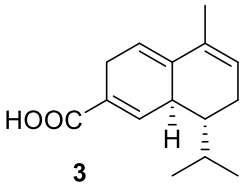
HOOC
H

3

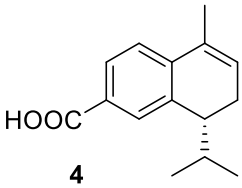
HOOC

4

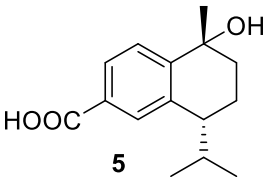
OH
HOOC

5

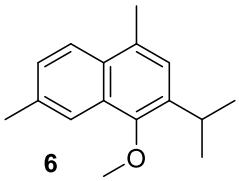
O

6

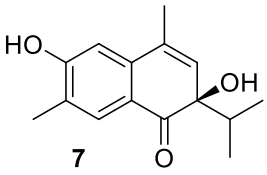
HO
OH
O

7

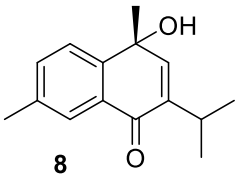
OH
O

8

JOURNAL OF NATURAL PRODUCTS

23

Article

pubs.acs.org/jnp

Cadinane-Type Sesquiterpenoids from *Heterotheca inuloides*: Absolute Configuration and Anti-inflammatory Activity

Verónica Egas,[†] Rubén A. Toscano,[†] Edelmira Linares,[‡] Robert Bye,[‡] Francisco J. Espinosa-García,[§] and Guillermo Delgado*[,†]

[†]Instituto de Química and [‡]Instituto de Biología, Universidad Nacional Autónoma de México, Circuito Exterior, Ciudad Universitaria, Coyoacán 04510, Mexico City, Mexico

[§]Instituto de Investigaciones en Ecosistemas y Sustentabilidad, Universidad Nacional Autónoma de México, Antigua carretera a Pátzcuaro No. 8701, Col. Ex-Hacienda de San José de la Huerta, 58190 Morelia, Michoacán, Mexico

Supporting Information

ABSTRACT: Eight cadinane-type sesquiterpenoids (**1**–**8**) together with some triterpenoids, flavonoids, and sterols were isolated from the aerial parts of *Heterotheca inuloides*. The structures of the new compounds (**1**–**4**) were elucidated on the basis of extensive 1D and 2D NMR spectroscopic data analysis. The structures of the new (**1**–**3**) and the known (**5**–**7**) sesquiterpenoids were confirmed by X-ray crystallography. The absolute configurations of metabolites **2**–**5** were determined by comparing their experimental and calculated electronic circular dichroism spectra and confirmed via refinement of the Flack parameter using anomalous X-ray scattering from the oxygen atoms and chemical correlation methods. The sesquiterpenoids were evaluated for their anti-inflammatory potential by applying the TPA-induced mouse ear edema model. The results revealed that some of these metabolites exhibit moderate anti-inflammatory activity. At a dose of 228 μg/ear compound **1** showed 43.14 ± 8.09% inhibition on ear edema, indicating an IC_{50} > 228 μg/ear.

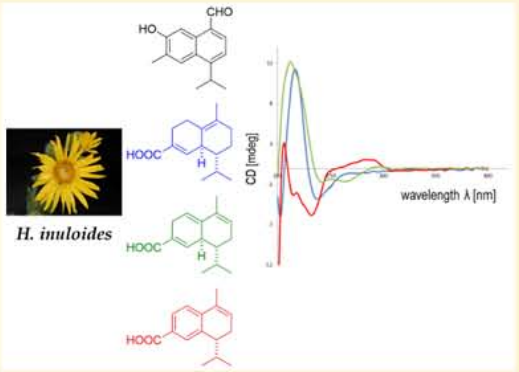

The genus *Heterotheca* Cass. (Asteraceae: Astereae) includes 24 species of herbaceous annuals and perennials distributed throughout Mexico, the United States, and the prairies and southern Rocky Mountains of western Canada.[1] *H. inuloides* Cass. is an endemic plant of Mexico that shares a natural distribution with *H. grandiflora* Nutt., *H. subaxilaris* (Lam.) Britton & Rusby, and *H. leptoglossa* DC.[2]

H. inuloides has continuously attracted attention because it is used as the treatment of choice in Mexican folk medicine for diverse ailments, mainly for those related to inflammatory processes.[3] Chemical investigations of this plant, also known as "Mexican arnica", have led to the isolation and identification of different metabolites including polyacetylenes, triterpenoids, sterols, flavonoids, and cadinanes.[4] Cadinanes may be considered representative constituents for the genus because they have been isolated from other species such as *H. latifolia*,[5,6] *H. grandiflora*,[7,8] and *H. subaxillaris*.[9] Cadinane-type sesquiterpenoids have shown diverse biological properties such as antioxidant,[10,11] anti-inflammatory,[4,12] antinociceptive,[13] inhibition of lipid peroxidation,[14] cytotoxic,[15] antimicrobial,[16] and antiparasitic properties.[17] Despite the significance of some of these metabolites in different bioassays, the absolute configuration of most of them has not been defined. The first studies concerning the configuration of cadinane derivatives were made by Ruzicka, who also defined the cadinane framework.[18] Chemical correlation methods permitted the assignment of the absolute configuration for many cadinane-type natural products, and these techniques were complemented by chiroptical methods, NMR, and anomalous X-ray scattering analyses. Some stereochemical assignments for this class of metabolites based solely on NMR arguments were later corrected by X-ray methods.[19]

In the present work, as part of efforts to identify additional cadinane-type sesquiterpenoids from *H. inuloides*,[4] to define their absolute configurations, and to explore their anti-inflammatory activities, we have isolated eight cadinane-type metabolites (**1**–**8**) and some flavonoids, triterpenoids, and sterols from the aerial parts of this species. Among these, four compounds (**1**–**4**) are new natural products. The absolute configurations were established by comparing their experimental and calculated electronic circular dichroism (ECD) spectra and confirmed by refinement of the Flack parameter using anomalous X-ray scattering from the oxygen atoms. In an attempt to provide additional information regarding structural features, the structures of compounds **5**–**8** were confirmed by X-ray analysis. The absolute configuration for one of these metabolites was also defined, and the in vivo anti-inflammatory properties of the cadinanes were evaluated.

Received: June 26, 2015
Published: November 13, 2015

DOI: 10.1021/acs.jnatprod.5b00571
J. Nat. Prod. 2015, 78, 2634–2641

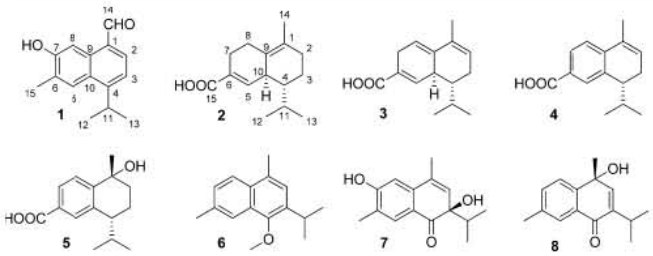

RESULTS AND DISCUSSION

The acetone extract of the aerial parts of *H. inuloides* was fractionated by vacuum liquid chromatography (VLC) using silica gel to obtain fractions that were pooled in 15 groups according to their TLC profiles. Further purifications of these fractions were carried out by repeated chromatographic separations to afford four new (**1**–**4**) and four known (**5**–**8**) cadinene-type sesquiterpenoids, together with nine known metabolites: 3β-friedelinol, α-amyrin, β-amyrin, α-spinasterol, α-spinasteryl β-D-glucopyranoside, quercetin, 3,7,3′-tri-*O*-methylquercetin, 7,3′-di-*O*-methyleriodictyol, and 3,7,3′,4′-tetra-*O*-methylquercetin. The known compounds were identified by comparison of their experimental and reported physical and spectroscopic data and by direct comparison with authentic samples.

Compound **1** was isolated as yellow crystals. The HRESIMS spectrum showed a protonated molecular ion at *m*/*z* 229.12229 $[M + H]^+$ (calcd for $C_{15}H_{17}O_2$, 229.12285), indicating a molecular formula of $C_{15}H_{16}O_2$ when taken in conjunction with the ^{13}C NMR data. The ^{13}C data of compound **1** (Table 1) exhibited signals for 15 carbons, which were classified in accordance with DEPT experiments as five sp^2 quaternary carbons (δ_C 153.6, 131.6, 127.9, 127.8, 127.1), one oxygenated sp^2 tertiary carbon (δ_C 156.8), three methyls (δ_C 23.5, 23.5, 17.2), five methines [four aromatic (δ_C 139.2, 125.4, 118.7, 107.9), and one aliphatic (δ_C 29.4)], and a formyl carbonyl group (δ_C 195.1). The latter functionality was confirmed by the presence of the band at 1676 cm^{-1} in the IR spectrum and a signal at δ_H 10.17 (1H, s) in the ^1H NMR data (Table 1). The ^1H NMR data were in agreement with the presence of four aromatic protons at δ_H 7.85 (1H, d, J = 7.6 Hz) and 7.41 (1H, d, J = 7.6 Hz) and two uncoupled signals at δ_H 9.14 (1H, s) and 7.98 (1H, s). Eight indices of hydrogen deficiency, together with the correlations observed in the HSQC experiment, permitted establishment of a tetrasubstituted naphthalene nucleus. The position of the formyl group was established according to HMBC correlations of the formyl proton δ_H 10.17 (1H, s) with C-1 (δ_C 127.1) and C-9 (δ_C 131.6). A methine signal at δ_H 3.80 (1H, hept, J = 6.8 Hz) coupled with two methyl groups at δ_H 1.42 (6H, d, J = 7.2 Hz) is characteristic for an isopropyl group, which was placed at C-4 due to the correlation of H-11 with C-4 and C-3 in the HMBC experiment establishing the cadinane-type skeleton. This arrangement was confirmed by single-crystal X-ray crystallographic analysis (Figure 1), and **1** was named 7-hydroxy-14-cadalenal.

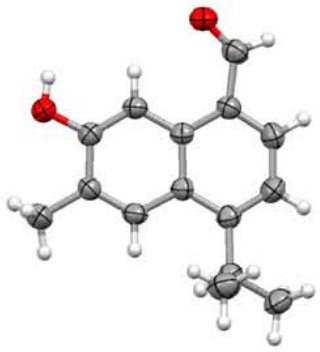

Figure 1. ORTEP drawing of the X-ray crystal structure of **1**.

Compound **2** was obtained as pink crystals. A molecular formula of $C_{15}H_{22}O_2$ was assigned from its ^{13}C NMR data and by the HRESIMS spectrum, which exhibited a protonated

Table 1. NMR Spectroscopic Data (400 MHz, $CDCl_3$, δ in ppm) for Compounds 1–4

	1		2		3		4	
position	δ_H (J in Hz)	δ_C, type	δ_H (J in Hz)	δ_C, type	δ_H (J in Hz)	δ_C, type	δ_H (J in Hz)	δ_C, type
1		127.1, C		126.6, C		132.0, C		131.5, C
2	7.85, d (7.6)	139.2, CH	1.98, br d (6.0)	32.2, CH_2	5.62, br t (3.6)	125.6, CH	5.89, t d (3.2, 1.2)	127.7, CH
3	7.41, d (7.6)	118.7, CH	α 1.690[a] β 1.269[a]	21.7, CH_2	2.06, br d (1.6)	26.0, CH_2	2.42, m	25.6, CH_2
4		153.6, C	1.194[a]	44.4, CH	1.66, m	44.4, CH	2.48, m	44.1, CH
5	7.98, s	125.4, CH	7.13, br s	145.1, CH	7.30, br d (2.4)	140.8, CH	7.83, br d (2.0)	130.1, CH
6		127.9, C		129.8, C		127.5, C		126.6, C
7		156.8, C	α 2.50, br dd (17.2, 5.4) β 2.195[a]	26.0, CH_2	3.04, m	25.5, CH_2	7.95, dd (8.0, 2.0)	128.7, CH
8	9.14, s	107.9, CH	α 2.79, ddd (13.2, 5.4, 2.0) β 1.87, br t (13.2)	26.3, CH_2	5.71, br t (4.4)	116.9, CH	7.29, d (8.0)	122.8, CH
9		131.6, C		127.8, C		135.4, C		140.9, C
10		127.8, C	2.73, br d (8.0)	40.6, CH	2.86, m	38.7, CH		139.3, C
11	3.80, hept (6.8)	29.4, CH	2.108[a]	27.0, CH	2.23, hept d (6.8, 3.6)	26.7, CH	1.92, hept d (13.6, 6.8)	30.4, CH
12	1.42, d (7.2)	23.5, CH_3	0.99, d (6.8)	21.6, CH_3	0.95, d (6.8)	21.0, CH_3	0.90, d (6.8)	20.3, CH_3
13	1.42, d (7.2)	23.5, CH_3	0.83, d (6.8)	15.9, CH_3	0.90, d (6.8)	15.1, CH_3	0.81, d (6.8)	21.4, CH_3
14	10.17, s	195.1, CH	1.663, s[a]	18.7, CH_3	1.82, br d (1.2)	19.5, CH_3	2.06, s	19.1, CH_3
15	2.50, s	17.2, CH_3		172.8, C		172.1, C		172.4, C

[a]Overlapped signals.

DOI: 10.1021/acs.jnatprod.5b00571
J. Nat. Prod. 2015, 78, 2634–2641

molecular ion at m/z 235.16880 $[M + H]^+$ (calcd for $C_{15}H_{23}O_2$, 235.16980). The IR spectrum showed absorption bands for a hydroxycarbonyl group (3526, 2930, 1686 cm^{-1}), confirmed by the signal in the ^{13}C NMR spectrum at δ_C 172.8. The ^1H NMR spectrum showed the same characteristic signals for an isopropyl group observed in **1** (Table 1) [a methine signal δ_H 2.108 (1H, m) correlated with two methyl groups δ_H 0.99 (3H, d, J = 6.8 Hz) and δ_H 0.83 (3H, d, J = 6.8 Hz) in the COSY experiment]. The ^{13}C NMR data of **2** (Table 1) showed 15 carbon resonances, which were categorized as three methyls (δ_C 21.6, 18.7, 15.9), four methylenes (δ_C 32.2, 26.3, 26.0, 21.7), four methines (three aliphatic, δ_C 44.4, 40.6, 27.0, and one vinylic, δ_C 145.1), three quaternary carbons (δ_C 129.8, 127.8, 126.6), and a hydroxycarbonyl group (δ_C 172.8), by analysis of DEPT data. Five indices of hydrogen deficiency for this compound, compared to **1**, indicated a higher degree of hydrogenation, thus establishing an unsaturated decalin system instead of a naphthalene nucleus. The vinylic proton observed in the ^1H NMR spectrum at δ_H 7.13 (1H, br s) was located in the β position with respect to the hydroxycarbonyl group, based on the correlation observed in the HMBC experiment. Unsaturation between C-1 and C-9 was determined according to HMBC correlations of the C-14 methyl group and both quaternary vinylic carbons. The proposed structure for compound **2** was confirmed by single-crystal X-ray crystallographic analysis (Figure 2). The *trans* orientation of H-4 and H-10 was evidenced after crystallographic analysis because overlapping signals in the ^1H NMR spectrum prevented calculating coupling constants for those hydrogens. The experimental ECD spectrum of **2** displayed negative and positive Cotton effects (CEs) at 238 ($\Delta\varepsilon$ = −3.81) and 217 nm ($\Delta\varepsilon$ = +12.26), respectively, associated with a π–π^* transition of an α,β-unsaturated carboxylic acid moiety. This curve, with characteristic Davydov-split CEs, made evident the chiral interaction between two isolated but spatially close chromophores, according to the exciton chirality method, which has been extended for determining the absolute configuration of molecules with carbonyl[20] and olefinic[21] chromophores. For compound **2** a negative chirality (*M*-helicity) is expected if the electric transition moment vectors of the two interacting chromophores, i.e., the α,β-unsaturated carboxylic acid moiety and the C-1−C-9 double bond, were oriented in a left-handed corkscrew fashion (Figure 3). The experimental ECD spectrum of **2** showed a negative first CE at 238 ($\Delta\varepsilon$ = −3.81); thus the absolute configuration of **2** was assigned as 4*R*,10*S*. This assignment agreed with that reported for frullanic acid, a cadinane-type sesquiterpenoid isolated from *Frullania serrata*.[22] Indeed, although the chromophores present in frullanic acid are different from those of compound **2**, its ECD spectra displayed quite similar CEs. To corroborate the 4*R*,10*S* assignment, nonempirical calculations using the π-electron SCF-CI-DV MO method (see the Experimental Section) were performed. The calculated ECD spectrum for the (4*R*,10*S*)-stereoisomer of **2** (Figure 4) closely matched the experimental results. Therefore, the structure of compound **2** was established as (4*R*,10*S*)-2,3,4,7,8,10-hexahydrocadalen-15-oic acid.

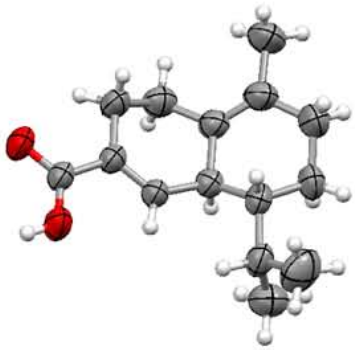

Figure 2. ORTEP drawing of the X-ray crystal structure of **2**. The ORTEP diagram represents the correct enantiomer defined by the Flack parameter, −0.12(13).

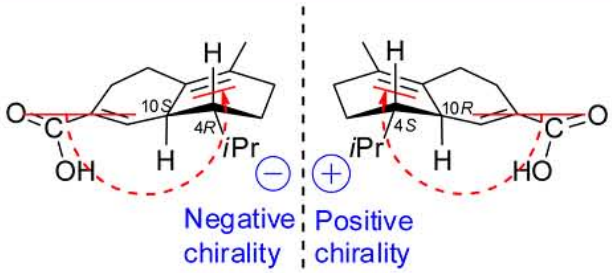

Figure 3. Exciton chirality of the two possible enantiomers for compound **2** (the 4*R*,10*R* enantiomer and its mirror image were discarded after establishing the *trans* orientation of H-4 and H-10 applying crystallographic analysis).

Compound **3** was isolated as colorless crystals. Its molecular formula was determined as $C_{15}H_{20}O_2$ by HRESIMS, from the protonated molecular ion at m/z 233.15330 $[M + H]^+$ (calcd for $C_{15}H_{21}O_2$, 233.15415) and by the ^{13}C NMR data. ^1H and ^{13}C NMR spectroscopic data (Table 1) showed some similarities to those of compound **2**, with characteristic signals for an isopropyl and a hydroxycarbonyl (δ_C 172.1) group. Six indices of hydrogen deficiency indicated the existence of a decalin system with three double bonds and the hydroxycarbonyl group. One of the three vinylic hydrogens in the ^1H NMR spectrum at δ_H 7.30 (1H, br d, J = 2.4 Hz) was located in the β position with respect to the α,β-unsaturated carboxylic acid moiety, because of its downfield chemical shift. The two remaining olefinic hydrogens at δ_H 5.71 (1H, br t, J = 4.4 Hz) and 5.62 (1H, br t, J = 3.6 Hz) were located adjacent to methylene carbons based on the observed multiplicity. The HMBC correlation of the three vinylic protons (H-5, H-8, and H-2) with the quaternary vinylic carbons (C-6, C-9, and C-1, respectively) determined the positions of the double bonds. X-ray diffraction data confirmed the proposed structure for **3** (Figure 5). The consistency of the ECD data of **3** with those of **2** suggested the same absolute configuration at the C-4 and C-10 stereocenters. The most significant CEs observed in the experimental ECD spectrum of **3** were at 243 nm ($\Delta\varepsilon$ = −1.76) and 212 nm ($\Delta\varepsilon$ = +13.19), in close proximity to those for **2** (Figure 4). The calculated ECD spectrum for the (4*R*,10*S*)-stereoisomer of **3** (Figure 4) showed an excellent fit with the experimental data. Therefore, compound **3** was named (4*R*,10*S*)-3,4,7,10-tetrahydrocadalen-15-oic acid. Interestingly, the specific rotations of compounds **2** and **3** were similar in magnitude but opposite in sign, $[\alpha]^{25}_D$ −75 (c 0.1, MeOH) and $[\alpha]^{25}_D$ +74.4 (c 0.1, MeOH), respectively, a remarkable observation for two compounds with a high degree of structural similarity and with the same configuration at their stereocenters. Comparison of the specific rotations may suggest that the configuration of one or both stereocenters for **3** might be opposite of that for **2**. To clarify these findings, the rotations were calculated using the Gaussian 09 package (see the

DOI: 10.1021/acs.jnatprod.5b00571
J. Nat. Prod. 2015, 78, 2634−2641

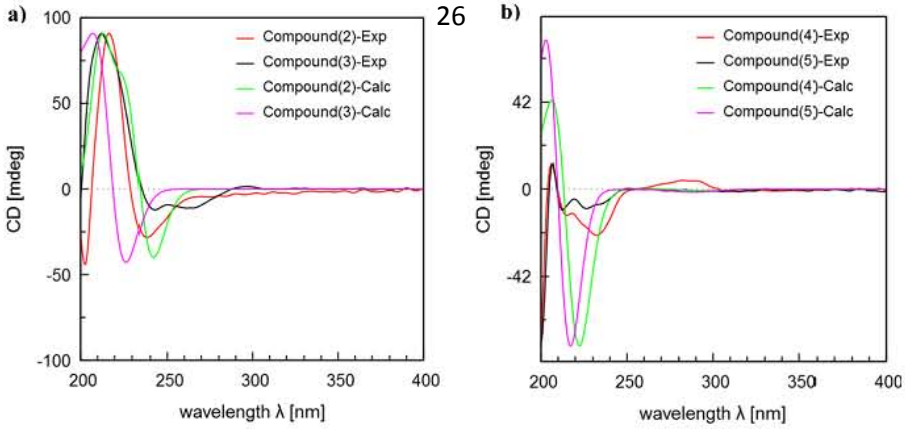

Figure 4. Calculated ECD spectra of (a) **2** (4*R*,10*S*)- and **3** (4*R*,10*S*)-isomers and (b) **4** (4*R*)- and **5** (1*R*,4*R*)-isomers and comparison with their respective experimental ECD spectra. The calculation was performed with the π-electron SCF-CI-DV MO method.

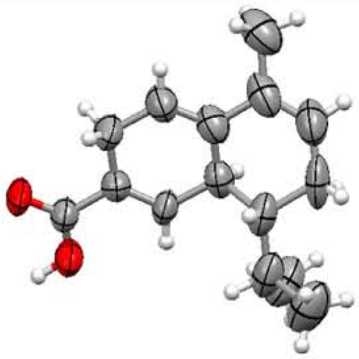

Figure 5. ORTEP drawing of the X-ray crystal structure of **3**. The ORTEP diagram represents the correct enantiomer defined by the Flack parameter, −0.20(3).

Experimental Section). The depicted configurations for **2** and **3** gave rotations with similar signs and approximate magnitudes to the experimental values [calculated specific rotation for compounds **2** and **3** with the 4*R*,10*S* configurations: $[\alpha]^{25}_{D}$ −84.05 (MeOH) and $[\alpha]^{25}_{D}$ +97.75 (MeOH), respectively]. To corroborate these absolute configuration assignments, the results were further checked by refinement of the Flack parameter using anomalous X-ray scattering from the oxygen atoms. The parameters for the absolute configuration were −0.12(13) and −0.20(3) for compounds **2** and **3**, respectively, indicating that the depicted formulas represent the correct enantiomers and confirmed that two closely related structures with the same orientations on their stereocenters and similar ECD spectra may display opposite specific rotation values. This outcome emphasizes the need for proper analysis of the results of chiroptical experiments before outlining conclusions about the absolute configuration of a molecule. Importantly, the reliability of the π-electron SCF-CI-DV MO method for determining absolute configuration was evidenced because it provided the same findings as those derived via X-ray crystallographic analysis.

Compound **4** was isolated as a white powder. Its molecular formula was established as $C_{15}H_{18}O_2$ based on analysis of the HRESIMS protonated molecular ion at *m*/*z* 231.13759 [M + H]$^+$ (calcd for $C_{15}H_{19}O_2$, 231.13850) and ^{13}C NMR data. The ^{1}H and ^{13}C NMR data (Table 1) displayed characteristic resonances that implied that **4** was also a cadinane-type sesquiterpenoid with a hydroxycarbonyl group. Seven indices of hydrogen deficiency were attributed to a dihydronaphthalene framework and a carbonyl group. Three signals were observed in the aromatic region of the ^{1}H NMR spectrum, with coupling constants that denoted an ABX system: δ_H 7.95 (1H, dd, *J* = 8.0 Hz, *J* = 2.0 Hz), δ_H 7.83 (1H, br d, *J* = 2.0 Hz), δ_H 7.29 (1H, d, *J* = 8.0 Hz). The HMBC correlation of the carbonyl carbon and H-5 and H-7 defined the location of the hydroxycarbonyl group. Unsaturation at C-1 was evidenced by the HMBC correlation of the vinylic proton at δ_H 5.89 (1H, td, *J* = 3.2, 1.2 Hz) with the 14-methyl carbon. The experimental ECD spectrum of **4** displayed CEs at 206 ($\Delta\varepsilon$ = +3.14), 215 ($\Delta\varepsilon$ = −3.33), 232 ($\Delta\varepsilon$ = −5.82), and 282 ($\Delta\varepsilon$ = +1.08) nm, similar to those for the calculated ECD spectrum of the (4*R*)-stereoisomer (Figure 4). Therefore, the structure of compound **4** was defined and named (4*R*)-3,4-dihydrocadalen-15-oic acid.

Reisolation of the known compound 1-hydroxy-1,2,3,4-tetrahydrocadalen-15-oic acid (**5**) as crystals suitable for X-ray crystallographic analysis allowed the determination of its absolute configuration. The Flack parameter, −0.01(3), determined an α-orientation for the C-4 *i*Pr group and a *trans* orientation of OH-1 and H-4; thus the stereogenic carbons were defined as (1*R*,4*R*) (Figure 6). The consistency of

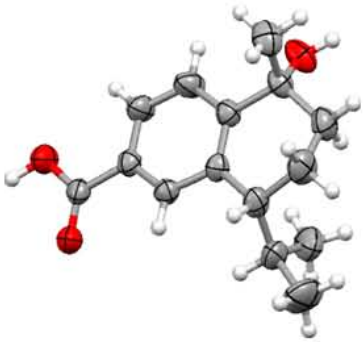

Figure 6. ORTEP drawing of the X-ray crystal structure of **5**. The ORTEP diagram represents the correct enantiomer defined by the Flack parameter, −0.01 (3).

the experimental and calculated ECD spectra for the 1*R*,4*R*-stereoisomer confirmed those assignments (Figure 4). Compound **5** has previously been isolated from *Heterotheca latifolia* as two C-1 epimers, and their relative configurations were assigned by the chemical shift differences for H-4, assuming that in the ^{1}H NMR spectrum of the *cis*-oriented *OH*-1 epimer the H-4 signal should have shifted downfield (in comparison

DOI: 10.1021/acs.jnatprod.5b00571
J. Nat. Prod. 2015, 78, 2634−2641

with the *trans*-isomer).[5] Nevertheless, the H-4 chemical shift and multiplicity reported in ref 5 for the *OH*-1 *cis*-oriented epimer (δ_H 2.69) were the same as those for compound **5**, reisolated from *H. inuloides*,[4] for which a *trans* orientation of OH-1 and H-4 was established by X-ray crystallographic analysis. Because the *i*Pr-4 α-orientation in compound **5** was evidenced by X-ray data, the established absolute configuration for compound **4** was corroborated, by considering that even though the matching of the experimental and calculated ECD spectra for this molecule is acceptable, there may be doubt about the position and relative intensity of CEs. Thus, alcohol **5** was dehydrated using *p*-toluenesulfonic acid to obtain compound **4**. The ^{1}H NMR spectrum of the reaction product was the same as that for the natural product **4**, and their ECD spectra were identical (Figure S27, Supporting Information); therefore the 4*R* assignment was confirmed.

Biogenetically, compounds **2**−**4** may be considered in the biosynthetic pathway that increases the degree of unsaturation of the bicyclic system, and the final hydration at C-1 in compound **4** afforded **5**. A cadinane skeleton with 1,9 and 5,6 double bonds observed for compound **2** had been previously reported for δ-cadinene, with the only difference being the oxidation state at C-15.

Experimental evidence has established that (+)-δ-cadinene is an early intermediate involved in the biosynthesis of cadinane sesquiterpenoids of *Gossypium hirsutum*, including 7-hydroxycadalene and 7-hydroxy-3,4-dihydrocadalene (also isolated from *H. inuloides*).[23,24] The absolute configuration of (+)-δ-cadinene from *G. hirsutum* has been established as (4*S*,10*R*).[25] Compound **2** [(−)-(4*R*,10*S*)-δ-cadinene-15-oic acid], isolated from *H. inuloides*, showed the opposite configuration of that observed for (+)-δ-cadinene from *G. hirsutum*. Thus, these findings were in agreement with previous results that established that the configuration of (+)-(4*S*)-7-hydroxy-3,4-dihydrocadalene [(+)-3-hydroxy-α-calacorene] from *G. hirsutum* is the opposite of that of the compound isolated from *H. inuloides*.[25] The 4*R* configuration has also been recently proven for inuloidin, a cadinene isolated from *H. inuloides*.[26]

X-ray crystal structures of the known compounds 4-methoxyisocadalene (**6**) and 3,7-dihydroxy-3(4*H*)-isocadalen-4-one (**7**) (not previously reported) were determined and are shown in Figures 7 and 8, respectively.

Results derived from the present study in comparison with the previous one[4] suggest that the metabolic variability of this species is associated with the morphophysiological condition of the plant. In the present research, the plant material was composed of fresh nonflowering branches with juvenile leaves that sprouted from pruned plants. Exhaustive fractionation of its acetone extract did not lead to the isolation of 7-hydroxycadalene and (4*R*)-7-hydroxy-3,4-dihydrocadalene, the major constituents previously found in flowering aerial parts collected in the same locality (and also collected during the end of the growing season) where the plant material studied in the present investigation was obtained.[4] Correlation between the concentration of some sesquiterpenoids and the morphophysiological conditions of *H. inuloides* has been previously demonstrated.[27]

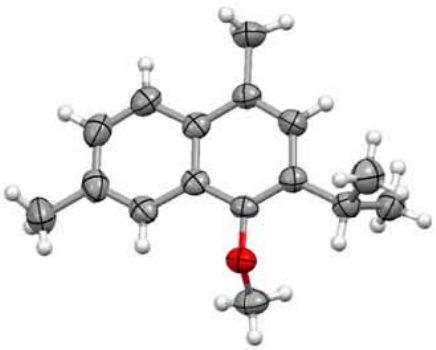

Figure 7. ORTEP drawing of the X-ray crystal structure of **6**.

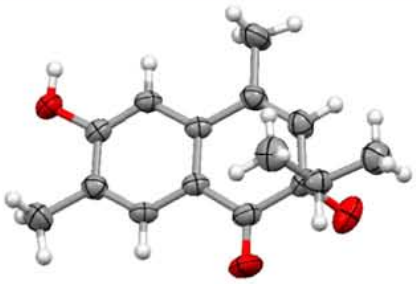

Figure 8. ORTEP drawing of the X-ray crystal structure of **7**.

Compounds **1**−**8** were evaluated as anti-inflammatory agents using the TPA-induced ear edema model. None of the tested compounds showed an $IC_{50} < 1$ μmol/ear (percentage values of inhibition on TPA-induced mouse ear edema are included in the Experimental Section). Therefore, the anti-inflammatory properties attributed to this species in folk medicine could not be related with the presence of these eight metabolites, due their relative low abundance and moderate activity. In previous studies performed with plant material having different morphophysiological conditions, different metabolites with higher anti-inflammatory activity were isolated.[4]

In summary, four new (**1**−**4**) and four known (**5**−**8**) cadinane sesquiterpenoids were isolated from the aerial parts of *H. inuloides*. The absolute configurations of compounds **2**−**5** were established by comparison of their experimental and calculated ECD spectra and were confirmed by single-crystal X-ray crystallographic diffraction. The finding that all compounds having a stereogenic center at C-4 with the same configuration supports previous studies regarding the configurations of cadinane sesquiterpenoids from *H. inuloides* and permitted the conclusion that this species biosynthesizes one enantiomeric series. In vivo anti-inflammatory studies revealed that some of these metabolites exhibit moderate activity.

EXPERIMENTAL SECTION

General Experimental Procedures. Melting points were determined in a Fisher-Johns apparatus (Cole Parmer). Optical rotations were measured using a PerkinElmer 343 polarimeter (MeOH, *c* in g/100 mL). UV spectra were taken on a Shimadzu UV−visible recording spectrophotometer. ECD spectra were obtained on a JASCO J-720 spectropolarimeter. IR spectra were recorded on a Bruker Tensor 27 spectrometer. ^{1}H and ^{13}C NMR spectra were recorded on a Bruker Avance III, 400 MHz NMR instrument. Chemical shifts are reported in parts per million (δ) relative to TMS, and coupling constants (*J*) are reported in Hz. The HRMS data were recorded on a Jeol The AccuTOF JMS T100LC system with a direct analysis in real time ESI+ ionization mode. X-ray data were collected using a Bruker Smart Apex CCD diffractometer (compounds **1** and **7**) or a Bruker D8 Venture κ-geometry diffractometer (compounds **2**, **3**, **5**, and **6**). Column chromatography was carried out using spherical silica gel with pore size 60 Å and 230−400 mesh particle size. TLC was performed using Merck silica gel 60 F_{254} plates (0.2 mm) visualized with either a UV lamp (254 and 365 nm) or a charring solution (12 g of ceric ammonium sulfate dihydrate, 22.2 mL of concentrated H_2SO_4,

DOI: 10.1021/acs.jnatprod.5b00571
J. Nat. Prod. 2015, 78, 2634−2641

and 350 g of ice). PLCs were done employing Merck silica gel 60 F_{254} glass plates (2 mm).

Plant Material. Aerial parts of *H. inuloides* (leaves and stems, material without flowers) were collected in Atlixco, Puebla, México, in October 2012 and identified by Edelmira Linares and Robert Bye. Voucher specimens (collection of E. Linares 2751 and R. Bye) were deposited in the National Herbarium (MEXU), Instituto de Biología de la Universidad Nacional Autónoma de México.

Extraction and Isolation. The dried and powdered plant material (4.47 kg) was extracted by maceration with acetone (3 times/24 h). The solvent was evaporated under vacuum to afford 235.9 g of extract, which was subjected to separation processes by vacuum liquid chromatography on silica gel using a hexanes−EtOAc gradient as mobile phase. As a result of the primary fractionation, 15 fractions were obtained (A−O). Fraction B (eluted with hexanes−EtOAc, 98:2) was subjected to a partition using MeOH in order to remove waxes. The MeOH-soluble fraction (64.7 mg) was purified by TLC using hexanes−EtOAc (98:2) to obtain 4.6 mg of 4-methoxyisocadalene[28] (**6**): mp 58−60 °C; ^{13}C NMR ($CDCl_3$, 100 MHz) δ_C 150.2 (C, C-4), 136.3 (C, C-3), 135.3 (C, C-6), 130.7 (C, C-9), 130.3 (C, C-1), 128.3 (C, C-10), 127.5 (CH, C-7), 124.5 (CH, C-8), 124.3 (CH, C-2), 121.8 (CH, C-5), 62.5 (CH_3, C-16), 26.4 (CH, C-11), 23.8 (CH_3, C-12), 23.8 (CH_3, C-13), 22.0 (CH_3, C-15), 19.4 (CH_3, C-14); UV (MeCN) λ_{max}(log ε) 235 (4.32), 253 (3.10), 292 (3.39) nm. From fraction D (eluted with hexanes−EtOAc, 95:5) was obtained 3β-friedelinol[29] (346.2 mg). This compound had not been previously described as a constituent of *H. inuloides*. Fraction E (8.9 g, eluted with hexanes−EtOAc, 95:5) was rechromatographed by VLC on silica gel using mixtures of hexanes−EtOAc as eluent, to give 13 subfractions (E1−E13). From subfraction E-7 was obtained **2** (9.0 mg) through crystallization from hexanes. Purification of subfraction E-8 was performed by TLC using CH_2Cl_2−MeOH (99:1), yielding a mixture of α-amyrin and β-amyrin (16.2 mg).[30,31] Fraction F (5.6 g, eluted with hexanes−EtOAc, 95:5) was subjected to silica gel column chromatography eluting with a gradient of hexanes−EtOAc to give eight subfractions (F1−F8). From subfraction F-5 was obtained **1** (5.8 mg) through recrystallization from hexanes. Subfraction F-6 (46.9 mg) was purified by TLC using benzene−EtOAc (94:6), affording 1-hydroxy-1(4*H*)-isocadalen-4-one[4,28] (**8**) (3.6 mg). ^{13}C NMR and UV spectroscopic data for 1-hydroxy-1(4*H*)-isocadalen-4-one (not previously reported): ^{13}C NMR ($CDCl_3$, 100 MHz) δ_C 184.3 (C, C-4), 145.2 (CH, C-2), 144.1 (C, C-9), 143.2 (C, C-3), 138.0 (C, C-6), 133.8 (CH, C-7), 129.6 (C, C-10), 127.0 (CH, C-5), 126.0 (CH, C-8), 68.1 (C, C-1), 30.9 (CH_3, C-14), 26.3 (CH, C-11), 21.8 (CH_3, C-12), 21.8 (CH_3, C-13), 21.1 (CH_3, C-15); UV (MeOH) λ_{max}(log ε) 210 (4.05), 226 (3.80), 235 (3.83), 243 (3.81), 249 (3.82), 267 (3.65), 275 (3.67) nm.

From fraction G (eluted with hexanes−EtOAc, 95:5) was obtained α-spinasterol[31,32] (349 mg) through recrystallization from hexanes. Fraction H (8.5 g, eluted with hexanes−EtOAc, 93:7) was submitted to VLC using a hexanes−EtOAc gradient as mobile phase to obtain 13 subfractions (H1−H13). Subfraction H-13 was rechromatographed by VLC using mixtures of hexanes−EtOAc to give 14 subfractions (H-13a−H13n). From subfraction H-13c was obtained **4** (43 mg), which was an unstable compound. Fraction I (9.7 g, eluted with hexanes−EtOAc, 90:10) was subjected to silica gel column chromatography eluting with a gradient of hexanes−EtOAc, to give 25 subfractions (I1−I25). From subfractions I-9, I-18, and I-23 were obtained **3** (4.1 mg), 3,7-dihydroxy-3(4*H*)-isocadalen-4-one[4] (**7**) (5.8 mg), and 7,3′-di-*O*-methyleriodictyol[33] (3.7 mg), respectively, through recrystallization from iPr$_2$O−hexanes. From fraction J (eluted with hexanes−EtOAc, 85:15) was obtained 3,7,3′,4′-tetra-*O*-methylquercetin[33] (1.6 mg) via recrystallization from iPr$_2$O−hexanes. This fraction was further purified by VLC using a hexanes−EtOAc gradient as mobile phase to afford 21 subfractions (J1−J21). From subfractions J12 and J16 were isolated 1-hydroxy-1,2,3,4-tetrahydrocadalen-15-oic acid[4,5] (**5**) (19.4 mg) and 3,7,3′-tri-*O*-methylquercetin[33] (2.3 mg), respectively, by recrystallization from EtOAc−hexanes. From fractions K (eluted with hexanes−EtOAc, 65:35) and O (eluted hexanes−EtOAc, 2:8) were obtained quercetin[33] (1.08 g) and α-spinasteryl β-D-glucopyranoside[34] (533 mg), respectively.

*7-Hydroxy-14-cadalenal (**1**):* yellow crystals; mp 153−155 °C; R_f 0.51 (hexanes−EtOAc, 80:20); UV (MeCN) λ_{max} (log ε) 207 (4.34), 235 (4.59), 280 (3.42), 322 (3.94), 336 (3.85), 355 (3.93) nm; IR ($CHCl_3$) ν_{max} 3581, 3270, 2968, 2928, 2744, 1676, 1577, 1462, 1243, 1227 cm^{-1}; ^{1}H and ^{13}C NMR (see Table 1); HRESIMS m/z 229.12229 [M + H]$^+$ (calcd for $C_{15}H_{17}O_2$, 229.12285).

*(4R,10S)-δ-Cadinen-15-oic acid (**2**):* pink crystals; mp 119−121 °C; R_f 0.44 (hexanes−EtOAc, 75:25); $[\alpha]^{25}_D$ −75 (c 0.1, MeOH); UV (MeOH) λ_{max} (log ε) 213 (5.22) nm; ECD (MeOH) 217 ($\Delta\varepsilon$ = +12.26), 238 ($\Delta\varepsilon$ = −3.81); IR ($CHCl_3$) ν_{max} 3526, 3041, 3008, 2962, 2930, 2871, 1686, 1640, 1431, 1286, 1233 cm^{-1}; ^{1}H and ^{13}C NMR (see Table 1); HRESIMS m/z 235.16880 [M + H]$^+$ (calcd for $C_{15}H_{23}O_2$, 235.16980).

*(4R,10S)-3,4,7,10-Tetrahydrocadalen-15-oic acid (**3**):* colorless crystals; mp 103−105 °C; R_f 0.38 (hexanes−EtOAc, 75:25); $[\alpha]^{25}_D$ +74.4 (c 0.1, MeOH); UV (MeOH) λ_{max} (log ε) 221 (4.21), 264 (3.23), 288 (3.36) nm; ECD (MeOH): 212 ($\Delta\varepsilon$ = +13.19), 243 ($\Delta\varepsilon$ = −1.76), 263 ($\Delta\varepsilon$ = −1.62), 296 ($\Delta\varepsilon$ = +0.21); IR ($CHCl_3$) ν_{max} 3524, 3023, 2963, 2930, 2874, 1695, 1272, 1221 cm^{-1}; ^{1}H and ^{13}C NMR (see Table 1); HRESIMS m/z 233.15330 [M + H]$^+$ (calcd for $C_{15}H_{21}O_2$, 233.15415).

*(4R)-3,4-Dihydrocadalen-15-oic acid (**4**):* white powder; R_f 0.31 (hexanes−EtOAc, 80:20); $[\alpha]^{25}_D$ +11.8 (c 0.25, MeOH); UV (MeOH) λ_{max}(log ε) 206 (4.16), 219 (4.00), 228 (4.03), 256 (3.49), 289 (3.82) nm; ECD (MeOH) 206 ($\Delta\varepsilon$ = +3.14), 215 ($\Delta\varepsilon$ = −3.33), 232 ($\Delta\varepsilon$ = −5.82), 282 ($\Delta\varepsilon$ = +1.08); IR ($CHCl_3$) ν_{max} 3589, 3522, 2929, 2857, 1695, 1425, 1271 cm^{-1}; ^{1}H and ^{13}C NMR (see Table 1); HRESIMS m/z 231.13759 [M + H]$^+$ (calcd for $C_{15}H_{19}O_2$, 231.13850).

Dehydration of Compound 5. Compound **5** (16.0 mg) was dissolved in EtOAc (2 mL) and placed in a 10 mL flask under a N_2 atmosphere. *p*-Toluenesulfonic acid (9.8 mg) dissolved in EtOAc (2 mL) was added, and the reaction mixture was heated with stirring at 70 °C for 1 h. TLC purification (hexanes−EtOAc, 70:30, two elutions) afforded **4** (4.9 mg) (for NMR data see Figure S25, Supporting Information).

Mouse Ear Inflammation Model. The in vivo anti-inflammatory activity was measured using the 12-*O*-tetradecanoylphorbol 13-acetate (TPA)-induced ear edema model.[35,36] The mice employed in these determinations were treated according the Mexican Official Norm MON-062-Z00-1999. Compounds **1**−**8** showed the following anti-inflammatory activities (% inhibition of edema, 1 μmol/ear): **1**, 43.14 ± 8.09; **2**, 21.51 ± 6.99; **4**, 12.93 ± 0.48; **6**, 15.32 ± 1.95; compounds **5**, **7**, and **8** displayed similar activities to those already reported,[4] and compound **3** did not display activity.

ECD Computational Calculations. An initial systematic conformational search of a given molecule was carried out by using the MMFF94 molecular mechanics force-field method, taking the solvent effect (MeOH) into consideration. The ECD and UV spectra for compounds **2**−**5** were calculated by the π-electron SCF-CI-DV MO method using the program CONFLEX.[37,38] For multiple conformers, an overall ECD spectrum was generated on the basis of Boltzmann weighting of individual conformers applying a shift based upon the difference between observed and calculated UV spectra. In the calculation of CD and UV spectra, the component CD and UV bands were approximated by the Gaussian distribution. This procedure was "tested" on the (−)-(4*R*)-7-hydroxy-3,4-dihydrocadalene [(−)-3-hydroxy-α-calacorene] (Figure S26, Supporting Information) also isolated by our research group from *H. inuloides* and whose absolute structure was previously determined independently.[25]

Specific Rotation Calculation. For compounds **2** and **3** the specific rotation were calculated using the Gaussian 09 package for the major conformers at the B3LYP/6-31G+(d) level with a PCM (MeOH) solvent model.

X-ray Crystal Structure Analysis. Crystals of compounds **2**, **3**, **5**, and **6** were obtained upon slow evaporation. In each case a colorless crystal was mounted on the goniometer of a Bruker D8 Venture k-geometry diffractometer operating with Cu Kα radiation (λ = 1.541 78

DOI: 10.1021/acs.jnatprod.5b00571
J. Nat. Prod. 2015, 78, 2634−2641

Å). The data collection routine, unit cell refinement, and data processing were carried out with the program APEX2.41. The structures were solved using SHELXS and refined using SHELXL-2014/7.42. The final refinement model involved anisotropic displacement parameters for non-hydrogen atoms. A riding model was used for the C-attached alkyl hydrogens. Hydrogen atom positions and isotropic displacement parameters were refined independently for the hydroxyl groups that are potentially involved in hydrogen bonding. The absolute configurations were established from anomalous dispersion effects.[39] Crystals of compounds **1** and **7** were mounted on the goniometer of a Bruker Apex CCD diffractometer operating with Mo Kα radiation (λ = 0.710 73 Å). The same procedure described above was followed except for the absolute configuration stage; every time the structures proved to be centrosymmetric.

*Crystal data of 7-hydroxy-14-cadalenal (**1**):* colorless, prism, $C_{15}H_{16}O_2$, M = 228.28, monoclinic, crystal size = 0.454 × 0.291 × 0.080 mm, a = 13.3320(3) Å, b = 9.8598(2) Å, c = 9.7860(2) Å, α = 90°, β = 106.6900(10)°, γ = 90°, V = 1232.19(5) Å^3, T = 298(2) K, space group $P2_1/c$, Z = 4, D_{cald} = 1.231 mg/m^3, λ(Mo Kα) = 0.710 73 Å, reflections collected = 10 405, independent reflections = 2257 [R(int) = 0.0609]. Final R indices for $I > 2\sigma(I)$, R_1 = 0.0444, wR_2 = 0.1000, R indices for all data R_1 = 0.0850, wR_2 = 0.1195.

*Crystal data of (4R,10S)-δ-cadinen-15-oic acid (**2**):* colorless, lamina, $C_{15}H_{22}O_2$, M = 234.32, monoclinic, crystal size = 0.277 × 0.155 × 0.045 mm, a = 8.5137(3) Å, b = 17.2957(6) Å, c = 9.8501(4) Å, α = 90°, β = 105.760(3)°, γ = 90°, V = 1395.90(9) Å^3, T = 298(2) K, space group $P2_1$, Z = 4, D_{cald} = 1.115 mg/m^3, λ(Cu Kα) = 1.541 78 Å, reflections collected = 47 866, independent reflections = 47 866 [R(int) = 0.0740]. Final R indices for $I > 2\sigma(I)$, R_1 = 0.0742, wR_2 = 0.1582, R indices for all data R_1 = 0.1353, wR_2 = 0.1899, Flack parameter = −0.12(13).

*Crystal data of (4R,10S)-3,4,7,10-tetrahydrocadalen-15-oic acid (**3**):* colorless, prism, $C_{15}H_{20}O_2$, M = 232.31, monoclinic, crystal size = 0.142 × 0.071 × 0.028 mm, a = 7.8341(10) Å, b = 17.4486(19) Å, c = 9.8795(14) Å, α = 90°, β = 90.053(10)°, γ = 90°, V = 1350.5(3) Å^3, T = 298(2) K, space group $P2_1$, Z = 4, D_{cald} = 1.143 mg/m^3, λ(Cu Kα) = 1.541 78 Å, reflections collected = 44 021, independent reflections = 5379 [R(int) = 0.1516]. Final R indices for $I > 2\sigma(I)$, R_1 = 0.0793, wR_2 = 0.1895, R indices for all data R_1 = 0.1638, wR_2 = 0.2435, Flack parameter = −0.2(3).

*Crystal data of (1R,4R)-1-hydroxy-1,2,3,4-tetrahydrocadalen-15-oic (**5**):* colorless, prism, $C_{15}H_{20}O_3$, M = 248.31, orthorhombic, crystal size = 0.316 × 0.304 × 0.112 mm, a = 8.6779(3) Å, b = 11.2141(4) Å, c = 14.2388(6) Å, α = 90°, β = 90°, γ = 90°, V = 1385.65(9) Å^3, T = 298(2) K, space group $P2_12_12_1$, Z = 4, D_{cald} = 1.190 mg/m^3, λ(Cu Kα) = 1.541 78 Å, reflections collected = 19 806, independent reflections = 2882 [R(int) = 0.0240]. Final R indices for $I > 2\sigma(I)$, R_1 = 0.0425, wR_2 = 0.1202, R indices for all data R_1 = 0.0439, wR_2 = 0.1223, Flack parameter = −0.01(3).

*Crystal data of 4-methoxyisocadalene (**6**):* colorless, prism, $C_{16}H_{20}O$, M = 228.32, orthorhombic, crystal size = 0.295 × 0.167 × 0.094 mm, a = 8.725(3) Å, b = 10.012(3) Å, c = 15.541(4) Å, α = 90°, β = 90°, γ = 90°, V = 1357.5(7) Å^3, T = 298(2) K, space group $P2_12_12_1$, Z = 4, D_{cald} = 1.117 mg/m^3, λ(Cu Kα) = 1.541 78 Å, reflections collected = 23 861, independent reflections = 2771 [R(int) = 0.0873]. Final R indices for $I > 2\sigma(I)$, R_1 = 0.0450, wR_2 = 0.1149, R indices for all data R_1 = 0.0643, wR_2 = 0.1281, Flack parameter = 0.2(2).

*Crystal data of 3,7-dihydroxy-3(4H)-isocadalen-4-one (**7**):* colorless, platy-prism, $C_{15}H_{18}O_3$, M = 246.29, monoclinic, crystal size = 0.487 × 0.368 × 0.060 mm, a = 8.2429(3) Å, b = 11.4497(4) Å, c = 13.7233(5) Å, α = 90°, β = 98.9450(10)°, γ = 90°, V = 1279.44(8) Å^3, T = 150(2) K, space group $P2_1/c$, Z = 4, D_{cald} = 1.279 mg/m^3, λ(Mo Kα) = 0.710 73 Å, reflections collected = 19 350, independent reflections = 2954 [R(int) = 0.0289]. Final R indices for $I > 2\sigma(I)$, R_1 = 0.0391, wR_2 = 0.0991, R indices for all data R_1 = 0.0459, wR_2 = 0.1049.

Crystallographic data for the structures reported in this paper have been deposited with the Cambridge Crystallographic Data Centre (compounds **1**−**3** and **5**−**7** deposition numbers: CCDC 1063660-CCDC 1063665, respectively). Copies of the data can be obtained, free of charge, on application to the Director, CCDC, 12 Union Road, Cambridge CB2 1EZ, UK (fax: + 44-(0)1223-336033 or e-mail: deposit@ccdc.cam.ac.uk).

■ ASSOCIATED CONTENT

Supporting Information

The Supporting Information is available free of charge on the ACS Publications website at DOI: 10.1021/acs.jnatprod.5b00571.

1D and 2D NMR spectra of compounds **1**−**4** (PDF)

■ AUTHOR INFORMATION

Corresponding Author

*Tel: +52 (55) 5622-4446. Fax: +52 (55) 5616-2217. E-mail: delgado@unam.mx.

Notes

The authors declare no competing financial interest.

■ ACKNOWLEDGMENTS

This work was taken from the Ph.D. thesis of V.E. The authors thank Universidad Nacional Autónoma de México (DGAPA, PAPIIT IG200514). The authors also acknowledge M. I. Chávez, B. Quiroz, A. León, R. Patiño, Á. Peña, E. Huerta, L. K. Calderón-Ortiz, A. Nieto, L. Delgado-Chávez, J. L. Rodríguez-Chávez, R. Ramos, L. Velasco, J. Pérez, and F. Novillo (Instituto de Química de la UNAM) for technical assistance. V.E. also thanks CONACyT for the graduate scholarship (257805) and Programa de Posgrado en Ciencias Químicas de la UNAM.

■ REFERENCES

(1) Semple, J. C. *Botany* **2008**, *86*, 886−900.
(2) Nesom, G. L. *Phytologia* **1990**, *69*, 282−294.
(3) Comisión Nacional Forestal. *Plantas Medicinales de la Farmacia Viviente del CEFOFOR: Usos Terapéuticos Tradicionales y Dosificación* **2010**, 12−13.
(4) Delgado, G.; Olivares, M.; Chávez, M.; Ramírez-Apan, T.; Linares, E.; Bye, R.; Espinosa-García, F. *J. Nat. Prod.* **2001**, *64*, 861−864.
(5) Bohlmann, F.; Gupta, R. K.; King, R. M.; Robinson, H. *Phytochemistry* **1982**, *21*, 2982−2984.
(6) Bohlmann, F.; Wolfrum, C.; Jakupovic, J.; King, R. M.; Robinson, H. *Phytochemistry* **1985**, *24*, 1101−1103.
(7) Bohlmann, F.; Zdero, C.; Robinson, H.; King, R. M. *Phytochemistry* **1979**, *18*, 1675−1680.
(8) El-Dahmy, T.; Sarg, T.; Farrag, N. M.; Ateya, A. M.; Jakupovic, J.; Bohlman, F.; King, R. M. *Phytochemistry* **1986**, *25*, 1474−1475.
(9) Bohlmann, F.; Zdero, C. *Phytochemistry* **1979**, *18*, 1185−1187.
(10) Coballase-Urrutia, E.; Pedraza-Chaverri, J.; Camacho-Carranza, R.; Cárdenas Rodríguez, N.; Huerta-Gertrudis, B.; Medina-Campos, O.; Mendoza-Cruz, M.; Delgado-Lamas, G.; Espinoza-Aguirre, J. *Toxicology* **2010**, *276*, 41−48.
(11) Haraguchi, H.; Ishikawa, H.; Sanchez, Y.; Ogura, T.; Kubo, Y.; Kubo, I. *Bioorg. Med. Chem.* **1997**, *5*, 865−871.
(12) Segura, L.; Freixa, B.; Ringbom, Th.; Vila, R.; Perera, P.; Adzet, T.; Bohlin, L.; Cañigueral, S. *Planta Med.* **2000**, *66*, 553−555.
(13) Rocha-Gonzáles, H.; Blaisdell-López, E.; Granados-Soto, V.; Navarrete, A. *Eur. J. Pharmacol.* **2010**, *649*, 154−160.
(14) Haraguchi, H.; Saito, T.; Ishikawa, H.; Sanchez, Y.; Ogura, T.; Kubo, I. *J. Pharm. Pharmacol.* **1996**, *48*, 441−443.
(15) Kubo, I.; Chaudhuri, S. K.; Kubo, Y.; Sanchez, Y.; Ogura, T.; Saito, T.; Ishkawa, H.; Haraguchi, H. *Planta Med.* **1996**, *62*, 427−430.
(16) Kubo, I.; Muroi, H.; Kubo, A.; Chaudhuri, S. K.; Sanchez, Y.; Ogura, T. *Planta Med.* **1994**, *60*, 218−221.

DOI: 10.1021/acs.jnatprod.5b00571
J. Nat. Prod. 2015, 78, 2634−2641

(17) Rodríguez-Chávez, J. L.; Rufino-González, Y.; Ponce-Macotela, M.; Delgado, G. *Parasitology* **2015**, *142*, 576−584.
(18) Herout, V.; Sykora, V. *Chem. Ind.* **1958**, 130−131.
(19) Ding, L.; Pfoh, R.; Rühl, S.; Qin, S.; Laatsch, H. *J. Nat. Prod.* **2009**, *72*, 99−101.
(20) Koreeda, M.; Harada, N.; Nakanishi, K. *J. Am. Chem. Soc.* **1974**, *96* (1), 266−268.
(21) Harada, N.; Iwabuchi, J.; Yokota, Y.; Uda, H. *J. Am. Chem. Soc.* **1981**, *103*, 5590−5591.
(22) Li, R.-J.; Zhu, R.-X.; Zhao, Y.; Morris-Natschke, S.; Chen, C.-H.; Wang, S.; Zhang, J.-Z.; Zhou, J.-C.; Lou, H.-X.; Lee, K.-H. *Nat. Prod. Res.* **2014**, *28*, 1519−1524.
(23) Davis, G.; Essenberg, M. *Phytochemistry* **1995**, *39*, 553−567.
(24) Wang, Y.-H.; Dávila-Huerta, G.; Essenberg, M. *Phytochemistry* **2003**, *63*, 219−225.
(25) Stipanovic, R. D.; Puckhaber, L. S.; Reibenspies, J. H.; Williams, H. J. *Phytochemistry* **2006**, *67*, 1304−1308.
(26) Kamatani, J.; Iwadate, T.; Tajima, R.; Kimoto, H.; Yamada, Y.; Masuoka, N.; Kubo, I.; Nihei, K. *Tetrahedron* **2014**, *70*, 3141−3145.
(27) Maldonado-Lopez, Y.; Linares-Mazari, E.; Bye, R.; Delgado, G.; Espinosa-García, F. *Econ. Bot.* **2008**, *62*, 161−170.
(28) Bohlmann, F.; Zdero, C. *Chem. Ber.* **1976**, *109*, 2021−2025.
(29) Salazar, G. C. M.; Silva, G. D. F.; Duarte, L. P.; Vieira Filho, S. A.; Lula, I. S. *Magn. Reson. Chem.* **2000**, *38*, 977−980.
(30) Mahato, S. B.; Kundu, A. P. *Phytochemistry* **1994**, *37*, 1517−1575.
(31) Willuhn, G.; Schneider, R. *Arch. Pharm. (Weinheim, Ger.)* **1987**, *320*, 393−396.
(32) Ragasa, C. Y.; Lim, K. *Philippine J. Sci.* **2005**, *134*, 83−87.
(33) Jerga, C.; Merfort, I.; Willuhn, G. *Planta Med.* **1990**, *56*, 122−123.
(34) Gafur, M. A.; Obata, T.; Kiuchi, F.; Tsuda, Y. *Chem. Pharm. Bull.* **1997**, *45*, 620−625.
(35) Della Logia, R.; Tubaro, A.; Sosa, S.; Becker, H.; Saar, St.; Isaac, O. *Planta Med.* **1994**, *60*, 516−529.
(36) Tubaro, A.; Dri, P.; Delbello, G.; Zilli, C.; Della Logia, R. *Agents Actions* **1985**, *17*, 347−349.
(37) Goto, H.; Osawa, E. *J. Am. Chem. Soc.* **1989**, *111*, 8950−8951.
(38) Goto, H.; Osawa, E. *J. Chem. Soc., Perkin Trans. 2* **1993**, *2*, 187−198.
(39) Parsons, S.; Flack, H.; Wagner, T. *Acta Crystallogr., Sect. B: Struct. Sci., Cryst. Eng. Mater.* **2013**, *B69*, 249−259.

DOI: 10.1021/acs.jnatprod.5b00571
J. Nat. Prod. 2015, 78, 2634−2641

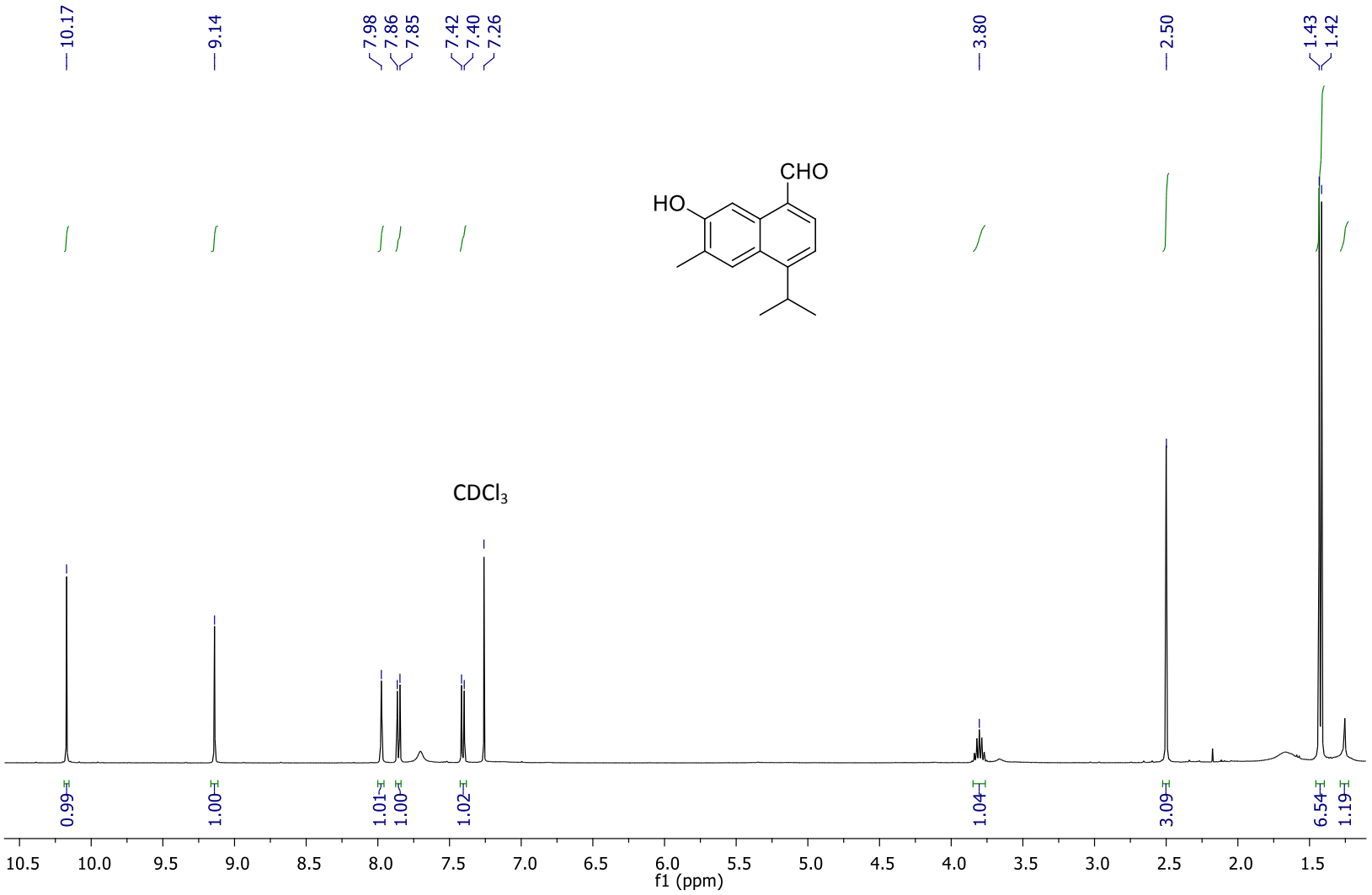

Espectro 1. RMN ^{1}H del compuesto **1** (400 MHz, $CDCl_3$).

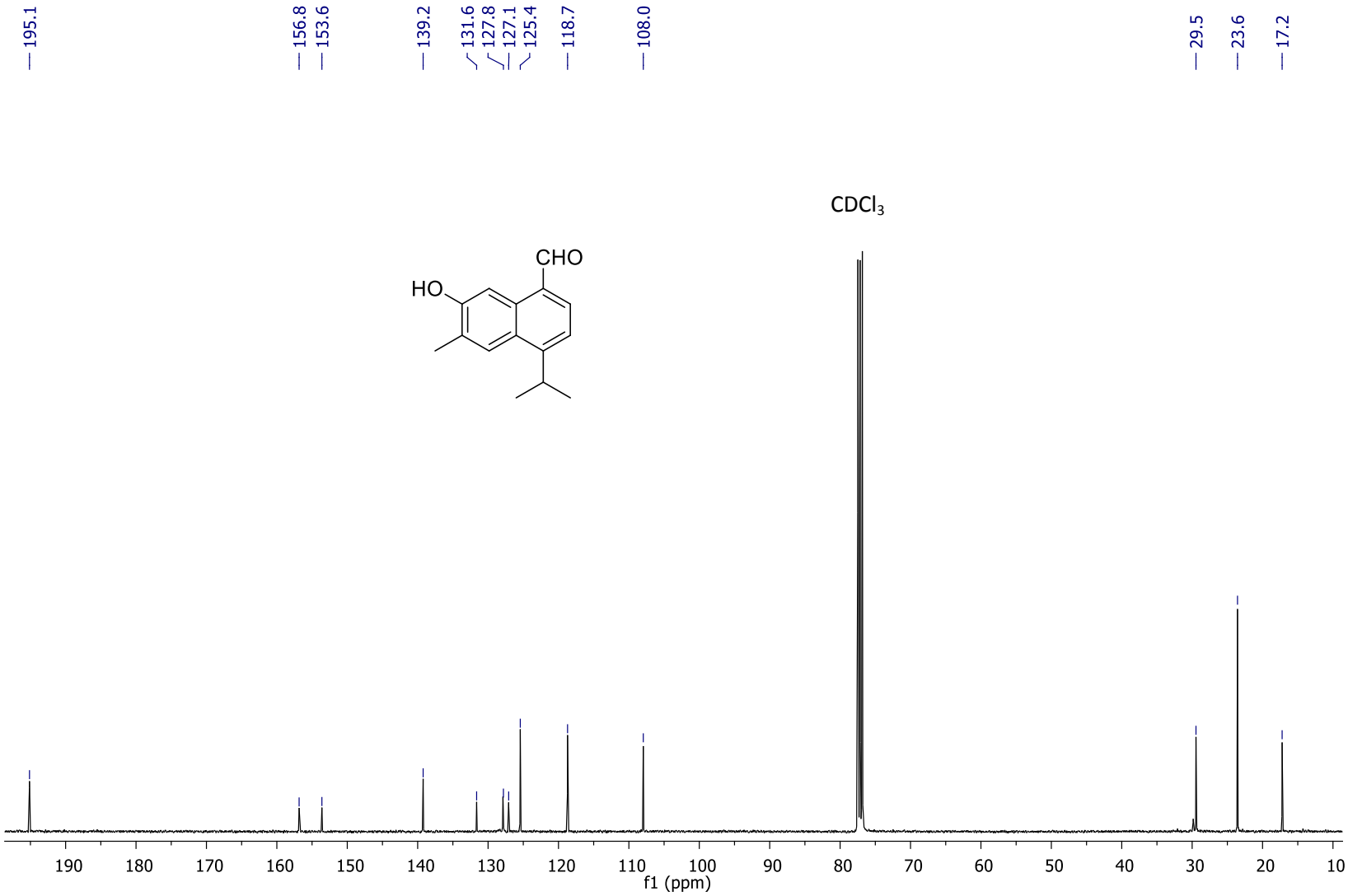

Espectro 2. RMN ^{13}C del compuesto **1** (100 MHz, $CDCl_3$).

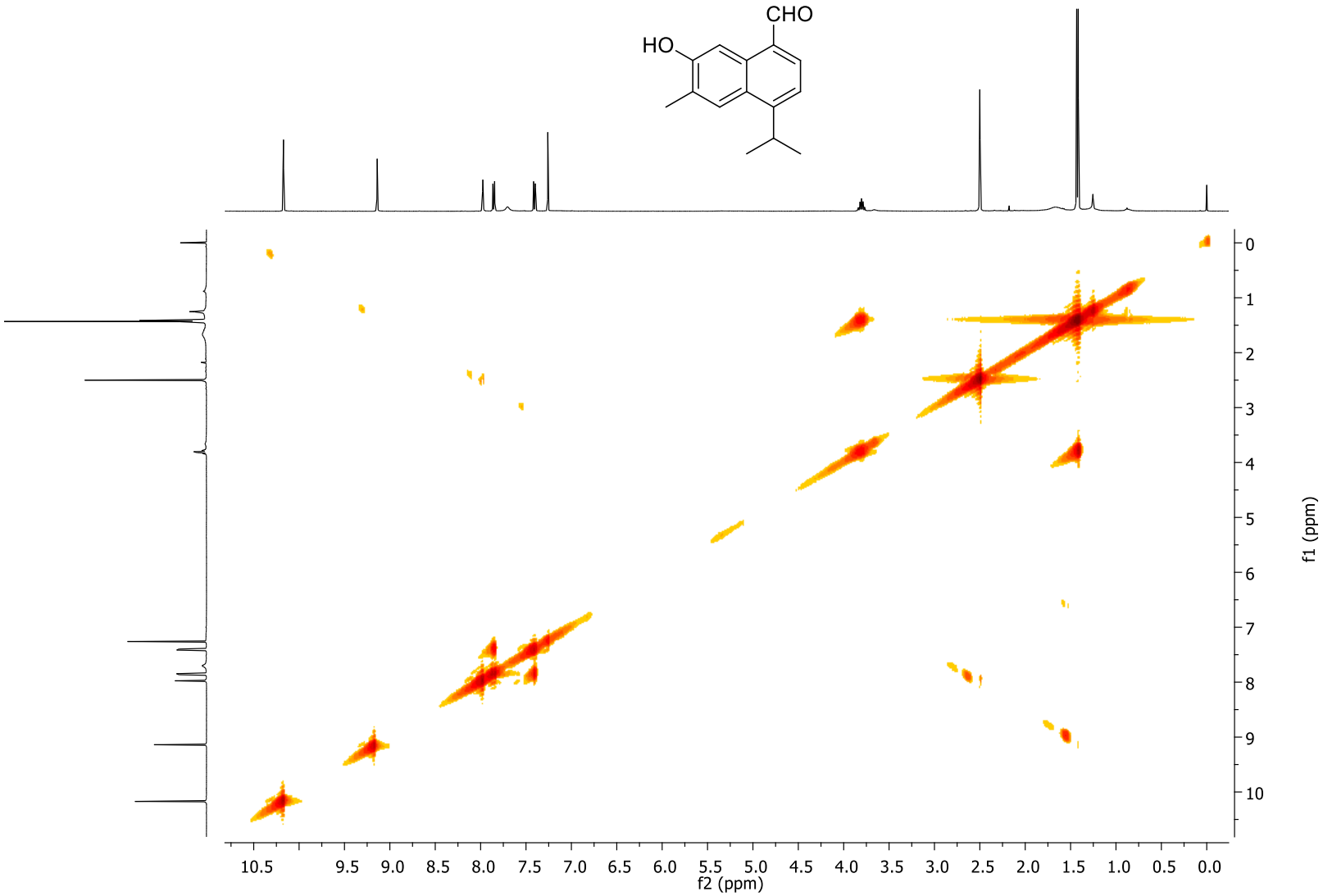

Espectro 3. COSY del compuesto **1** ($CDCl_3$).

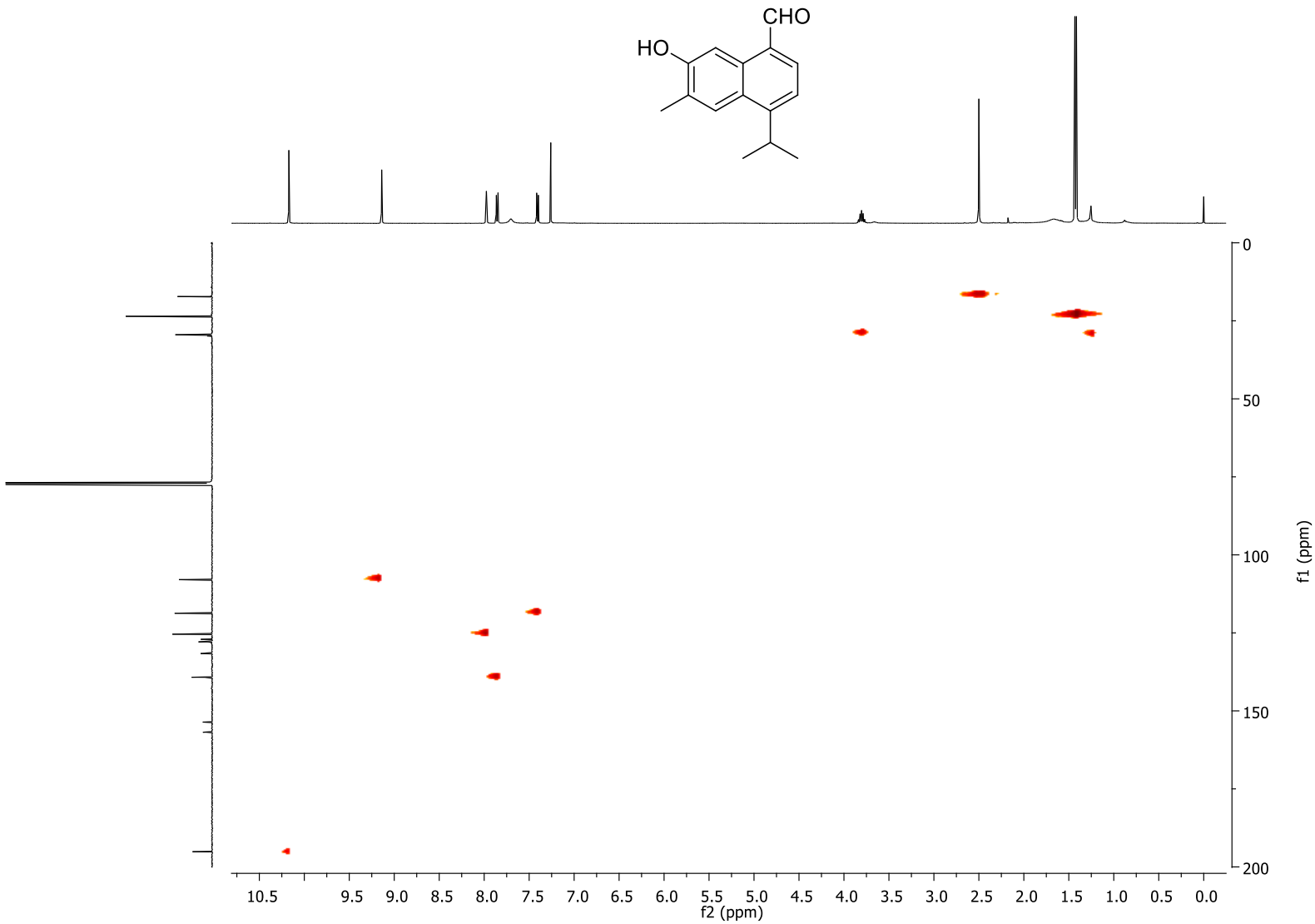

Espectro 4. HSQC del compuesto **1** ($CDCl_3$).

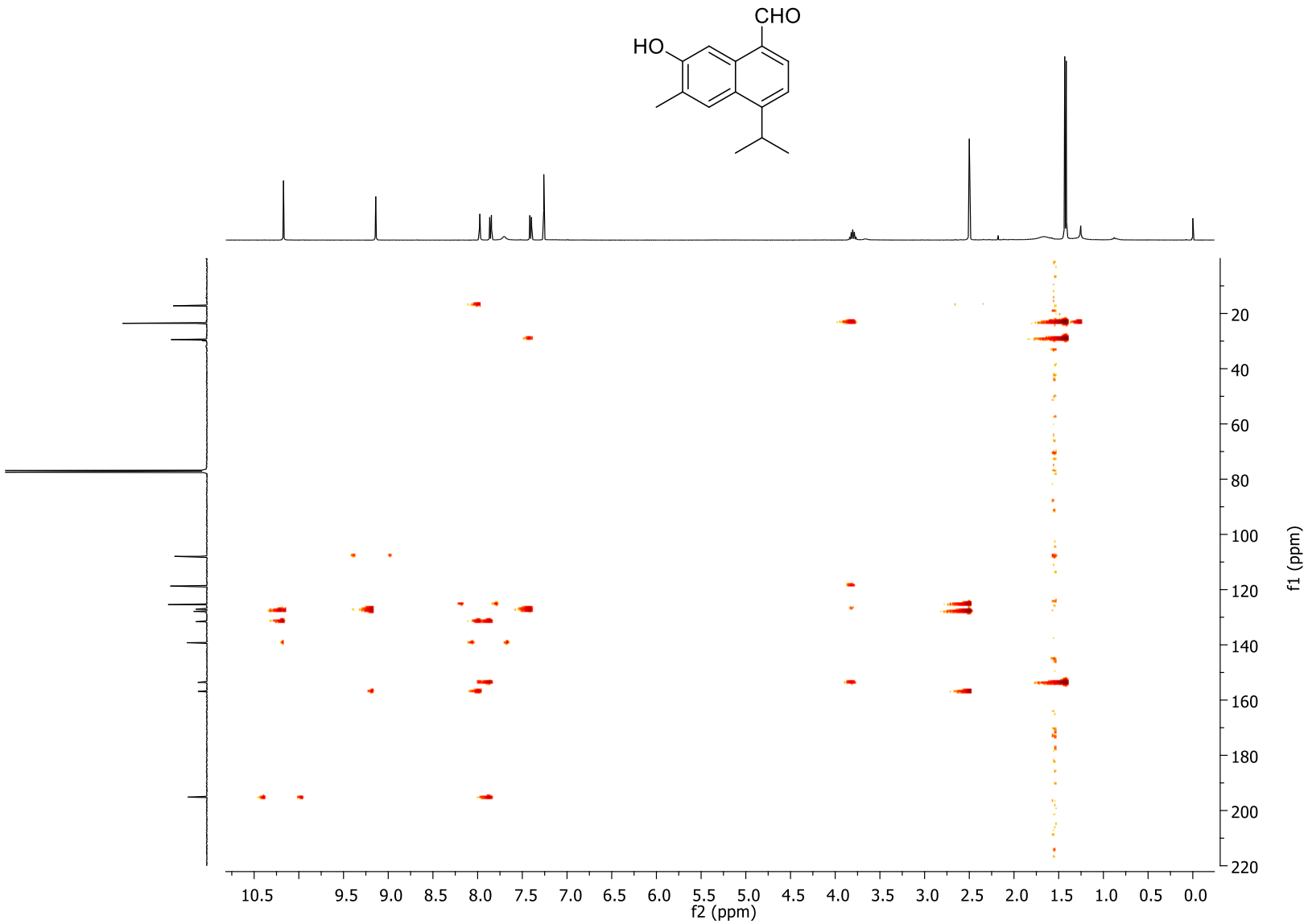

Espectro 5. HMBC del compuesto **1** ($CDCl_3$).

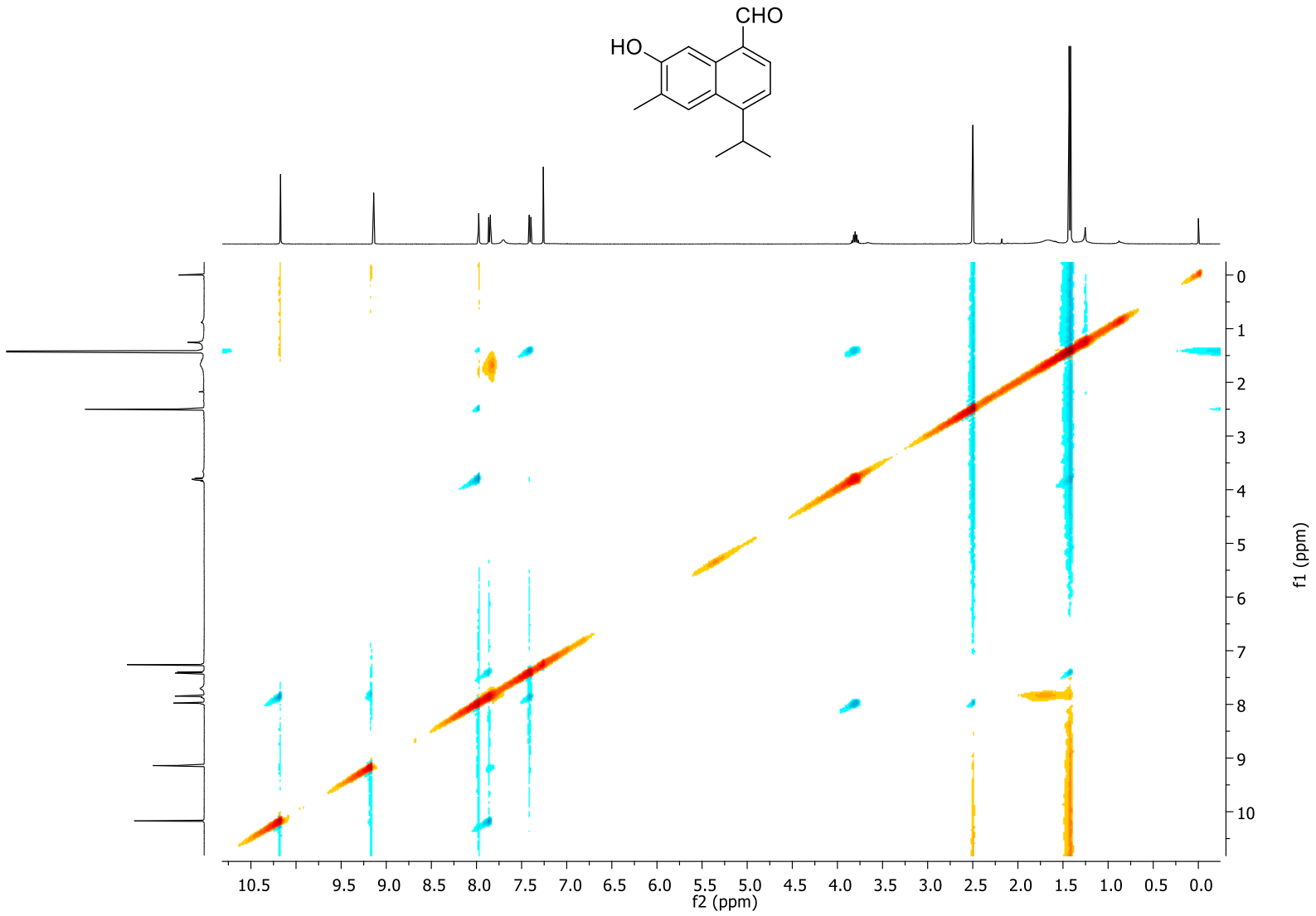

Espectro 6. NOESY del compuesto **1** ($CDCl_3$).

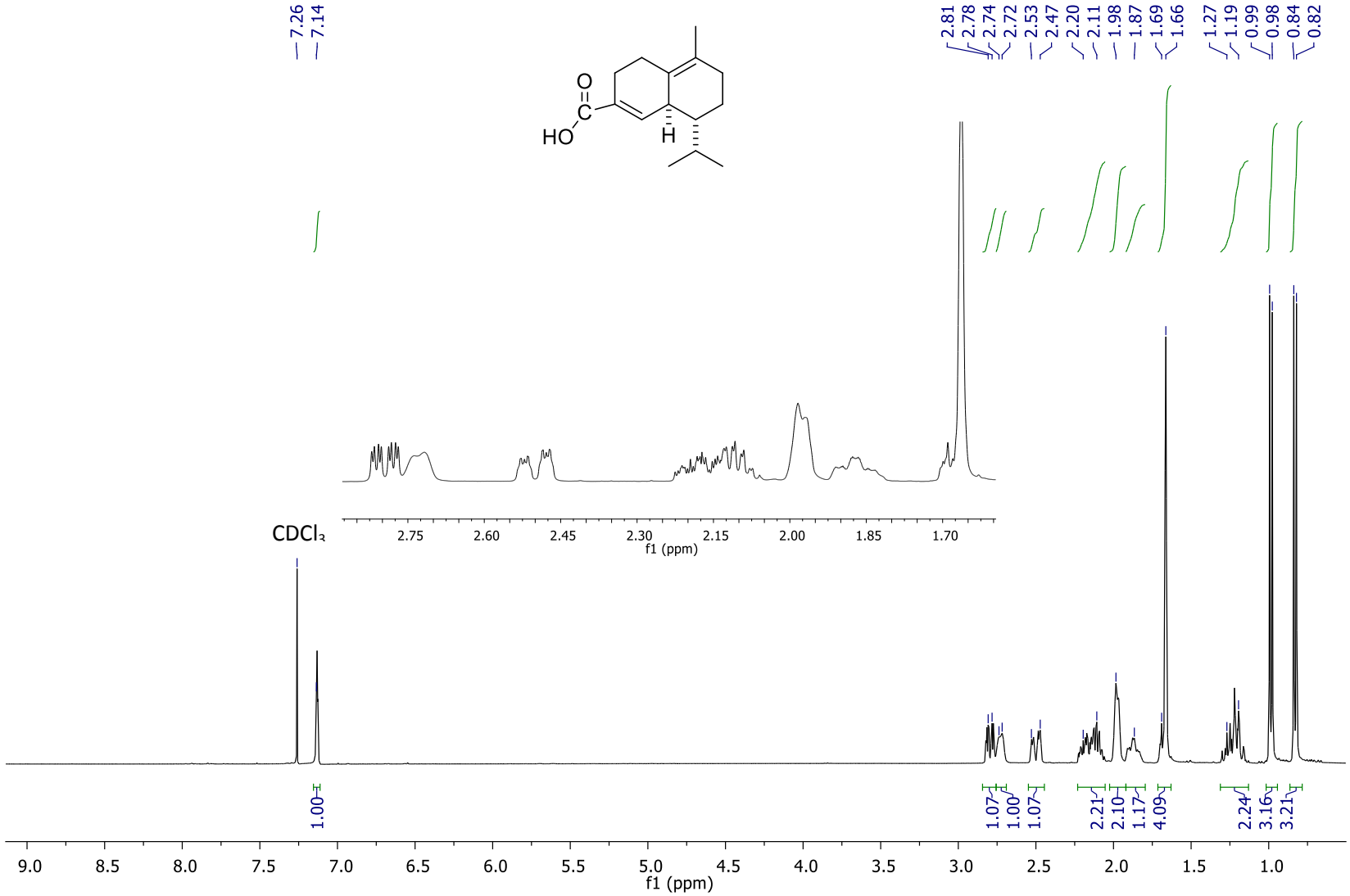

Espectro 7. RMN ^{1}H del compuesto **2** (400 MHz, $CDCl_3$).

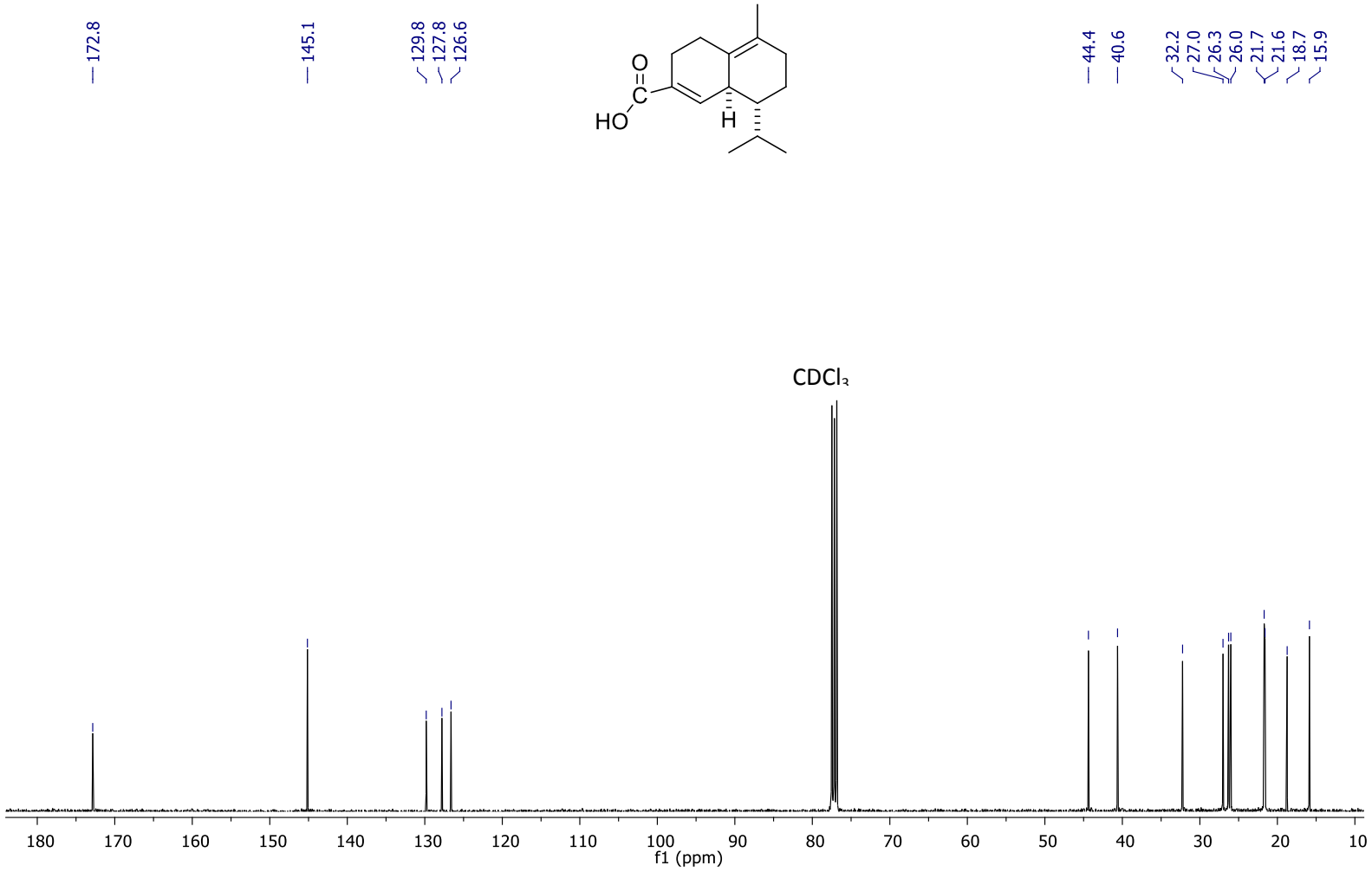

Espectro 8. RMN ^{13}C del compuesto **2** (100 MHz, $CDCl_3$).

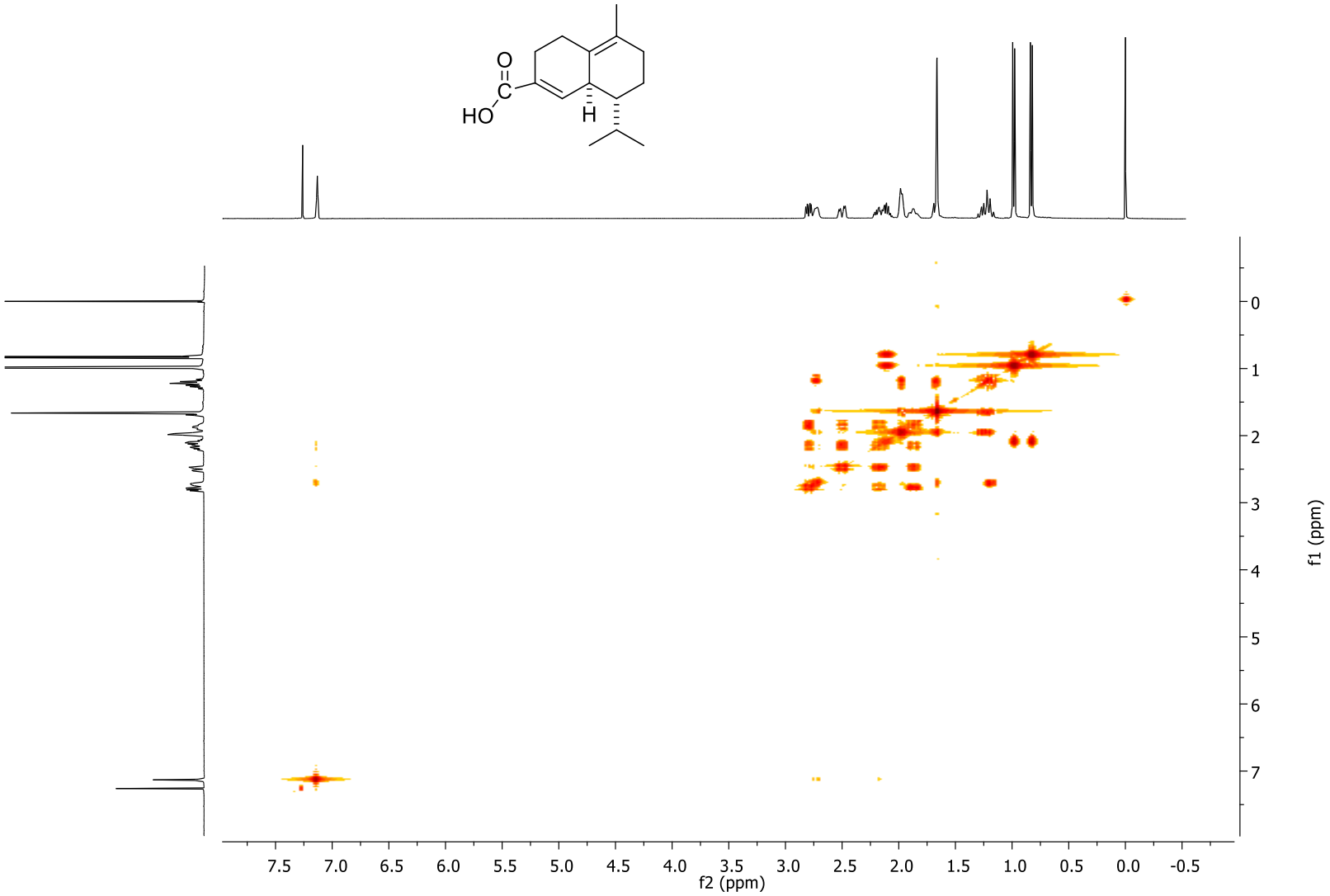

Espectro 9. COSY del compuesto **2** ($CDCl_3$).

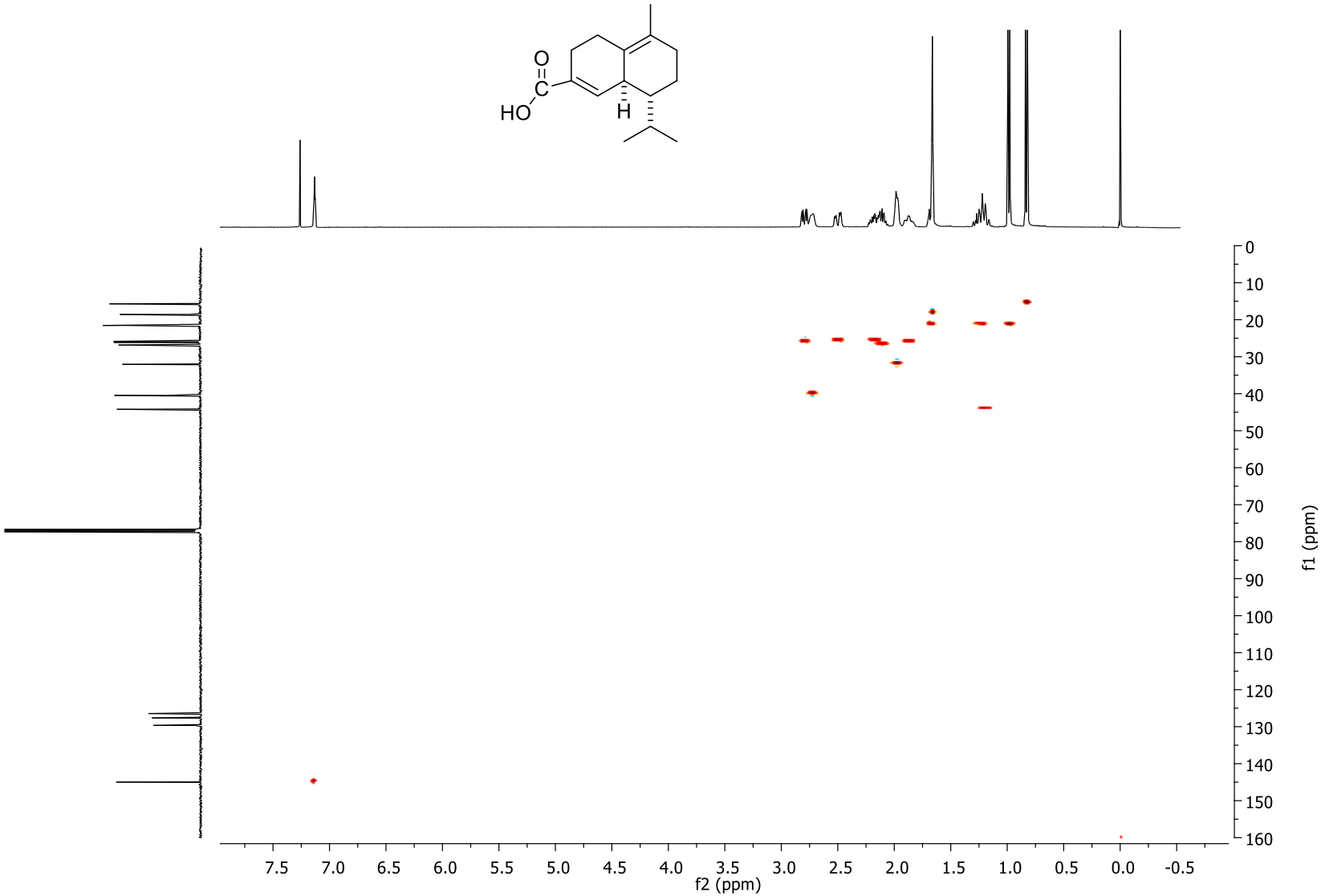

Espectro 10. HSQC del compuesto **2** ($CDCl_3$).

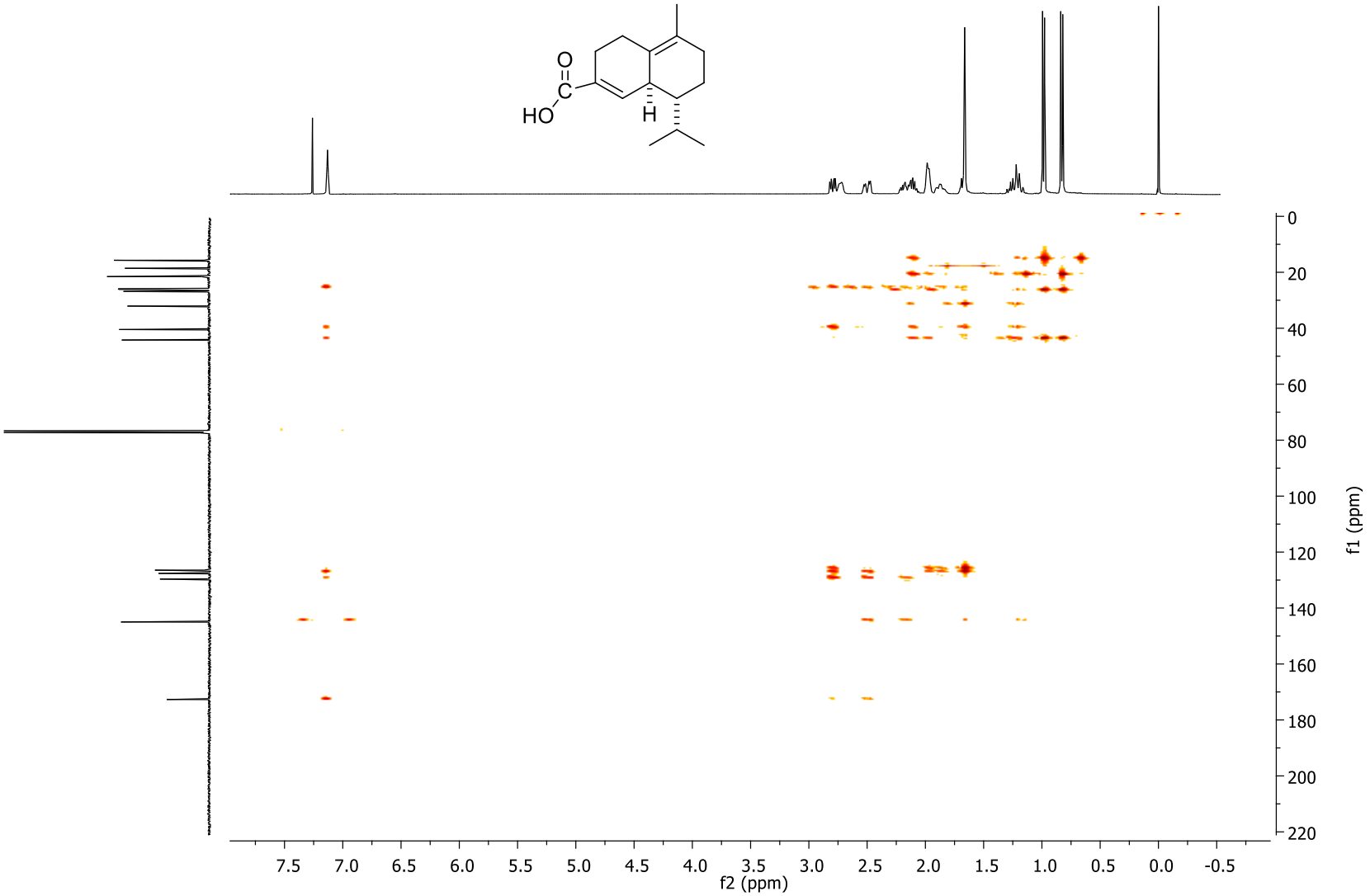

Espectro 11. HMBC del compuesto **2** ($CDCl_3$).

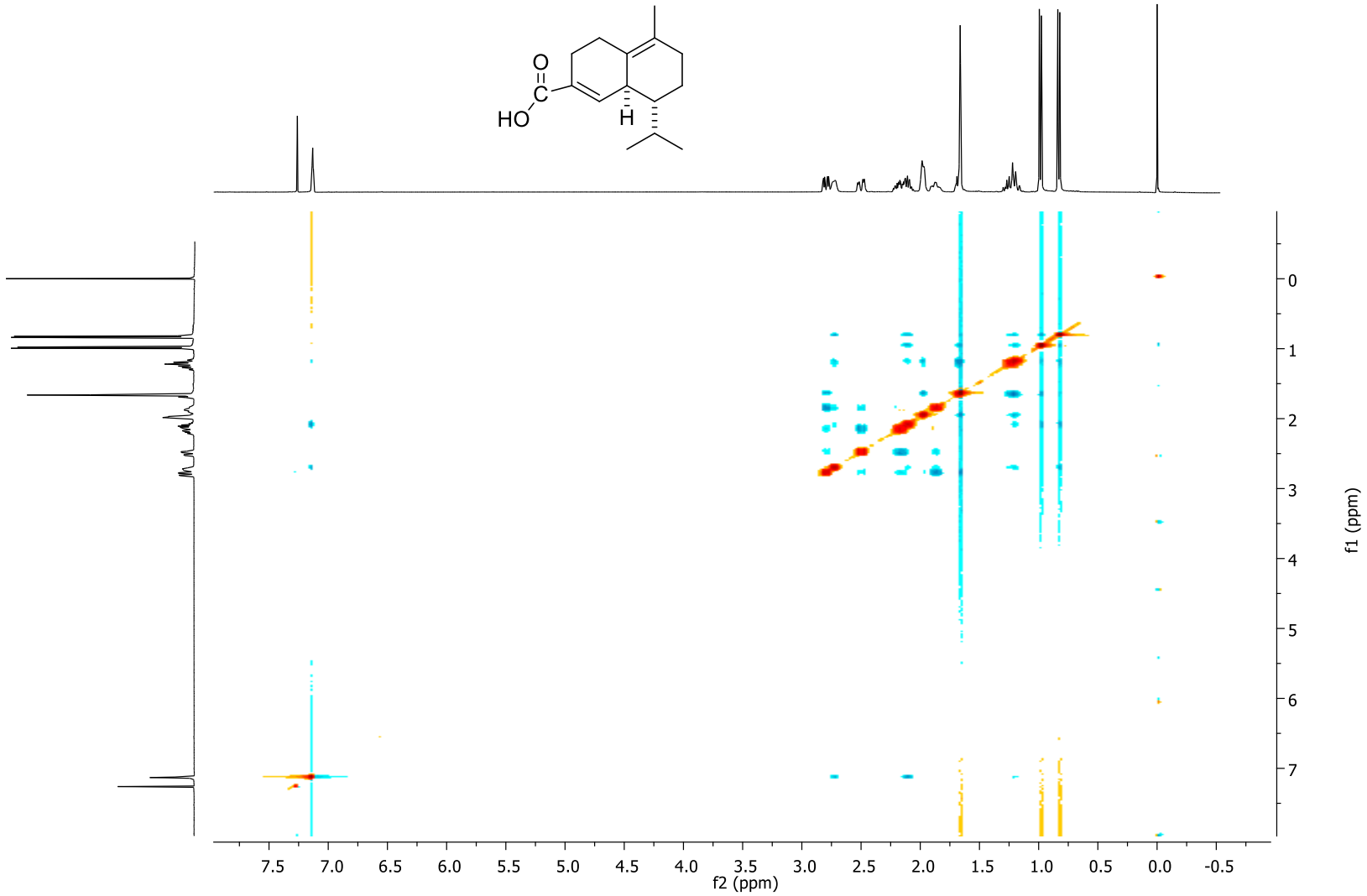

Espetro 12. NOESY del compuesto **2** ($CDCl_3$).

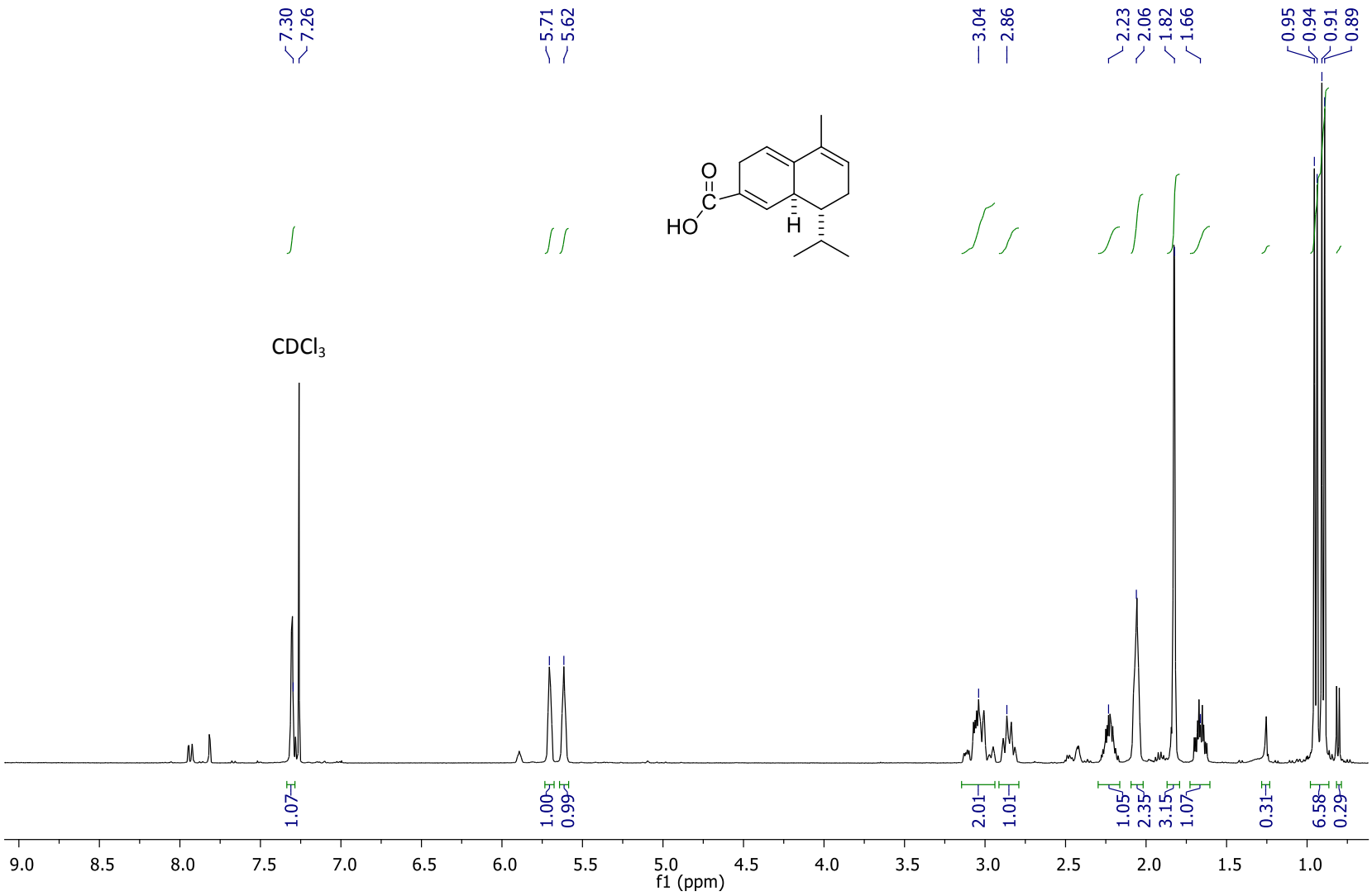

Espectro 13. RMN ^{1}H del compuesto **3** (400 MHz, $CDCl_3$).

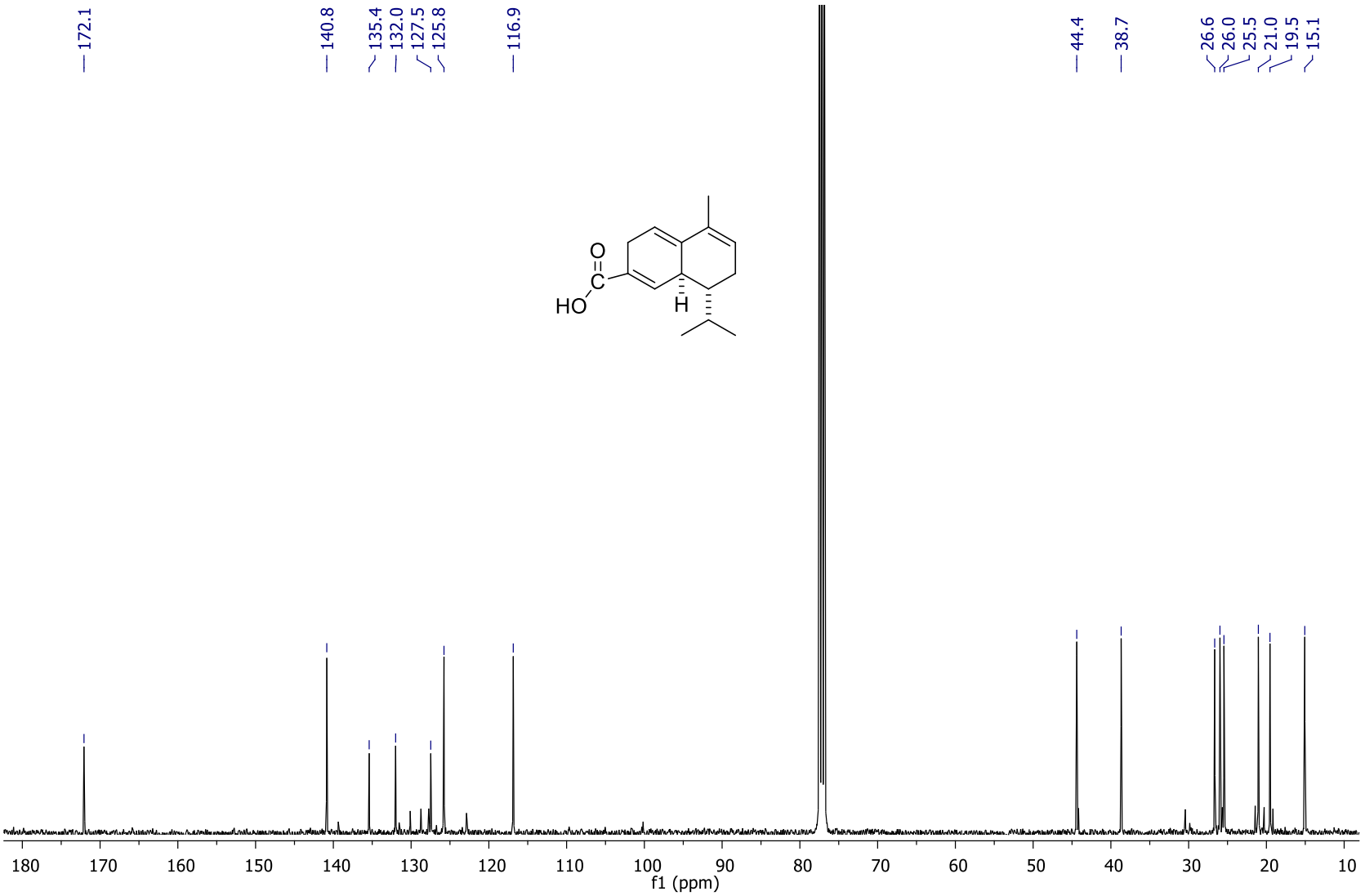

Espectro 14. RMN ^{13}C del compuesto **3** (100 MHz, $CDCl_3$).

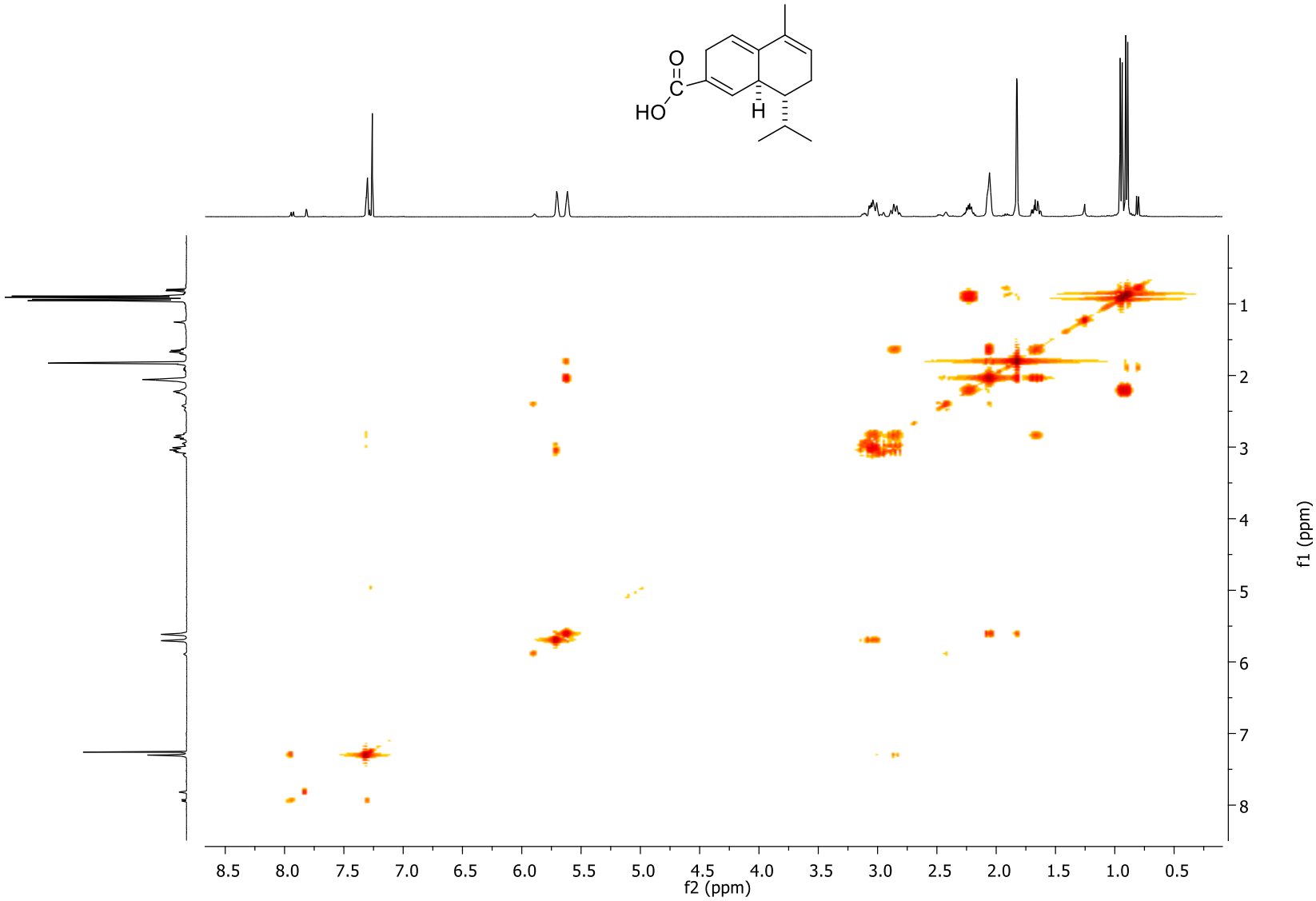

Espectro 15. COSY del compuesto **3** ($CDCl_3$).

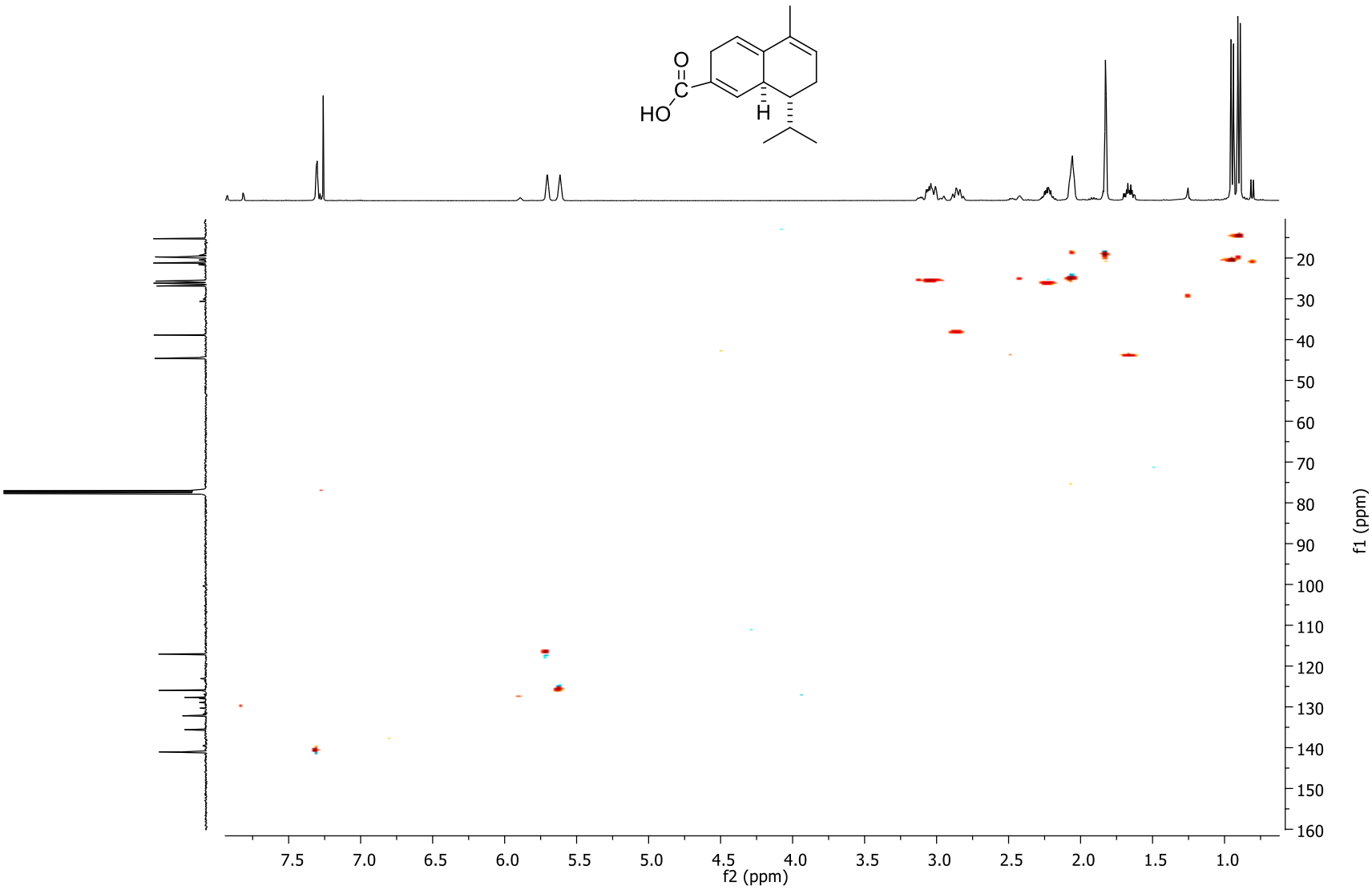

Espectro 16. HSQC del compuesto **3** ($CDCl_3$).

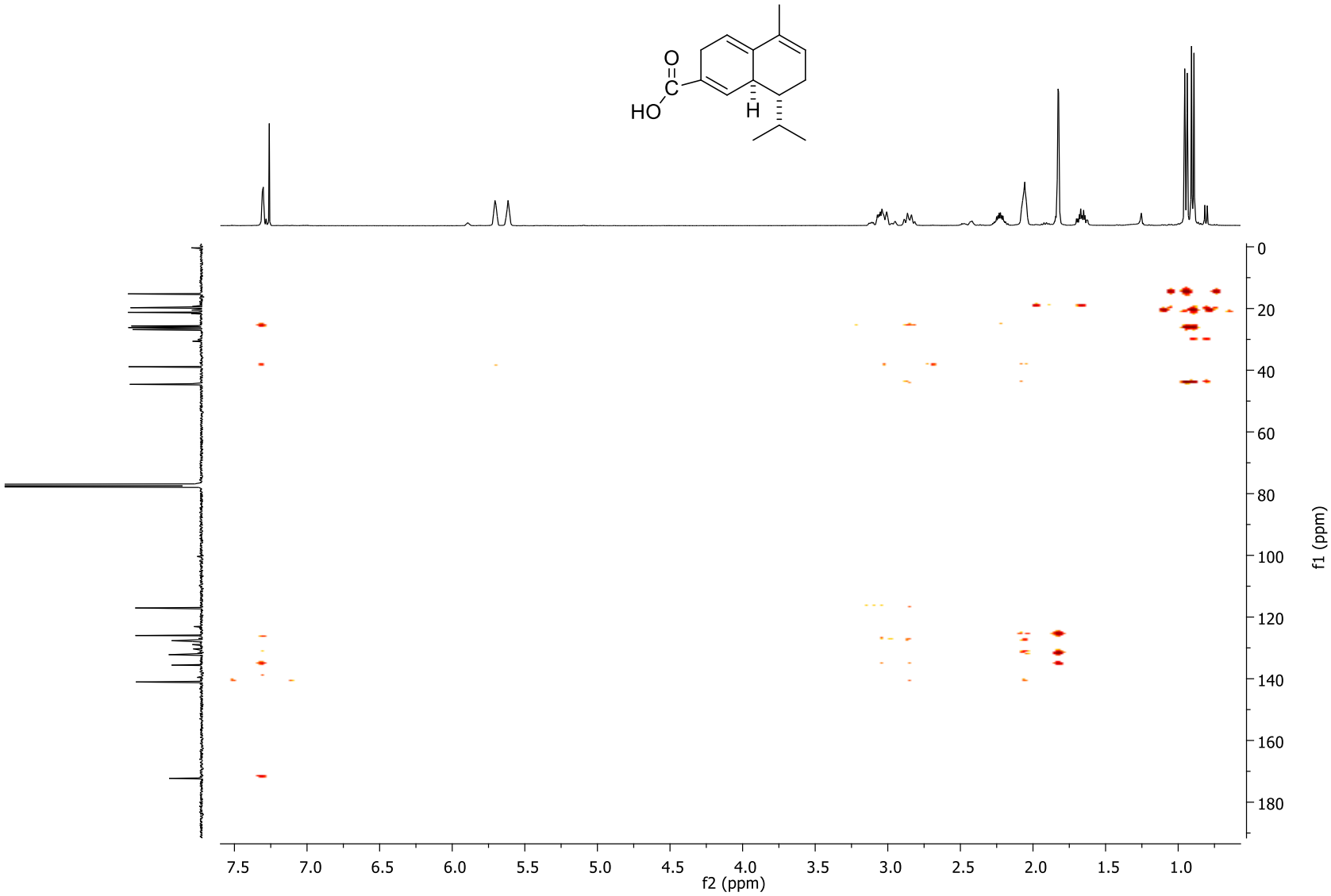

Espectro 17. HMBC del compuesto **3** ($CDCl_3$).

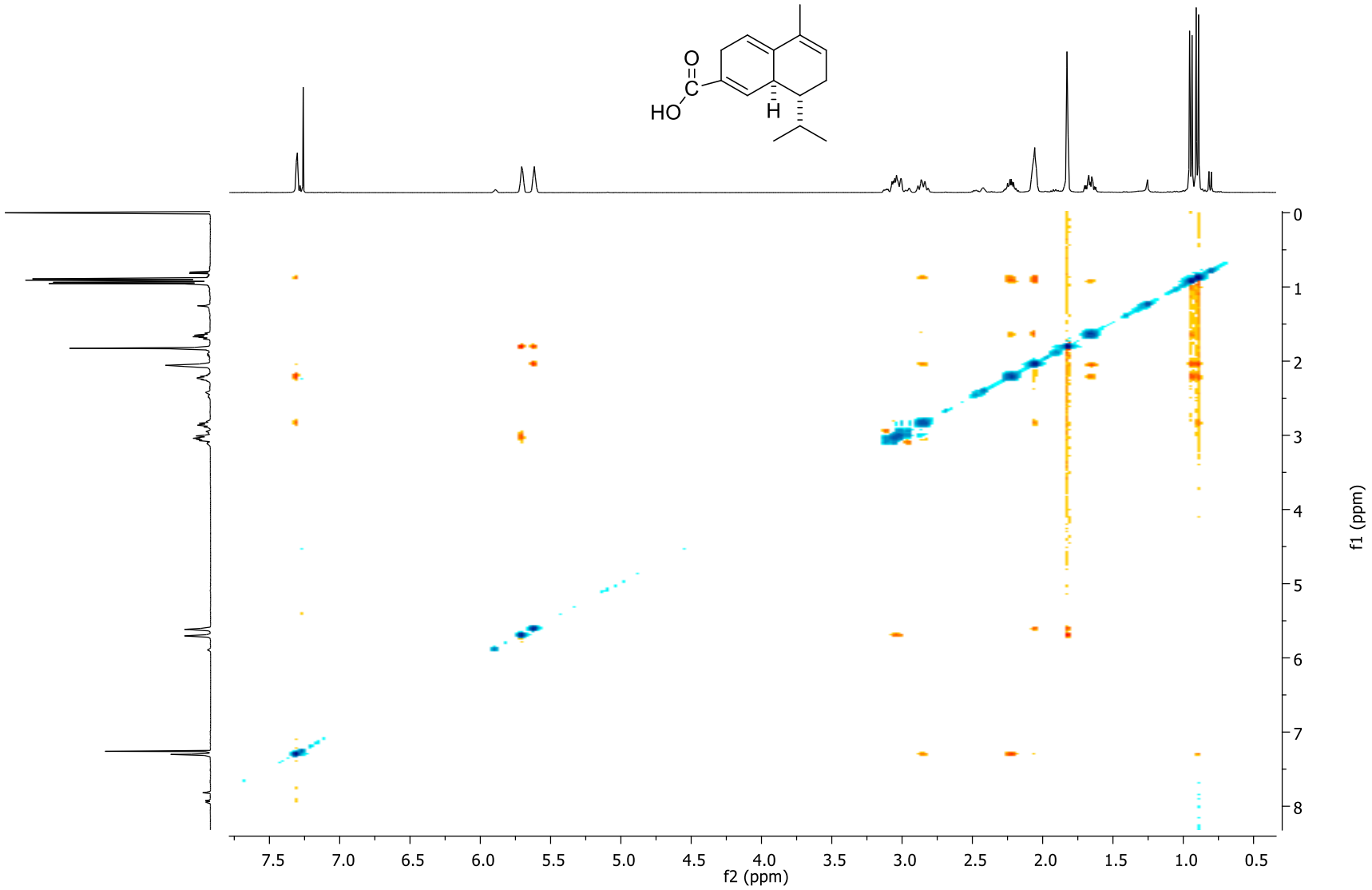

Espectro 18. NOESY del compuesto **3** ($CDCl_3$).

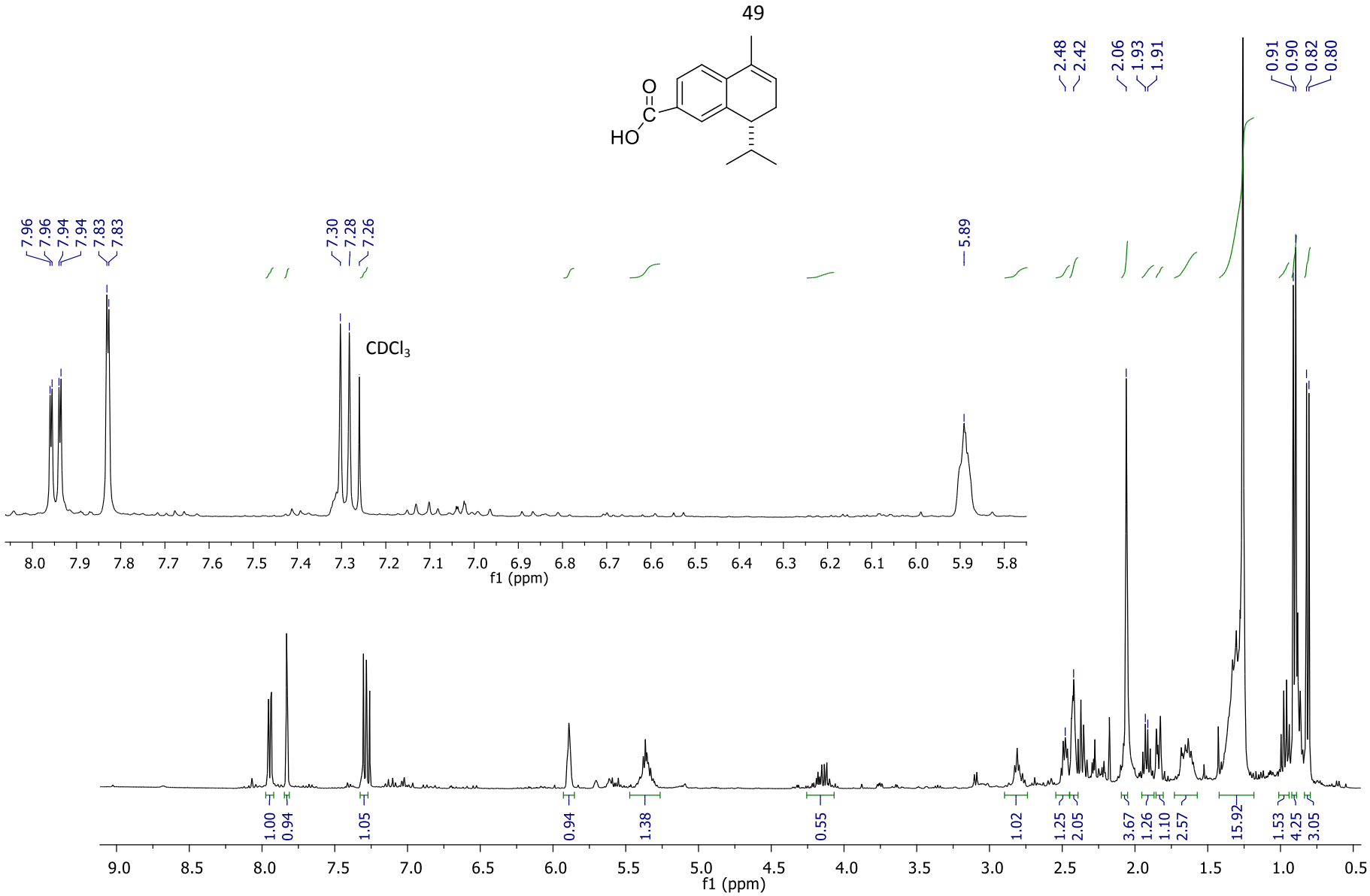

Espectro 19. RMN ^{1}H del compuesto **4** (400 MHz, $CDCl_3$).

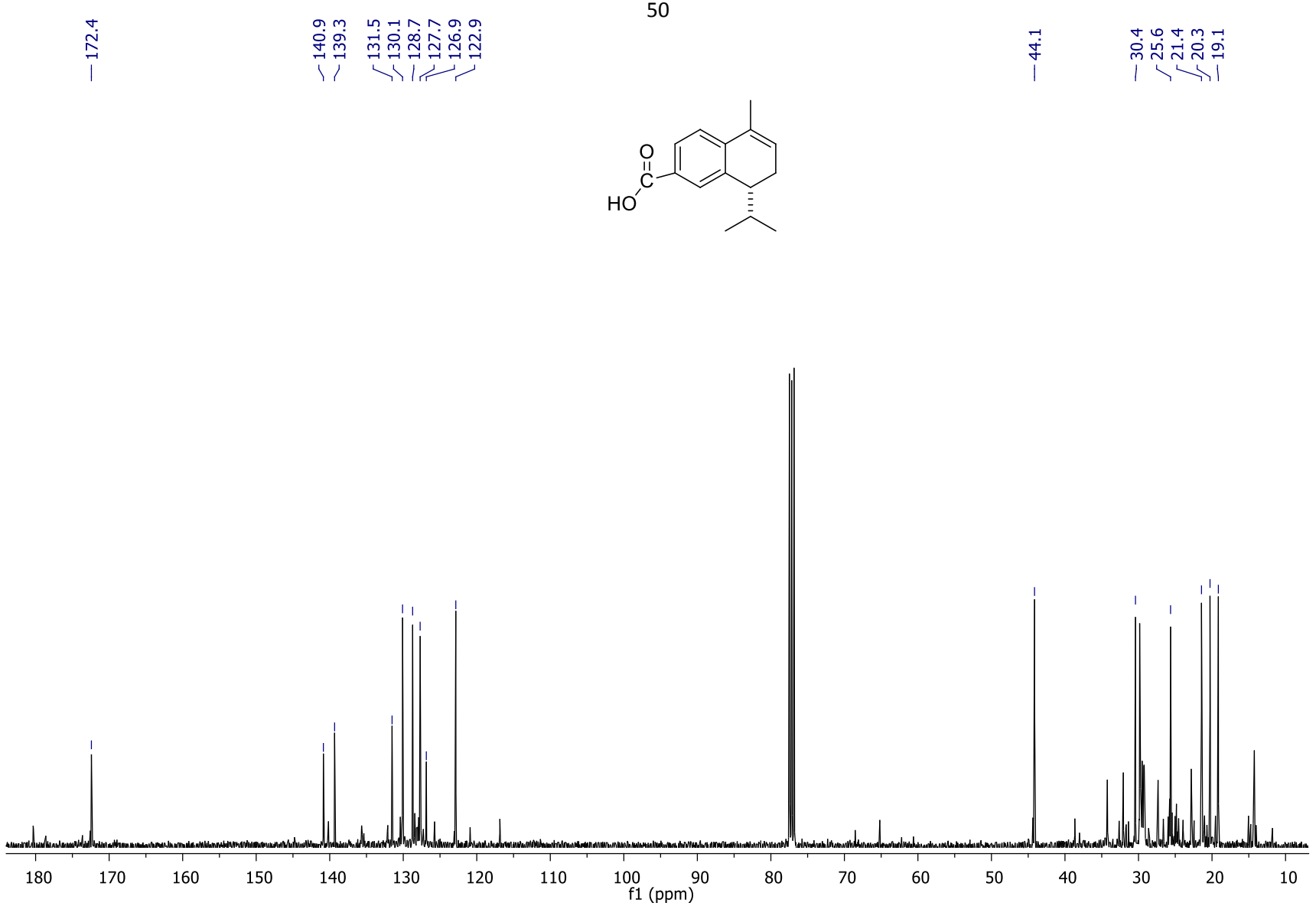

Espectro 20. RMN ^{13}C del compuesto **4** (100 MHz, $CDCl_3$).

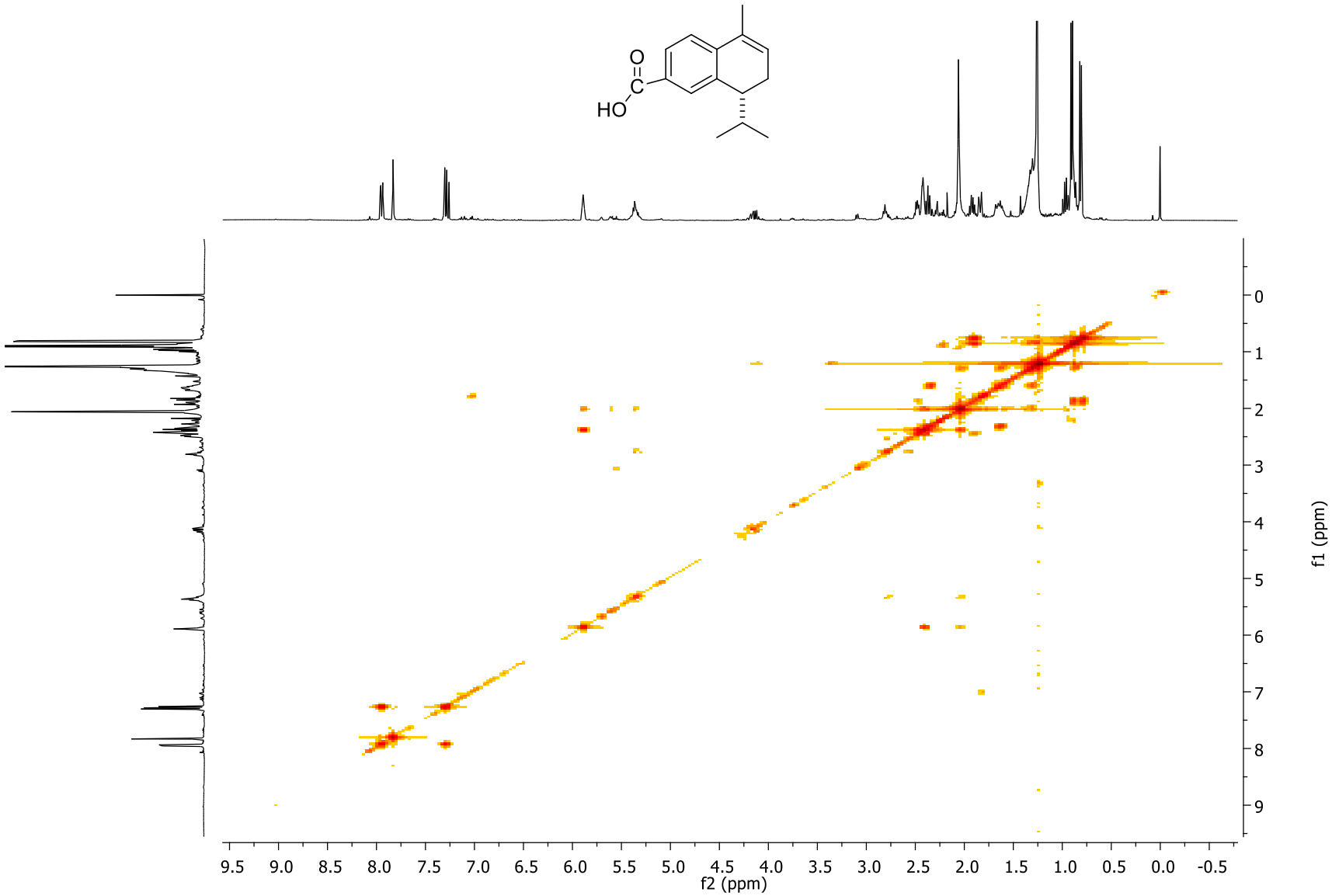

Espectro 21. COSY del compuesto **4** ($CDCl_3$).

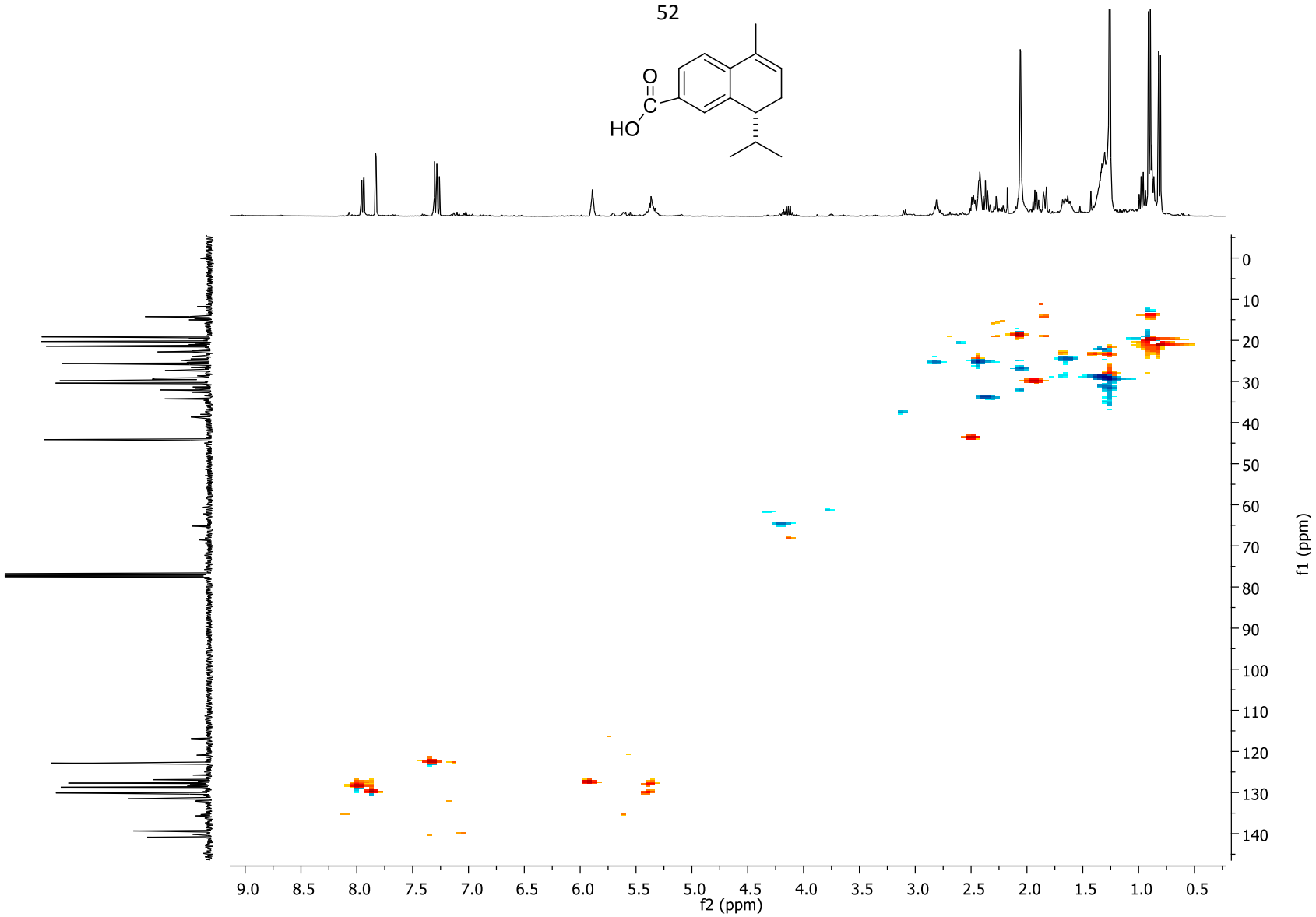

Espetro 22. HSQC del compuesto **4** ($CDCl_3$).

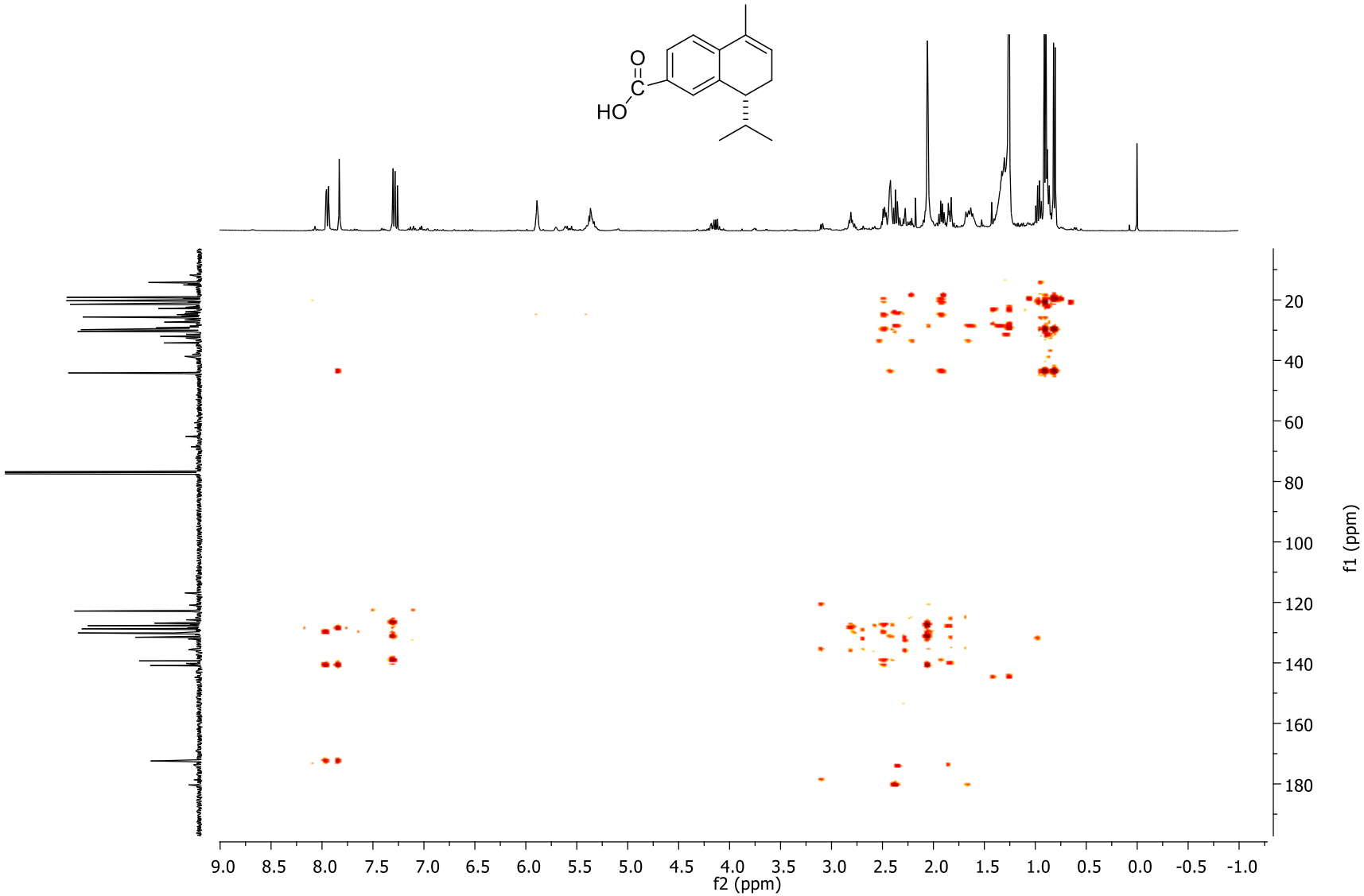

Espectro 23. HMBC del compuesto **4** ($CDCl_3$).

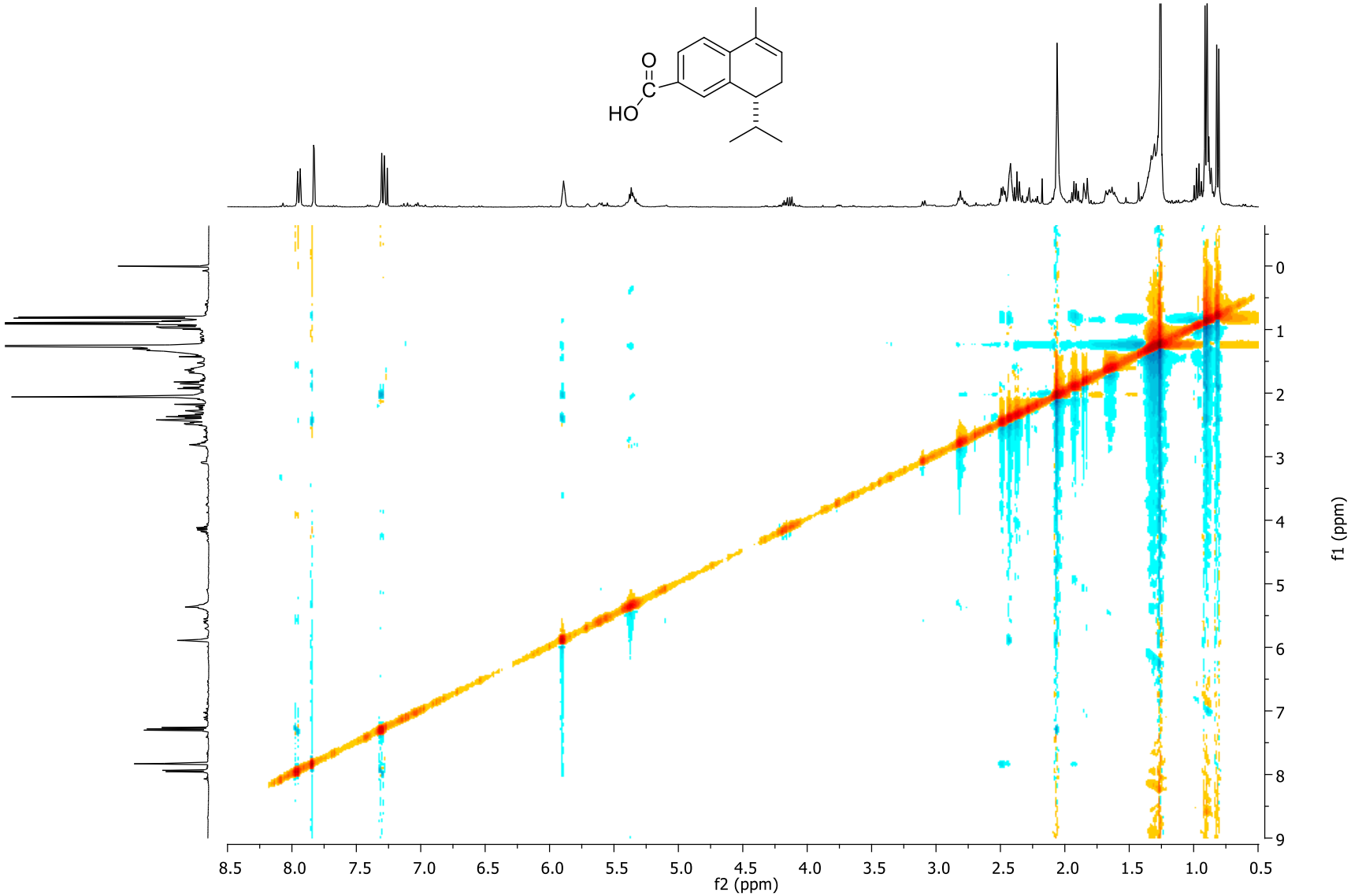

Espectro 24. NOESY del compuesto **4** ($CDCl_3$).

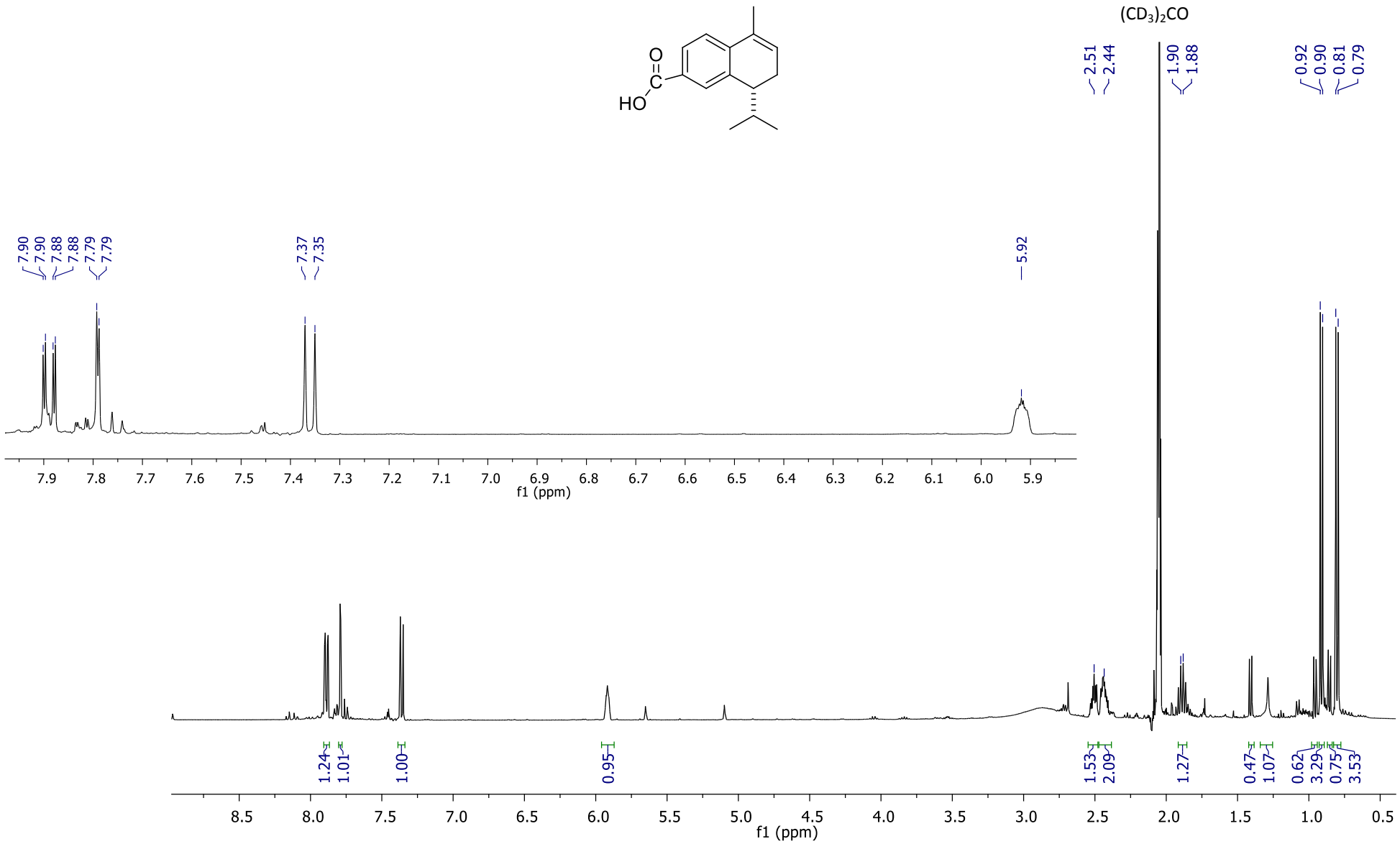

Espectro 25. RMN ^{1}H del compuesto **4** obtenido a partir de la deshidratación del compuesto **5** (400 MHz, $(CD_3)_2CO$).

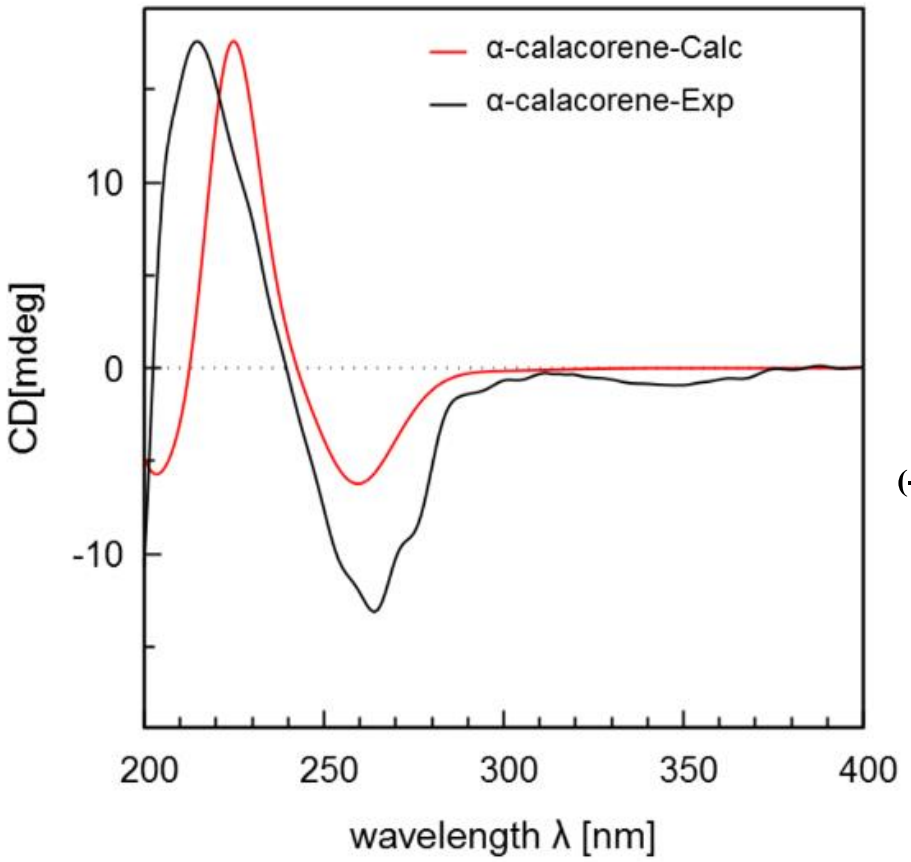

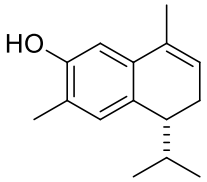

(-)-3-hydroxy-α-calacorene

Espectros de Dicroísmo Circular Electrónico experimental y calculado para el compuesto (-)-3-hidroxi-α-calacoreno

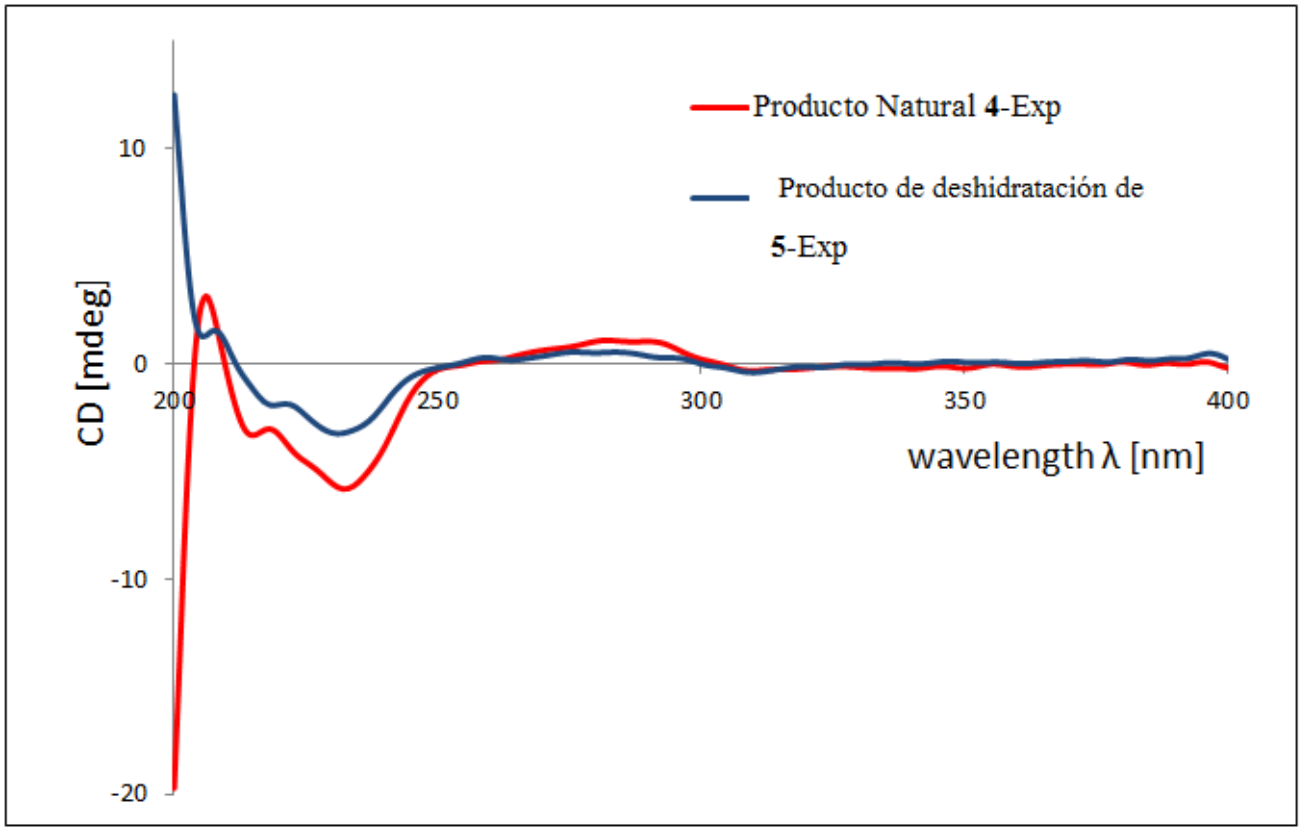

Comparación de los espectros de Dicroísmo Circular Electrónico del producto natural **4** y del producto de deshidratación de **5.**

CAPÍTULO II

Efecto de los sesquiterpenos de tipo cadinano naturales y semisintéticos obtenidos a partir de *Heterotheca inuloides* sobre las vías de sañalización de los factores de transcripción NF-κB, Nrf2 y STAT3. Evaluación de su actividad citotóxica *in vitro* sobre líneas celulares de cáncer humano

Egas, V.; Millán, E.; Collado, J. A.; Ramírez-Apan, T.; Méndez-Cuesta, C. A.; Muñoz, E.; Delgado, G.

[a]Instituto de Química, Universidad Nacional Autónoma de México, Circuito Exterior, Ciudad Universitaria, Coyoacán 04510, Mexico City, Mexico

[b]Maimonides Biomedical Research Institute of Córdoba, Reina Sofía University Hospital, Department of Cell Biology, Physiology and Immunology, University of Córdoba, Avenida Menéndez Pidal s/n, 14004, Córdoba, Spain

[c]Universidad Autónoma Metropolitana Unidad Xochimilco, Calzada del Hueso 1100, Mexico City 04960, Mexico

Manuscrito publicado en Bioorganic & Medicinal Chemistry (En prensa) DOI: http://dx.doi.org/10.1016/j.bmc.2017.03.069

Resumen

El efecto de diez sesquiterpenos de tipo cadinano aislados a partir de *H. inuloides*, sobre los factores de transcripción NF-κB, Nrf2 y STAT3, se estudió por primera vez. El principal constituyente en esta especie, el 7-hidroxi-3,4-dihidrocadaleno (**1**), mostró actividad anti-NF-κB y fue capaz de activar la ruta antioxidante del Nrf2, lo cual puede explicar las propiedades reportadas en el uso tradicional de esta planta. Además del metabolito mayoritario, otro compuesto estructuralmente similar, el 7-hidroxi-cadaleno (**2**), también mostró actividad anti-NF-κB. Por lo tanto, estos compuestos naturales se utilizaron en la preparación de un grupo de derivados semisintéticos que incluyen ésteres y carbamatos. La actividad antiproliferativa *in vitro* de estas sustancias fue

evaluada sobre seis líneas celulares de cáncer humano. Los derivados de tipo carbamato **32** y **33** mostraron una potente actividad inhibidora de la proliferación sobre células de adenocarcinoma colorrectal (IC_{50} 0.03±0.01 μM y 3.88±0.5μM, respectivamente) y una selectividad notable sobre células cancerosas. Entre los derivados de tipo éster, el compuesto **13** desarrolló una mayor actividad en la inhibición del NF-κB y activación del Nrf2, que el producto natural originario 7-hidroxi-3,4-dihydrocadaleno (**1**). Este compuesto también disminuye los niveles de fosfo-IκBα, un complejo proteínico involucrado en la activación de la vía de señalización del NF-κB. Estudios teóricos de reconocimiento molecular sugieren que todos los compuestos activos interactúan con los sitios de activación de la subunidad IKKβ del complejo IKK, el cual es responsable de la fosforilación del IκBα.

Abstract

The effect of ten natural cadinane sesquiterpenoids isolated from *Heterotheca inuloides*, on NF-κB, Nrf2 and STAT3 transcription factors, was studied for the first time. The main constituent in this species, 7-hydroxy-3,4-dihydrocadalene (**1**), showed anti-NF-κB activity and activated the antioxidant Nrf2 pathway, which may explain the properties reported for the traditional use of the plant. In addition to the main metabolite, a structurally similar compound, 7-hydroxy-cadalene (**2**), also displayed anti-NF-κB activity. Thus, both natural compounds were used as templates for the preparation of a novel semi-synthetic derivative set, including esters and carbamates, which were evaluated for potential in vitro antiproliferative activity against six human cancer cell lines. Carbamate derivatives **32** and **33** were found to exhibit potent activity against human colorectal adenocarcinoma and showed important selectivity on cancer cells. Among ester derivatives, compound **13** was determined to be more potent NF-κB inhibitor and Nrf2 activator than its parent 7-hydroxy-3,4-dihydrocadalene (**1**). Furthermore, this compound decreases levels of phospho-IκBα, a protein complex involved in the NF-κB activation pathway. Molecular simulations suggest that all active compounds interact with the activation loop of the IKKβ subunit at the IKK complex, which is the responsible of IκBα phosphorylation.

Key words: *Heterotheca inuloides*, cadinanes, transcription factors, semisynthesis, antiproliferative activity.

1. Introduction

The relationship between inflammation and the development of cancer is now widely accepted. Although this connection could be complicated, evidence suggests that long-standing inflammation predisposes one to cancer.[1,2] Furthermore, the molecular pathways that link inflammation and cancer are now known. These extrinsic and intrinsic pathways converge resulting in the activation of transcription factors in tumor cells, mainly nuclear factor-κB (NF-κB), signal transducer and activator of transcription 3 (STAT3) and hypoxia-inducible factor 1α (HIF1α).[3] Activation of NF-κB in inflammatory cells leads to the production of secreted factors that enhance the growth, survival and vascularization of carcinoma cells.[4,5] STAT3 is considered one of the most promising new targets for cancer therapy. Its activation in tumor cells and the tumor microenvironment promotes cell proliferation, survival and invasion, and facilitates cancer development through inflammation.[6] Another transcription factor known to play an important protective role in suppressing oxidative stress and inhibiting carcinogenesis is the Nuclear factor-erythroid 2 p45-related factor 2 (Nrf2). Activation of Nrf2 inhibits inflammation and facilitates the adaptation by upregulating the repair and degradation of damaged macromolecules.[7,8] The aforementioned knowledge facilitates the research and development of substances that target the inflammatory components of the cancer microenvironment. Indeed, several experimental, epidemiologic, and clinical studies suggest that anti-inflammatory agents are promising as cancer therapeutics.[9,10]

Naturally occurring compounds are a representative group of substances displaying chemopreventive effects, many of them resulting from anti-inflammatory properties.[11] It has been demonstrated that some natural products could exert regulation at a transcriptional level in the molecular mechanisms involved in inflammation and cancer, so they represent an interesting source of potentially useful agents for prevention and therapy.[12] Despite the biological activities of many natural products being broadly studied, the identification of the cellular targets involved in these activities represents a challenge that could explain the traditional uses of several species in folk medicine.[13]

Cadinane-type sesquiterpenoids are secondary metabolites widely distributed in nature and are considered representative constituents of the species *Heterotheca inuloides* (Mexican arnica). This plant is highly regarded in Mexican traditional medicine mainly for the treatment of inflammatory ailments, motivating investigations of its chemical constituents and their biological activities.[14] These sesquiterpenoids have been found to possess anti-

inflammatory properties,[15,16] however, the molecular mechanism associated with their activity has not been investigated.

Here we report the evaluation of ten natural cadinanes on well-defined targets involved in inflammation and carcinogenesis, and the semi-synthesis of a derivative set starting from the active compounds. The cytotoxic effect of derivatives was tested on six human cancer cell lines and correlated with the inhibition or activation of the NF-κB, STAT3, and Nrf2 pathways. To understand how these compounds inhibit NF-κB, computational docking was performed using the crystal structure of a protein involved in the NF-κB activation pathway.

2. Results and discussion

2.1 Isolation and initial biological screening on well-defined targets involved in inflammation and carcinogenesis

From the aerial parts of *H.* inuloides, a total of ten sesquiterpene-type metabolites displaying anti-inflammatory activities,[15,16] were obtained (Figure 1). 7-Hydroxy-3,4-dihydrocadalene (**1**) and 7-hydroxy-cadalene (**2**) were re-isolated by conventional chromatographic methods (experimental section), and compounds **1-8** were obtained in previous studies carried out in our laboratory.[16] The isolated compounds were tested in NF-κB, Nrf2 and STAT3-dependent luciferase gene reporter assays, where the amount of the luciferase gene product reflects the extent of transcription factor activation.

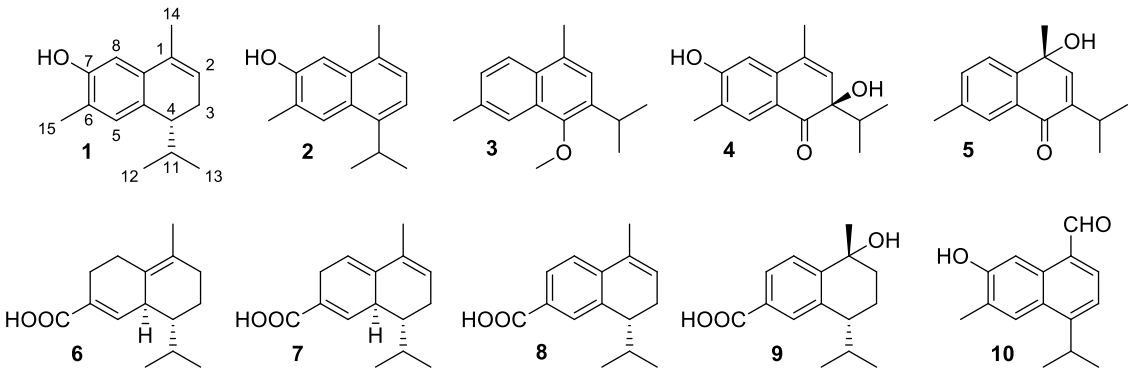

Figure 1. Structure of cadinane type sesquiterpenoids isolated from *H. inuloides.*

Interestingly, we found that although compounds **1-10** have a high structural similarity, only two of them showed activity on the evaluated targets, evidencing their high selectivity (Table 1). 7-Hydroxy-3,4-dihydrocadalene (**1**) and 7-hydroxy-cadalene (**2**), showed anti-NF-κB activities, and 7-hydroxy-3,4-dihydrocadalene was also able to activate antioxidant Nrf2 pathway. All compounds were ineffective as STAT3 inhibitors. These results could explain the ancestral use of *H. inuloides* in Mexican folk medicine, since both NF-κB and Nrf2 transcription factors regulate inflammatory processes that are the most common conditions for which this plant is largely used. Furthermore, 7-hydroxy-3,4-dihydrocadalene (**1**) is the main constituent in this species, so it might significantly contribute to the anti-inflammatory activity observed for its extracts. Our observation confirms previous studies demonstrating that NF-κB

inhibition is one of the most important mechanisms exerted by many natural products with therapeutic and preventive effects.[17]

2.2 Semi-synthesis, biological evaluations and molecular docking

Metabolites **1** and **2** showed positive activity on the primary screening and were selected as scaffolds for the preparation of a novel semi-synthetic derivative set by simple reactions where the existing functional group could be manipulated to afford additional structures. The reactive phenol was thus transformed to the corresponding benzoates having electron donating or electron withdrawing substituents in *meta* and *para* positions (Scheme 1). In the course of generating novel structures, two carbamate derivatives were obtained by reaction of chosen natural products with phenyl isocyanate (Scheme 1).

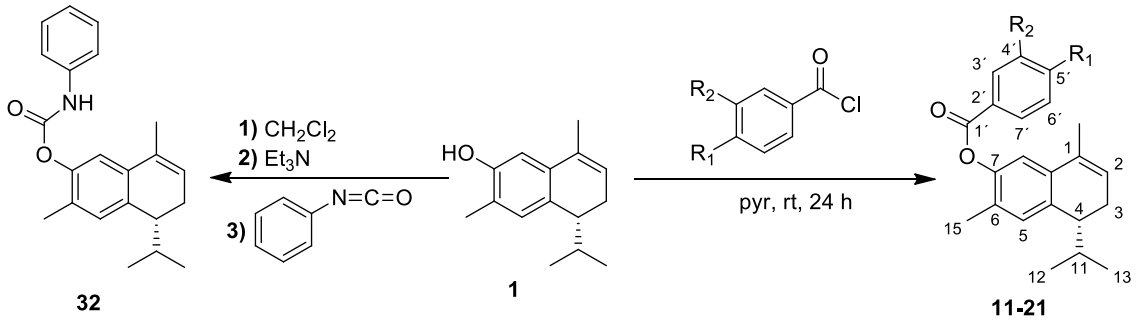

Compound	R_1	R_2
11	H	H
12	Cl	H
13	CH_3	H
14	OCH_3	H
15	CF_3	H
16	NO_2	H
17	H	Cl
18	H	CH_3
19	H	OCH_3
20	H	CF_3
21	H	NO_2

Scheme 1. Semi-synthesis of ester and carbamate derivatives prepared from cadinane-type natural products.

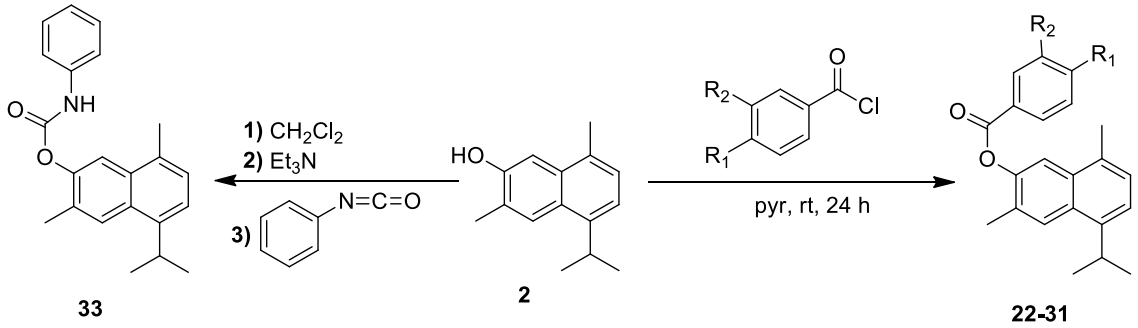

Compound	R_1	R_2
22	H	H
23	Cl	H
24	CH_3	H
25	OCH_3	H
26	CF_3	H
27	NO_2	H
28	H	CH_3
29	H	OCH_3
30	H	CF_3
31	H	Cl

Scheme 1. Continuation

All semi-synthetic compounds were then subjected to a new biological screening on the selected targets to analyze how structural modifications undertaken might have affected their activity. Table 2 summarizes the results of this primary screening along with the cytotoxic effect of derivatives on six human cancer cell lines. The anti-NF-κB activity previously observed for 7-hydroxy-3,4-dihydrocadalene (**1**) was improved in compound **13** and totally lost in all its semi-synthetic derivatives. Nrf2 activating effect improvement was detected in derivatives **11**, **13** and **16**, indicating that some structural modifications on the benzoyl group are tolerated. The presence of methyl- and nitro-groups on the benzoyl moiety seems to be advantageous, and it was clear that the *para*-position is preferred for the interaction with the receptor since a change in the location of these substituents results in loss of activity. This effect was also observed on the cytotoxic properties, which were generally lower for the *meta*- derivatives.

Among ester derivatives prepared from 7-hydroxy-3,4-dihydrocadalene (**1**), compound **13** showed the highest cytotoxicity over four of the six cancer cell lines evaluated with an IC_{50} of 30.94±2.2 μM on leukemia. This indicates that its activity could be related to the inhibition of the NF-κB transcription factor, as it has been demonstrated that its signaling pathway is active in cancer cells, and that some anticancer agents that have shown anti-NF-κB activity may exert their effects by lessening a proliferative, antiapoptotic or inflammatory activity of NF-κB.[17]All the ester derivatives obtained from 7-hydroxy-cadalene (**2**) lost their activity on NF-κB and Nrf2 pathways. Although compound **27** showed good cytotoxicity over all cell lines with the highest efficacy on leukemia (IC_{50}=2.28±0.2 μM), its ineffectiveness as NF-κB inhibitor makes it less interesting, since it is desirable that new potential anticancer compounds affect a particular target or pathway involved in the process of malignancy.[18] The potential of compounds showing NF-κB inhibition and Nrf2 activation properties on the primary screening were then compared through dose-response experiments where luciferase activities were measured on cells pre-treated with increasing concentrations of the substances (Figure 2). The most active compound among those showing anti-NF-κB activity was 7-hydroxy-cadalene (**2**) with an IC_{50} of 16.5±2.2 μM, followed by compound **13** and 7-hydroxy-3,4-dihydrocadalene (**1**) with an IC_{50} of 47.1±2.9 μM and 72.0±3.4 μM, respectively. Decrease on luciferase activity produced by these compounds was not a consequence of its cytotoxicity over the employed cell line.

Through kinetic assays, we determined that these compounds are not cytotoxic at the concentrations at which the anti-NF-κB activities were evaluated.

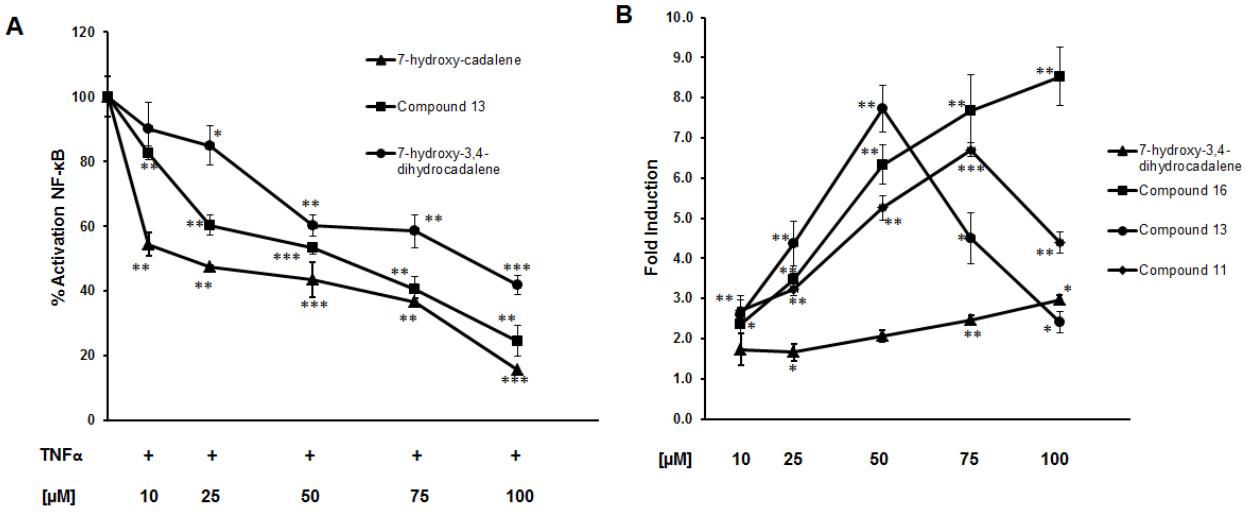

Figure 2. Effects of *H. inuloides* compounds and some semisynthetic derivatives on NF-κB and Nrf2 activation. (A) NIH-3T3-KBF-Luc cells (fibroblasts) were pre-treated with increasing concentrations of the compounds for 15 min and then stimulated with TNFα for 6 h, after which the luciferase activities were measured in the cell lysates and expressed as percentage of activation considering 100% the value of TNFα-induced NF-κB activation. (B) HaCaT-ARE-Luc cells (keratinocytes) were treated with increasing concentrations of the compounds for 6 h. Luciferase activity was measured in the cell lysates and expressed as fold induction over basal levels.

Compound **13** was clearly the best promoter of Nrf2 activation, showing its optimum effect at doses lower than 50 μM because its activity decreases at higher concentrations. As Nrf2 transcription factor regulates the cellular redox status, some substances that behave as oxidizing agents could indirectly activate the Nrf2 pathway. For this reason, we decide to find out whether the activating effect on the Nrf2 pathway exerted by compound **13** is a simple consequence of its cell oxidant effect. Hence, the intracellular accumulation of reactive oxygen species (ROS) was monitored on keratinocytes pre-incubated with increasing concentrations of compound **13**. Figure 3 shows the fluorometric detection of ROS using the free radical sensor CM-H2DCFDA (see Experimental section for details). The results revealed that compound **13** does not induce the production of ROS; on the contrary, it reduces its concentration induced by *tert*-butyl-hydroperoxide (TBHP) similar to the antioxidant molecule *N*-acetylcysteine (NAC).

ROS production was quantified by changes in fluorescence through imaging analysis of the total green object integrated intensity (Figure 4).

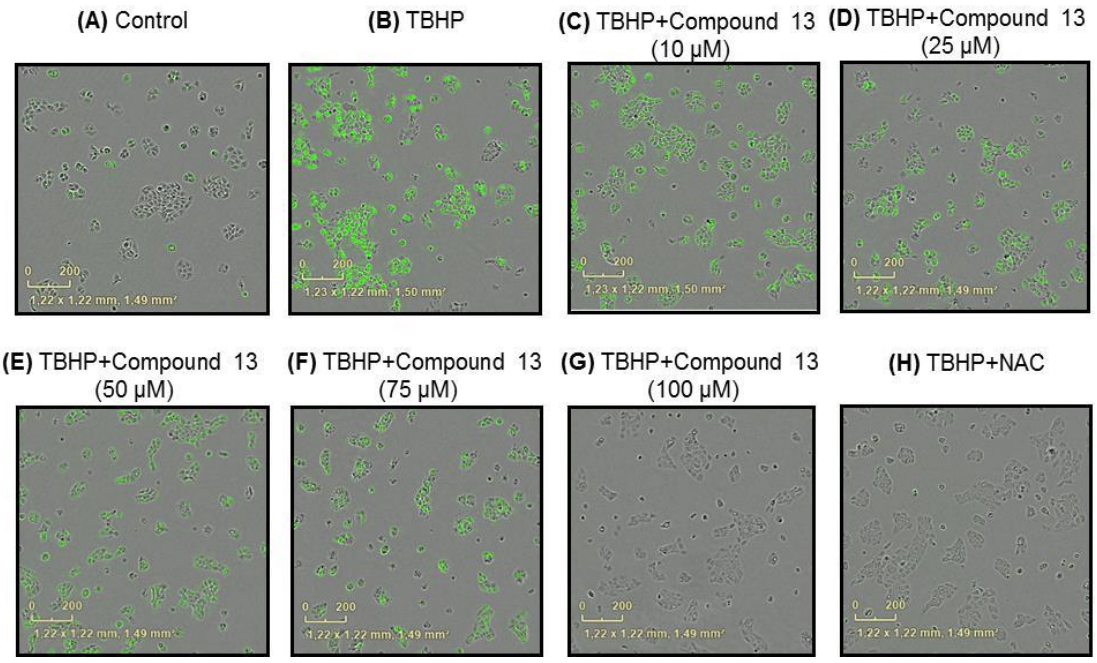

Figure 3. Fluorometric detection of ROS using the free radical sensor CM-H2DCFDA on HaCaT cell line. (A) Cells over basal conditions. (B) Cells treated with the oxidant compound TBHP (0.4 mM). (C-G) Cells pre-incubated with increasing concentration of compound **13** and then treated with TBHP (0.4 mM). (H) Cells pre-incubated with the antioxidant NAC (15 mM) and then treated with TBHP (0.4 mM).

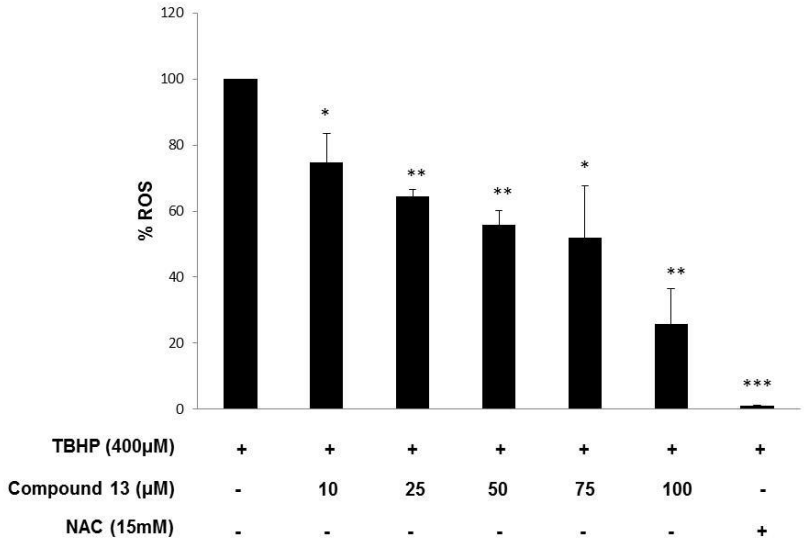

Figure 4. Compound **13** reduces intracellular accumulation of ROS. HaCaT cells were treated with the indicated doses of compound **13** and ROS were measured by changes in fluorescence through imaging analysis of the total green object integrated intensity and expressed as percentage of ROS considering 100% the value of TBHP induction. The results were compared with the effect of the antioxidant NAC.

Considering that the signaling pathways involved in the activation of the studied transcription factors represent a focus for pharmacological intervention in situations of chronic inflammation or in cancer, we can say that among ester derivatives, compound **13** showed the best biological profile in vitro having three important properties. It was able to activate the Nrf2 pathway, neutralize ROS production, and inhibit the transcription factor NF-κB, which could generally be considered as a beneficial consequence for cells. For these reasons we decided to evaluate its possible mechanism of action by evaluating its effect over phospho-IκBα, a protein complex involved in the NF-κB activation pathway. In most cells NF-κB dimers such as p50/RelA are retained in the cytoplasm by interaction with an independent IκB protein (often IκBα). Activation of NF-κB dimers is the result of the phosphorylation, ubiquitination and degradation of the IκB inhibitor mediated by the IKK complex, which enables the NF-κB dimers to enter the nucleus and activate specific target gene expression.[19] Therefore, western blot analysis was carried out to detect levels of endogenous protein expression on cells treated with compound **13**. The results revealed that levels of phospho-IκBα

decreased on cells incubated with this semi-synthetic derivative and then treated with TNFα to induce IκBα phosphorylation (Figure 5). The above observations mean that compound **13** prevents the phosphorylation and degradation of the cytoplasmic IκBα protein. Many substances have been described that inhibit IκB phosphorylation driving to block proteasomal degradation of IκB and allowing it to sequester NF-κB in the cytoplasm in an inactivated state.[18] It is well known that inhibition of NF-κB activation can occur by several mechanisms at different levels of the pathway. One of them is the inhibition of IκB phosphorylation by agents that act directly at the IKK complex.[17] This complex is activated by phosphorylation of its main subunit, IKKβ, in the activation loop at two sites, Ser-177 and Ser-181.[20] To clarify if it is possible that compound **13** targets the IKK complex, we performed molecular docking studies to identify important binding modes. Analyses showed that ATP-binding pockets of the IKKβ subunit are occupied by compound **13** in a similar fashion as the staurosporine analog K252a, a potent kinase inhibitor which has been crystalized bound to the IKKβ subunit [21] (Figure 6). These results could explain the inhibitory activity of compound **13**, since it was positioned at the activation loop in the protomer B (residues 166-194), which assumes a conformation characteristic of an active kinase.[21] Those residues are close to the key residues (Ser-177 and Ser-181) for the phosphorylation and subsequent activation of the IKK complex. In this way, the complex protein-compound **13** destabilizes the correct folding of the activation loop. The inactive form IKK complex cannot phosphorylate IκB inhibitor, thus preventing NF-κB release.

Additionally, the molecular structures of 7-hydroxy-cadalene (**2**) and 7-hydroxy-3,4-dihydrocadalene (**1**), both showing anti-NF-κB activities, were docked at the IKKβ subunit. The results revealed that these compounds not only occupy ATP-binding pockets in IKKβ subunit but also make hydrogen bond contact from the 7-hydroxyl to the carbonyl oxygen Cys-97 as well as to the amine on Cys-99 (Figure 7). These analyses allowed us to propose, in a preliminary way, that similar binding modes exist in the staurosporine analog K252a and cadinane sesquiterpenoids. Moreover, the protein-ligand interactions between IKKβ and staurosporine analog K252a, found by computational analyses applying our model, were similar to those reported for the co-crystallized form (Figure S44, supporting information).

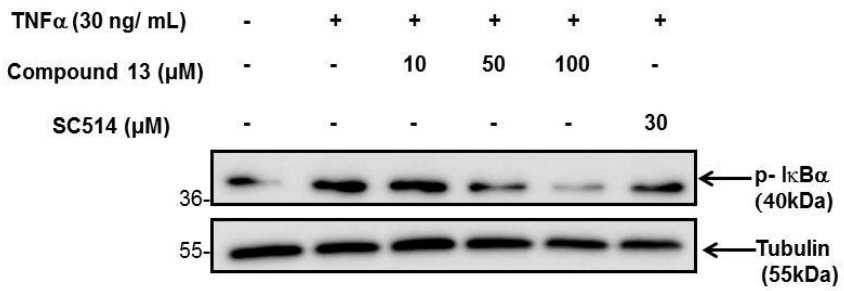

Figure 5. Compound **13** inhibits phospho-IκBα protein expression. NIH-3T3-KBF-Luc cells were incubated with either increasing concentrations of compound **13** or with the IKKβ inhibitor SC514 during 15 min and then stimulated with TNFα for 20 min. Total cell content was extracted and analyzed to detect the level of the phospho-IκBα protein expression by western blot.

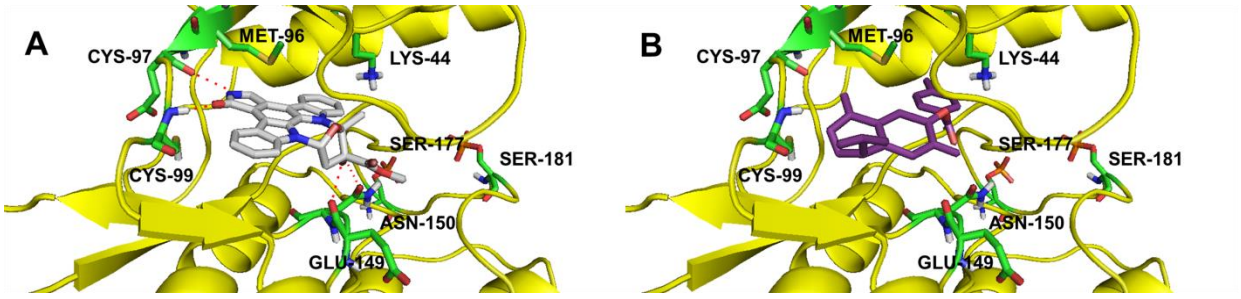

Figure 6. Docking of staurosporine analog K252 and compound **13** at the protomer B of the human IKKβ crystal structure (PDB ID: 4kik). (A) Staurosporine analog K252 interacts with the ATP-binding pockets through hydrogen bonds with the amino acids Cys-97, Cys-99, Glu-149 and Asn-150 (B) Compound **13** interacts with the ATP-binding pockets by Van der Waals forces (ΔG = -9.43 Kcal/mol).

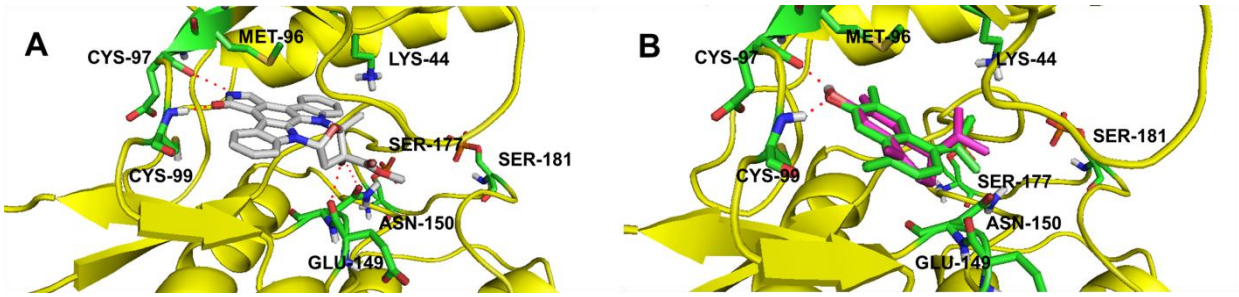

Figure 7. Docking of staurosporine analog K252, 7-hydroxy-3,4-dihydrocadalene and 7-hydroxy-cadalene at the protomer B of the human IKKβ crystal structure (PDB ID: 4kik). (A) Staurosporine analog K252 interacts with the ATP-binding pockets through hydrogen bonds with the amino acids Cys-97, Cys-99, Glu-149 and Asn-150 (B) 7-hydroxy-3,4-dihydrocadalene (pink) and 7-hydroxy-cadalene (green) interact with the ATP-binding pockets; the 7-hydroxyl group makes hydrogen bond interaction with the residue Cys-97 and Cys-99.

Carbamate derivatives **32** and **33** were the most cytotoxic substances on human colorectal adenocarcinoma with an IC_{50} of 0.035±0.01 µM and 3.88±0.5 µM, respectively (Table 2). Considering that cytotoxicity does not define a specific cellular death mechanism and that compounds **32** and **33** were not effective on NF-κB nor STAT3 inhibition, we decided to evaluate its cytotoxicity on a primary cell culture from human oral tissue (gingival fibroblast) to clarify whether these compounds could be selective against cancer cells or may exert important cytotoxic effects over non-tumorigenic cells. The observed results revealed that compound **32** showed a 38.24±1.7% of inhibition of cell proliferation at a concentration of 50 µM, indicating a low toxicity over healthy cells. Moreover, at this concentration compound **32** produces a 92% of inhibition of cell proliferation on human colorectal adenocarcinoma (Table 2). Although compound **33** was less potent than **32** on inhibition of human colorectal adenocarcinoma cell proliferation, it was not cytotoxic on gingival fibroblast, which makes it interesting in terms of selectivity. Taken together, the results suggest that these carbamate-type derivatives could be exerting an important cytotoxic effect on cancer cells through a mechanism involving different targets from those evaluated. A variety of mechanisms of cell death have been demonstrated for compounds containing the carbamate functionality. For instance, Entinostat, a synthetic benzamide derivative containing a pyridylmethyl carbamate functionality acts as an antitumor agent through

histone deacetylase inhibition,[22] and Mitomycin C, a natural chemotherapeutic agent in the treatment of several types of cancer, interacts with ribosomal RNA producing inhibition of protein translation.[23] Recently, the discovery of a potent semi-synthetic phenyl carbamate showing in vitro activity against breast cancer cells through a mechanism involving the receptor tyrosine kinase c-Met has been reported.[24]

The ability of carbamates to modulate inter- and intramolecular interactions with the target enzymes or receptors has been widely used in medicinal chemistry,[25] hence it is clear that evaluation of alternative cytotoxic mechanisms not involving NF-κB and STAT3 receptors is necessary for compounds **32** and **33**.

3. Conclusions

The molecular targets involved in the anti-inflammatory activity of cadinane sesquiterpenoids isolated from *H. inuloides* were identified. The results obtained indicated that 7-hydroxy-3,4-dihydrocadalene (**1**), the main constituent in this species, possesses anti-NF-κB activity and is able to activate antioxidant Nrf2 pathway, which may correlate with the ancestral use of this species in Mexican folk medicine.

A novel semi-synthetic set, including ester and carbamate derivatives, was prepared using the active natural cadinanes as scaffolds. Derivative **13** showed be more potent on NF-κB inhibition and Nrf2 activation when compared with its parent 7-hydroxy-3,4-dihydrocadalene (**1**). Additionally, compound **13** reduces the intracellular accumulation of ROS induced by TBHP and decreases levels of phospho-IκBα, a protein complex involved in the NF-κB activation pathway. Docking analyses revealed that compound **13** is positioned at the activation loop of the IKKβ subunit, which explains how it prevents IκBα phosphorylation and agrees with evidence found by western blot.

Carbamate derivatives **32** and **33** showed potent in vitro cytotoxic activity against human colorectal adenocarcinoma with minimal toxicity on human gingival fibroblast cells. These compounds were ineffective on NF-κB, Nrf2 and STAT3 transcription factors, indicating a cell death mechanism involving different targets. Thus, further research is needed.

Cadinane sesquiterpenoids now could be considered a novel class of natural NF-κB and Nrf2 modulators, which can be useful as templates for the development and optimization of new substances with anti-inflammatory and anticancer activities.

4. Experimental section

4.1 General methods

UV spectra were obtained on a Shimadzu UV-VISIBLE recording Spectrophotometer. IR spectra were recorded on a Bruker Tensor 27 spectrometer. ^{1}H and ^{13}C NMR spectra were measured on a Bruker Avance III, 400 MHz NMR instrument. Chemical shifts are reported in parts per million (δ) relative to TMS, and coupling constants (J) are reported in Hz. The complete assignment of ^{1}H and ^{13}C signals was carried out by an analysis of the correlated homonuclear H,H-COSY, and heteronuclear H,C-HSQC and H,C-HMBC spectra. The HRMS data were taken on a Jeol The AccuTOF JMS T100 LC system with a direct analysis in real time ESI+ ionization mode.

Vacuum liquid chromatography (VLC) was carried out using spherical silica gel with pore size 60 Å and 230-400 mesh particle size. Reactions were monitored by TLC employing Merck silica gel 60 F_{254} plates (0.2 mm) visualized with either a UV lamp (254 and 365 nm) or a charring solution (12 g of ceric ammonium sulfate dihydrate, 22.2 mL of concentrated H_2SO_4, and 350 g of ice). PLCs were conducted using Merck silica gel 60 F_{254} glass plates (2 mm).

4.2 Plant material

H. inuloides (aerial parts) was collected in the region of Ozumba, in Estado de México, Mexico in October 2012. Voucher specimen was authenticated by Edelmira Linares and Robert Bye (collection of E. Linares 2754 and R. Bye) and deposited in the National Herbarium (MEXU), Instituto de Biología de la Universidad Nacional Autónoma de México.

4.3 Extraction and isolation

7-hydroxy-3,4-dihydrocadalene (**1**) and 7-hydroxy-cadalene (**2**) preparative amounts were obtained by fractionation of an acetonic extract (348.6 g) prepared by maceration (3 times / 24 h) of dried and powdered plant material (10 kg). This extract was concentrated under reduced pressure and subjected to separation processes by VLC using a hexanes-EtOAc gradient as mobile phase. From fractions eluted with hexanes-EtOAc 75:25 and 70:30 were obtained 2.7 g of 7-hydroxy-3,4-dihydrocadalene and 331 mg of 7-hydroxy-cadalene, respectively, which were purified through recrystallization from hexanes. Spectroscopic data were compared with authentic samples from our

laboratory. Metabolites **1-8** were isolated in previous investigations carried out by our group.[16]

4.4 Semi-synthetic derivatives

4.4.1 General procedure for esterification of 7-hydroxy-3,4-dihydrocadalene (1) and 7-hydroxy-cadalene (2)

A solution of either 7-hydroxy-3,4-dihydrocadalene (1.0 equiv) or 7-hydroxy-cadalene (1.0 equiv) in anhydrous pyridine (1 mL/20 mg of natural product) was flushed with nitrogen gas and then a balloon filled with helium gas was connected to the septum. This solution was treated with the aproppiated benzoyl chloride reagent (2.0 equiv) having electron donating or electron withdrawing substituents in *meta* and *para* positions (Sigma Aldrich). After 24 hours stirring the mixture was quenched with ice-cold water and the organic phase was extracted with EtOAc. Excess pyridine was neutralized with HCl (10%), and subsequent addition of a saturated solution of $NaHCO_3$ avoided acidification of the medium. The resulting mixture was treated with a saturated solution of NaCl and the organic phase was passed over Na_2SO_4 to remove remaining water. Purification of each one of the corresponding semisynthetic esters was carried out by PLC (hexanes-EtOAc 90:10, two or three elutions). Preparation and structural characterization of derivatives **11** and **22** have been previously described by our research group.[26]

4.4.1.1 7-(*p*-Chlorobenzoyloxy)-3,4-dihydrocadalene (12). Yellow oil; 34.4 mg 81% yield; UV (MeOH) λ_{max}(log ε) 204 (4.77), 224 (4.52), 239 (4.63) nm; IR ($CHCl_3$) ν_{max} 3536, 2961, 1734, 1594, 1260, 1130, 1093 cm^{-1}; ^{1}H-NMR (400 MHz, $CDCl_3$) 0.84 (3H, d, $J_{13,11}$ 6.8 Hz, CH_3-13), 0.91 (3H, d, $J_{12,11}$ 6.8 Hz, CH_3-12), 1.91 (1H, hept, $J_{11,12;11,13}$ 6.8 Hz, H-11),1.99 (3H, br s, CH_3-14), 2.19 (3H, s, CH_3-15), 2.38 (3H, overlapped, H-3,4), 5.72 (1H, br d, $J_{2,3}$ 1.2 Hz, H-2), 6.96 (1H, s, H-8), 7.00 (1H, s, H-5), 7.50, (2H, br d, $J_{3',4';6',7'}$ 6.8 Hz, H-4',6'), 8.17, (2H, br d, $J_{3',4';6',7'}$ 6.8 Hz, H-3',7'); ^{13}C NMR (100 MHz, $CDCl_3$) 16.0 (CH_3-15), 18.9 (CH_3-14), 20.2 (CH_3-12), 21.4 (CH_3-13), 25.5 (CH_2-3), 30.2 (CH-11), 43.8 (CH-4), 116.2 (CH-8), 124.0 (CH-2), 127.3 (C-6), 128.1 (C-5'), 128.9 (CH-4',6'), 131.1 (CH-5), 131.5 (CH-3',7', C-9), 134.8 (C-1), 137.0 (C-10), 140.0 (C-2'), 147.8 (C-7), 164.2 (C-1'); HRESIMS *m/z* 355.14561 $[M + H]^+$ (calcd for $C_{22}H_{24}ClO_2$, 355.14648).

4.4.1.2 7-(*p*-Methylbenzoyloxy)-3,4-dihydrocadalene (13). White solid; 32.2 mg 77% yield; UV (MeOH) λ_{max}(log ε) 211 (4.67), 261 (4.57) nm; IR ($CHCl_3$) ν_{max} 3538, 3038, 2961, 1726, 1606, 1256, 1233, 1130 cm^{-1}; ^{1}H-NMR (400 MHz, $CDCl_3$) 0.84 (3H, d, $J_{13,11}$ 6.8 Hz, CH_3-13), 0.91 (3H, d, $J_{12,11}$ 6.8 Hz, CH_3-12), 1.91 (1H, hept, $J_{11,12;11,13}$ 6.8 Hz, H-11),1.99 (3H, br s, CH_3-14), 2.20 (3H, s, CH_3-15), 2.38 (3H, overlapped, H-3,4), 2.46 (3H, s, CH_3-8'), 5.71 (1H, br d, $J_{2,3}$ 1.6 Hz, H-2), 6.98 (1H, s, H-8), 7.0, (1H, s, H-5), 7.32, (2H, d, $J_{4',3';6',7'}$ 9.2 Hz, H-4',6'), 8.12, (2H, d, $J_{3',4';7',6'}$ 8.12 Hz, H-3',7'); ^{13}C NMR (100 MHz, $CDCl_3$) 16.0 (CH_3-15), 19.0 (CH_3-14), 20.2 (CH_3-12), 21.4 (CH_3-13), 21.7 (CH_3-8'), 25.5 (CH_2-3), 30.2 (CH-11), 43.8 (CH-4), 116.3 (CH-8), 123.9 (CH-2), 126.9 (C-2'), 127.5 (C-6), 129.3 (CH-4',6'), 130.2 (CH-3',7'), 131.0 (CH-5), 131.2 (C-9), 134.7 (C-1), 136.7 (C-10), 144.2 (C-5'), 147.9 (C-7), 165.1 (C-1'); HRESIMS *m/z* 335.20016 $[M + H]^+$ (calcd for $C_{23}H_{27}O_2$, 335.20110).

4.4.1.3 7-(*p*-Methoxybenzoyloxy)-3,4-dihydrocadalene (14). White solid; 22.5 mg 69% yield; UV (MeOH) λ_{max}(log ε) 204 (4.80), 239 (4.63) nm; IR ($CHCl_3$) ν_{max} 3533, 3019, 2961, 1730, 1263, 1233, 1131 cm^{-1}; ^{1}H-NMR (400 MHz, $CDCl_3$) 0.84 (3H, d, $J_{13,11}$ 6.8 Hz, CH_3-13), 0.91 (3H, d, $J_{12,11}$ 6.8 Hz, CH_3-12), 1.90 (1H, hept, $J_{11,12;11,13}$ 6.8 Hz, H-11),1.99 (3H, br s, CH_3-14), 2.20 (3H, s, CH_3-15), 2.38 (3H, overlapped, H-3,4), 3.90 (3H, s, CH_3-8'), 5.70 (1H, br d, $J_{2,3}$ 1.6 Hz, H-2), 6.97 (1H, s, H-8), 6.99 (3H, m, H-5,4',6'), 8.18 (2H, d, $J_{3',4';7',6'}$ 8.8 Hz, H-3',7'); ^{13}C NMR (100 MHz, $CDCl_3$) 16.0 (CH_3-15), 19.0 (CH_3-14), 20.2 (CH_3-12), 21.4 (CH_3-13), 25.5 (CH_2-3), 30.2 (CH-11), 43.8 (CH-4), 55.5 (CH_3-8'), 113.8 (CH-4',6'), 116.4 (CH-8), 122.0 (C-2'), 123.8 (CH-2), 127.5 (C-6), 131.0 (CH-5), 131.2 (C-9), 132.2 (CH-3',7'), 134.7 (C-1), 136.7 (C-10), 148.0 (C-7), 163.8 (C-5'), 164.7 (C-1'); HRESIMS *m/z* 351.19493 $[M + H]^+$ (calcd for $C_{23}H_{27}O_3$, 351.19602).

4.4.1.4 7-(*p*-Trifluoromethylbenzoyloxy)-3,4-dihydrocadalene (15). White solid; 22.1 mg 73% yield; UV (MeOH) λ_{max}(log ε) 204 (4.53), 209 (4.51), 229 (4.69), 251 (4.02), 264 (4.03) nm; IR ($CHCl_3$) ν_{max} 2960, 1737, 1325, 1263,1175, 1133 cm^{-1}; ^{1}H-NMR (400 MHz, $CDCl_3$) 0.83 (3H, d, $J_{13,11}$ 6.8 Hz, CH_3-13), 0.91 (3H, d, $J_{12,11}$ 6.8 Hz, CH_3-12), 1.91 (1H, hept, $J_{11,12;11,13}$ 6.8 Hz, H-11), 1.99 (3H, br s, CH_3-14), 2.19 (3H, s, CH_3-15), 2.38 (3H, overlapped, H-3,4), 5.72 (1H, br d, $J_{2,3}$ 1.6 Hz, H-2), 6.97 (1H, s, H-8), 7.01 (1H, s, H-5), 7.79, (2H, br d, $J_{4',3';6',7'}$ 8.8 Hz, H-4',6'), 8.34, (2H, br d, $J_{3',4';7',6'}$ 8.8 Hz, H-3',7'); ^{13}C NMR (100 MHz, $CDCl_3$) 16.0 (CH_3-15), 18.9 (CH_3-14), 20.2 (CH_3-12), 21.4 (CH_3-13), 25.5 (CH_2-3), 30.3 (CH-11), 43.8 (CH-4), 116.1 (CH-8),

124.2 (CH-2), 125.6 (CH-4',6'), 127.2 (C-6), 130.5 (CH-3',7'), 131.0 (C-9), 131.2 (CH-5), 133.0 (C-5'), 134.9 (C-1, C-2'), 137.2 (C-10), 147.7 (C-7), 163.9 (C-1'); HRESIMS *m/z* 389.17176 $[M + H]^+$ (calcd for $C_{23}H_{24}F_3O_2$, 389.17284).

4.4.1.5 7-(*p*-Nitrobenzoyloxy)-3,4-dihydrocadalene (16). Yellow oil; 23.1 mg 84% yield; UV (MeOH) λ_{max}(log ε) 205 (3.72), 244 (3.42), 258 (3.46) nm; IR ($CHCl_3$) ν_{max} 3558, 3020, 2960, 1739, 1530, 1262, 1232, 1129 cm^{-1}; ^{1}H-NMR (400 MHz, $CDCl_3$) 0.83 (3H, d, $J_{13,11}$ 6.8 Hz, CH_3-13), 0.91 (3H, d, $J_{12,11}$ 6.8 Hz, CH_3-12), 1.90 (1H, hept, $J_{11,12;11,13}$ 6.8 Hz, H-11), 1.99 (3H, br s, CH_3-14), 2.20 (3H, s, CH_3-15), 2.38 (3H, overlapped, H-3,4), 5.73 (1H, br d, $J_{2,3}$ 1.2 Hz, H-2), 6.97 (1H, s, H-8), 7.01 (1H, s, H-5), 6.97 (4H, m, H-3',4',6',7'); ^{13}C NMR (100 MHz, $CDCl_3$) 16.0 (CH_3-15), 18.9 (CH_3-14), 20.2 (CH_3-12), 21.4 (CH_3-13), 25.4 (CH_2-3), 30.2 (CH-11), 43.8 (CH-4), 115.9 (CH-8), 123.7 (CH-4',6'), 124.3 (CH-2), 127.0 (C-6), 130.9 (CH-5), 131.2 (CH-3',7', C-9), 134.9 (C-1), 135.0 (C-2'), 137.3 (C-10), 147.5 (C-7), 150.8 (C-5'), 163.1 (C-1'); HRESIMS *m/z* 366.16922 $[M + H]^+$ (calcd for $C_{22}H_{24}NO_4$, 366.17053).

4.4.1.6 7-(*m*-Chlorobenzoyloxy)-3,4-dihydrocadalene (17). Colorless oil; 46.5 mg 77% yield; UV (MeOH) λ_{max}(log ε) 206 (4.55), 225 (4.37), 234 (4.41),), 271 (3.70) nm; IR ($CHCl_3$) ν_{max} 2962, 1711, 1363, 1248, 1131 cm^{-1}; ^{1}H-NMR (400 MHz, $CDCl_3$) 0.83 (3H, d, $J_{13,11}$ 6.8 Hz, CH_3-13), 0.91 (3H, d, $J_{12,11}$ 6.8 Hz, CH_3-12), 1.91 (1H, hept, $J_{11,12;11,13}$ 6.8 Hz, H-11), 1.98 (3H, br s, CH_3-14), 2.19 (3H, s, CH_3-15), 2.38 (3H, overlapped, H-3,4), 5.72 (1H, br d, $J_{2,3}$ 1.6 Hz, H-2), 6.95 (1H, s, H-8), 7.00 (1H, s, H-5), 7.47 (1H, t, $J_{6',5';6',7'}$ 8.0 Hz, H-6'), 7.62 (1H, ddd, $J_{5',6'}$ 8.0 Hz, $J_{5',3'}$ 2.0 Hz, $J_{5'7'}$ 1.2 Hz, H-5'), 8.11 (1H, dt, $J_{7',6'}$ 8.0 Hz, $J_{7',5'}$ 1.2 Hz, H-7'), 8.21 (1H, t, $J_{3',5'}$ 2.0 Hz, H-3'); ^{13}C NMR (100 MHz, $CDCl_3$) 16.0 (CH_3-15), 18.9 (CH_3-14), 20.2 (CH_3-12), 21.4 (CH_3-13), 25.5 (CH_2-3), 30.2 (CH-11), 43.8 (CH-4), 116.1 (CH-8), 124.1 (CH-2), 127.2 (C-6), 128.2 (CH-7'), 129.9 (CH-6'), 130.1 (CH-3'), 131.1 (CH-5), 131.4 (C-1), 133.5 (CH-5'), 133.6 (C-2'), 134.7 (C-4'), 134.8 (C-9), 137.0 (C-10), 147.7 (C-7), 163.8 (C-1'); HRESIMS *m/z* 355.14559 $[M + H]^+$ (calcd for $C_{22}H_{24}ClO_2$, 355.14648).

4.4.1.7 7-(*m*-Methylbenzoyloxy)-3,4-dihydrocadalene (18). Yellow oil; 45.1 mg 89% yield; UV (MeOH) λ_{max}(log ε) 205 (4.66), 225 (4.40), 235 (4.45) nm; IR ($CHCl_3$) ν_{max} 3579, 2964, 1732, 1276, 1195, 1129, 1070 cm^{-1}; ^{1}H-NMR (400 MHz, $CDCl_3$) 0.85 (3H, d, $J_{13,11}$ 6.8 Hz, CH_3-13), 0.92 (3H, d, $J_{12,11}$ 6.8 Hz, CH_3-12), 1.92 (1H, hept, $J_{11,12;11,13}$ 6.8 Hz, H-11), 2.00 (3H, br s, CH_3-14), 2.22 (3H, s, CH_3-15), 2.40 (3H,

overlapped, H-3,4), 2.47 (3H, s, CH_3-8'), 5.70 (1H, br d, $J_{2,3}$ 0.8 Hz, H-2), 6.99 (1H, s, H-8), 7.01 (1H, s, H-5), 7.44, (2H, m, H-5',6'), 8.05, (2H, m, H-3',7'); ^{13}C NMR (100 MHz, $CDCl_3$) 16.0 (CH_3-15), 18.9 (CH_3-14), 20.2 (CH_3-12), 21.3 (CH_3-8'), 21.4 (CH_3-13), 25.5 (CH_2-3), 30.2 (CH-11), 43.8 (CH-4), 116.3 (CH-8), 123.9 (CH-2), 127.3 (CH-7'), 127.4 (C-6), 128.4 (CH-6'), 129.6 (C-2'), 130.6 (CH-3'), 131.0 (CH-5), 131.1 (C-1), 134.2 (CH-5'), 134.7 (C-9), 136.7 (C-10), 138.2 (C-4'), 147.9 (C-7), 165.2 (C-1'); HRESIMS *m/z* 335.20129 $[M + H]^+$ (calcd for $C_{23}H_{27}O_2$, 335.20110).

4.4.1.8 7-(*m*-Methoxybenzoyloxy)-3,4-dihydrocadalene (19). Yellow oil; 83.0 mg 95% yield; UV (MeOH) λ_{max}(log ε) 214 (4.75), 347 (2.34) nm; IR ($CHCl_3$) ν_{max} 3558, 2962, 1732, 1491, 1277, 1233, 1129 cm^{-1}; ^{1}H-NMR (400 MHz, $CDCl_3$) 0.86 (3H, d, $J_{13,11}$ 6.8 Hz, CH_3-13), 0.93 (3H, d, $J_{12,11}$ 6.8 Hz, CH_3-12), 1.93 (1H, hept, $J_{11,12;11,13}$ 6.8 Hz, H-11), 2.00 (3H, br s, CH_3-14), 2.23 (3H, s, CH_3-15), 2.40 (3H, overlapped, H-3,4), 3.90 (3H, s, CH_3-8'), 5.73 (1H, br d, $J_{2,3}$ 1.2 Hz, H-2), 7.00 (1H, s, H-8), 7.02 (1H, s, H-5), 7.19, (1H, ddd, $J_{5',6'}$ 8.0 Hz, $J_{5',3'}$ 2.8 Hz, $J_{5',7'}$ 1.2 Hz, H-5'), 7.44 (1H, t, $J_{6',5';6',7'}$ 8Hz, H-6'), 7.76 (1H, t, $J_{3',5'}$ 2.8 Hz, H-3'); 7.86 (1H, dt, $J_{7',6'}$ 8.0 Hz, $J_{7',5'}$ 1.2 Hz, H-7'); ^{13}C NMR (100 MHz, $CDCl_3$) 16.0 (CH_3-15), 18.9 (CH_3-14), 20.2 (CH_3-12), 21.4 (CH_3-13), 25.5 (CH_2-3), 30.2 (CH-11), 43.8 (CH-4), 55.4 (CH_3-8'), 114.5 (CH-3'), 116.2 (CH-8), 120.0 (CH-5'), 122.5 (CH-7'), 123.9 (CH-2), 127.4 (C-6), 129.5 (CH-6'), 130.9 (C-2'), 131.0 (CH-5), 131.1 (C-10), 134.7 (C-1), 136.8 (C-9), 147.9 (C-7), 159.7 (C-4'), 164.8 (C-1'); HRESIMS *m/z* 351.19599 $[M + H]^+$ (calcd for $C_{23}H_{27}O_3$, 351.19602).

4.4.1.9 7-(*m*-Trifluoromethylbenzoyloxy)-3,4-dihydrocadalene (20). Colorless oil; 22.1 mg 88% yield; UV (MeOH) λ_{max}(log ε) 203 (4.64), 215 (4.55), 226 (4.59) nm; IR ($CHCl_3$) ν_{max} 3576, 2965, 1740, 1336, 1174, 1136, 1073 cm^{-1}; ^{1}H-NMR (400 MHz, $CDCl_3$) 0.84 (3H, d, $J_{13,11}$ 6.8 Hz, CH_3-13), 0.91 (3H, d, $J_{12,11}$ 6.8 Hz, CH_3-12), 1.91 (1H, hept, $J_{11,12;11,13}$ 6.8 Hz, H-11), 1.99 (3H, br s, CH_3-14), 2.21 (3H, s, CH_3-15), 2.39 (3H, overlapped, H-3,4), 5.73 (1H, br d, $J_{2,3}$ 1.2 Hz, H-2), 6.97 (1H, s, H-8), 7.01 (1H, s, H-5), 7.68 (1H, m, H-6'), 7.90, (1H, br d, $J_{5',6'}$ 8.4 Hz, H-5'), 8.41 (1H, d, $J_{7',6'}$ 7.6 Hz, H-7'), 8.50 (1H, s, H-3'); ^{13}C NMR (100 MHz, $CDCl_3$) 16.0 (CH_3-15), 18.9 (CH_3-14), 20.2 (CH_3-12), 21.4 (CH_3-13), 25.5 (CH_2-3), 30.2 (CH-11), 43.8 (CH-4), 116.0 (CH-8), 124.1 (CH-2), 127.0 (CH-3'), 127.2 (C-6), 129.3 (CH-6'), 130.0 (CH-5'), 130.1 (C-2'), 130.5 (C-4'), 131.0 (C-1), 131.1 (CH-5), 133.3 (CH-7'), 135.0 (C-9), 137.1 (C-10), 147.6 (C-7), 163.7 (C-1'); HRESIMS *m/z* 389.17234 $[M + H]^+$ (calcd for $C_{23}H_{24}F_3O_2$, 389.17284).

4.4.1.10 7-(*m*-Nitrobenzoyloxy)-3,4-dihydrocadalene (21). Yellow oil; 32.2 mg 72% yield; UV (MeOH) λ_{max}(log ε) 223 (4.70), 245 (4.19), 260 (4.20) nm; IR ($CHCl_3$) ν_{max} 2959, 1741, 1536, 1353, 1255, 1133 cm^{-1}; ^{1}H-NMR (400 MHz, $CDCl_3$) 0.84 (3H, d, $J_{13,11}$ 6.8 Hz, CH_3-13), 0.91 (3H, d, $J_{12,11}$ 6.8 Hz, CH_3-12), 1.91 (1H, hept, $J_{11,12;11,13}$ 6.8 Hz, H-11), 1.99 (3H, br s, CH_3-14), 2.21 (3H, s, CH_3-15), 2.39 (3H, overlapped, H-3,4), 5.73 (1H, br d, $J_{2,3}$ 1.6 Hz, H-2), 6.98 (1H, s, H-8), 7.02 (1H, s, H-5), 7.74 (1H, t, $J_{6',5';6',7'}$ 8Hz, H-6'), 8.50, (1H, ddd, $J_{5',6'}$ 8.0 Hz, $J_{5',3'}$ 2.4 Hz, $J_{5',7'}$ 1.2 Hz, H-5'), 8.55 (1H, dt, $J_{7',6'}$ 8.0 Hz, $J_{7',5'}$ 1.2 Hz, H-7'), 9.06 (1H, t, $J_{3',5'}$ 2.4 Hz, H-3'); ^{13}C NMR (100 MHz, $CDCl_3$) 16.0 (CH_3-15), 18.9 (CH_3-14), 20.2 (CH_3-12), 21.4 (CH_3-13), 25.5 (CH_2-3), 30.3 (CH-11), 43.8 (CH-4), 115.9 (CH-8), 124.3 (CH-2), 125.1 (CH-3'), 127.1 (C-6), 127.9 (CH-5'), 129.9 (CH-6'), 131.0 (C-1), 131.2 (CH-5), 131.5 (C-2'), 135.0 (C-9), 135.7 (CH-7'), 137.3 (C-10), 147.6 (C-7), 148.5 (C-4'), 163.0 (C-1'); HRESIMS *m/z* 366.17023 $[M + H]^+$ (calcd for $C_{22}H_{24}NO_4$, 366.17053).

4.4.1.11 7-(*p*-Chlorobenzoyloxy)-cadalene (23). White crystals; 28.2 mg 78% yield; UV (MeOH) λ_{max}(log ε) 208 (4.84), 216 (4.81), 235 (4.91) nm; IR ($CHCl_3$) ν_{max} 2967, 1735, 1267, 1092 cm^{-1}; ^{1}H-NMR (400 MHz, $CDCl_3$) 1.39 (6H, d, $J_{12,11;13,11}$ 6.8 Hz, CH_3-12,13), 2.41 (3H, s, CH_3-15), 2.60 (3H, s, CH_3-14), 3.71 (1H, hept, $J_{11,12;11,13}$ 6.8 Hz, H-11), 7.26 (2H, overlapped, H-2,3), 7.51 (2H, d, $J_{4',3';6',7'}$ 8.8 Hz, H-4',6'), 7.75 (1H, s, H-8), 8.03 (1H, s, H-5), 8.21 (2H, d, $J_{3',4';7',6'}$ 8.8 Hz, H-3',7'); ^{13}C NMR (100 MHz, $CDCl_3$) 17.2 (CH_3-15), 19.4 (CH_3-14), 23.6 (CH_3-12,13), 28.5 (CH-11), 116.5 (CH-8), 121.4 (CH-3), 125.8 (CH-5), 126.4 (CH-2), 128.0 (C-5'), 128.5 (C-6), 129.0 (CH-4',6'), 130.0 (C-10), 131.6 (CH-3',7', C-1), 132.5 (C-9), 140.2 (C-2'), 142.2 (C-4), 147.6 (C-7), 164.4 (C-1'); HRESIMS *m/z* 353.12940 $[M + H]^+$ (calcd for $C_{22}H_{22}ClO_2$, 353.13083).

4.4.1.12 7-(*p*-Methylbenzoyloxy)-cadalene (24). White crystals; 24.7 mg 82% yield; UV (MeOH) λ_{max}(log ε) 208 (7.73), 211 (4.70), 237 (4.87), 281 (4.05) nm; IR ($CHCl_3$) ν_{max} 3693, 2966, 1731, 1611, 1442, 1269, 1129, 1077 cm^{-1}; ^{1}H-NMR (400 MHz, $CDCl_3$) 1.39 (6H, d, $J_{11,12;\ 11,13}$ 6.8 Hz, CH_3-12,13), 2.42 (3H, s, CH_3-15), 2.46 (3H, s, CH_3-8'), 2.60 (3H, s, CH_3-14), 3.71 (1H, hept, $J_{11,12;11,13}$ 6.8 Hz, H-11), 7.25 (2H, overlapped, H-2,3), 7.33 (2H, d, $J_{4',3';6',7'}$ 8.0 Hz, H-4',6'), 7.75 (1H, s, H-8), 8.02 (1H, s, H-5), 8.17 (2H, d, $J_{3',4';7',6'}$ 8.4 Hz, H-3',7'); ^{13}C NMR (100 MHz, $CDCl_3$) 17.2 (CH_3-15), 19.4 (CH_3-14), 21.7 (CH_3-8'), 23.6 (CH_3-12,13), 28.4 (CH-11), 116.5 (CH-8), 121.2 (CH-3), 125.7 (CH-5), 126.2 (CH-2), 126.7 (C-2'), 128.8 (C-6), 129.2 (CH-4',6'), 129.9 (C-10), 130.3 (CH-3',7'), 131.6 (C-1), 132.5 (C-9), 142.1 (C-4), 144.4 (C-5'),

147.8 (C-7), 165.3 (C-1'); HRESIMS *m/z* 333.18453 $[M + H]^+$ (calcd for $C_{23}H_{25}O_2$, 333.18545).

4.4.1.13 7-(*p*-Methoxybenzoyloxy)-cadalene (25). Colorless crystals; 24.2 mg 84% yield; UV (MeOH) λ_{max}(log ε) 215 (4.82), 225 (4.76), 231 (4.78), 244 (4.42), 261 (4.59) nm; IR ($CHCl_3$) ν_{max} 3554, 2967, 1728, 1606, 1512, 12259, 1168,1129,1077 cm^{-1}; ^{1}H-NMR (400 MHz, $CDCl_3$) 1.39 (6H, d, $J_{12,11;13,11}$ 6.8 Hz, CH_3-12,13), 2.42 (3H, s, CH_3-15), 2.60 (3H, s, CH_3-14), 3.71 (1H, hept, $J_{11,12;11,13}$ 6.8 Hz, H-11), 3.90 (3H, s, CH_3-8'), 7.01 (2H, d, $J_{4',3';6',7'}$ 8.8 Hz, H-4',6'), 7.25 (2H, overlapped, H-2,3), 7.75 (1H, s, H-8), 8.02 (1H, s, H-5), 8.23 (2H, d, $J_{3',4';7',6'}$ 8.8 Hz, H-3',7'); ^{13}C NMR (100 MHz, $CDCl_3$) 17.2 (CH_3-15), 19.4 (CH_3-14), 23.6 (CH_3-12,13), 28.4 (CH-11), 55.5 (CH_3-8'), 113.9 (CH-4',6'), 116.6 (CH-8), 121.1 (CH-3), 121.8 (C-2'), 125.6 (CH-5), 126.3 (CH-2), 128.9 (C-6), 129.9 (C-10), 131.6 (C-1), 132.2 (CH-3',7'), 132.5 (C-9), 142.1 (C-4), 147.9 (C-7), 163.9 (C-5'), 164.9 (C-1'); HRESIMS *m/z* 349.17915 $[M + H]^+$ (calcd for $C_{23}H_{25}O_3$, 349.18037).

4.4.1.14 7-(*p*-Trifluoromethylbenzoyloxy)-cadalene (26). White crystals; 39.6 mg 89% yield; UV (MeOH) λ_{max}(log ε) 235 (4.65), 257 (3.65), 281 (4.76) nm; IR ($CHCl_3$) ν_{max} 3569, 2967, 1738, 1412, 1325, 1269, 1131, 1082 cm^{-1}; ^{1}H-NMR (400 MHz, $CDCl_3$) 1.42 (6H, d, $J_{12,11;13,11}$ 6.8 Hz, CH_3-12,13), 2.45 (3H, s, CH_3-15), 2.63 (3H, s, CH_3-14), 3.73 (1H, hept, $J_{11,12;11,13}$ 6.8 Hz, H-11), 7.30 (2H, overlapped, H-2,3), 7.79 (1H, s, H-8), 7.82 (2H, d, $J_{4',3';6',7'}$ 8.0 Hz, H-4',6'), 8.07 (1H, s, H-5), 8.42 (2H, d, *J* $J_{3',4';7',6'}$ 8.0 Hz, H-3',7'); ^{13}C NMR (100 MHz, $CDCl_3$) 17.1 (CH_3-15), 19.3 (CH_3-14), 23.6 (CH_3-12,13), 28.5 (CH-11), 116.4 (CH-8), 121.5 (CH-3), 122.17 (CH_3-8'), 125.7 (CH-4',6'), 125.9 (CH-5), 126.5 (CH-2), 128.4 (C-6), 130.1 (C-10), 130.6 (CH-3',7'), 131.6 (C-1), 132.5 (C-9), 132.7 (C-5'), 135.0 (C-2'), 142.2 (C-4), 147.5 (C-7), 164.1 (C-1'); HRESIMS *m/z* 387.15549 $[M + H]^+$ (calcd for $C_{23}H_{22}F_3O_2$, 387.15719).

4.4.1.15 7-(*p*-Nitrobenzoyloxy)-cadalene (27). Yellow crystals; 28.2 mg 86% yield; UV (MeOH) λ_{max}(log ε) 233 (5.03), 249 (4.59), 257 (4.60) nm; IR ($CHCl_3$) ν_{max} 3575, 2966, 1741, 1530, 1267, 1233, 1128 cm^{-1}; ^{1}H-NMR (400 MHz, $CDCl_3$) 1.39 (6H, d, $J_{12,11;13,11}$ 6.8 Hz, CH_3-12,13), 2.43 (3H, s, CH_3-15), 2.61 (3H, s, CH_3-14), 3.71 (1H, hept, $J_{11,12;11,13}$ 6.8 Hz, H-11), 7.28 (2H, overlapped, H-2,3), 7.73 (1H, s, H-8), 8.05 (1H, s, H-5), 8.36 (2H, d, $J_{4',3';6',7'}$ 8.4 Hz, H-4',6'), 8.43 (2H, d, $J_{3',4';7',6'}$ 8.4 Hz, H-3',7'); ^{13}C NMR (100 MHz, $CDCl_3$) 17.1 (CH_3-15), 19.3 (CH_3-14), 23.6 (CH_3-12,13), 28.5

(CH-11), 116.3 (CH-8), 121.6 (CH-3), 123.7 (CH-4',6'), 126.0 (CH-5), 126.6 (CH-2), 128.1 (C-6), 130.1 (C-10), 131.3 (CH-3',7'), 131.6 (C-1), 132.3 (C-9), 134.9 (C-2'), 142.2 (C-4), 147.3 (C-7), 150.9 (C-5'), 163.4 (C-1'); HRESIMS *m/z* 364.15363 $[M + H]^+$ (calcd for $C_{22}H_{22}NO_4$, 364.15488).

4.4.1.16 7-(*m*-Methylbenzoyloxy)-cadalene (28). White crystals; 30.0 mg 75% yield; UV (MeOH) λ_{max}(log ε) 205 (4.81), 210 (4.78), 236 (4.90), 264 (4.02), 281 (4.09) nm; IR ($CHCl_3$) ν_{max} 2967, 1732, 1276, 1233, 1197 cm^{-1}; ^{1}H-NMR (400 MHz, $CDCl_3$) 1.39 (6H, d, $J_{11,12;13,11}$ 6.8 Hz, CH_3-12,13), 2.43 (3H, s, CH_3-15), 2.46 (3H, s, CH_3-8'), 2.60 (3H, s, CH_3-14), 3.71 (1H, hept, $J_{11,12;11,13}$ 6.8 Hz, H-11), 7.25 (2H, overlapped, H-2,3), 7.43 (2H, overlapped, H-5',6'), 7.74 (1H, s, H-8), 8.02 (1H, s, H-5), 8.07 (1H, overlapped, H-7'), 8.09 (1H, s, H-3'); ^{13}C NMR (100 MHz, $CDCl_3$) 17.2 (CH_3-15), 19.4 (CH_3-14), 21.3 (CH_3-8'), 23.6 (CH_3-12,13), 28.4 (CH-11), 116.5 (CH-8), 121.2 (CH-3), 125.7 (CH-5), 126.3 (CH-2), 127.4 (CH-7'), 128.5 (CH-6'), 128.8 (C-6), 129.4 (C-2'), 129.9 (C-10), 130.7 (CH-3'), 131.6 (C-1), 132.5 (C-9), 134.4 (CH-5'), 138.5 (C-4'), 142.1 (C-4), 147.8 (C-7), 165.4 (C-1'); HRESIMS *m/z* 333.18570 $[M + H]^+$ (calcd for $C_{23}H_{25}O_2$, 333.18545).

4.4.1.17 7-(*m*-Methoxybenzoyloxy)-cadalene (29). Yellow oil; 9.1 mg 78% yield; UV (MeOH) λ_{max}(log ε) 215 (4.95), 225 (4.91), 233 (4.95), 266 (4.00), 293 (4.16) nm; IR ($CHCl_3$) ν_{max} 3404, 3007, 1711, 1362, 1277, 1237 cm^{-1}; ^{1}H-NMR (400 MHz, $CDCl_3$) 1.39 (6H, d, $J_{12,11;13,11}$ 6.8 Hz, CH_3-12,13), 2.43 (3H, s, CH_3-15), 2.61 (3H, s, CH_3-14), 3.71 (1H, hept, $J_{11,12;11,13}$ 6.8 Hz, H-11), 3.90 (3H, s, CH_3-8'), 7.21 (1H, ddd, $J_{5',6'}$ 8.4 Hz, $J_{5',3'}$ 2.8 Hz, $J_{5',7'}$ 1.2 Hz, H-5'), 7.26 (2H, overlapped, H-2,3), 7.45 (1H, t, $J_{6',5';6',7'}$ 8.0 Hz, H-6'), 7.76 (1H, s, H-8), 7.78 (1H, br t, $J_{3',5'}$ 2.4 Hz, H-3'), 7.89 (1H, dt, $J_{7',6'}$ 8.0 Hz, $J_{7',5'}$ 1.2 Hz, H-7'), 8.03 (1H, s, H-5); ^{13}C NMR (100 MHz, $CDCl_3$) 17.2 (CH_3-15), 19.4 (CH_3-14), 23.6 (CH_3-12,13), 28.5 (CH-11), 55.5 (CH-8'), 114.6 (CH-3'), 116.4 (CH-8), 120.2 (CH-5'), 121.3 (CH-3), 122.6 (CH-7'), 125.8 (CH-5), 126.4 (CH-2), 128.7 (C-6), 129.2 (CH-6'), 130.0 (C-10), 130.1 (C-2'), 131.6 (C-1), 132.5 (C-9), 142.1 (C-4), 147.8 (C-7), 159.8 (C-4'), 165.1 (C-1'); HRESIMS *m/z* 349.18091 $[M + H]^+$ (calcd for $C_{23}H_{25}O_3$, 349.18037).

4.4.1.18 7-(*m*-Trifluoromethylbenzoyloxy)-cadalene (30). White crystals; 59.5 mg 94% yield; UV (MeOH) λ_{max}(log ε) 235 (4.89), 258 (3.89), 280 (3.98) nm; IR ($CHCl_3$) ν_{max} 2965, 1740, 1336, 1133 cm^{-1}; ^{1}H-NMR (400 MHz, $CDCl_3$) 1.39 (6H, d, $J_{12,11;12,13}$

6.8 Hz, CH_3-12,13), 2.43 (3H, s, CH_3-15), 2.61 (3H, s, CH_3-14), 3.71 (1H, hept, $J_{11,12;11,13}$ 6.8 Hz, H-11), 7.27 (2H, overlapped, H-2,3), 7.66 (1H, t, $J_{6',5';6',7'}$ 7.6 Hz, H-6'), 7.77 (1H, s, H-8), 7.90 (1H, d, $J_{5',6'}$ 7.6 Hz, H-5'), 8.05 (1H, s, H-5), 8.45 (1H, d, $J_{7',6'}$ 7.6 Hz, H-7'), 8.56 (1H, s, H-3'); ^{13}C NMR (100 MHz, $CDCl_3$) 17.1 (CH_3-15), 19.4 (CH_3-14), 23.6 (CH_3-12,13), 28.5 (CH-11), 116.4 (CH-8), 121.4 (CH-3), 125.9 (CH-5), 126.5 (CH-2), 127.1 (CH-3'), 128.4 (C-6), 129.3 (CH-6'), 130.1 (CH-5', C-2'), 130.4 (C-10), 131.2 (C-4'), 131.6 (C-1), 132.5 (C-9), 133.4 (CH-7'), 142.2 (C-4), 147.5 (C-7), 164.0 (C-1'); HRESIMS *m/z* 387.15648 $[M + H]^+$ (calcd for $C_{23}H_{22}F_3O_2$, 387.15719).

4.4.1.19 7-(*m*-Chlorobenzoyloxy)-cadalene (31). White crystals; 30.8 mg 91% yield; UV (MeOH) λ_{max}(log ε) 208 (4.73), 216 (4.70), 235 (4.86), 261 (3.87), 282 (4.00) nm; IR ($CHCl_3$) ν_{max} 3559, 2963, 1739, 1243, 1130 cm^{-1}; ^{1}H-NMR (400 MHz, $CDCl_3$) 1.39 (6H, d, $J_{12,11;13,11}$ 6.8 Hz, CH_3-12,13), 2.42 (3H, s, CH_3-15), 2.60 (3H, s, CH_3-14), 3.71 (1H, hept, $J_{11,12;11,13}$ 6.8 Hz, H-11), 7.26 (2H, overlapped, H-2,3), 7.48 (1H, t, $J_{6',5';6',7'}$ 7.6 Hz, H-6'), 7.63 (1H, ddd, $J_{5',6'}$ 8.0 Hz, $J_{5',3'}$ 2.0 Hz, $J_{5',7'}$ 0.8 Hz, H-5'), 7.74 (1H, s, H-8), 8.03 (1H, s, H-5), 8.16 (1H, dt, $J_{7',6'}$ 8.0 Hz, $J_{7',5'}$ 0.8 Hz, H-7'), 8.26 (1H, t, $J_{3',5'}$ 2.0 Hz, H-3'); ^{13}C NMR (100 MHz, $CDCl_3$) 17.2 (CH_3-15), 19.4 (CH_3-14), 23.6 (CH_3-12,13), 28.5 (CH-11), 116.4 (CH-8), 121.4 (CH-3), 125.8 (CH-5), 126.5 (CH-2), 128.3(CH-7'), 128.5 (C-6), 129.9 (CH-6'), 130.1 (C-10), 130.2 (CH-3'), 131.3 (C-2'), 131.6 (C-1), 132.5 (C-9), 133.6 (CH-5'), 134.8 (C-4'), 142.2 (C-4), 147.5 (C-7), 164.1 (C-1'); HRESIMS *m/z* 353.13062 $[M + H]^+$ (calcd for $C_{22}H_{22}ClO_2$, 353.13083).

4.4.2 Carbamates

7-Hydroxy-3,4-dihydrocadalene (1.0 equiv, 40 mg) was dissolved in CH_2Cl_2 (1 mL) and a nitrogen atmosphere was generated in the flask containing this solution. Et_3N (3.0 equiv, 76.7 µL) and phenyl isocyanate (3.0 equiv, 60.3 µL) were added and the mixture was stirred at room temperature overnight. Next, the reaction was quenched by adding ice-cold water and the organic phase was extracted with EtOAc and passed over Na_2SO_4. The desired product was purified by PLC (benzene-EtOAc 96:4, two elutions). The above methodology was applied to obtain the corresponding semisynthetic carbamate from 7-hydroxy-cadalene.

4.4.2.1 7-(Phenylcarbamate)-3,4-dihydrocadalene (32). Yellow oil; 20.5 mg 77% yield; UV (MeOH) λ_{max}(log ε) 204 (4.87), 225 (4.64), 236 (4.68) nm; IR ($CHCl_3$) ν_{max} 3433, 2960, 1746, 1602, 1524, 1442, 1248, 1175, 1131 cm^{-1}; ^{1}H-NMR (400 MHz, $CDCl_3$) 0.82 (3H, d, $J_{13,11}$ 6.8 Hz, CH_3-13), 0.90 (3H, d, $J_{12,11}$ 6.8 Hz, CH_3-12), 1.89 (1H, hept, $J_{11,12;11,13}$ 6.8 Hz, H-11), 1.99 (3H, br s, CH_3-14), 2.24 (3H, s, CH_3-15), 2.36 (3H, overlapped, H-3,4), 5.70 (1H, br d, $J_{2,3}$ 1.2 Hz, H-2), 6.97 (2H, overlapped, H-5,8), 7.03 (1H, br s, NH-2'), 7.10 (1H, d, $J_{6',5';6',7'}$ 7.6 Hz, H-6'), 7.34 (2H, br t, $J_{5',6';7',6'}$ 7.6 Hz, H-5',7'), 7.46 (2H, d, $J_{4',5';8'7'}$ 8.0 Hz, H-4',8'); ^{13}C NMR (100 MHz, $CDCl_3$) 15.9 (CH_3-15), 18.9 (CH_3-14), 20.2 (CH_3-12), 21.4 (CH_3-13), 25.4 (CH_2-3), 30.2 (CH-11), 43.8 (CH-4), 116.5 (CH-8), 118.6 (C-1'), 123.7 (CH-6'), 123.9 (CH-2), 127.8 (C-6), 129.1 (CH-5',7',4',8'), 131.0 (CH-5), 131.1 (C-9), 134.7 (C-1), 136.8 (C-10), 137.6 (C-3'), 147.4 (C-7); HRESIMS *m/z* 336.19620 $[M + H]^+$ (calcd for $C_{22}H_{26}NO_2$, 336.19635).

4.4.2.2 7-(Phenylcarbamate)-cadalene (33). White solid; 20.6 mg 79% yield; UV (MeOH) λ_{max}(log ε) 204 (4.80), 209 (4.79), 213 (4.80), 220 (4.79), 238 (4.96), 265 (3.88), 281 (3.99) nm; IR ($CHCl_3$) ν_{max} 3433, 2967, 1754, 1527, 1539, 1130 cm^{-1}; ^{1}H-NMR (400 MHz, $CDCl_3$) 1.38 (6H, d, $J_{12,11;13,11}$ 6.8 Hz, CH_3-12,13), 2.47 (3H, s, CH_3-15), 2.61 (3H, s, CH_3-14), 3.70 (1H, hept, $J_{11,12;11,13}$ 6.8 Hz, H-11), 7.10 (2H, d, $J_{4',5';8',7'}$ 7.2 Hz, H-4',8'), 7.26 (2H, overlapped, H-2,3), 7.32 (2H, t, $J_{5',4';7',8'}$ 7.6 Hz, H-5',7'), 7.46 (2H, overlapped, H-6',NH-2'), 7.75 (1H, s, H-8), 7.99 (1H, s, H-5); ^{13}C NMR (100 MHz, $CDCl_3$) 17.1 (CH_3-15), 19.4 (CH_3-14), 23.6 (CH_3-12,13), 28.4 (CH-11), 116.7 (CH-8), 118.7 (CH-6'), 121.2 (CH-3), 123.9 (CH-4',8'), 125.7 (CH-5), 126.3 (CH-2), 129.0 (C-6), 129.1 (CH-5',7'), 129.3 (C-1'), 129.9 (C-10), 131.6 (C-1), 132.5 (C-9), 137.5 (C-3'), 142.1 (C-4), 147.2 (C-7); HRESIMS *m/z* 334.18054 $[M + H]^+$ (calcd for $C_{22}H_{24}NO_2$, 334.18070).

4.5 Biological studies

4.5.1 Cell cultures

HaCaT cells (human keratinocytes) were obtained from CLS Cell Lines Service GmbH (Germany), HaCaT-ARE-Luc, (human keratinocytes), NIH-3T3-KBF-Luc (mouse fibroblasts), HeLa-STAT3-Luc (human cervix carcinoma) cell lines were constructed in our lab and the characterization of the cells has been previously described.[27] NIH-3T3-NucLight-Red cells were also generated in our lab by infection with a lentivirus encoding a nuclear restricted Red Fluorescent Protein under the EF-1□ promoter and

selected with puromycin. All the cell lines were grown in supplemented DMEM medium containing 10% fetal bovine serum and 1% penicillin/streptomycin antibiotics, at 37ºC in a humidified atmosphere of 5% CO_2.

4.5.2. Luciferase Assays

For the anti-NF-κB activity NIH-3T3-KBFLuc cells were stimulated with TNFα (30 ng/mL) in the presence or the absence of the compounds for 6 h. For the activation of the antioxidant response element that is activated by Nrf2, HaCaTARE-Luc cells were stimulated with the compounds for 6 h. For the anti-STAT3 activity HeLa-STAT-3-Luc cells were stimulated with IFN-γ (25 IU/mL) in the presence or the absence of the compounds for 6 h. After the treatment the cells were washed twice in PBS and lysed in 25 mM Tris-phosphate pH 7.8, 8 mM MgCl2, 1 mM DTT, 1% Triton X-100, and 7% glycerol during 15 min at RT in a horizontal shaker. After centrifugation, luciferase activity in the supernatant was measured using a GloMax 96 microplate luminometer (Promega) following the instructions of the luciferase assay kit (Promega, Madison, WI, USA). For NF-κB inhibition the RLU was calculated and the results were expressed as percentage of inhibition of NF-κB activity induced by TNFα (100% activation). For STAT3 inhibition the RLU were calculated and results were expressed as percentage of inhibition of STAT3 activity induced by IFN-γ (100% activation). The specific Nrf2 activation was expressed as fold induction over basal levels (untreated cells). The experiments for each concentration of the compounds were performed in triplicate wells.

4.5.3 Cellular antioxidant activity

The intracellular accumulation of ROS was detected by fluorometry using the free radical sensor 5-(and-6)-chloromethyl-2',7'-dichlorosihydrofluorescein diactetate, acetyl ester (CM-H2DCFDA) (Life Technologies). HaCaT cells (1 x 10^4/well) were seeded the day before the assay in a 96-well plate using DMEM supplemented with 10% FBS. After 24 hours cells were pre-incubated with the compounds for 30 min and ROS production was induced with 0.4 mM Tert-butyl-hydroperoxide (TBHP) (Sigma-Aldrich, Saint Louis, USA). After 3 hours cells were incubated with CM-H2DCFDA at a concentration of 10 μM during 30 min at 37ºC. ROS production was measured by changes in fluorescence using the Incucyte FLR software; the data were analyzed by the total green object integrated intensity (GCUxμm^{2}xWell) of the imaging system IncuCyte HD (Essen BioScience).

4.5.4 Western Blots

NIH-3T3-KBF-Luc cells were treated with increasing concentrations of either compound **13** or with SC514, an IKKβ inhibitor, during 15 min at 37ºC and subsequently stimulated with TNFα (30 ng/mL) for 20 min at 37ºC. Total cell content was extracted in 100 µL of lysis buffer (20 mM Hepes pH 8.0, 10 mM KCl, 0.15 mM EGTA, 0.15 mM EDTA, 0.5 mM Na3 VO4, 5 mM NaF, 1 mM DTT, leupeptin 1 mg/mL, pepstatin 0.5 mg/mL, aprotinin 0.5 mg/mL, and 1 mM PMSF) containing 0.5% NP-40. After incubation of the lysate at 4 °C during 15 min, proteins were obtained by centrifugation at 13000 rpm (4 °C for 10 min), boiled in Laemmli buffer and electrophoresed in 10% SDS polyacrylamide gels. Separated proteins were transferred to PVDF membranes. Blots were blocked in TBS solution containing 0.1% Tween 20 and 5% nonfat dry milk overnight at 4 °C. Primary antiphospho-IκBα (#9246, Cell Signaling Technology) and anti-αTubulin antibodies (Sigma-Aldrich) were employed to detect specific proteins.

4.5.5 Cytotoxic Assays over Human cancer cell lines and gingival fibroblasts

The cytotoxic effects of semi-synthetic derivatives were evaluated on tumor cells provided by the National Cancer Institute (USA) and on human gingival fibroblasts (HGF), applying the protein-binding dye sulforhodamine B (SRB) in a microculture assay to measure cell growth.[28] Colon (HCT-15), breast (MCF-7), leukemia (K-562), central nervous system (U-251, Glia), lung (SK-LU-1), and prostate cancer (PC-3) cells were cultured in RPMI-1640, and HGF were cultured in DMEM, both supplemented with 10% fetal bovine serum, 2 µM L-glutamine, 100 IU/mL penicillin G, 100 µg/mL streptomycin sulfate, and 0.25 µg/ mL amphotericin B and were maintained at 37 °C in a 5% CO_2 atmosphere with 95% humidity. For the assay, 100 µL/well of cell suspension containing 5×10^4 cells/mL (K-562, MCF-7), 7.5×10^4 cells/mL (U-251, PC-3, SK-LU-1), 10×10^4 cells/mL (HCT-15, HGF), were seeded in 96-well microtiter plates and incubated to allow cell attachment. After 24 h, 100 µL of each test compound or positive control was added (all test substances were dissolved in DMSO). After 48 h, adherent cell cultures were fixed in situ by adding 50 µL of cold 50% (w/v) aqueous trichloroacetic acid (TCA) and incubated for 60 min at 4 °C. The supernatant was discarded, and the plates were washed three times with water and then dried. Cultures fixed with TCA were stained for 30 min with 100 µL of 0.4% SRB solution. Protein-bound dye was extracted with 10 µM unbuffered Tris base, and optical densities were

measured at 515 nm on an Ultra microplate reader (Elx808, Bio-Tek Instruments, Inc.). The results were expressed as percentages of inhibition of cell proliferation at a concentration of 50 μM or as IC_{50} values (μM inhibitory concentration at which 50% of cell proliferation is inhibited), estimated by linear regression equations of dose-response curves.

4.5.6 Statistical analysis

Data analysis was performed using at least three independent experiments. For NF-κB, Nrf2 and ROS inhibition reporting results, sample population means were compared against control population means in an unpaired two-tailed Student's t test. A p value < 0.05 was considered statistically significant. NF-κB IC_{50} calculations were performed using the GraphPad Prism Program (Graph Pad Software, San Diego, CA, USA).

4.6 Molecular docking

7-Hydroxy-3,4-dihydrocadalene, 7-hydroxycadalene and compound **13** structures were built using previoulsly reported X-ray crystallography data.[16] Geometries were optimized applying the semi-empirical quantum mechanical method PM3. MGL tools 1.5.4 with AutoDock 4.2[29] were used to set up and perform blinded docking calculations between compounds and IKKβ crystal structure (PDB ID: 4kik).[21,30] Molecules were docked over the entire protein to identify its binding sites. For docking calculations, Lamarckian genetic algorithms (LGA) were implemented in AutoDock 4.2. The final positions of the compounds were ranked by lowest interaction energy values (docking score expressed in Kcal/mol). H-bond interactions between the compounds and protein were explored. The output obtained from AutoDock was further analyzed with PyMOL software package. Validation of the employed computational protocol was established through comparison of docking results carried out using data of co-crystallized ligand (staurosporine analog K252a) bound to the IKKβ subunit, with the docking pose of experimental crystal data [21] (Figure S44, Supporting Information). A docked pose with a RMSD <2 Å is considered acceptable.[31]

References and notes

1. Coussens, L. M.; Werb, Z. *Nature* **2002**, 420, 860.
2. Mantovani, A.; *Nature*. **2005**, 435, 752.
3. Mantovani, A.; Allavena, P.; Sica, A.; Balkwill, F.; *Nature* **2008**, 454, 436.
4. Karin, M.; *Nature* **2006**, 441, 431.
5. Pikarsky, E.; Porat, R.M.; Stein, I.; Abramovithc, R.; Amit, S.; Kasem, S.; Gutcovich-Pyest, E.; Urieli-Shoval, S.; Galun, E.; Ben-Neriah, Y. *Nature* **2004**, 431, 461.
6. Yu, H.; Lee, H.; Herrmann, A.; Buettner, R.; Jove, R. *Nat. Rev. Cancer*. **2014**, 14, 736.
7. Hayes, J. D.; Dikova-Kostova, A. T. *Trends Biochem Sci*. **2014**, 39, 199.
8. Sporn, M. B.; Liby, K. T. *Nat. Rev. Cancer*. **2012**, 12, 564.
9. Kashfi, K. *Adv Pharmacol*. **2009**, 57, 31.
10. Thun, J. T.; Henley, S. J.; Patrono, C. *J. Natl. Cancer Inst.* **2002**, 94, 252.
11. Bremner, P.; Heinrich, M. *J. Pharm. Pharmacol*. **2002**, 54, 453.
12. Orlikova, B.; Legran, N.; Panning, J.; Dicato, M.; Diederich, M. *Cancer Treat Res*. **2014**, 159, 123.
13. Wright, M. H.; Sieber, S.A. *Nat Prod Rep*. **2016**, 33, 681.
14. Rodríguez-Chávez, J. L., Egas, V.; Linares, E.; Bye, R.; Hernández, T.; Espinosa-García, F. J.; Delgado, G. *J Ethnopharmacol* **2017**, 195, 39.
15. Delgado, G.; Olivares, M.; Chávez, M.; Ramírez-Apan, T.; Linares, E.; Bye, R.; Espinosa-García, F. *J. Nat. Prod*. **2001**, 64, 681.
16. Egas, V.; Toscano, R.; Linares, E.; Bye, R.; Espinosa-García, F.; Delgado, G. *J. Nat. Prod*. **2015**, 78, 2634.
17. Gilmore, T. D.; Herscovitch, M. *Oncogene* **2006**, 25, 6887.
18. Luqman, S.; Pezzuto, J. M. *Phytother. Res*. **2010**, 24, 949.
19. Gilmore, T. D. *Oncogene* **2006**, 25, 6680.
20. Mercurio, F.; Zhu, H.; Murray, B. W.; Shevchenko, A.; Bennett, B. L.; Li, J. W.; Young, D. B.; Barbosa, M.; Mann, M.; Manning, A.; Rao. A. *Science* **1997**, 278, 860.
21. Liu, S.; Misquitta, Y. R.; Olland, A.; Johnson, M. A.; Kelleher, K. S.; Kriz, R.; Lin, L. L.; Stahl, M.; Mosyak, L. *J. Biol. Chem*. **2013**, 288, 22758.

22. Saito, A.; Yamashita, T.; Mariko, Y.; Nosaka, Y.; Tsuchiya, K.; Ando, T.; Suzuki, T.; Tsuruo, T.; Nakanishi, O. *Proc. Natl. Acad. Sci. USA*. **1999**, 96, 4592.
23. Snodgrass, R.; Collier, A. C.; Coon, A. E.; Pritsos, C. A. *J. Biol. Chem*. **2010**, 285, 19068.
24. Ebrahim, H. Y.; Mohyeldin, M. M.; Hailat, M. M.; El Sayed, K. A. *Bioorg. Med. Chem*. **2016**, 24, 5748.
25. Ghosh, A. K.; Brindisi, M. *J. Med. Chem*. **2015**, 58, 2895.
26. Rodríguez-Chávez, J. L.; Rufino-Gonzáles, Y.; Ponce-Macotela, M.; Delgado, G. *Parasitology* **2015**, 142, 576.
27. Del Prete, D.; Millán, E.; Pollastro, F.; Chianese, G.; Luciano, P.; Collado, J. A.; Munoz, E.; Appendino, G.; Taglialatela-Scafati, O. *J. Nat. Prod*. **2016**, 79, 267.
28. Monks, A.; Scudiero, D.; Skehan, P.; Shoemaker, R.; Paull, K.; Vistica, D.; Hose, C.; Langley, J.; Cronise, P.; Vaigro-Wolff, A.; GrayGoodrich, M.; Campbell, H.; Mayo, J.; Boyd, M. *J. Natl. Cancer Inst*. **1991**, 83, 757.
29. Morris, G. M.; Goodsell, D. S.; Halliday, R. S.; Huey, R.; Hart, W. E.; Belew, R. K.; Olson, A. J. *J. Comput. Chem*. **1998**, 19, 1639.
30. Schrödinger, L. The PyMOL Molecular Graphics System. **2004**.
31. Carugo, O.; Pongor, S. *Protein Sci*. **2001**, 10, 1470.

Table 1. Primary screening of some natural cadinane-type sesquiterpenoids on three molecular targets involved in inflammation and carcinogenesis. A minimal value of 50% of inhibition of NF-κB or STAT3 activation and at least two fold inductions over Nrf2 pathway at a concentration of 50 μM was considered as positive result.

Compound	NF-κB inhibition	Nrf2 activation	STAT3 inhibition
1	+	+	–
2	+++	–	–
3	–	–	–
4	–	–	–
5	–	–	–
6	–	–	–
7	–	–	–
8	–	–	–
9	–	–	–
10	–	–	–

Table 2. Cytotoxic effects of semi-synthetic derivatives against six human cancer cell lines and its activity on specific targets involved in inflammation and carcinogenesis.

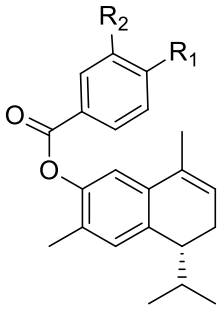

11-21

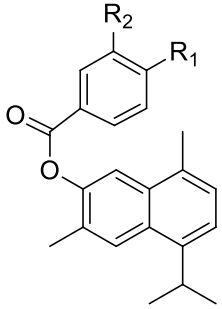

22-31

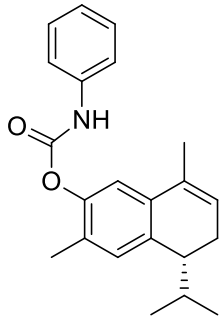

32

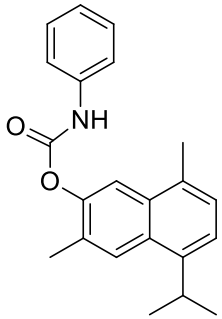

33

Compound	**Substituent**		**Percentage of inhibition of cell proliferation at a concentration of 50 µM** [IC_{50}, µM]						**Activity in transcription factors pathways at a concentration of 50 µM** Results are represented as the mean ± standard deviation of at least three different experiments		
	R_1	**R_2**	**U-251**	**PC-3**	**K-562**	**HCT-15**	**MCF-7**	**SK-LU-1**	**NF-κB inhibition** (percentage)	**Nrf2 activation** (fold induction)	**STAT3 inhibition** (percentage)
11	H	H	25.8	22.5	NC	49.5	60.7	37.0	47.2±5.3	6.6±0.5	2.4±0.8
12	Cl	H	25.6	34.1	58.9	47.4	79.7	17.4	36.1±3.2	1.3±0.4	2.7±1.0
13	CH_3	H	67.7	49.6	100	78.9	65.0	85.4	76.0±6.6	9.4±0.6	3.1±0.2

					[30.94±2.2]	[40.32±4.1]		[33.88±2.2]			
14	OCH_3	H	37.0	60.6 [32.17±2.5]	46.5	30.8	80.1	18.6	49.2±4.5	1.9±0.4	1.8±0.7
15	CF_3	H	14.7	12.3	9.0	6.4	40.4	NC	25.4±4.9	1.6±0.4	2.5±0.5
16	NO_2	H	16.8	36.7 [42.47±2.4]	89.0	67.8 [56.33±4.9]	72.9	47.5 [42.89±3.3]	7.2±3.9	8.5±0.7	1.6±0.3
17	H	Cl	0.9	23.4	NC	5.3	40.4	30.6	22.5±5.0	1.4±0.2	1.5±0.6
18	H	CH_3	16.8	38.6	NC	5.3	54.9	NC	44.2±6.7	1.7±0.4	2.3±0.6
19	H	OCH_3	NC	16.3	NC	NC	11.9	24.2	41.2±2.5	1.6±0.5	3.3±0.7
20	H	CF_3	29.3	25.4	45.5	15.0	86.0	18.3	4.4±4.1	1.9±0.2	1.7±0.5
21	H	NO_2	44.0	36.9	15.9	45.9	29.3	60.4	3.5±4.7	1.5±0.4	3.2±0.8
22	H	H	41.5	21.2	44.3	72.0	51.0	63.0	34.5±7.2	1.9±0.7	0.5±0.4
23	Cl	H	92.8 [35.45±0.7]	81.1 [44.01±3.6]	95.4 [19.08±1.8]	82.2 [33.95±1.1]	76.0 [32.13±3.0]	100 [23.85±2.2]	15.5±5.4	1.7±0.5	1.3±0.6
24	CH_3	H	100 [22.79±2.1]	72.3 [23.72±2.0]	100 [8.37±0.6]	86.5 [12.0±0.5]	90.2 [8.20±1.3]	100 [10.23±1.6]	30.3±2.9	1.8±0.3	2.9±0.7

25	OCH_3	H	42.6	10.4	88.6	84.0	93.4	32.8	26.9±4.8	1.3±0.2	2.5±0.8
26	CF_3	H	16.5	100 [34.04±3.5]	45.1	55.6	16.8	28.7	5.2±3.9	1.7±0.5	0.9±0.3
27	NO_2	H	100 [7.75±0.3]	100 [17.57±1.7]	100 [2.28±0.2]	97.6 [7.88±0.7]	100 [7.90±1.7]	100 [9.37±0.9]	18.5±3.0	1.8±0.3	1.6±0.6
28	H	CH_3	5.2	52.4 [47.13±0.7]	17.1	27.6	50.4	NC	4.8±2.7	1.8±0.6	2.0±0.3
29	H	OCH_3	NC	12.5	14.2	35.2	31.8	30.6	2.8±1.9	1.5±0.2	0.8±0.5
30	H	CF_3	NC	26.7	NC	NC	41.5	17.3	4.8±2.0	1.9±0.5	2.7±0.4
31	H	Cl	0.8	4.2	NC	NC	11.4	11.6	25.6±3.7	1.7±0.3	1.8±0.6
32	----		100 [0.46±0.03]	93.2 [7.93±0.6]	92.6 [0.30±0.04]	92.0 [0.03±0.01]	75.1 [4.05±0.1]	100 [0.12±0.01]	4.2±2.1	1.6±0.3	3.3±0.7
33	----		100 [15.78±1.6]	44.7 [8.62±1.1]	100 [13.97±0.4]	84.7 [3.88±0.5]	100	90.4 [10.05±0.8]	13.3±4.1	1.4±0.4	3.0±0.9
Cisplatin	----		3.31±0.6	8.30±0.7	5.34±1.2	10.02±1.0	9.43±1.1	2.03±0.1	----	----	----

U-251 = Central Nervous System (Glia) **PC-3** = Prostate **K-562** = Leukemia **HCT-15** = Colon **MCF-7** = Breast **SK-LU-1** = Lung **NC** = No cytotoxic

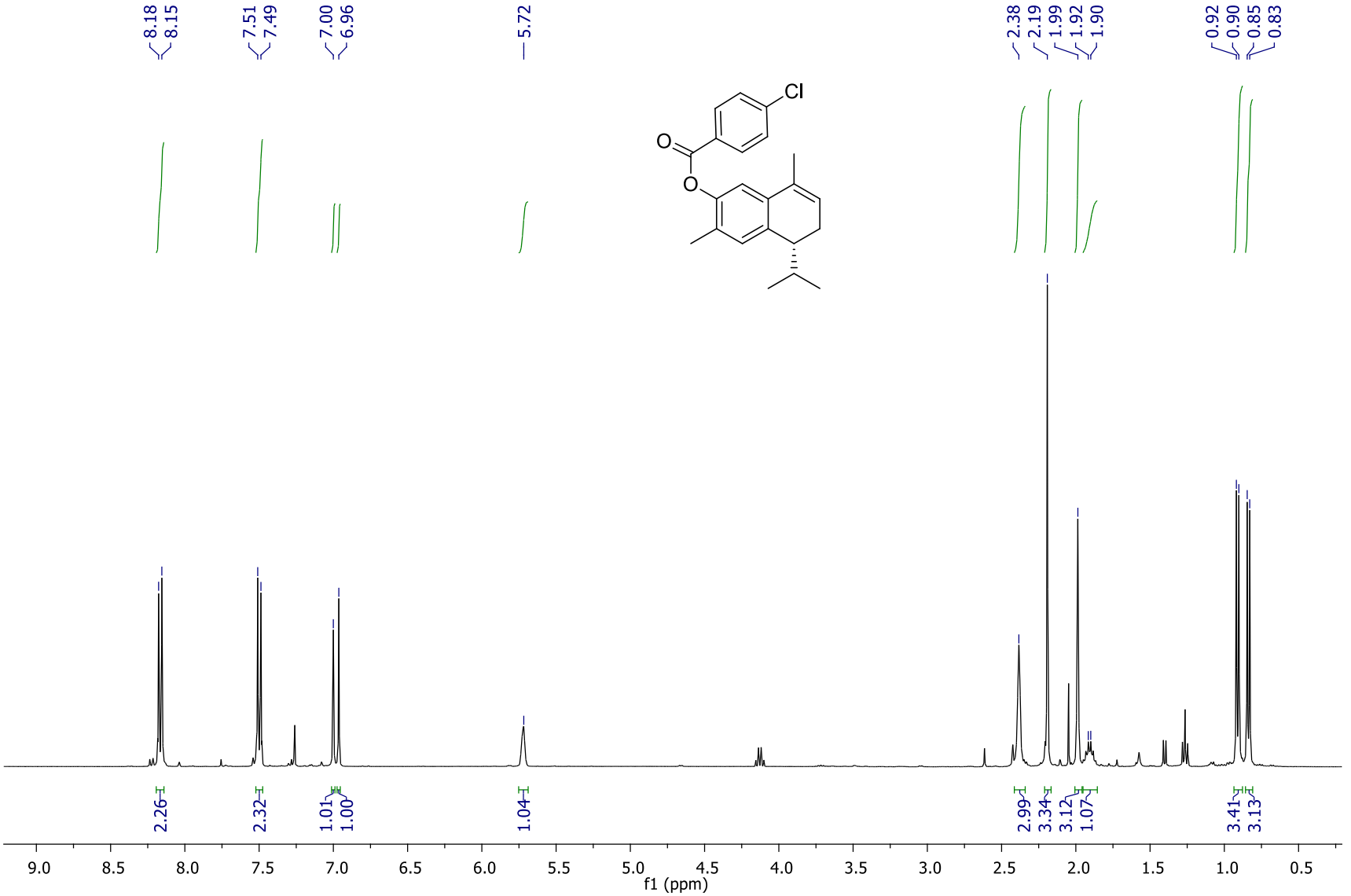

Espectro 1. RMN ^{1}H del compuesto **12** (400 MHz, $CDCl_3$).

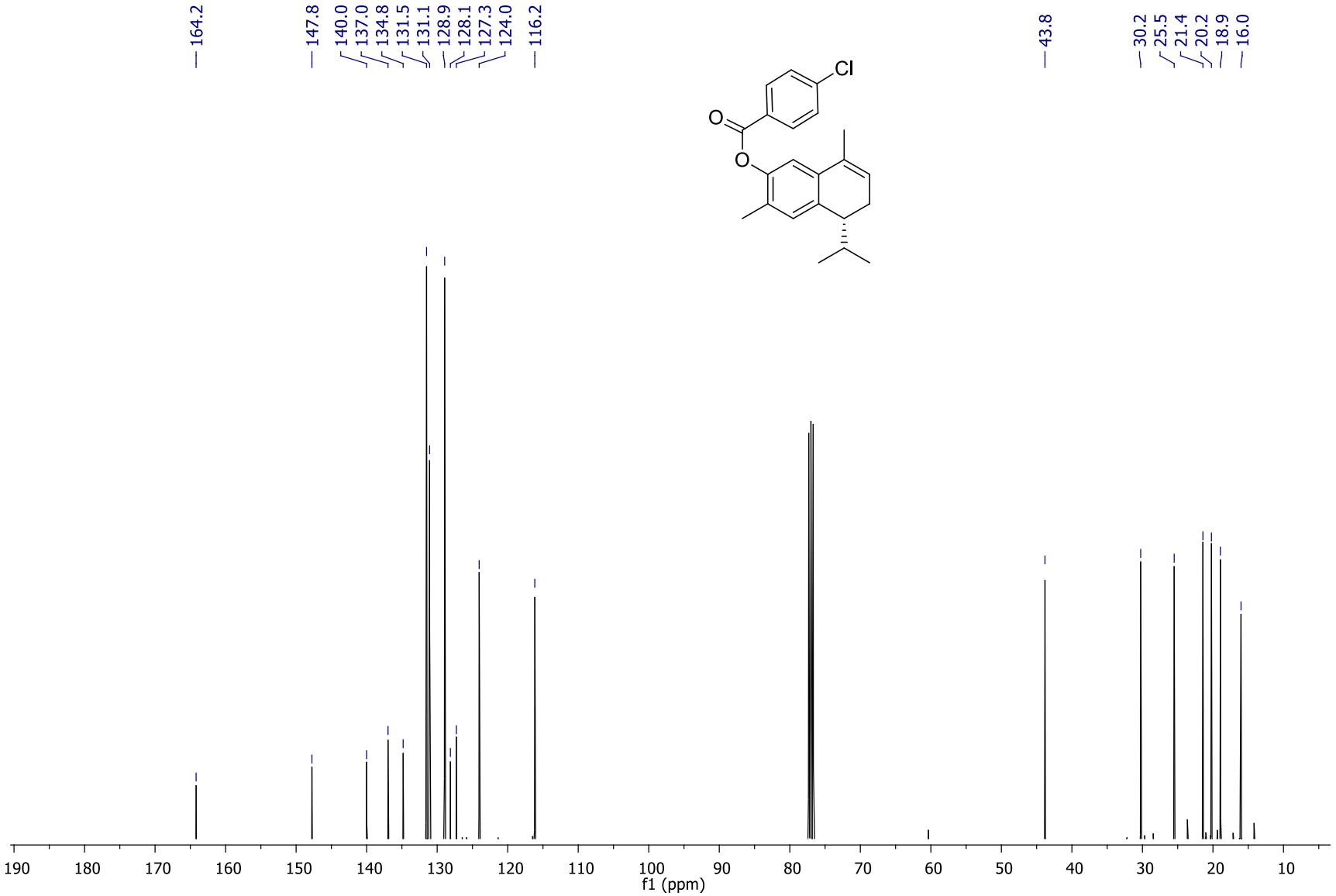

Espectro 2. RMN ^{13}C del compuesto **12** (100 MHz, $CDCl_3$).

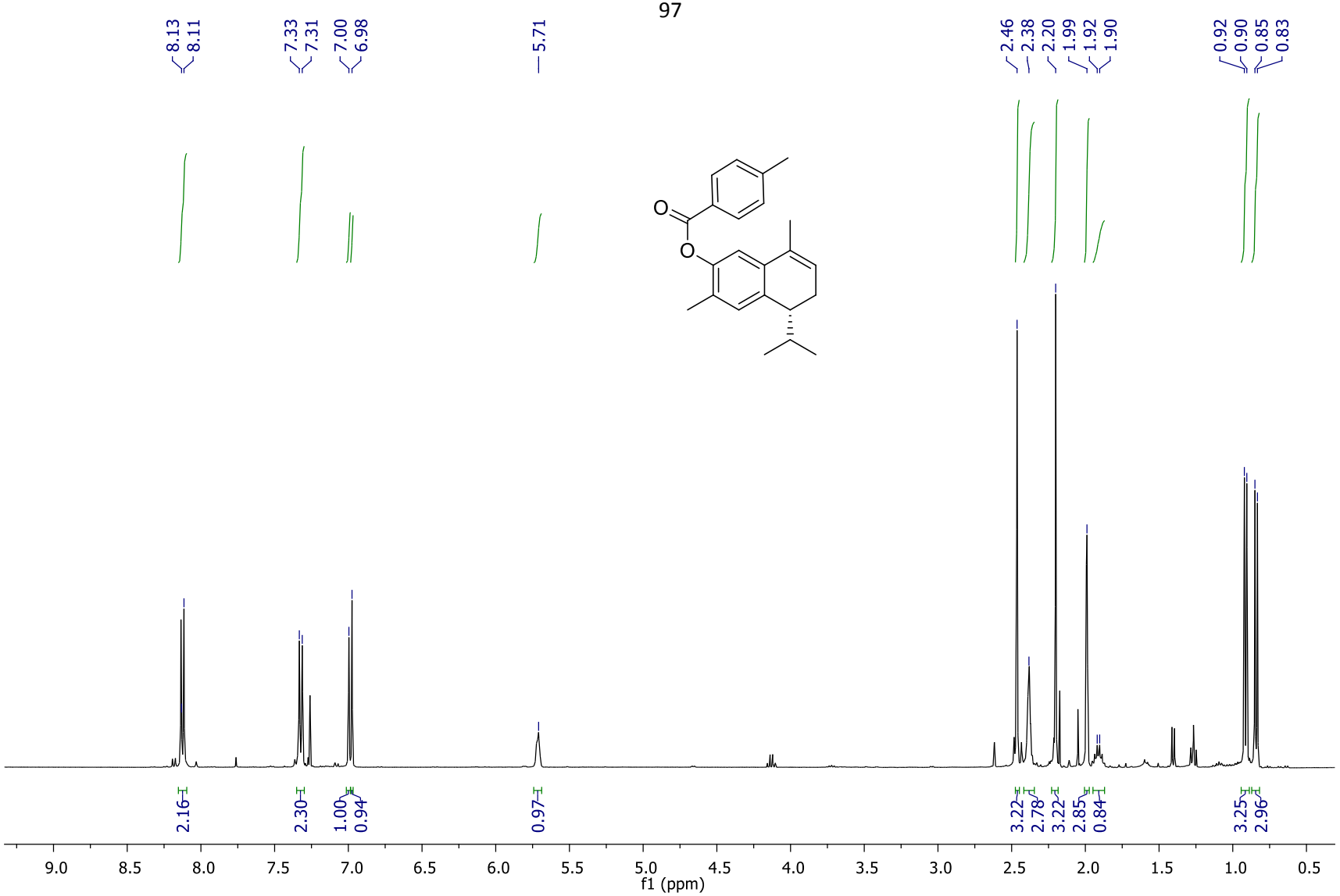

Espectro 3. RMN ^{1}H del compuesto **13** (400 MHz, $CDCl_3$).

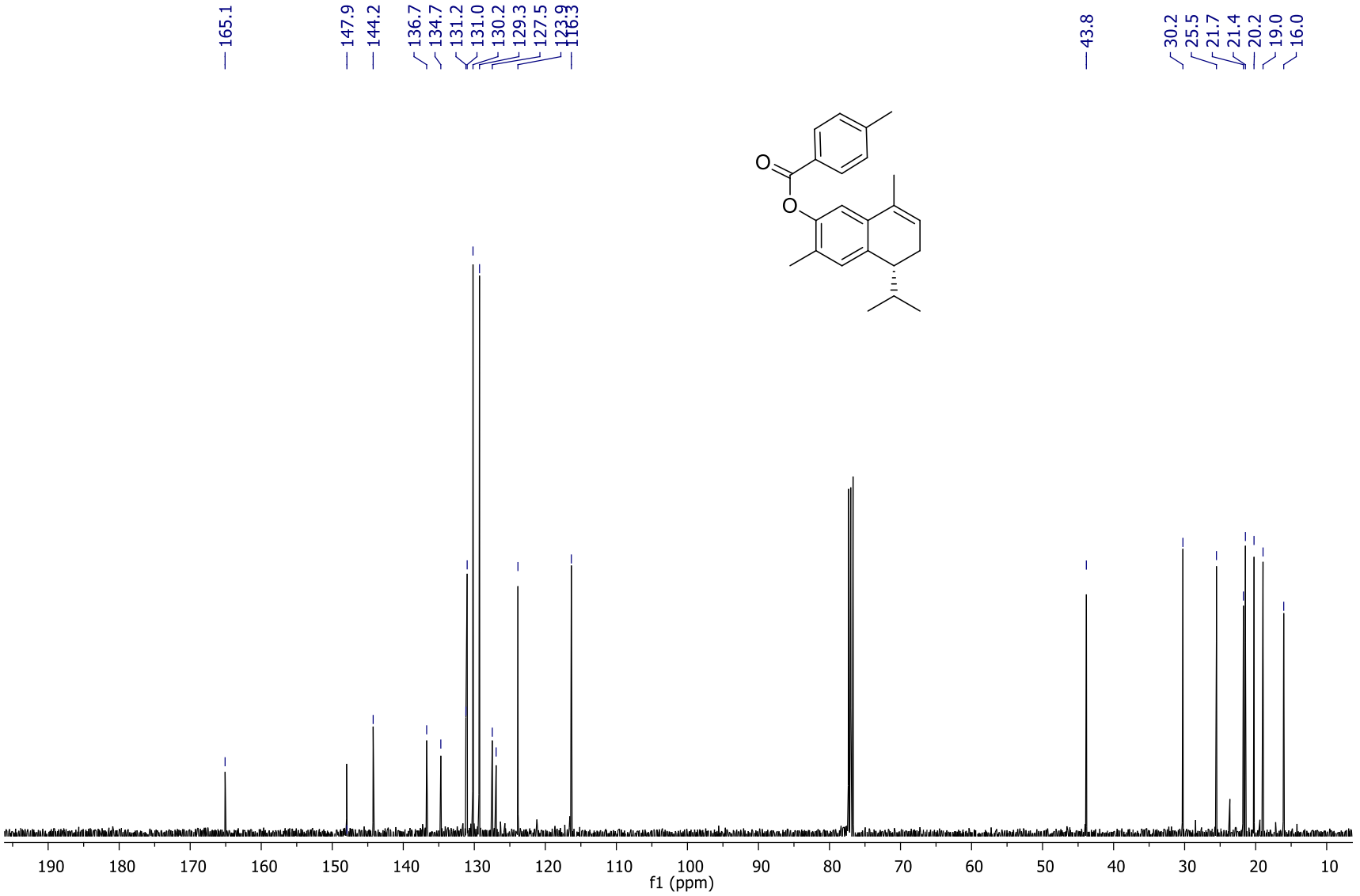

Espectro 4. RMN ^{13}C del compuesto **13** (100 MHz, $CDCl_3$).

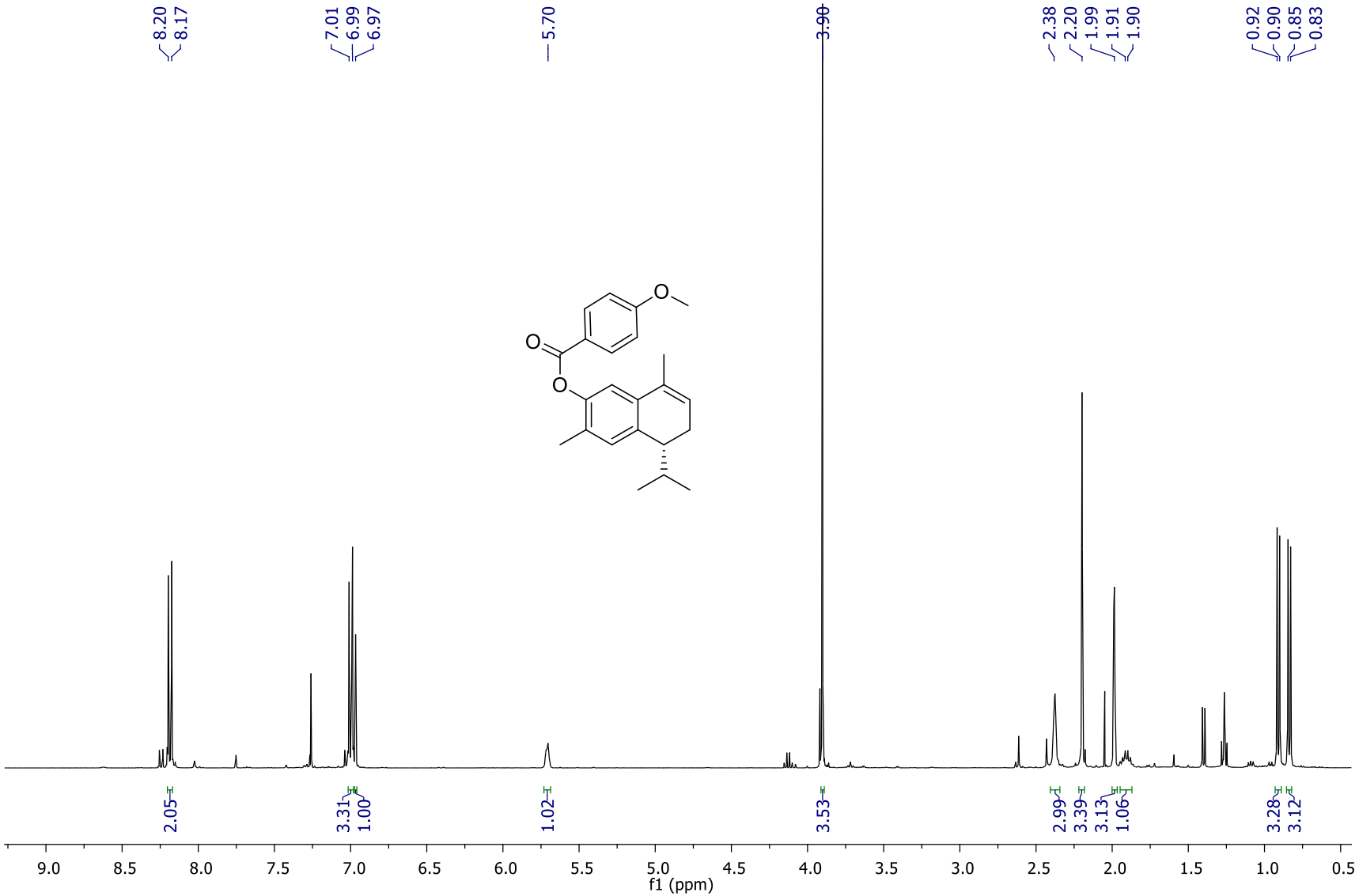

Espectro 5. RMN ^{1}H del compuesto **14** (400 MHz, $CDCl_3$).

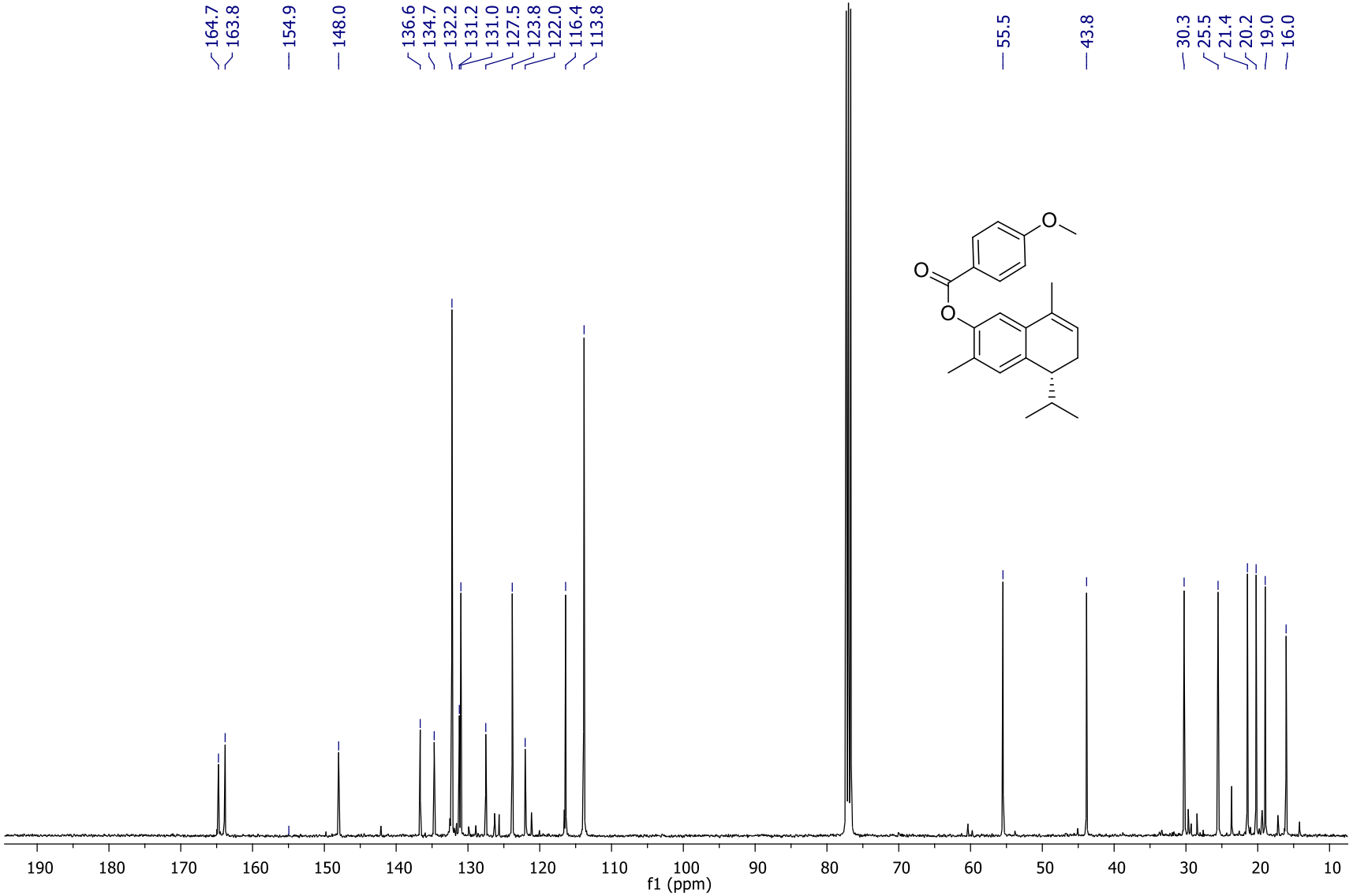

Espectro 6. RMN ^{13}C del compuesto **14** (100 MHz, $CDCl_3$).

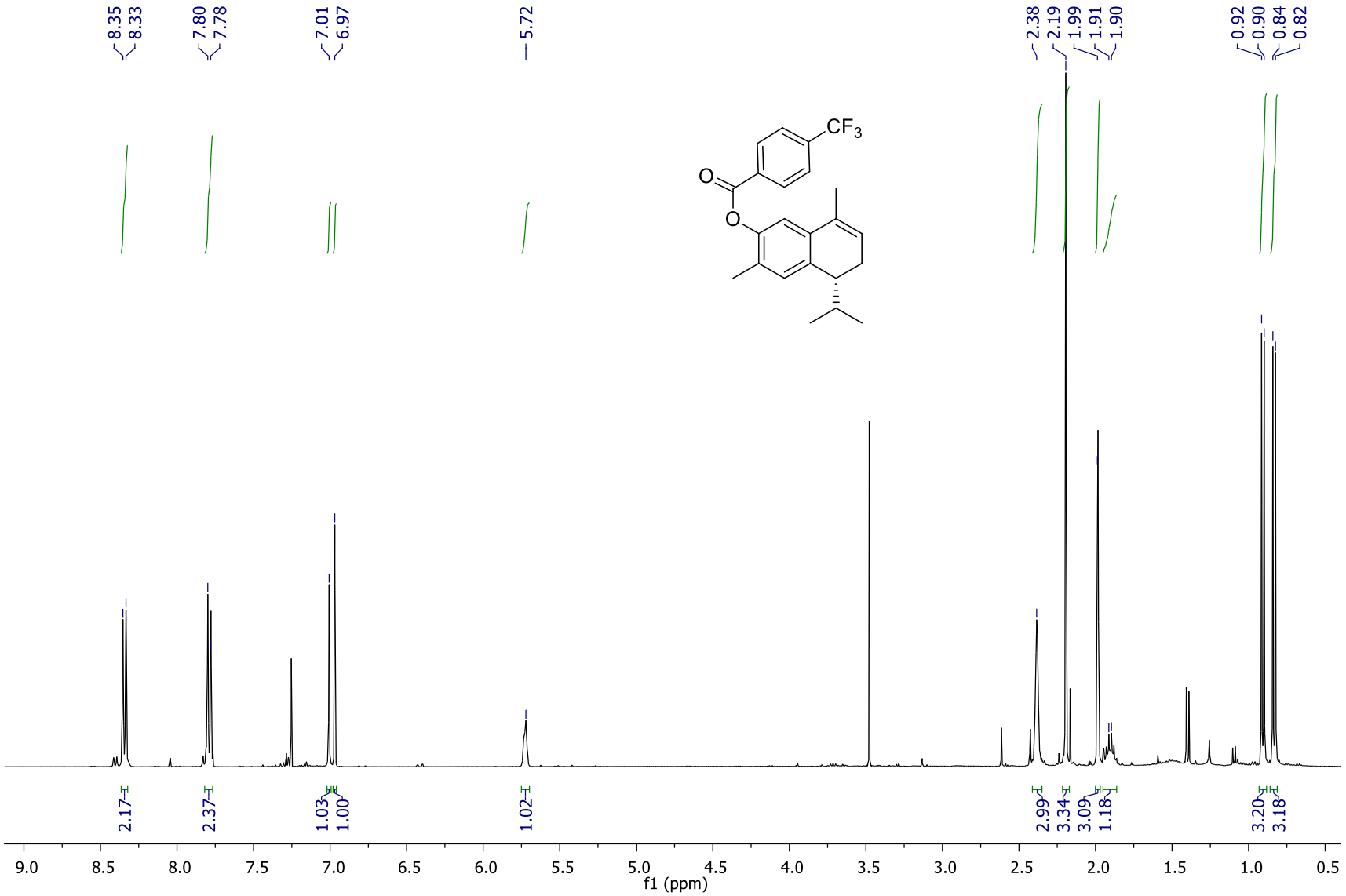

Espectro 7. RMN ^{1}H del compuesto **15** (400 MHz, $CDCl_3$).

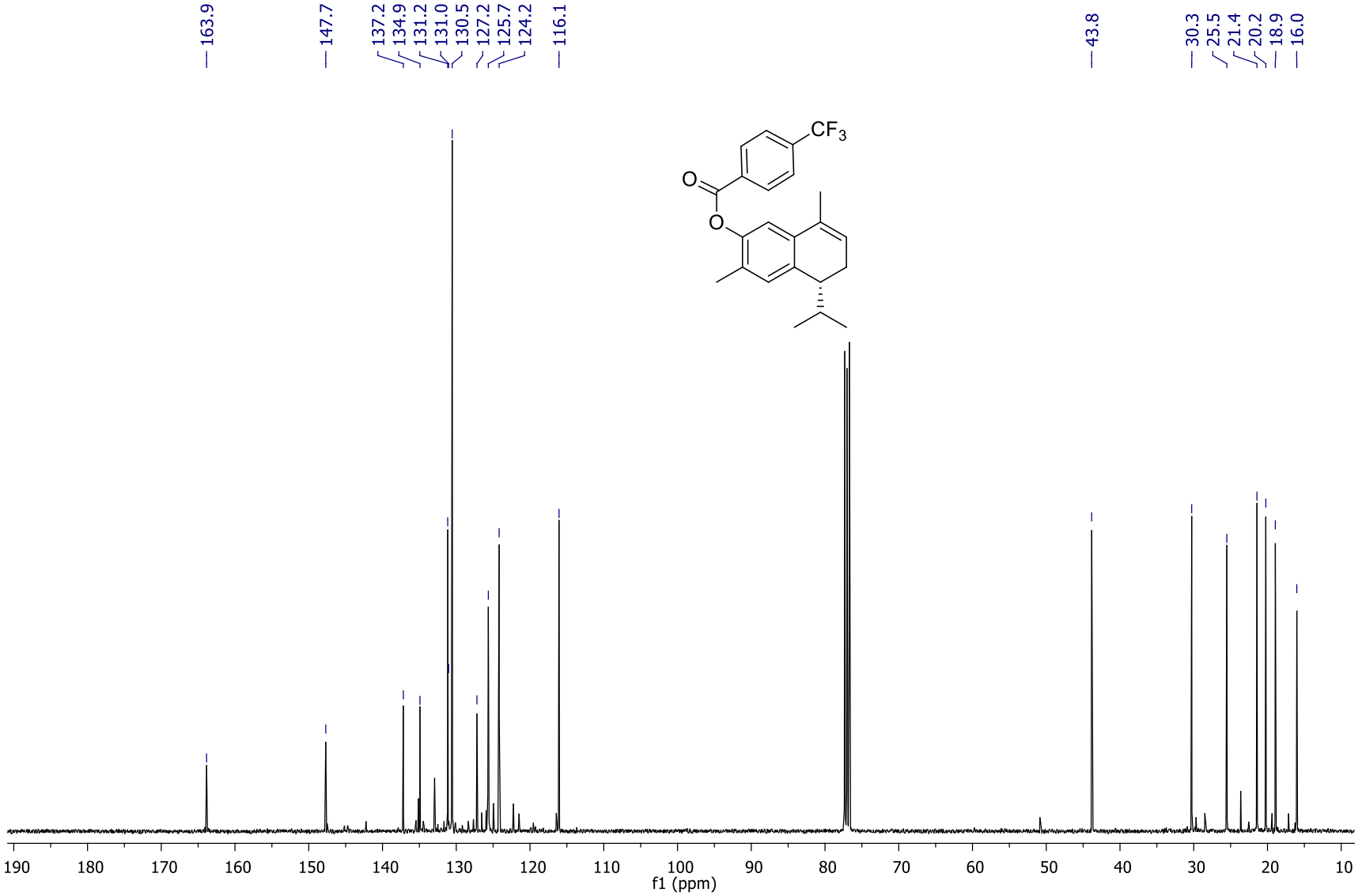

Espectro 8. RMN ^{13}C del compuesto **15** (100 MHz, $CDCl_3$).

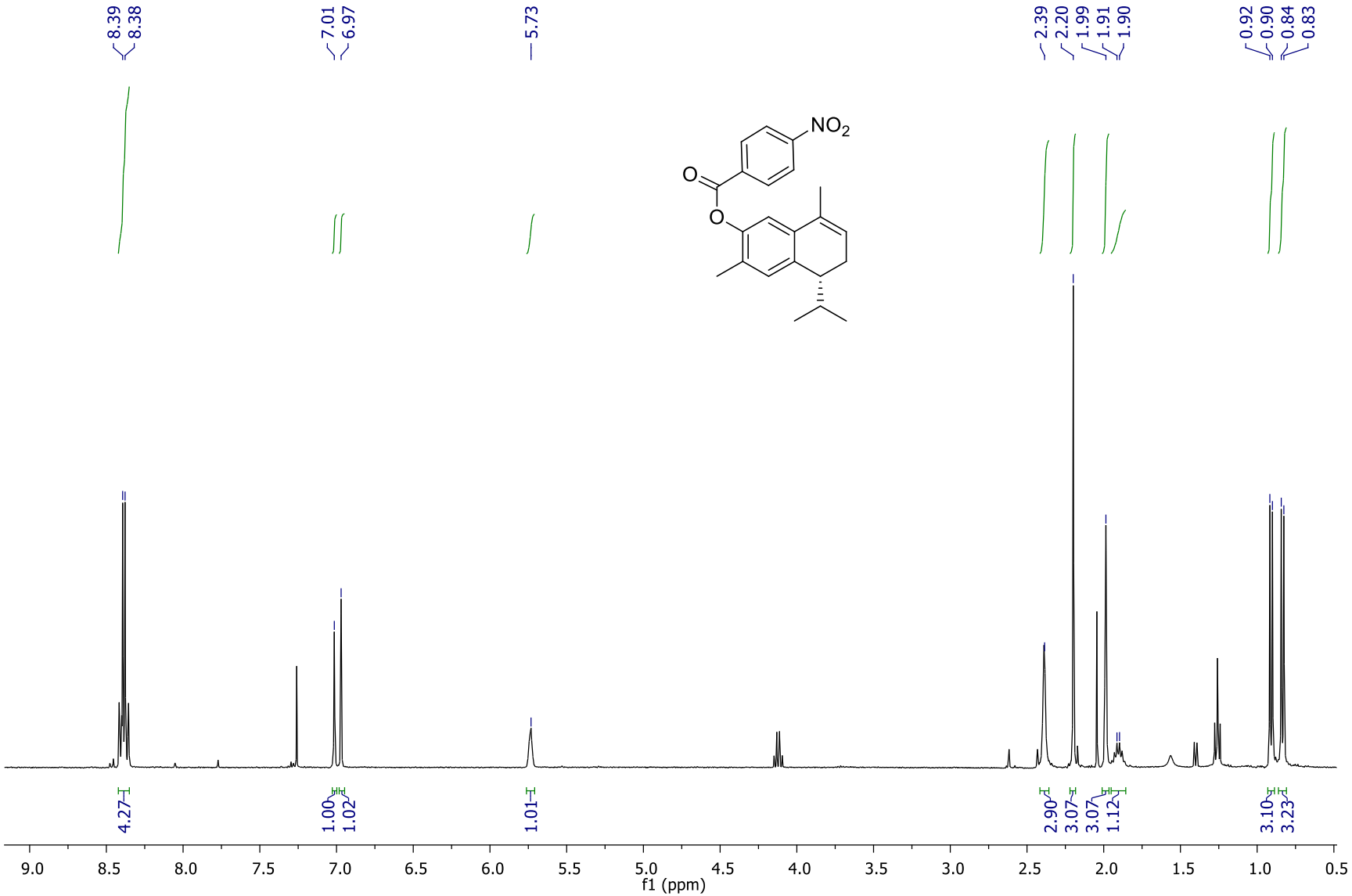

Espectro 9. RMN ^{1}H del compuesto **16** (400 MHz, $CDCl_3$).

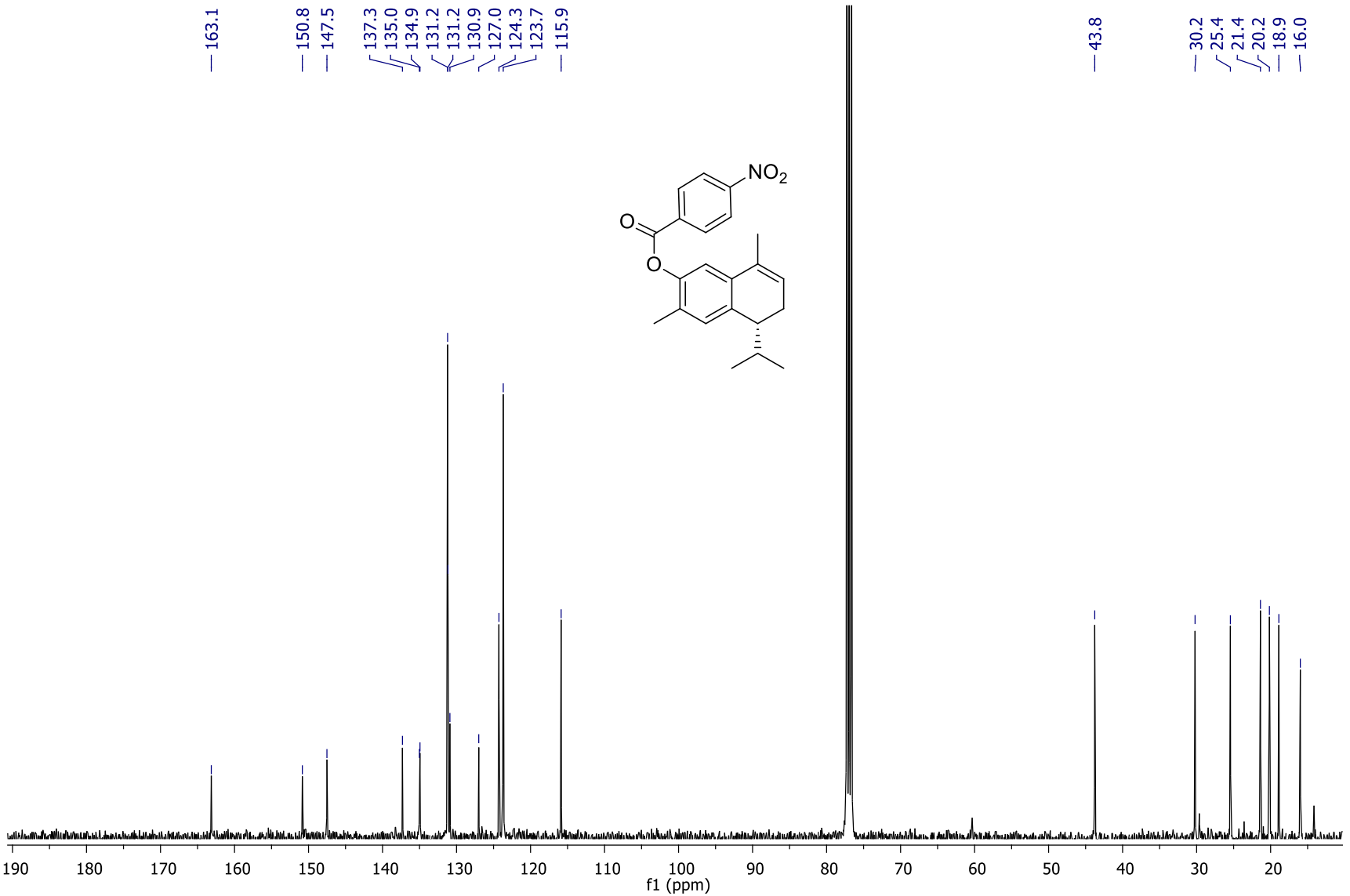

Espectro 10. RMN ^{13}C del compuesto **16** (100 MHz, $CDCl_3$).

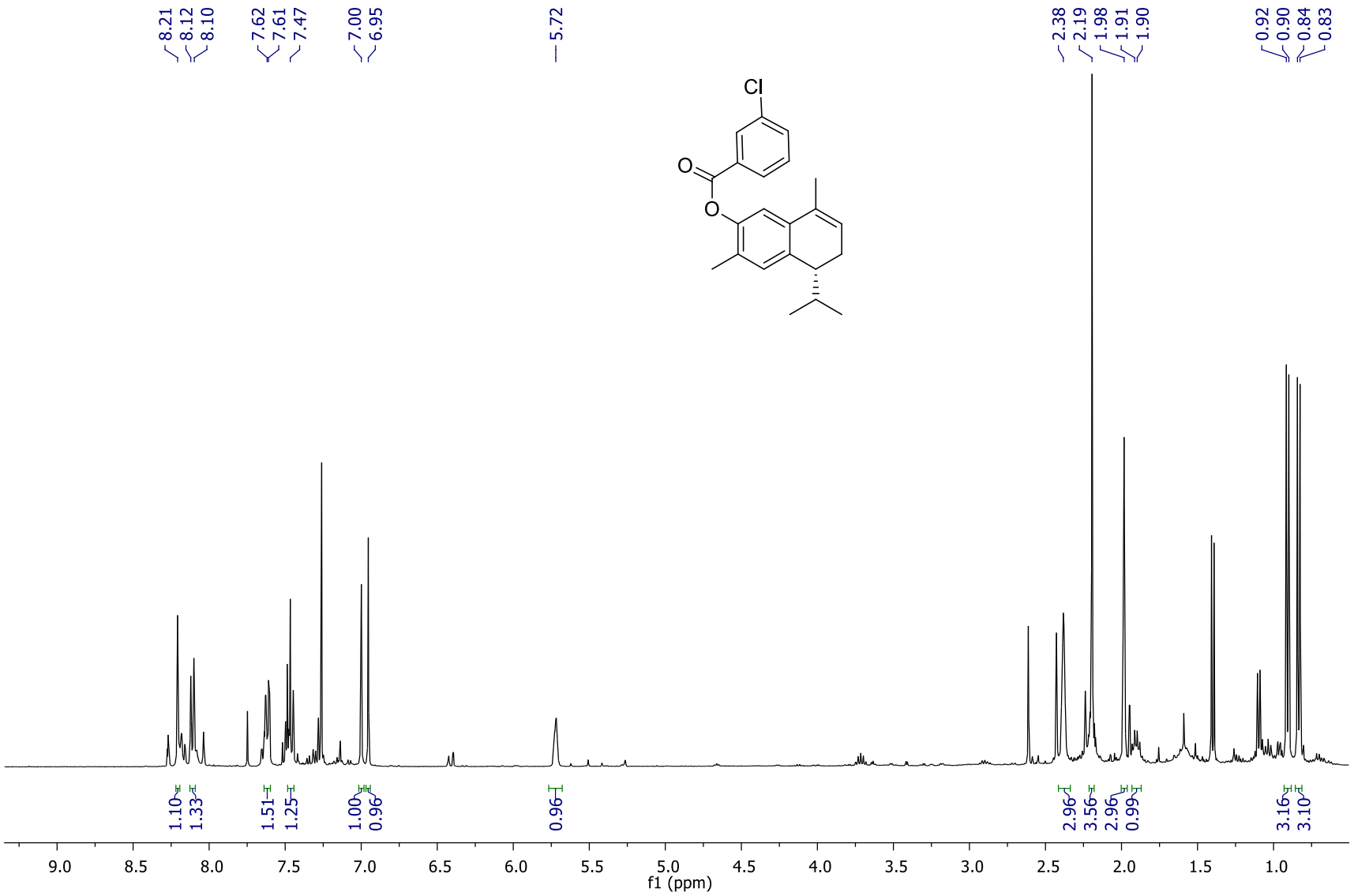

Espectro 11. RMN ^{1}H del compuesto **17** (400 MHz, $CDCl_3$).

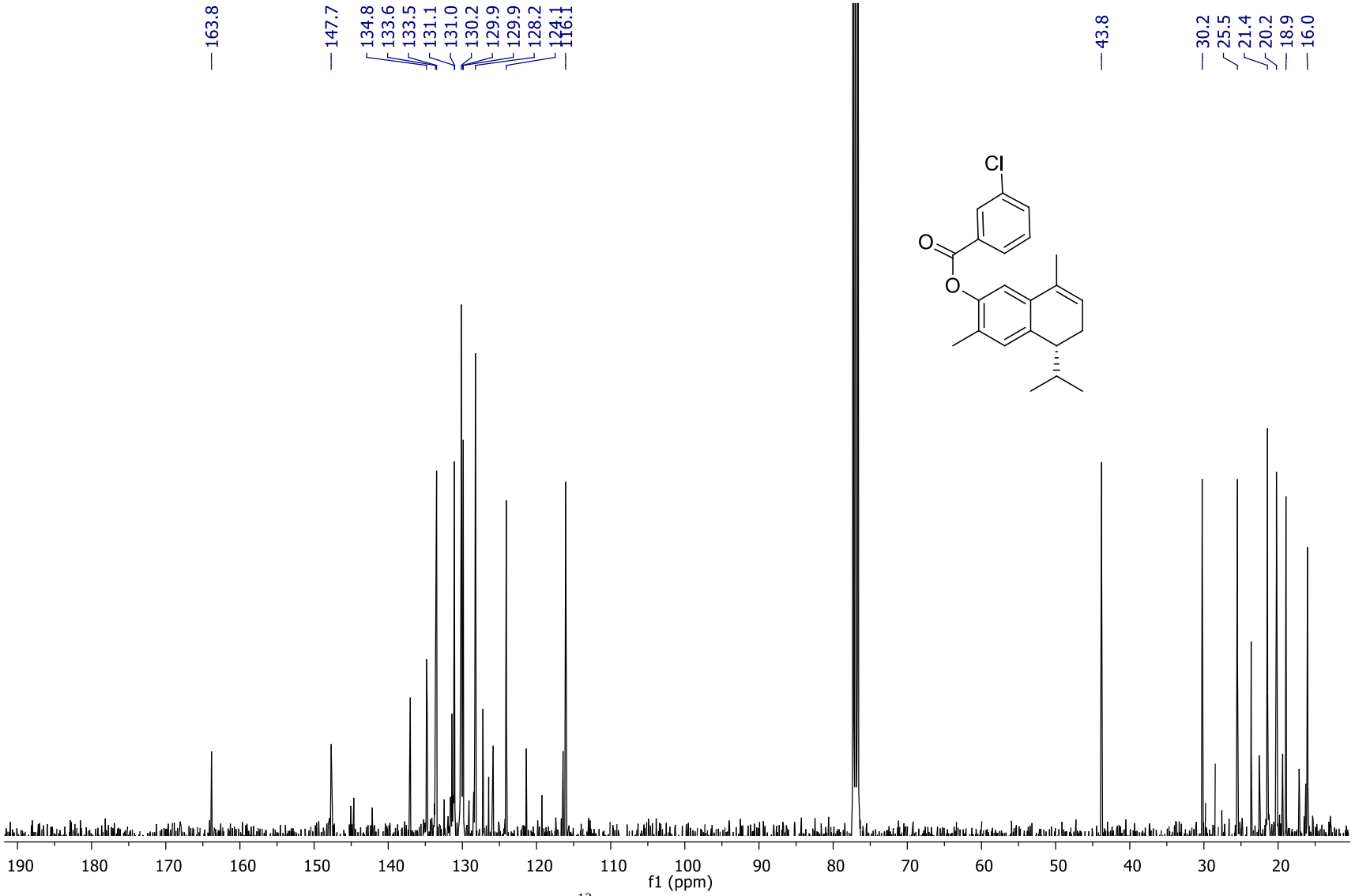

Espectro 12. RMN ^{13}C del compuesto **17** (100 MHz, $CDCl_3$).

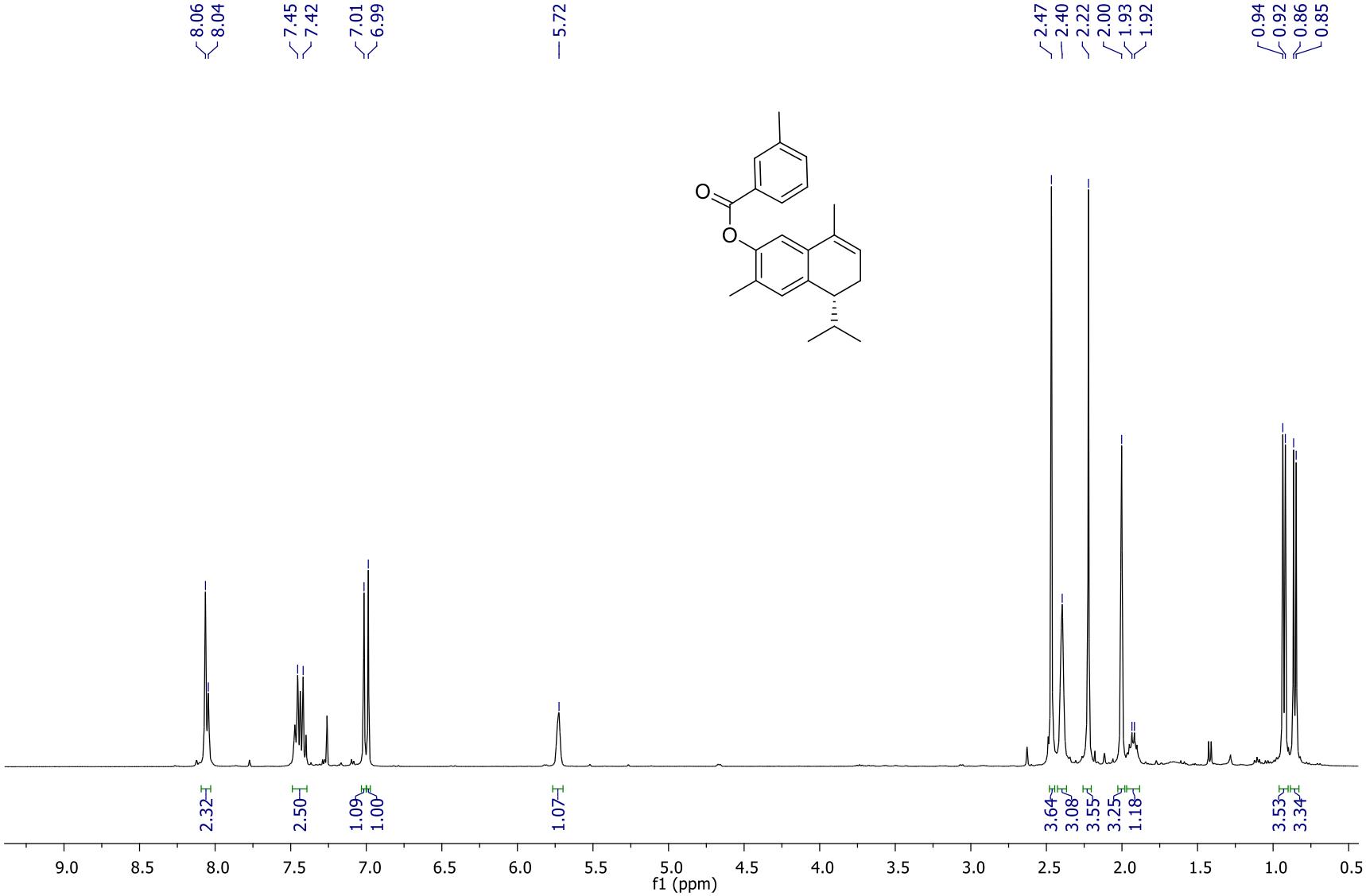

Espectro 13. RMN ^{1}H del compuesto **18** (400 MHz, $CDCl_3$).

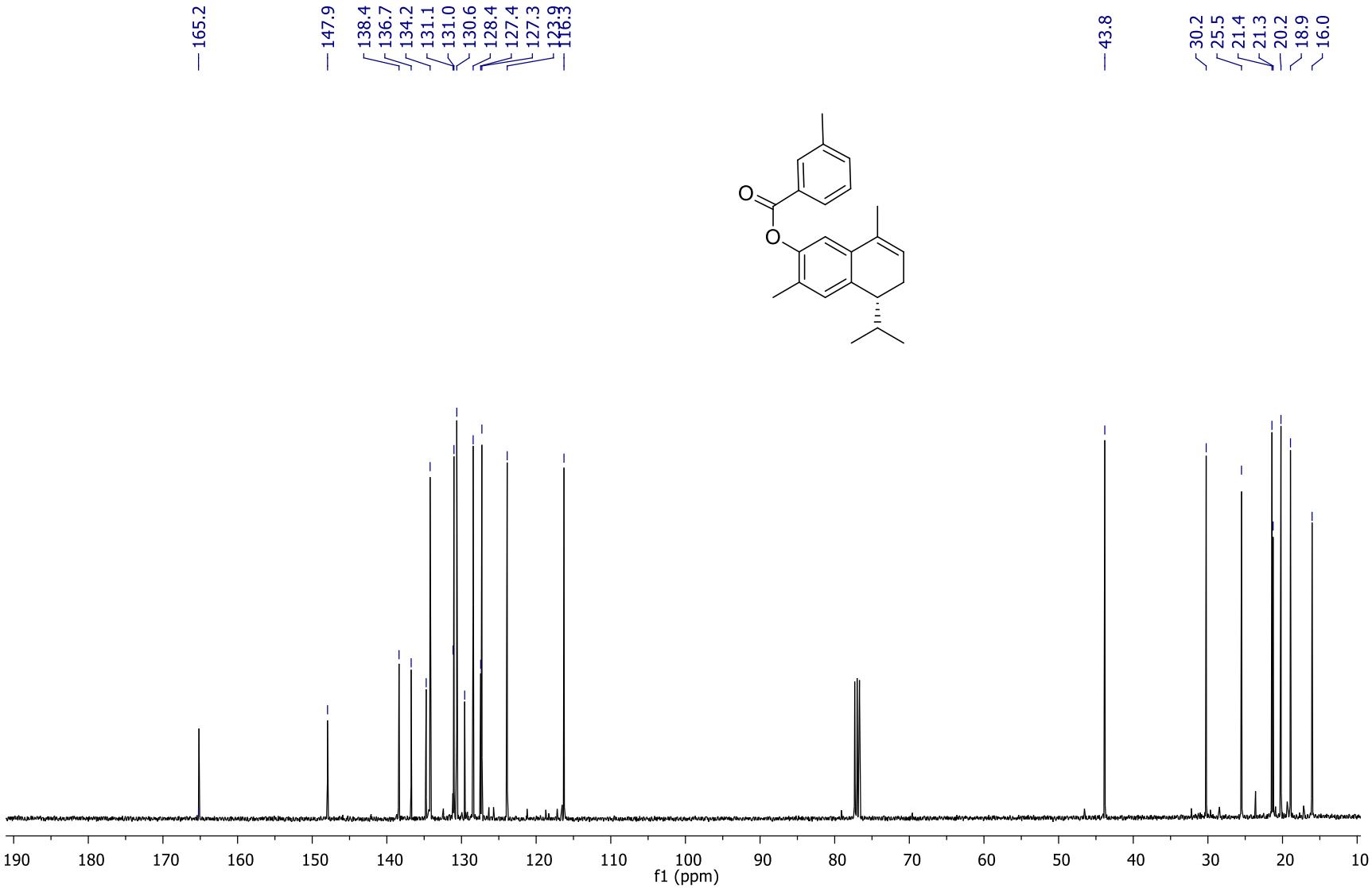

Espectro 14. RMN ^{13}C del compuesto **18** (100 MHz, $CDCl_3$).

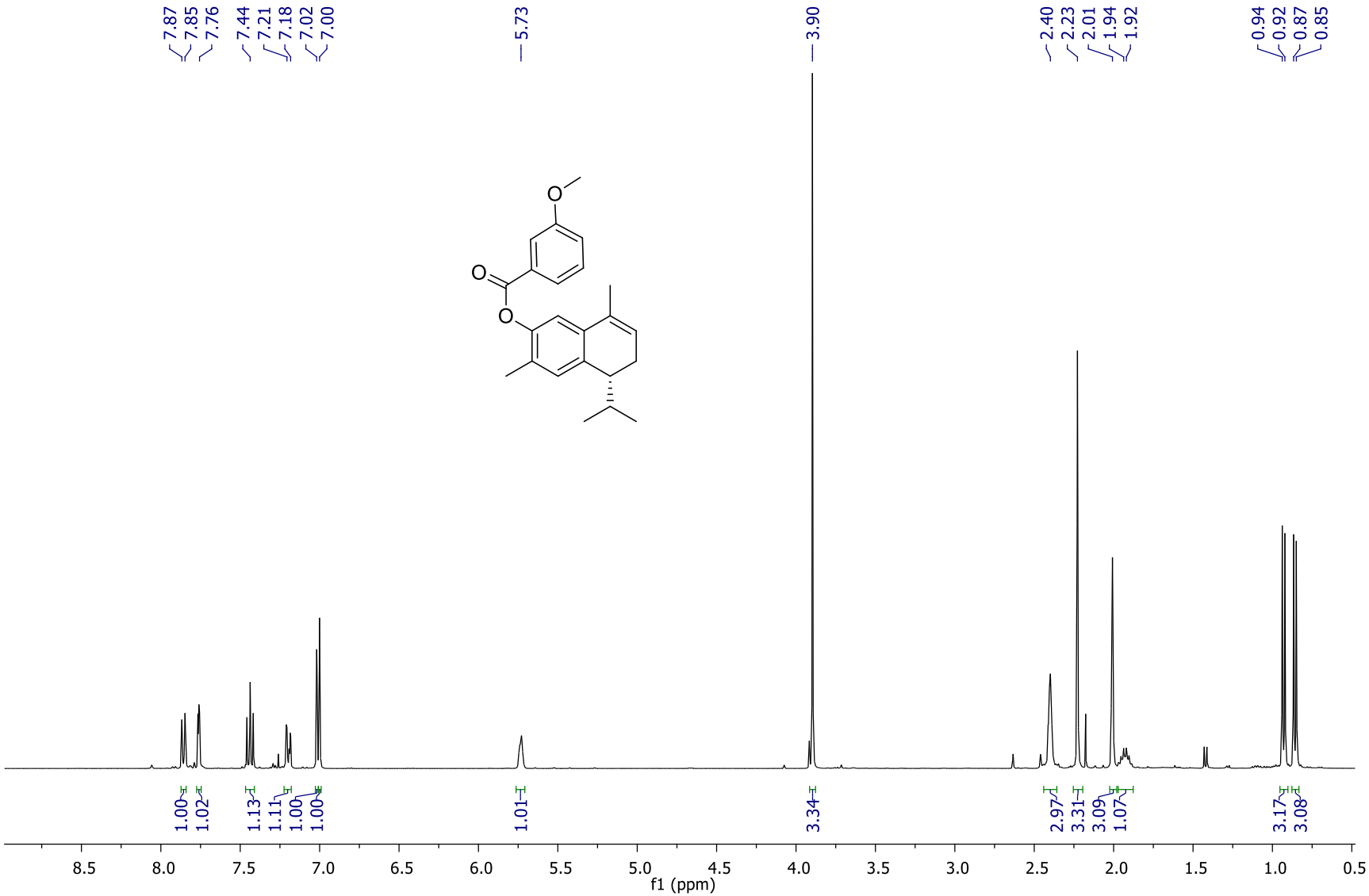

Espectro 15. RMN ^{1}H del compuesto **19** (400 MHz, $CDCl_3$).

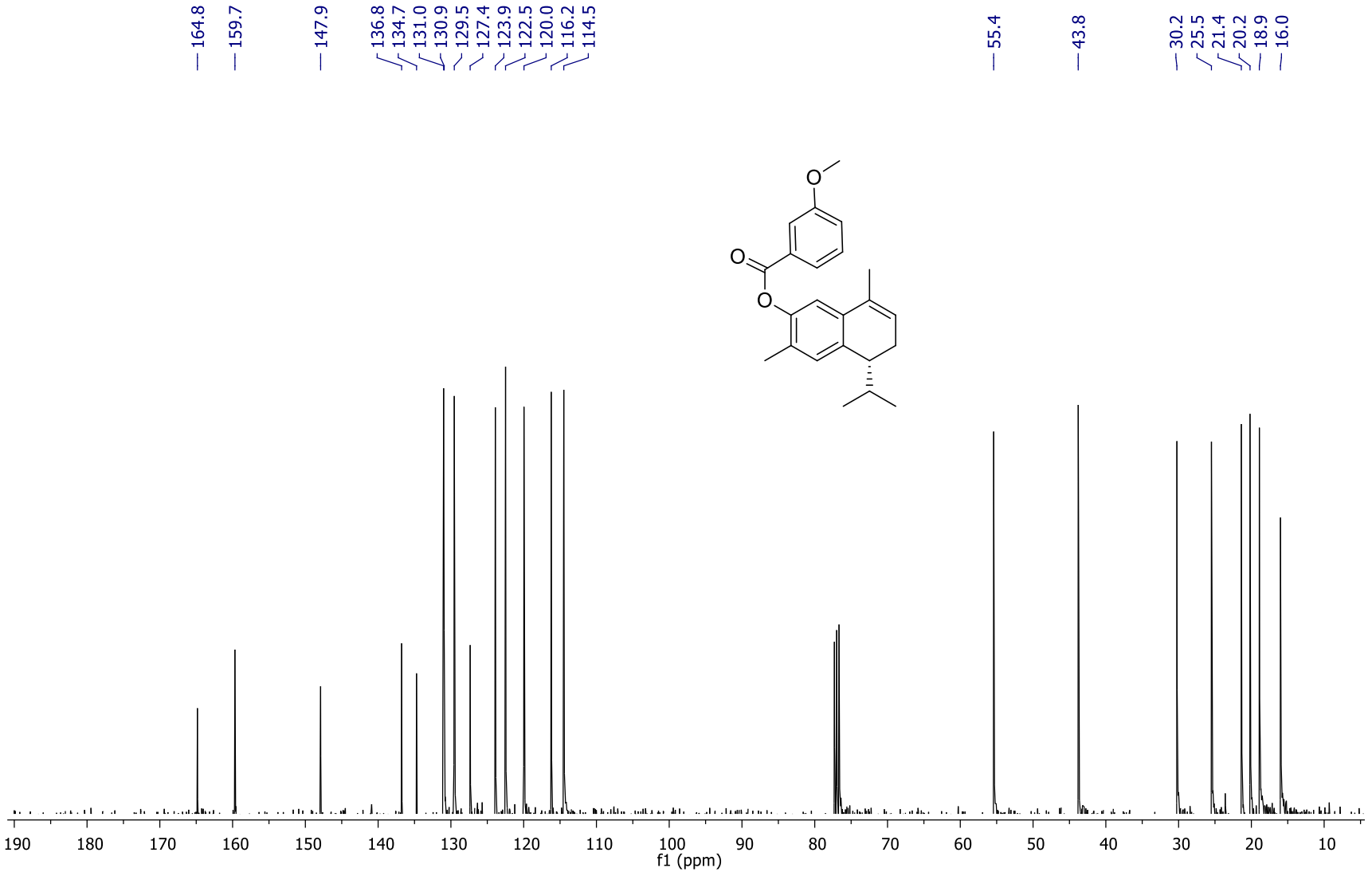

Espectro 16. RMN ^{13}C del compuesto **19** (100 MHz, $CDCl_3$).

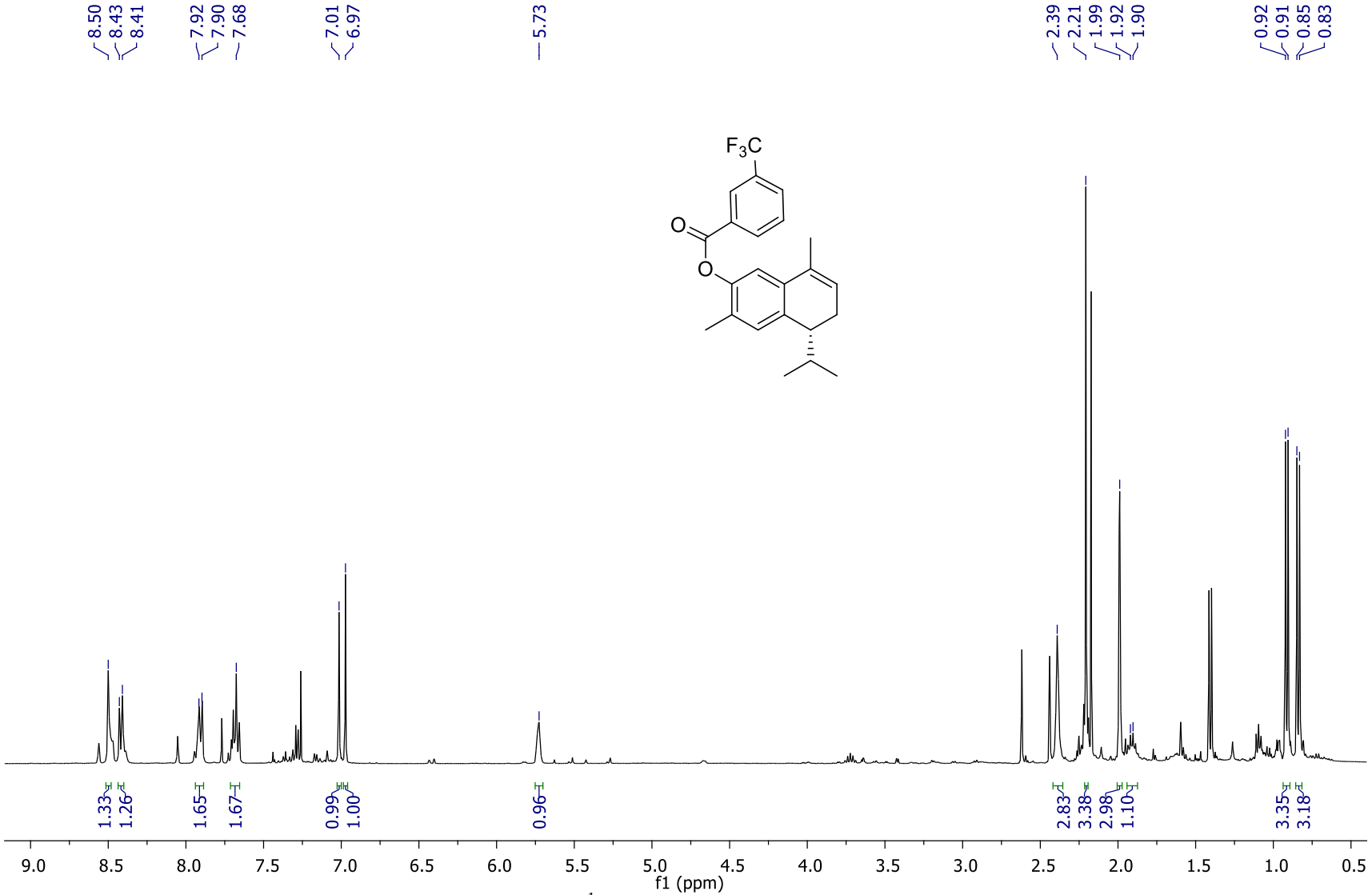

Espectro 17. RMN ^{1}H del compuesto **20** (400 MHz, $CDCl_3$).

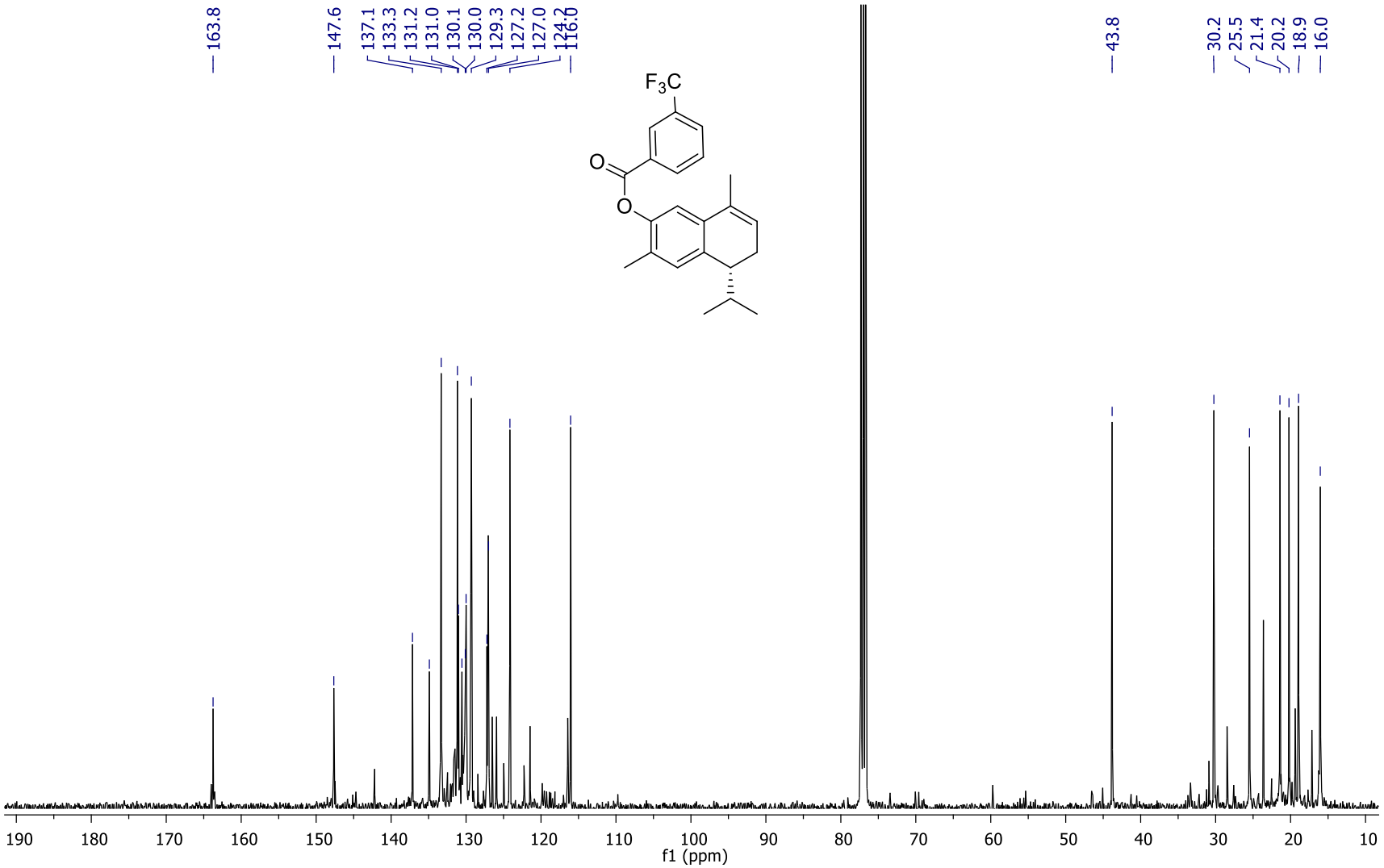

Espectro 18. RMN ^{13}C del compuesto **20** (100 MHz, $CDCl_3$).

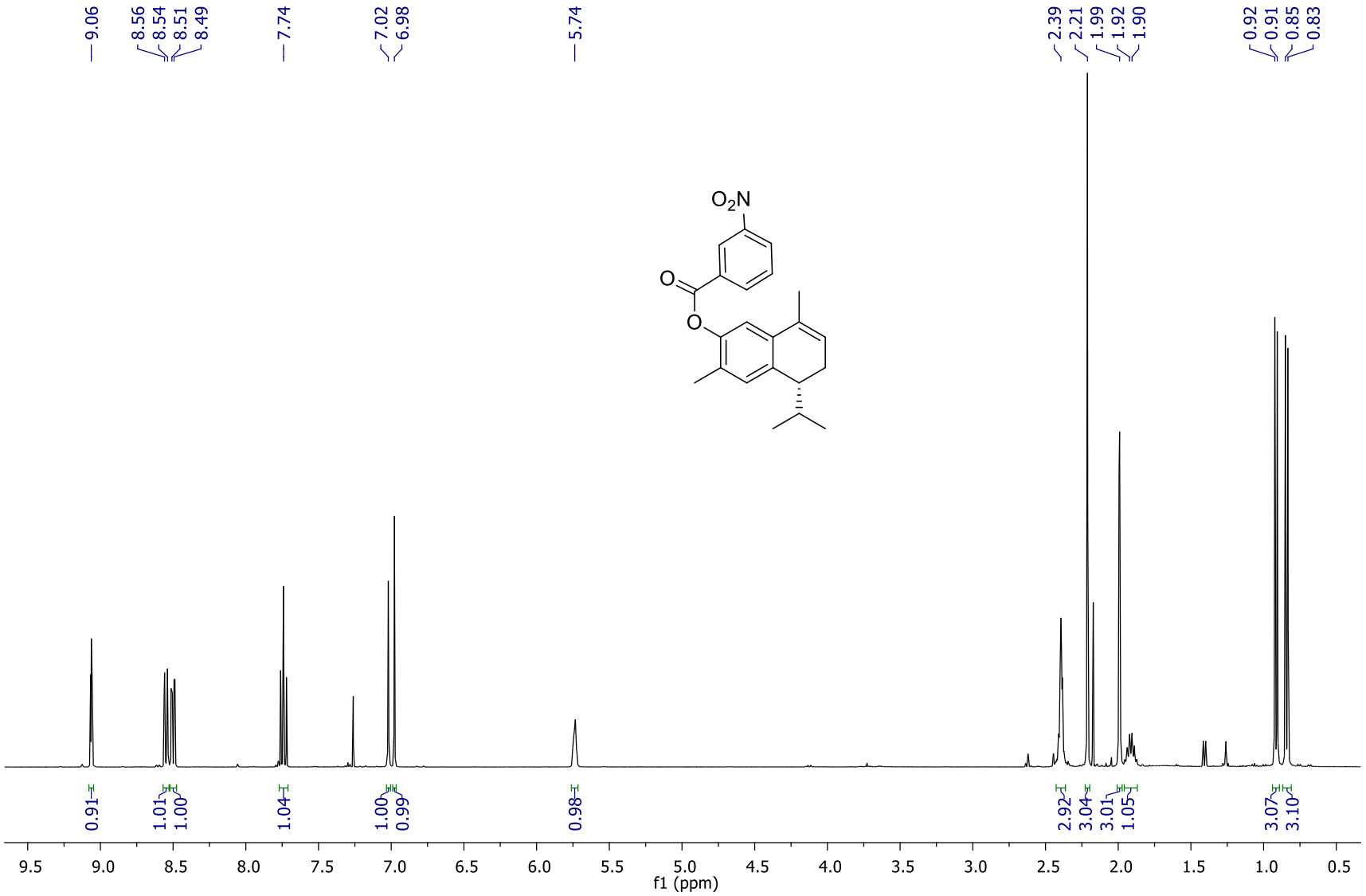

Espectro 19. RMN ^{1}H del compuesto **21** (400 MHz, $CDCl_3$).

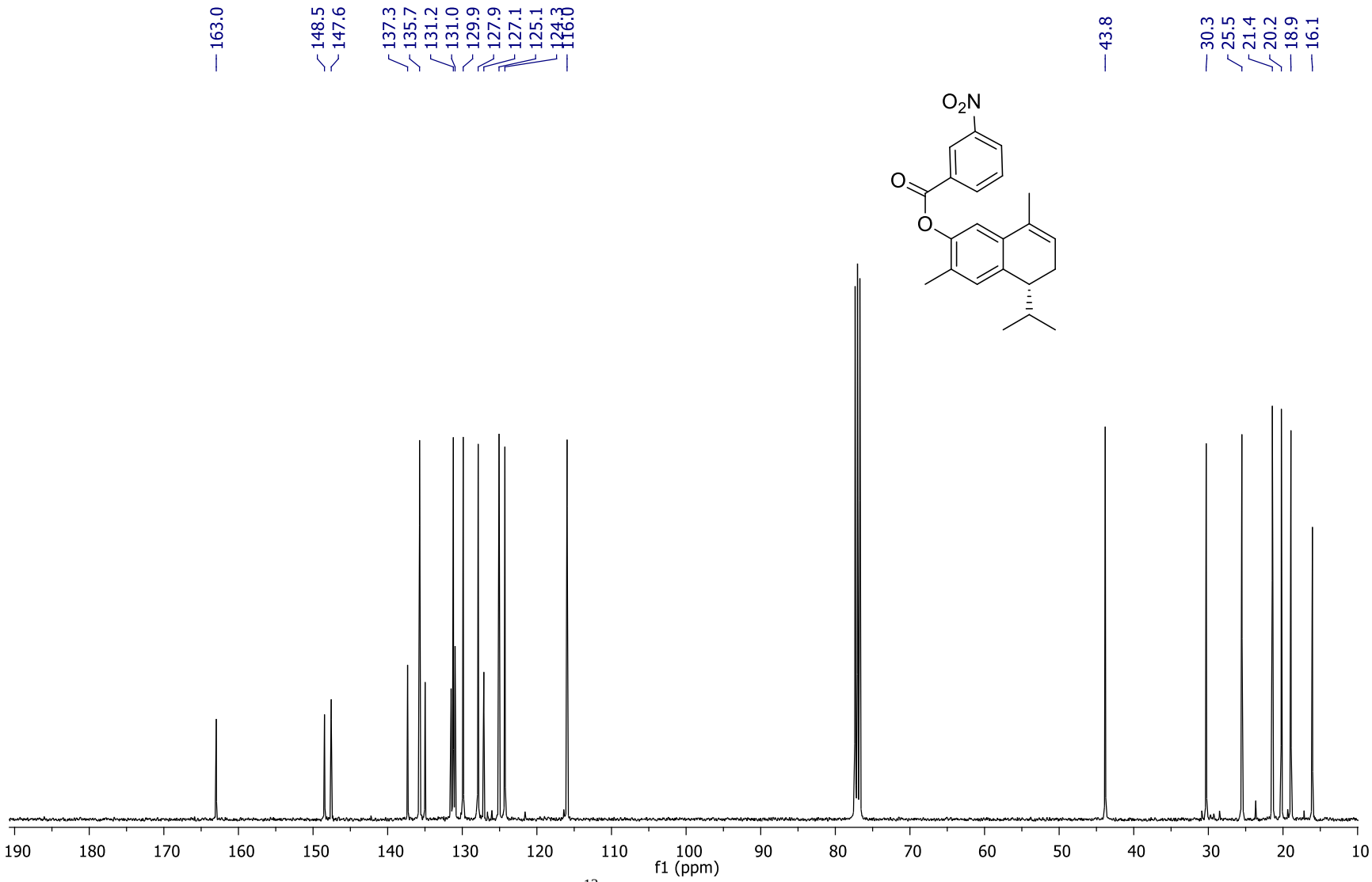

Espectro 20. RMN ^{13}C del compuesto **21** (100 MHz, $CDCl_3$).

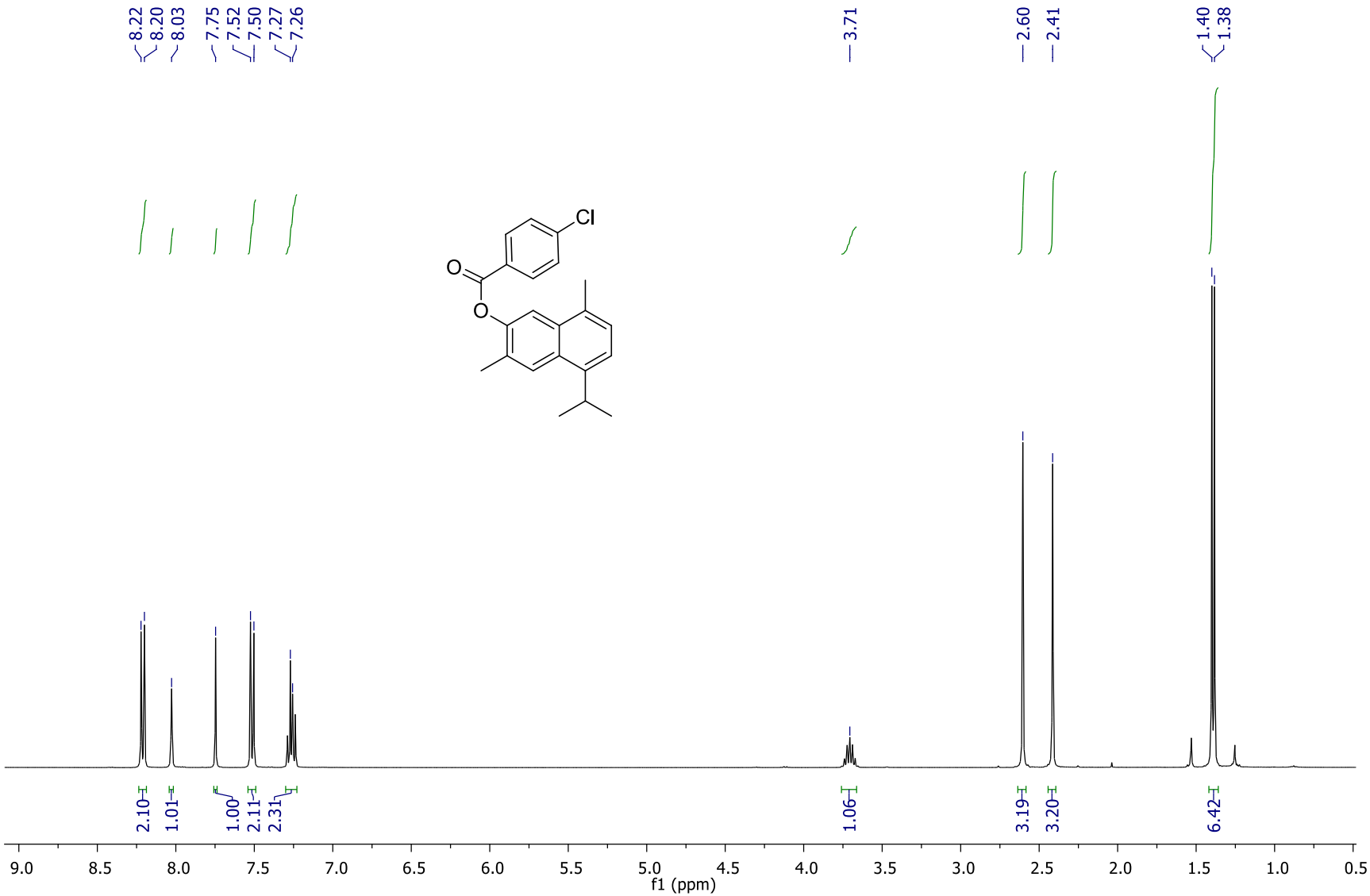

Espectro 21. RMN ^{1}H del compuesto **23** (400 MHz, $CDCl_3$).

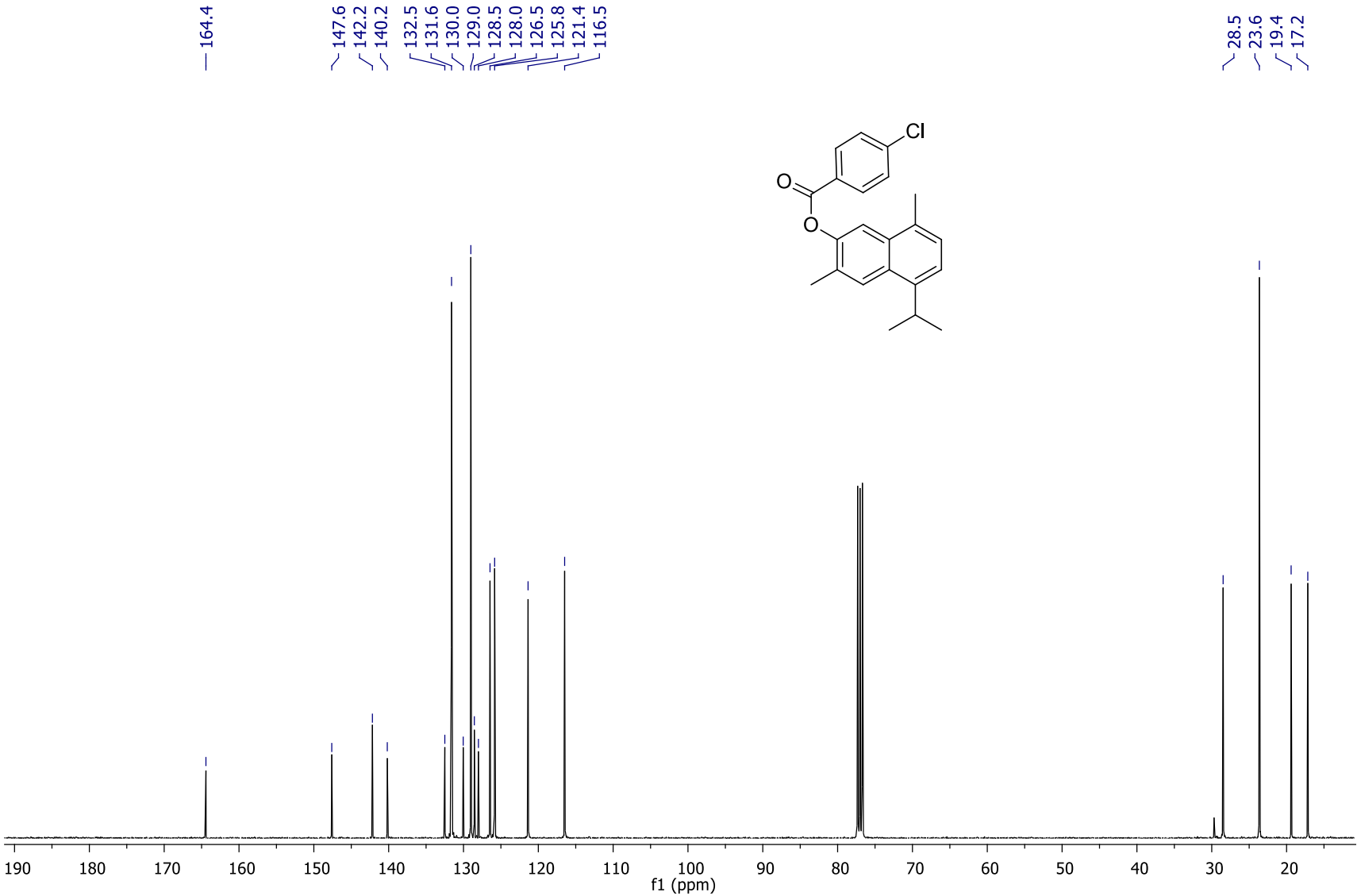

Espectro 22. RMN ^{13}C del compuesto **23** (100 MHz, $CDCl_3$).

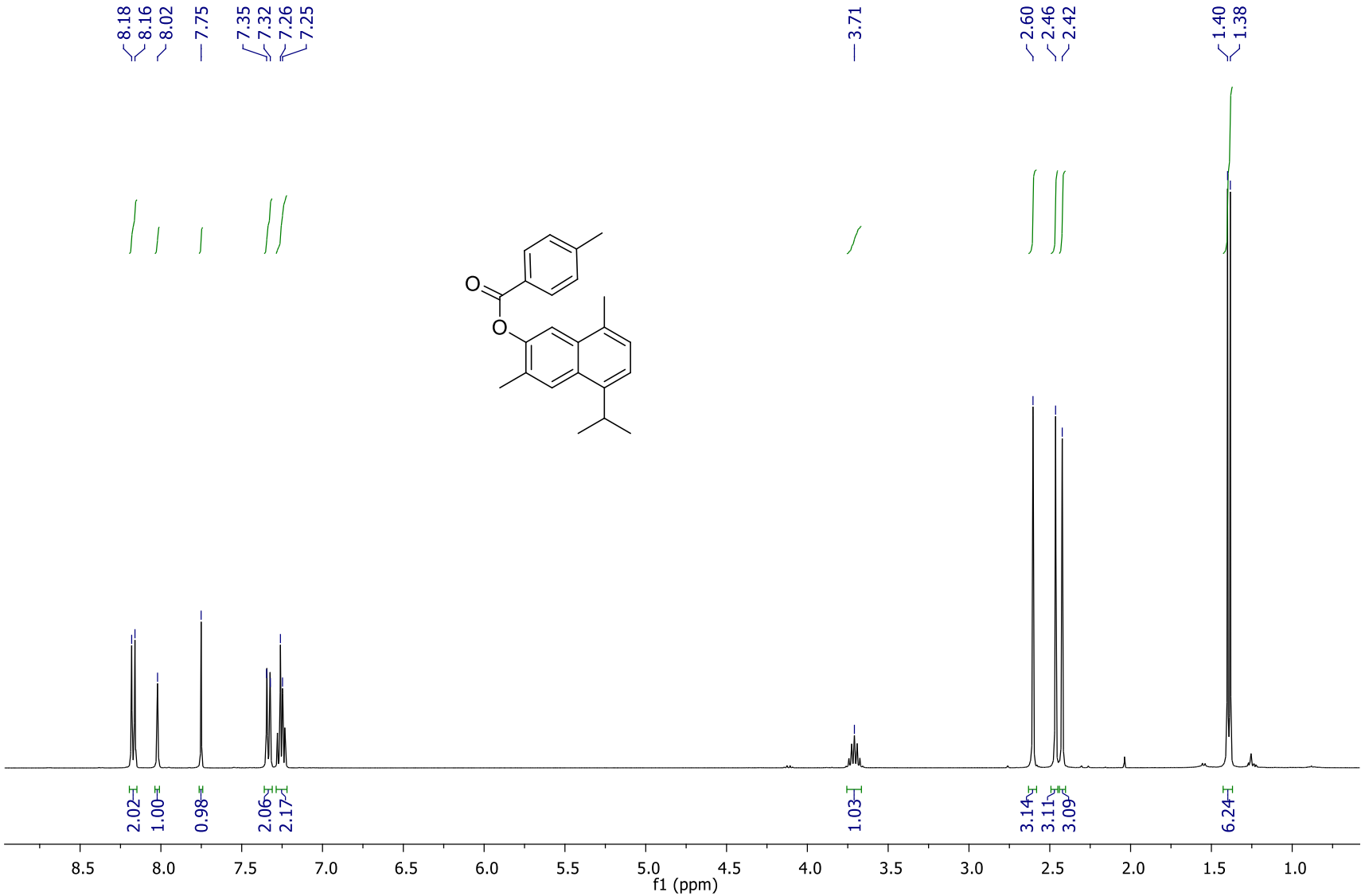

Espectro 23. RMN ^{1}H del compuesto **24** (400 MHz, $CDCl_3$).

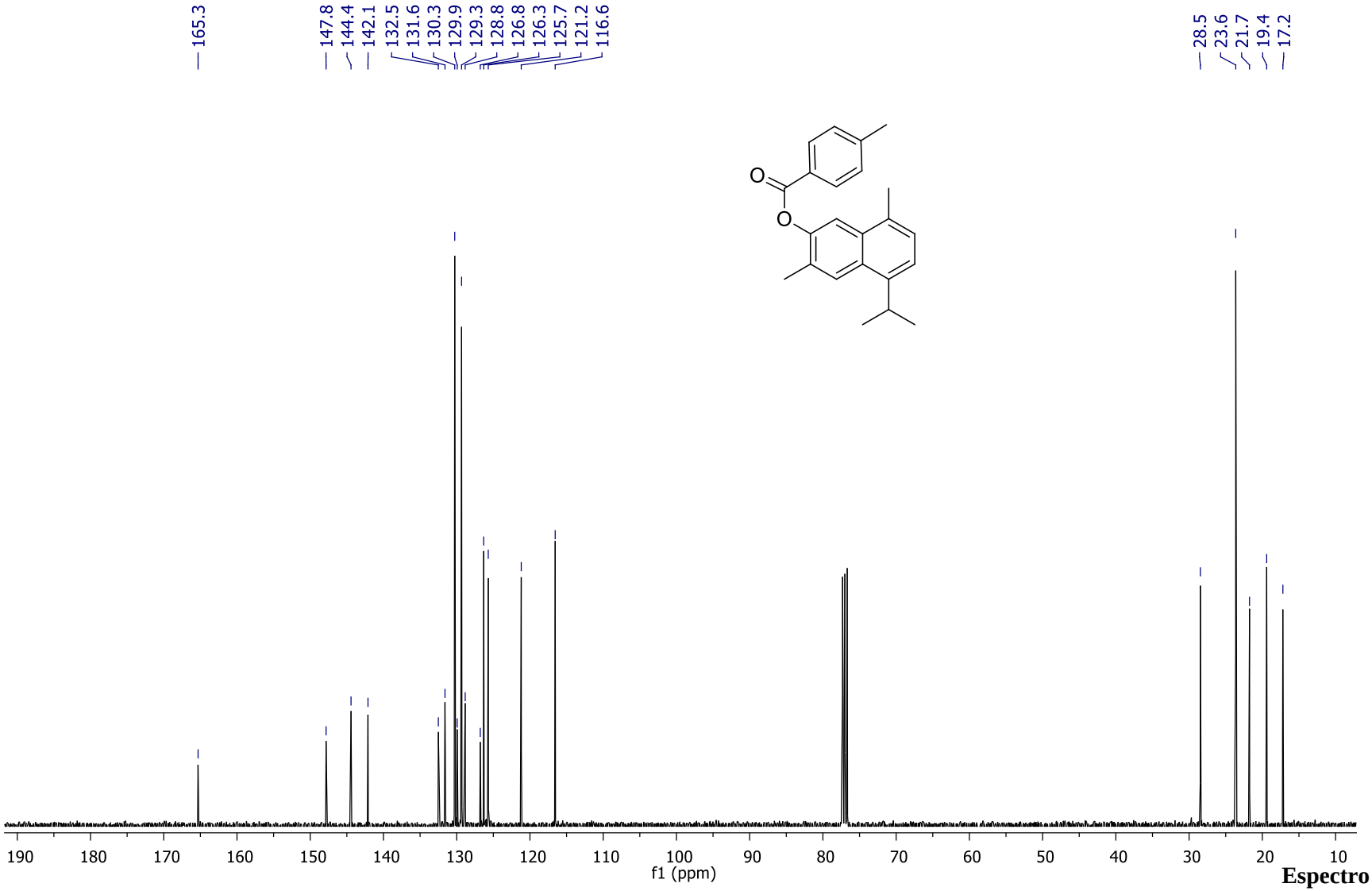

24. RMN ^{13}C del compuesto **24** (100 MHz, $CDCl_3$).

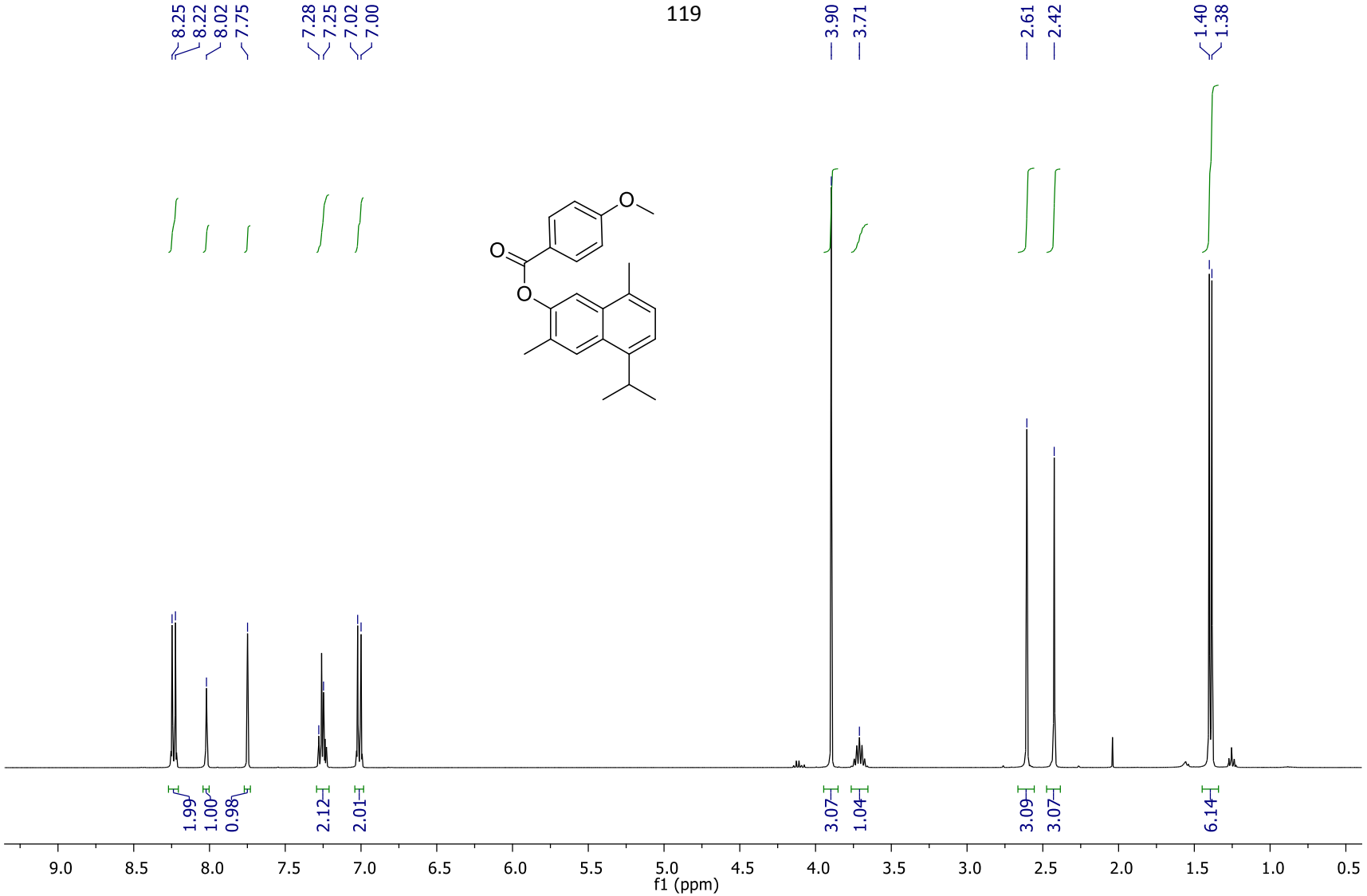

Espectro 25. RMN ^{1}H del compuesto **25** (400 MHz, $CDCl_3$).

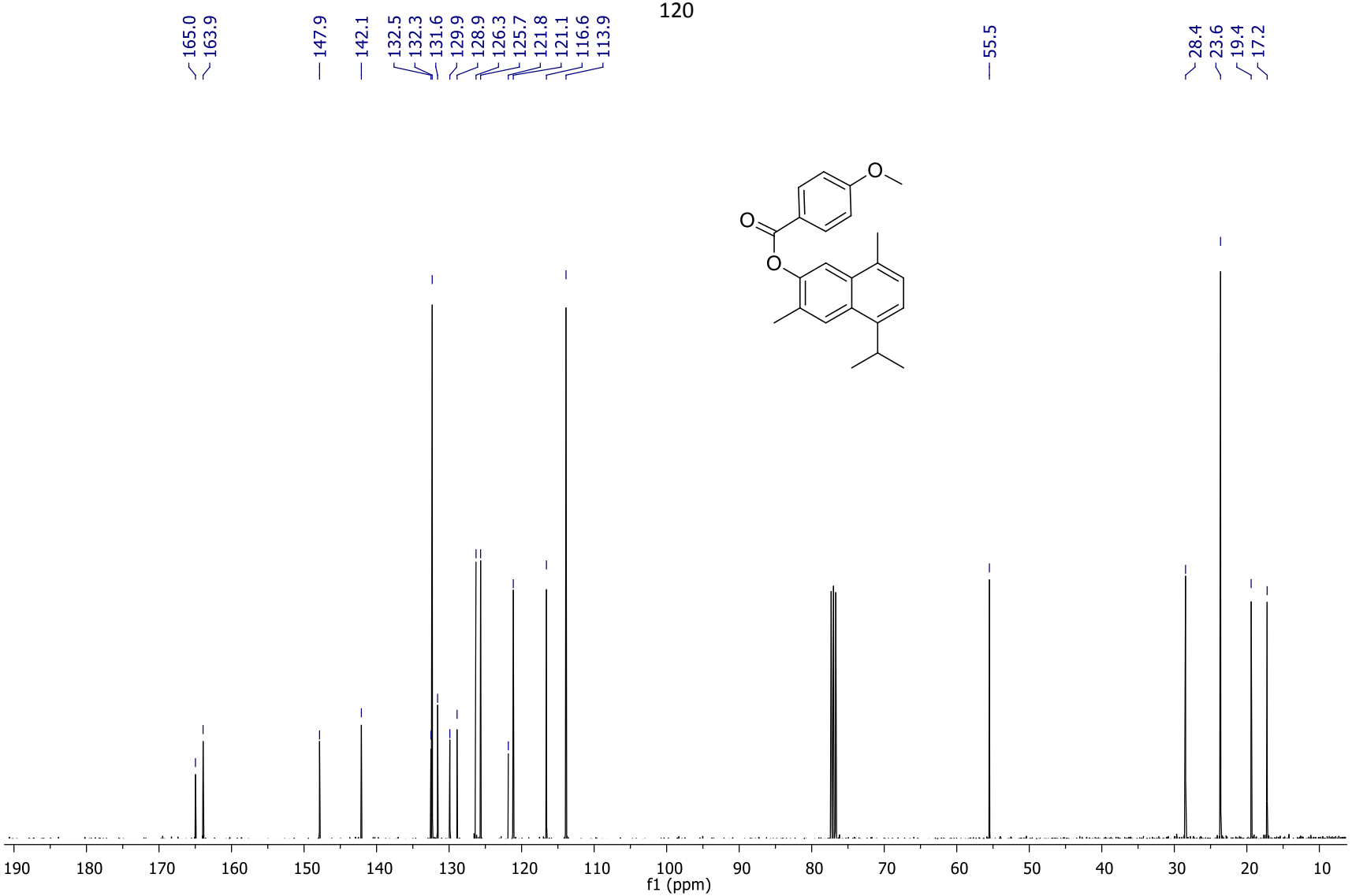

Espectro 26. RMN ^{13}C del compuesto **25** (100 MHz, $CDCl_3$).

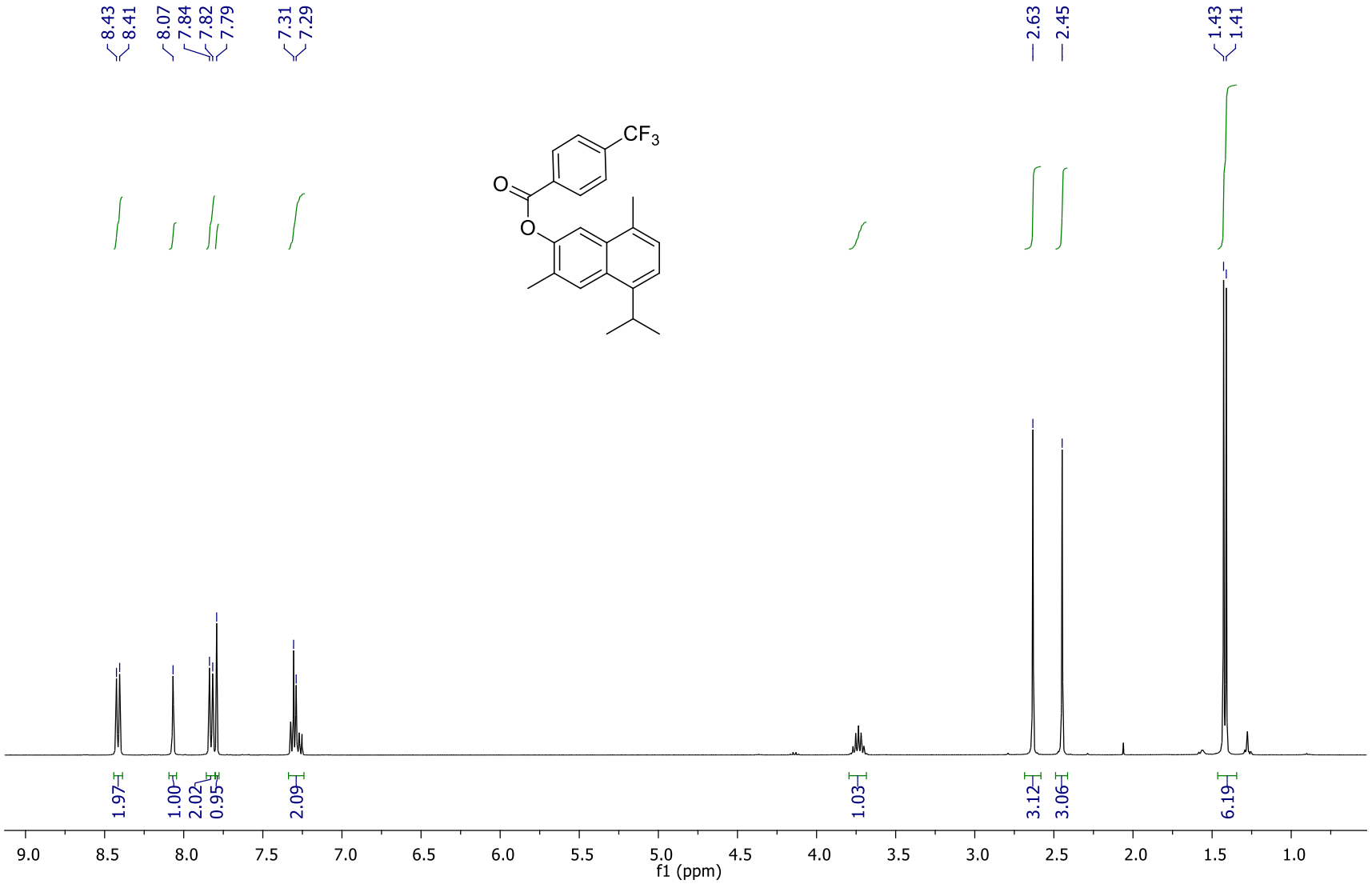

Espectro 27. RMN ^{1}H del compuesto **26** (400 MHz, $CDCl_3$).

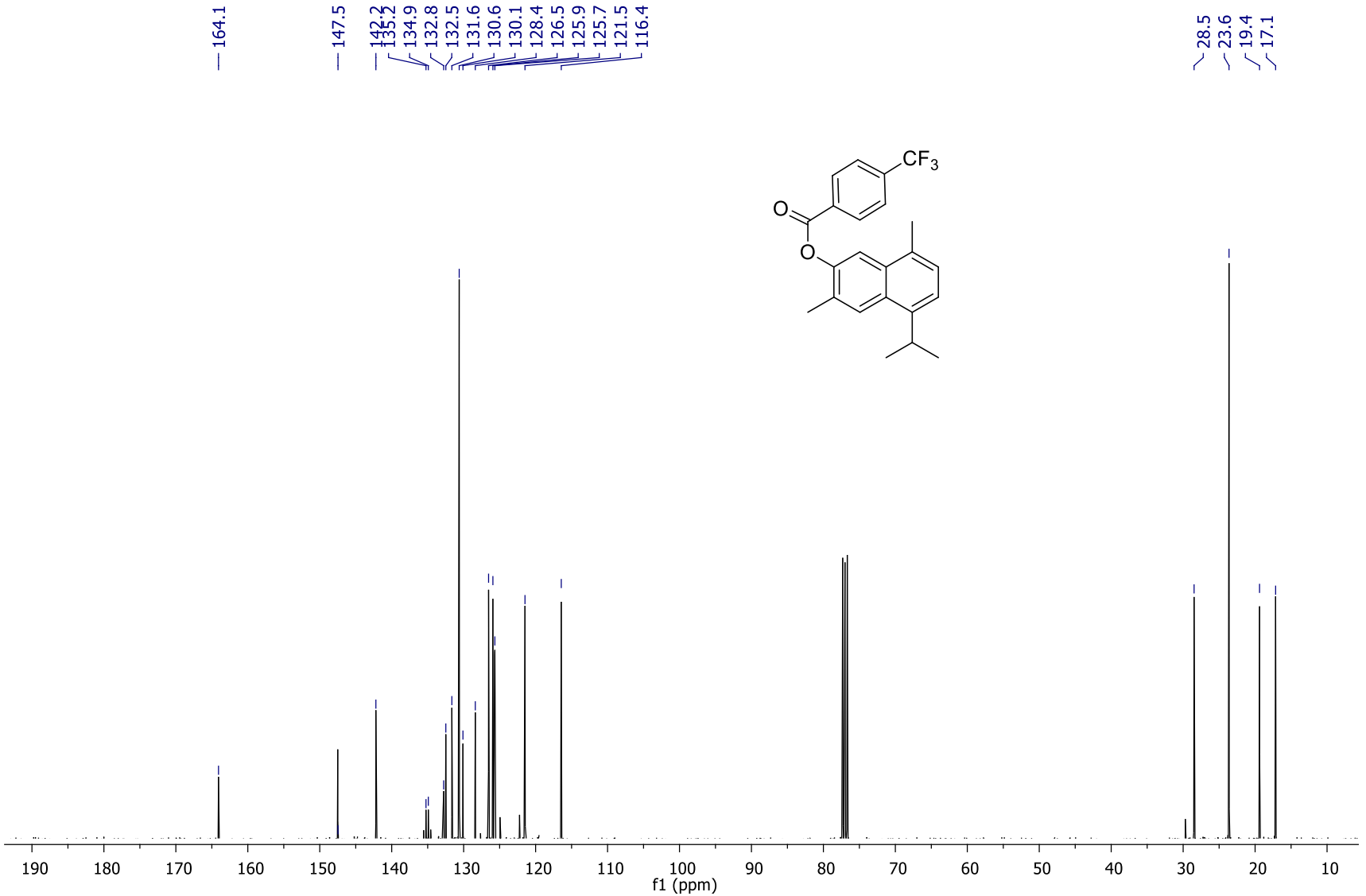

Espectro 28. RMN ^{13}C del compuesto **26** (100 MHz, $CDCl_3$).

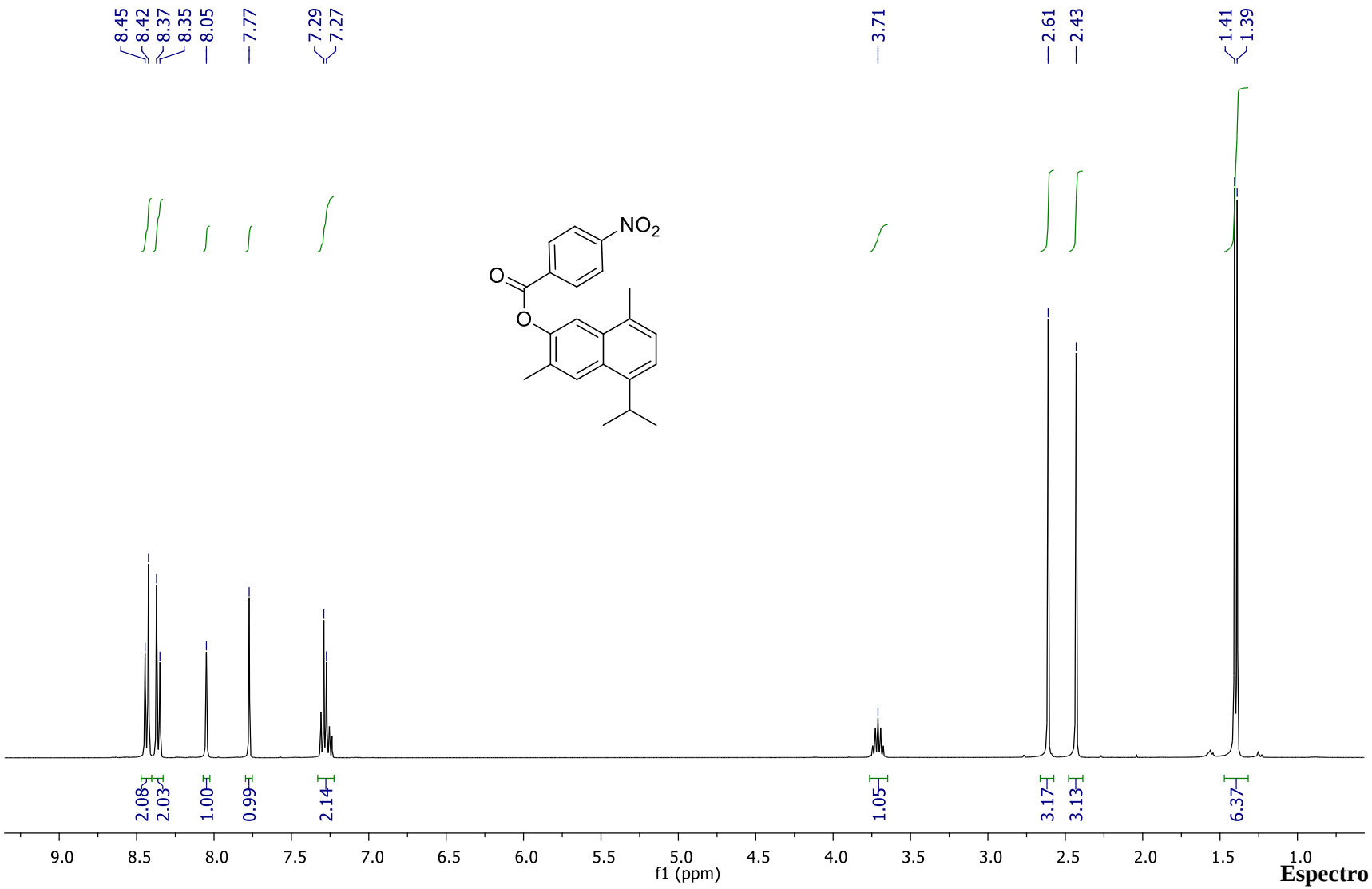

29. RMN ^{1}H del compuesto **27** (400 MHz, $CDCl_3$).

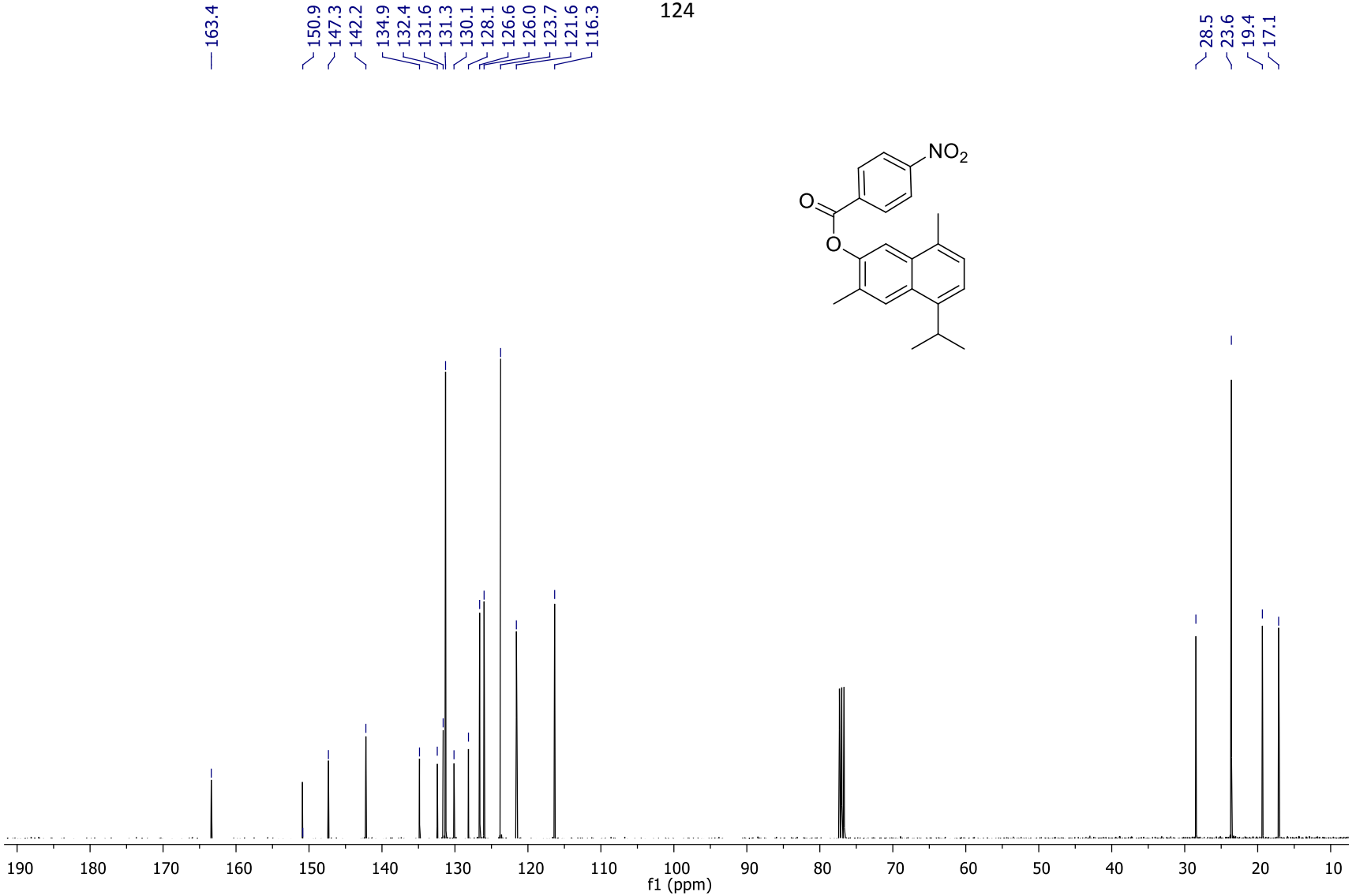

Espectro 30. RMN ^{13}C del compuesto **27** (100 MHz, $CDCl_3$).

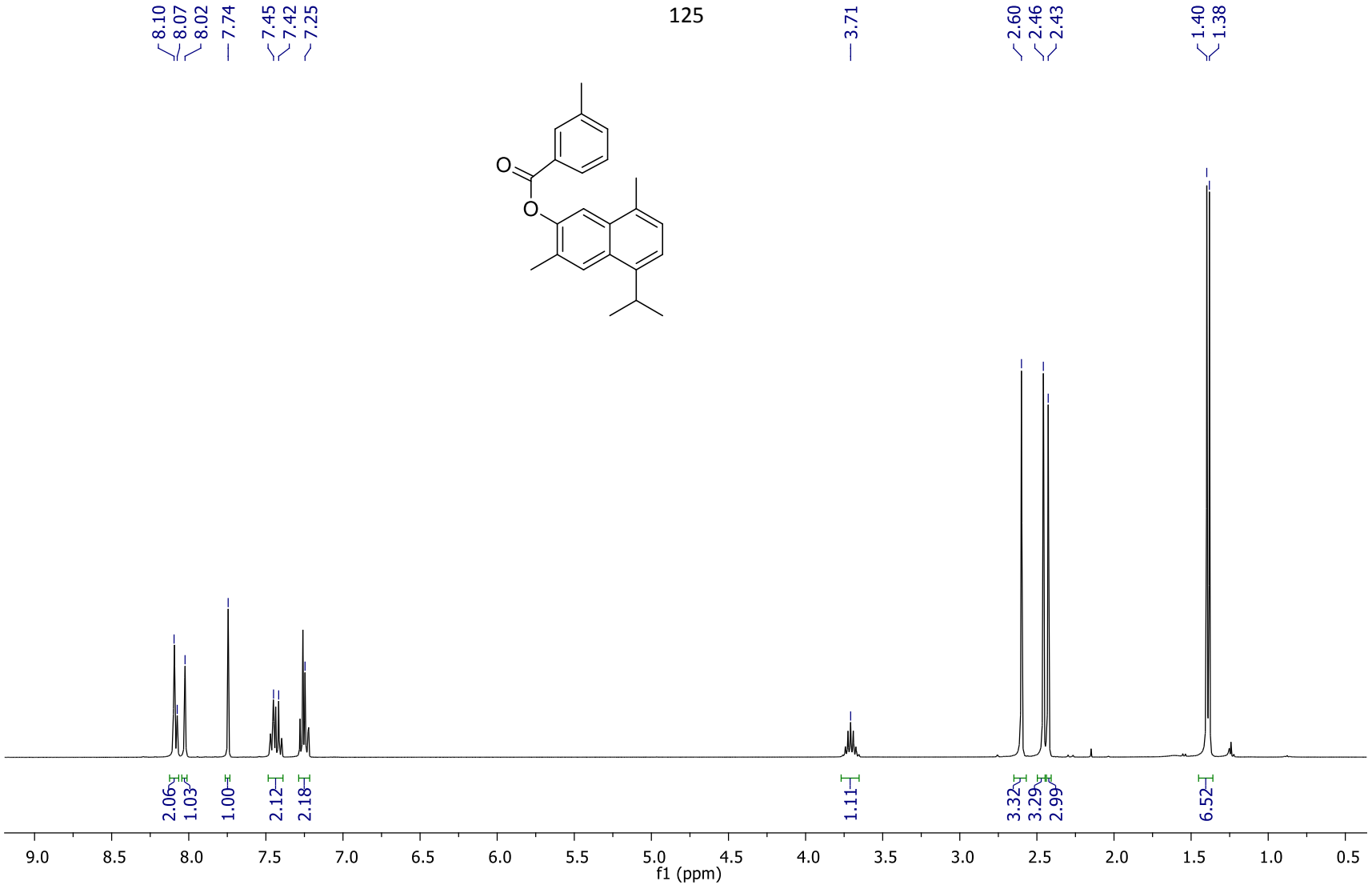

Espectro 31. RMN ^{1}H del compuesto **28** (400 MHz, $CDCl_3$).

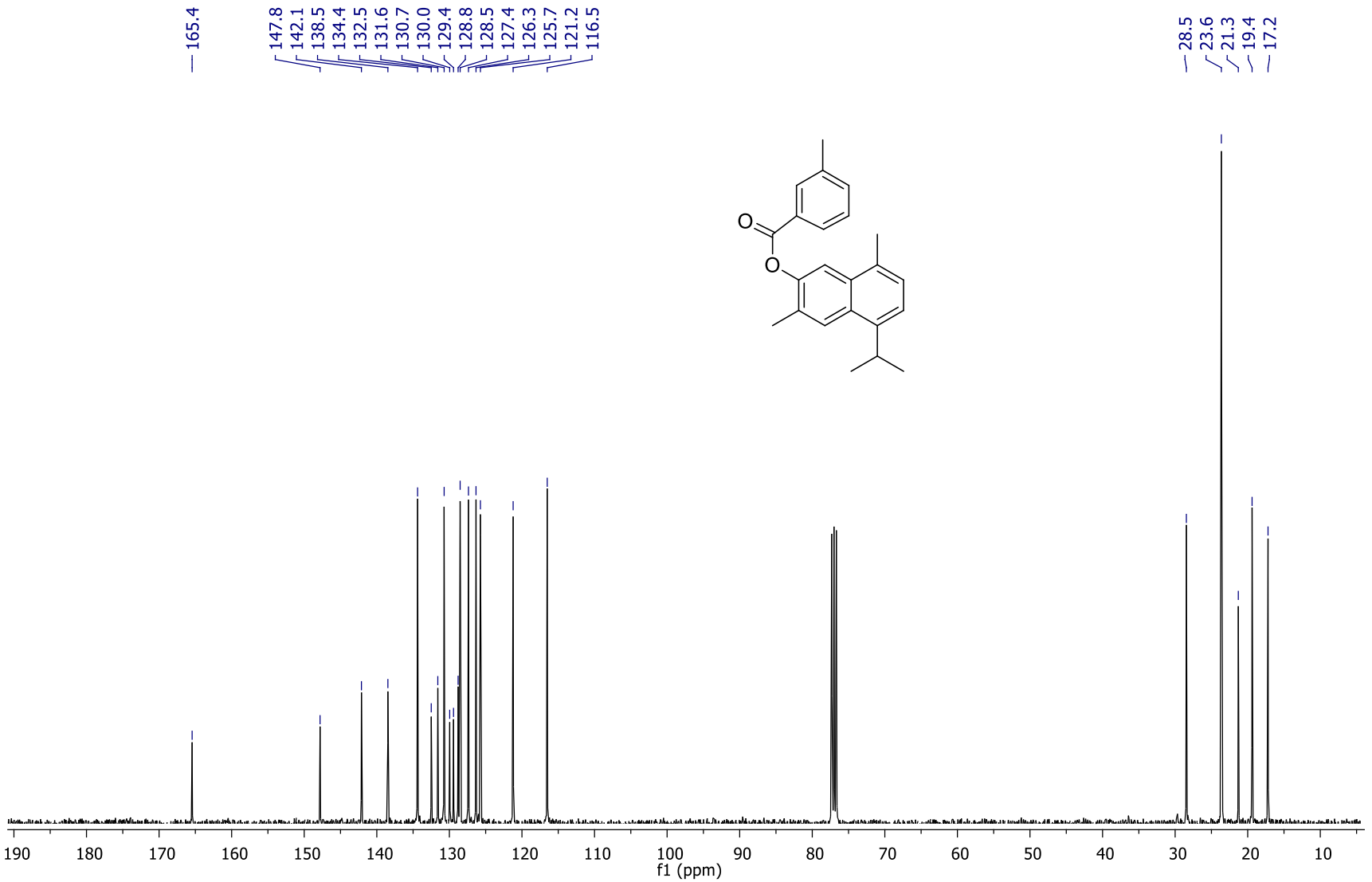

Espectro 32. RMN ^{13}C del compuesto **28** (100 MHz, $CDCl_3$).

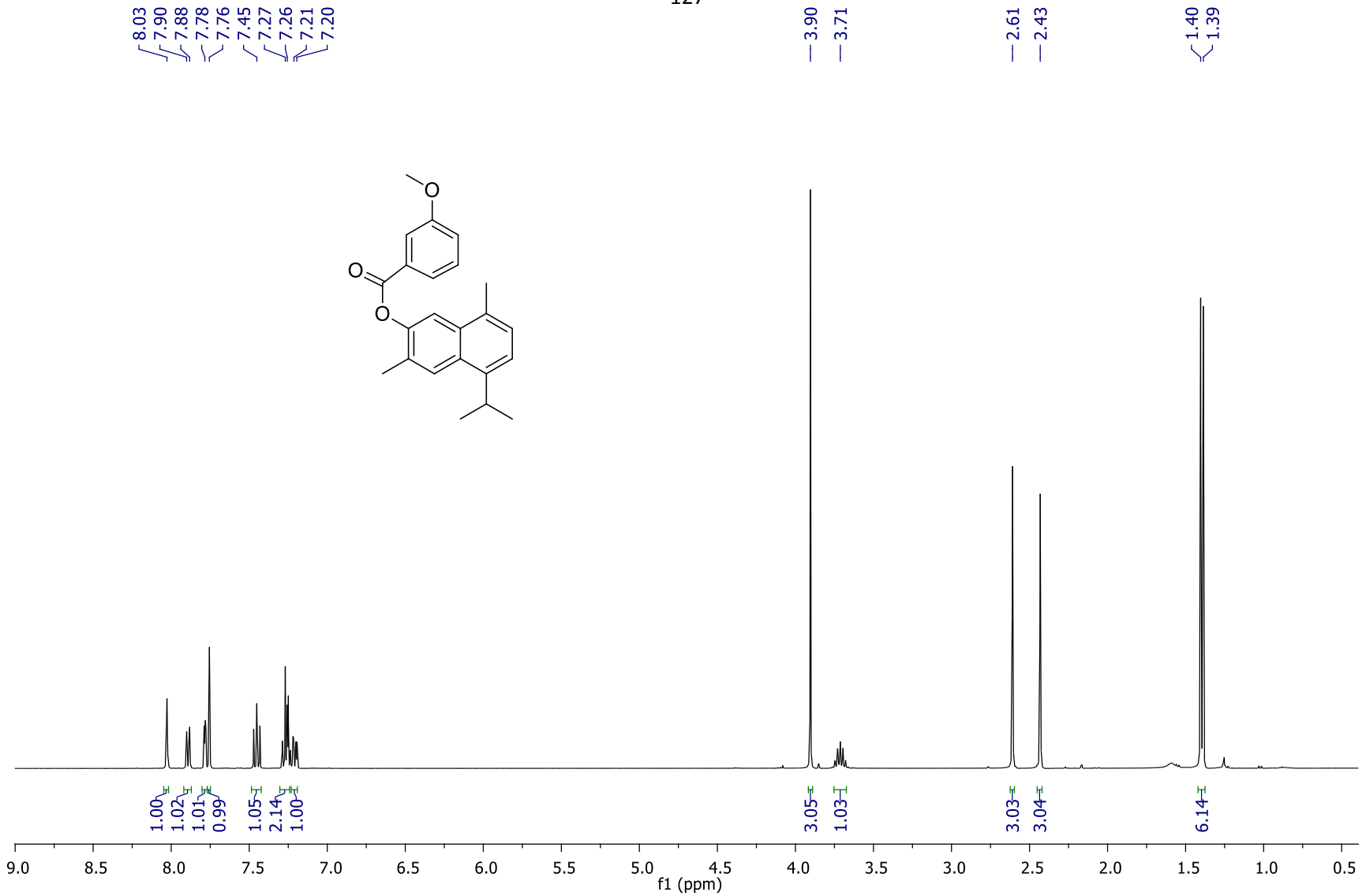

Espectro 33. RMN ^{1}H del compuesto **29** (400 MHz, $CDCl_3$).

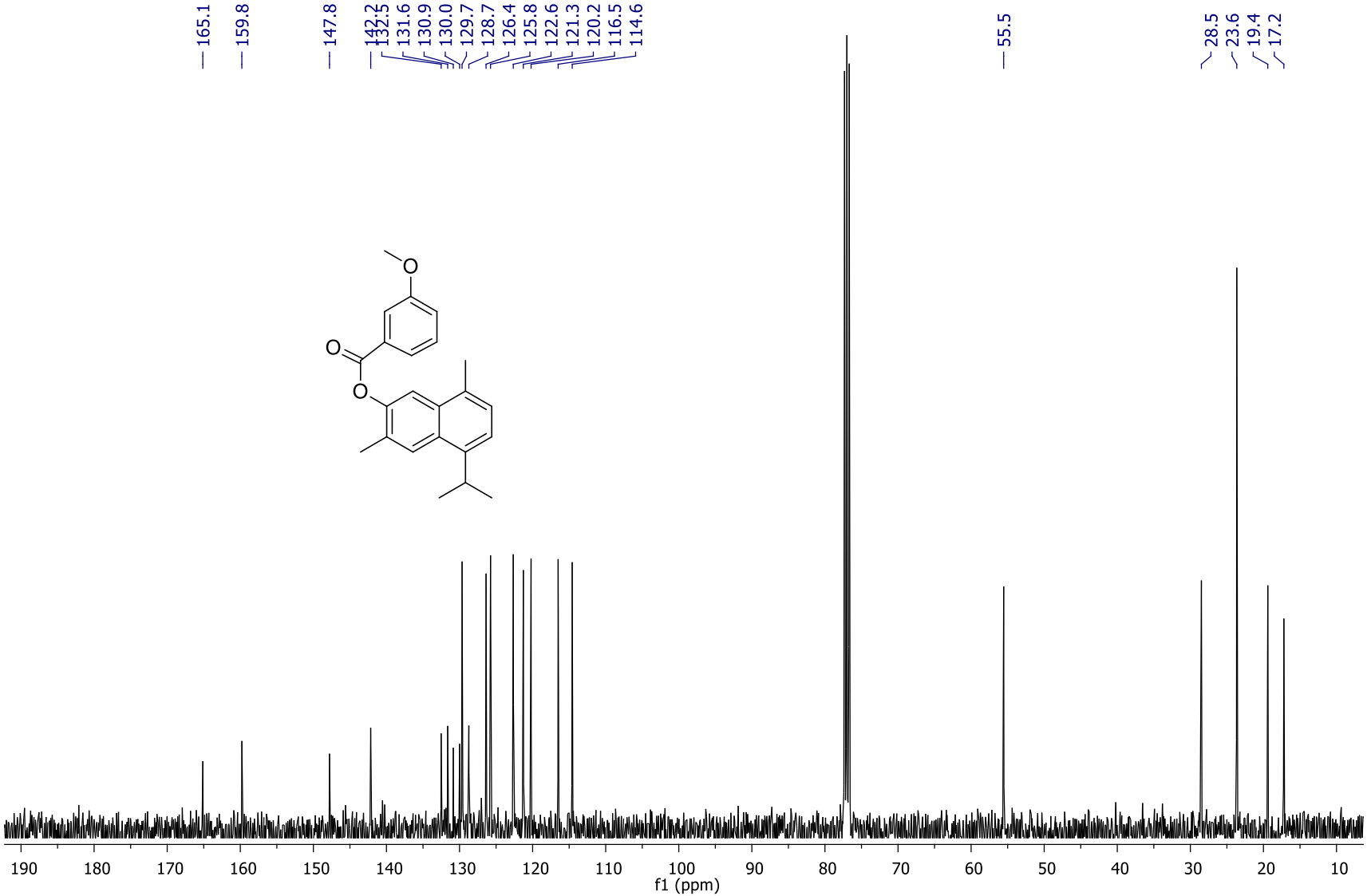

Espectro 34. RMN ^{13}C del compuesto **29** (100 MHz, $CDCl_3$).

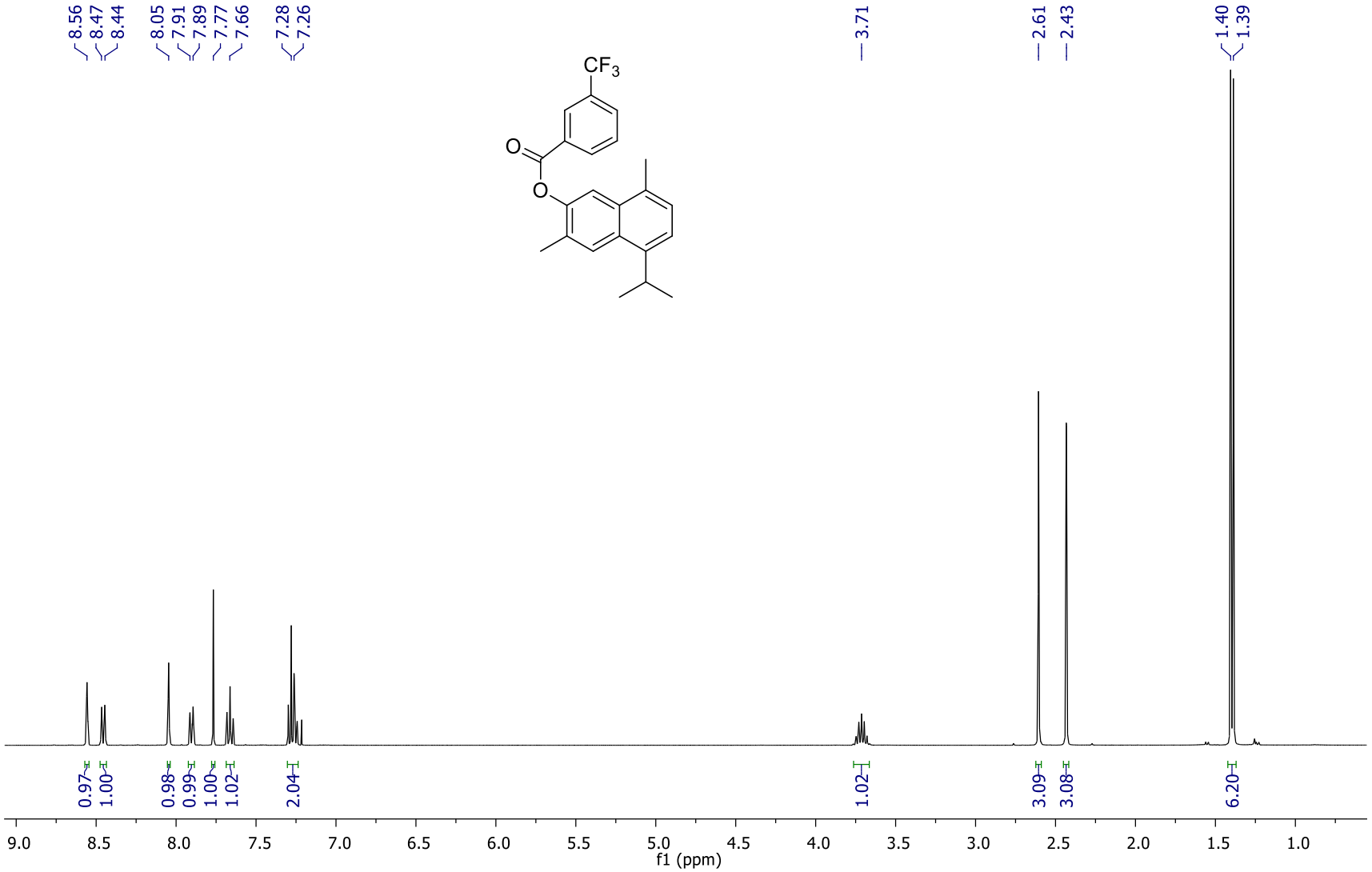

Espectro 35. RMN ^{1}H del compuesto **30** (400 MHz, $CDCl_3$).

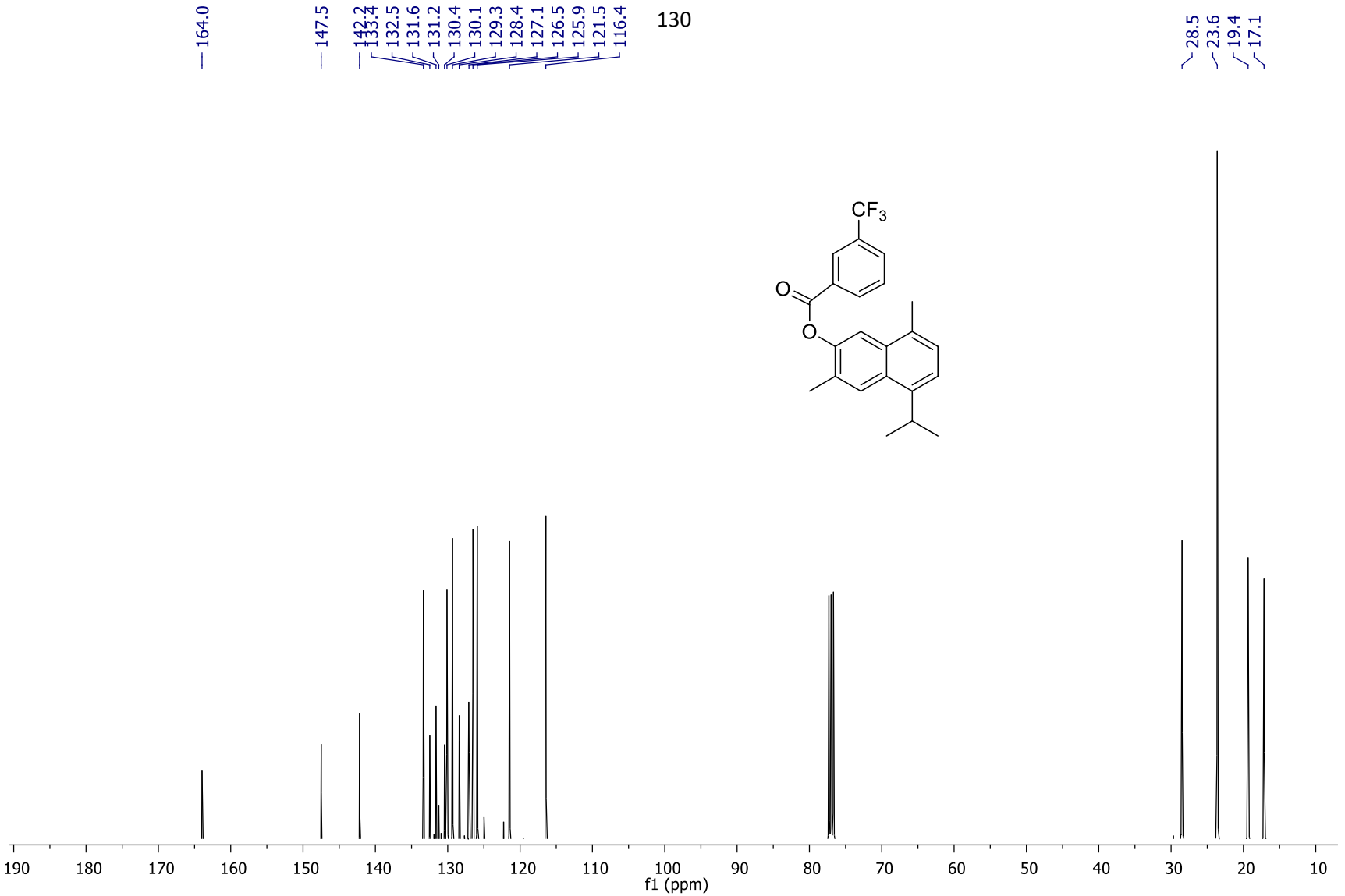

Espectro 36. RMN ^{13}C del compuesto **30** (100 MHz, $CDCl_3$).

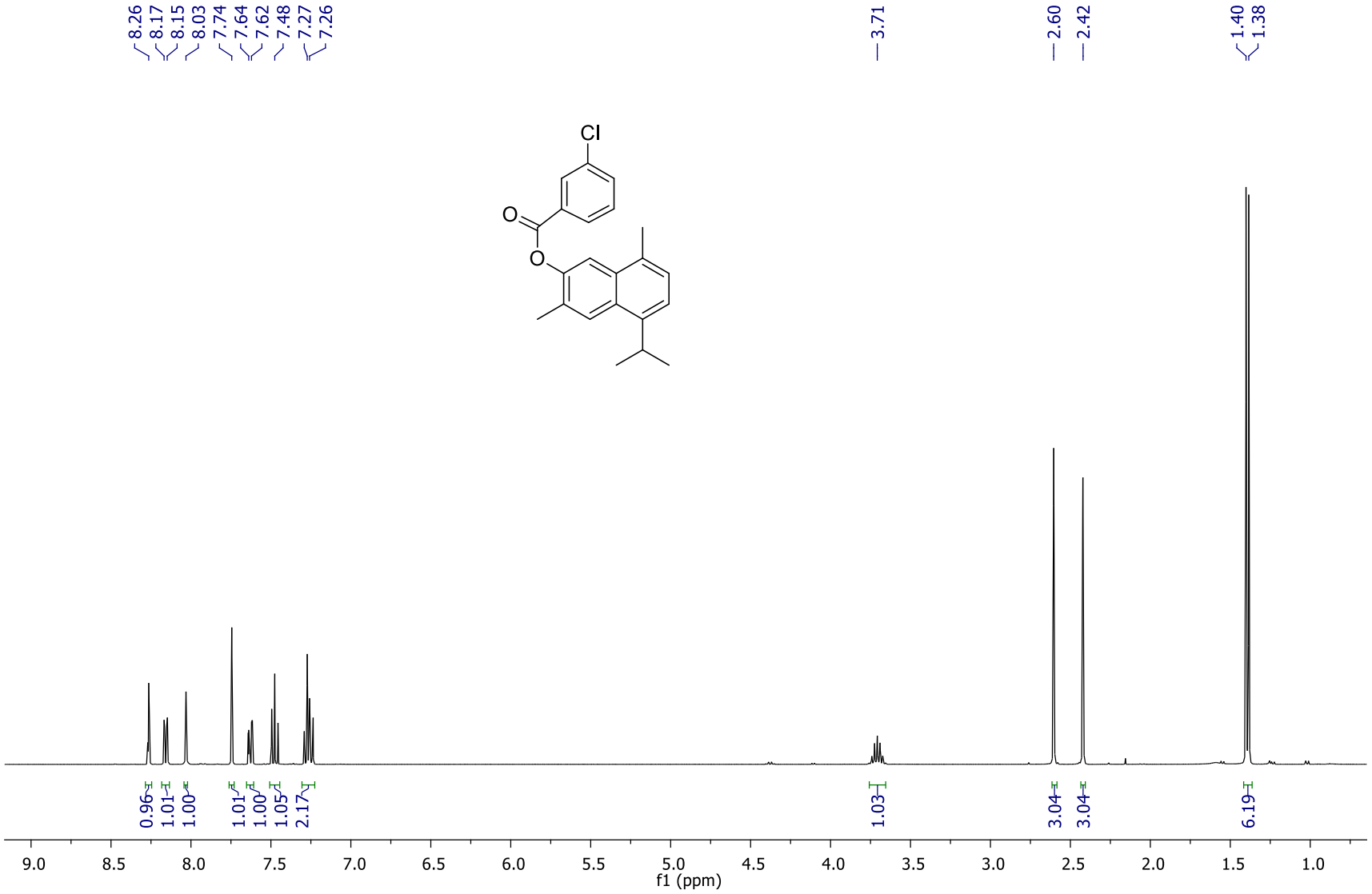

Espectro 37. RMN ^{1}H del compuesto **31** (400 MHz, $CDCl_3$).

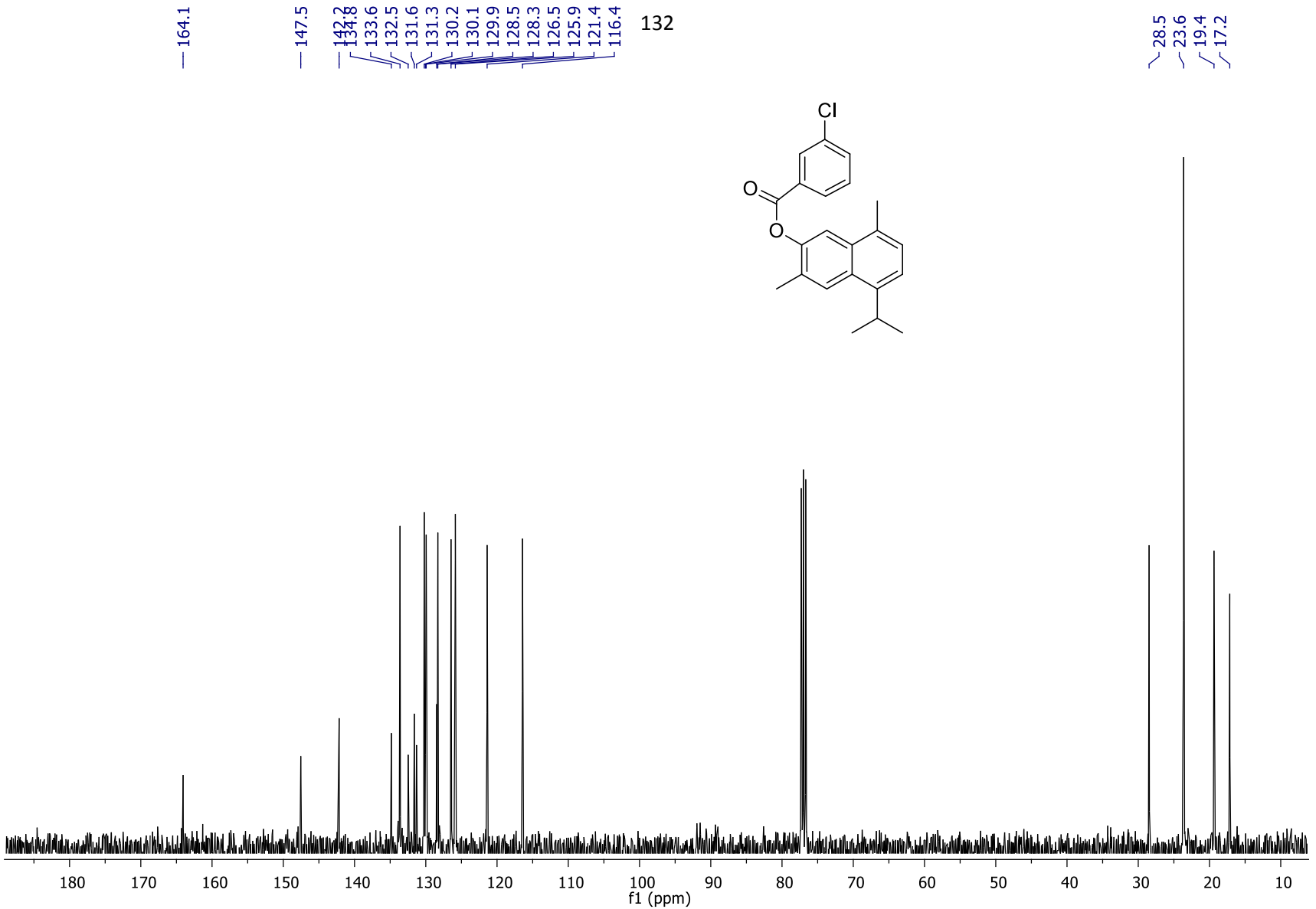

Espectro 38. RMN ^{13}C del compuesto **31** (100 MHz, $CDCl_3$).

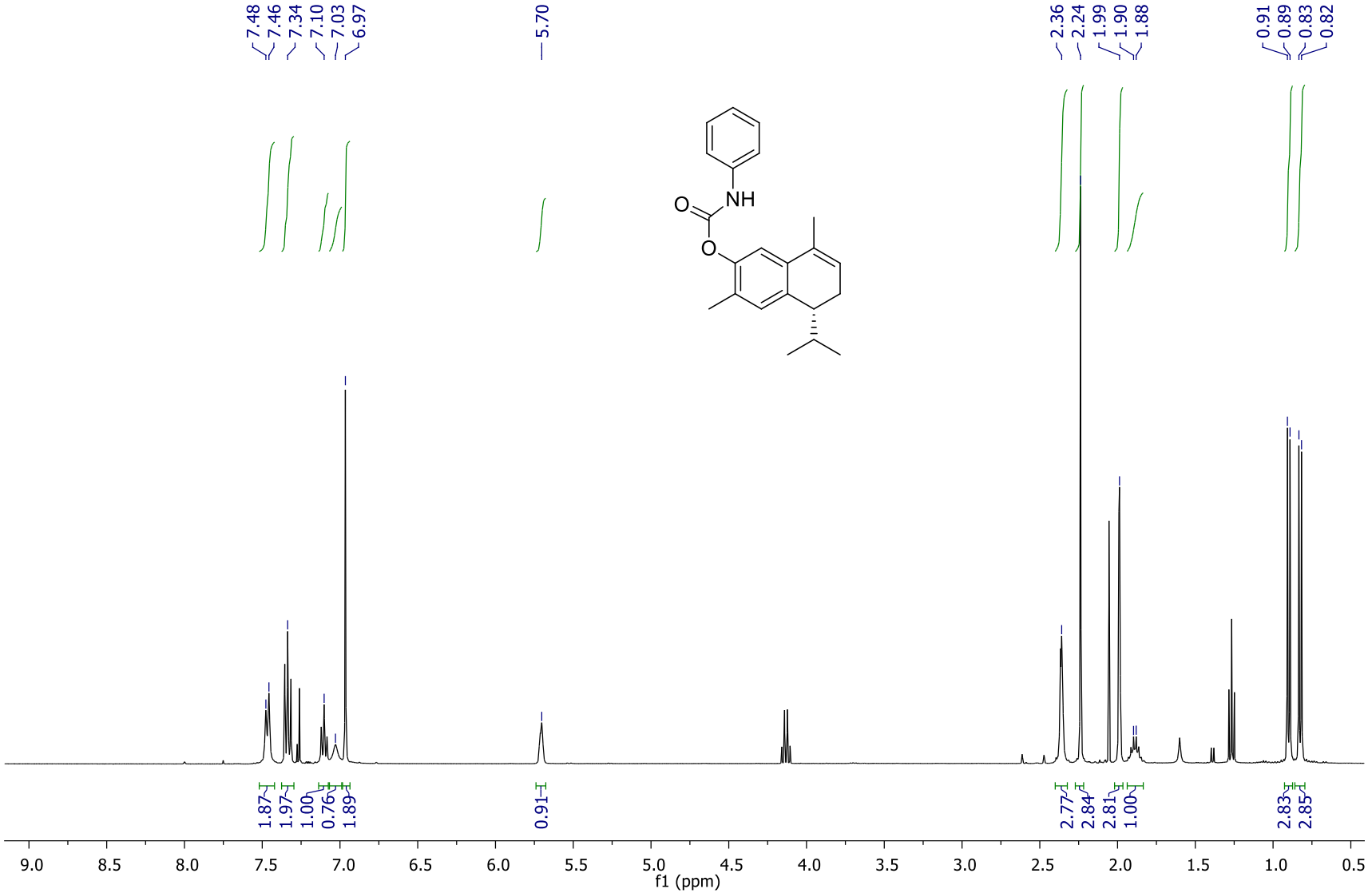

Espectro 39. RMN ^{1}H del compuesto **32** (400 MHz, $CDCl_3$).

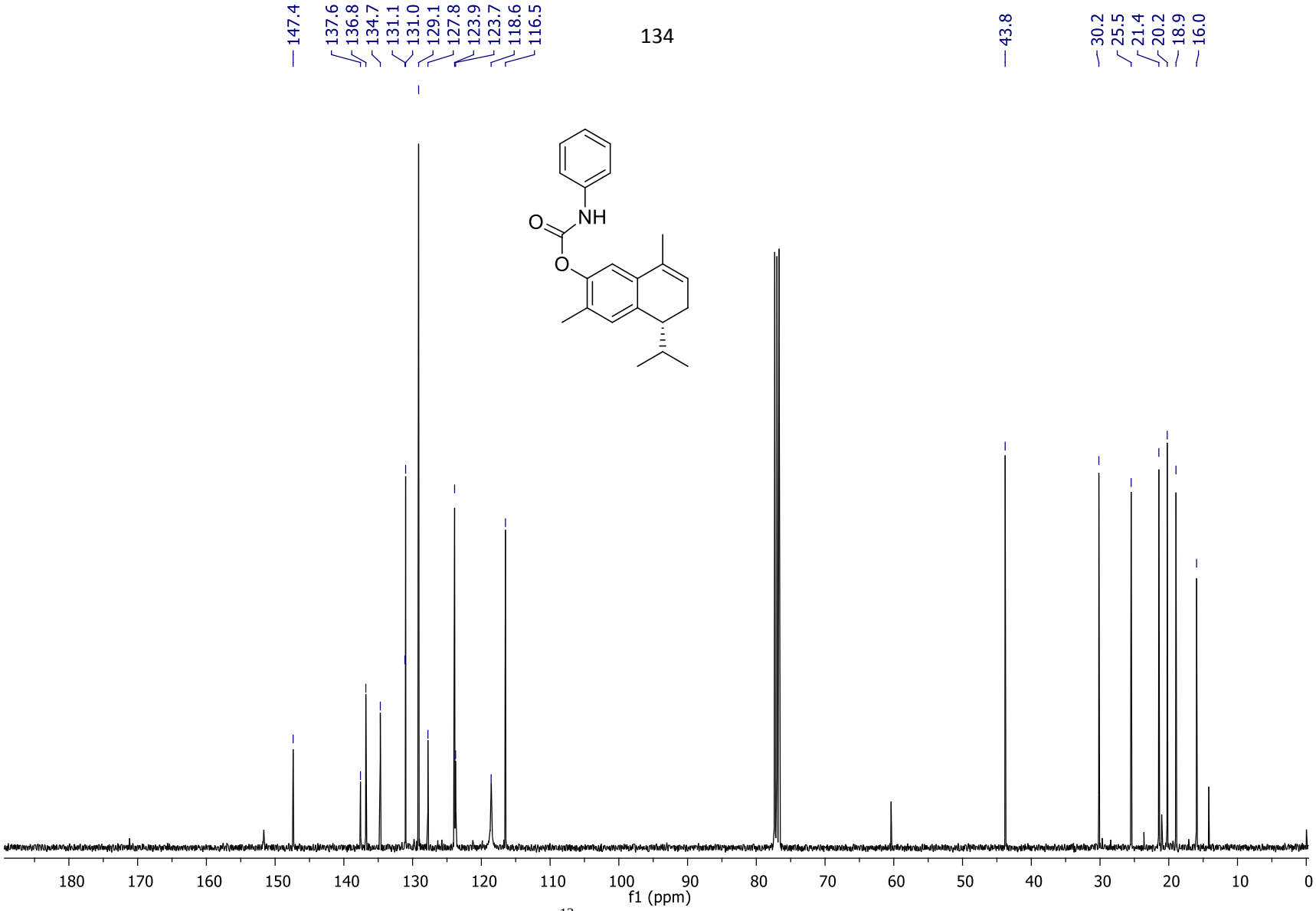

Espectro 40. RMN ^{13}C del compuesto **32** (100 MHz, $CDCl_3$).

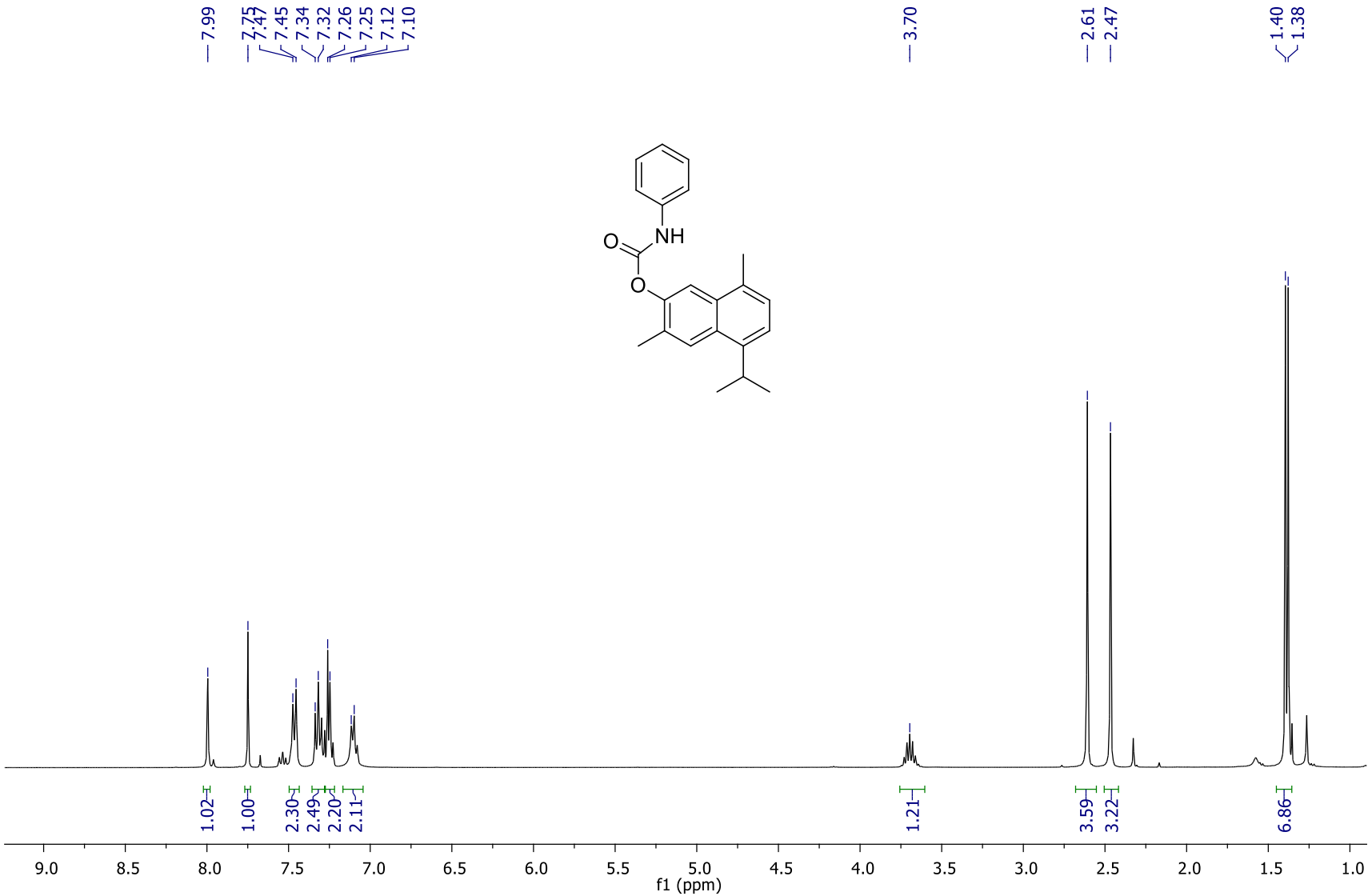

Espectro 41. RMN ^{1}H del compuesto **33** (400 MHz, $CDCl_3$).

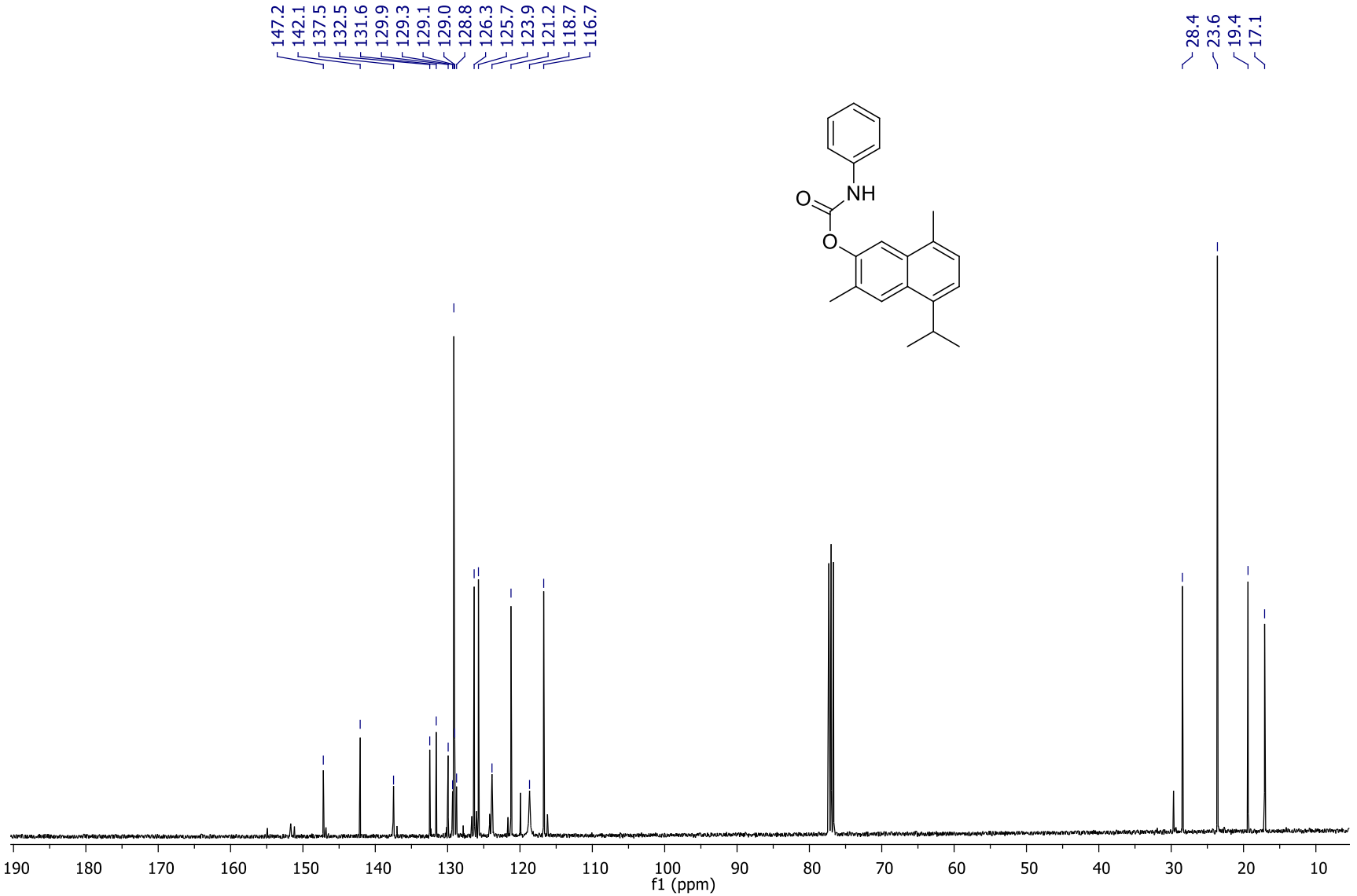

Espectro 42. RMN ^{13}C del compuesto **33** (100 MHz, $CDCl_3$).

Bioorganic & Medicinal Chemistry xxx (2017) xxx-xxx

Contents lists available at ScienceDirect

Bioorganic & Medicinal Chemistry

journal homepage: www.elsevier.com

Effect of natural and semi-synthetic cadinanes from *Heterotheca inuloides* on NF-κB, Nrf2 and STAT3 signaling pathways and evaluation of their in vitro cytotoxicity in human cancer cell lines

Verónica Egas[a], Estrella Millán[b], Juan A. Collado[b], Teresa Ramírez-Apan[a], Carlos A. Méndez-Cuesta[c], Eduardo Muñoz[b], Guillermo Delgado[a,*]

[a] *Instituto de Química, Universidad Nacional Autónoma de México, Circuito Exterior, Ciudad Universitaria, Coyoacán 04510, Mexico City, Mexico*
[b] *Maimonides Biomedical Research Institute of Córdoba, Reina Sofía University Hospital, Department of Cell Biology, Physiology and Immunology, University of Córdoba, Avenida Menéndez Pidal s/n, 14004 Córdoba, Spain*
[c] *Universidad Autónoma Metropolitana Unidad Xochimilco, Calzada del Hueso 1100, Mexico City 04960, Mexico*

ARTICLE INFO

Article history:
Received 19 December 2016
Received in revised form 24 March 2017
Accepted 30 March 2017
Available online xxx

Keywords:
Heterotheca inuloides
Cadinanes
Transcription factors
Semisynthesis
Antiproliferative activity

ABSTRACT

The effects of ten natural cadinane sesquiterpenoids isolated from *Heterotheca inuloides* on the pathways of the NF-κB, Nrf2 and STAT3 transcription factors were studied for the first time. The main constituent in this species, 7-hydroxy-3,4-dihydrocadalene (**1**), showed anti-NF-κB activity and activated the antioxidant Nrf2 pathway, which may explain the properties reported for the traditional use of the plant. In addition to the main metabolite, a structurally similar compound, 7-hydroxy-cadalene (**2**), also displayed anti-NF-κB activity. Thus, both natural compounds were used as templates for the preparation of a novel semi-synthetic derivative set, including esters and carbamates, which were evaluated for their potential in vitro antiproliferative activities against six human cancer cell lines. Carbamate derivatives **32** and **33** were found to exhibit potent activity against human colorectal adenocarcinoma and showed important selectivity in cancer cells. Among ester derivatives, compound **13** was determined to be a more potent NF-κB inhibitor and Nrf2 activator than its parent, 7-hydroxy-3,4-dihydrocadalene (**1**). Furthermore, this compound decreases levels of phospho-IκBα, a protein complex involved in the NF-κB activation pathway. Molecular simulations suggest that all active compounds interact with the activation loop of the IKKβ subunit in the IKK complex, which is the responsible of IκBα phosphorylation. Thus, we identified two natural, and one semi-synthetic, NF-κB and Nrf2 modulators and two new promising cytotoxic compounds.

1. Introduction

The relationship between inflammation and the development of cancer is now widely accepted. Although this connection could be complicated, evidence suggests that long-standing inflammation predisposes to cancer.[1,2] Furthermore, the molecular pathways that link inflammation and cancer are now known. These extrinsic and intrinsic pathways converge, which results in the activation of transcription factors, mainly nuclear factor-κB (NF-κB), signal transducer and activator of transcription 3 (STAT3) and hypoxia-inducible factor 1α (HIF1α), in tumor cells.[3] Activation of NF-κB in inflammatory cells leads to the production of secreted factors that enhance the growth, the survival and the vascularization of carcinoma cells.[4,5] STAT3 is considered one of the most promising new targets for cancer therapy. Its activation in tumor cells and the tumor microenvironment promotes cell proliferation, survival and invasion and facilitates cancer development through inflammation.[6] Another transcription factor known to play an important protective role in suppressing oxidative stress and inhibiting carcinogenesis is the nuclear factor-erythroid 2 p45-related factor 2 (Nrf2). Activation of Nrf2 inhibits inflammation and facilitates adaptation by upregulating repair and degradation of damaged macromolecules.[7,8]

The aforementioned knowledge facilitates the investigation and development of substances that target the inflammatory components of the cancer microenvironment. Indeed, several experimental, epidemiologic, and clinical studies suggest that anti-inflammatory agents are promising as cancer therapeutics.[9,10]

Naturally occurring compounds are a representative group of substances displaying chemopreventative effects, and many of them result from anti-inflammatory properties.[11] It has been demonstrated that some natural products could exert regulation at a transcriptional level in the molecular mechanisms involved in inflammation and cancer. Thus, they represent an interesting source of potentially useful agents for prevention and therapy.[12]

Despite the biological activities of many natural products being broadly studied, the identification of the cellular targets or pathways involved in these activities represents a challenge that could explain the traditional uses of several species in folk medicine.[13]

Heterotheca inuloides (*H. inuloides*) is a highly regarded plant in Mexican traditional medicine, mainly for the treatment of inflammatory ailments, motivating investigations of its chemical constituents and their biological activities.[14] These studies have shown that

* Corresponding author.
Email address: delgado@unam.mx (G. Delgado)

http://dx.doi.org/10.1016/j.bmc.2017.03.069
0968-0896/

sesquiterpenoids are the major secondary metabolites from this plant. It has been demonstrated that these compounds exhibit anti-inflammatory properties;[15,16] however, the molecular mechanism associated with their activity has not been investigated.

Here, we report the evaluation of ten natural cadinanes on well defined pathways involved in inflammation and carcinogenesis, and the semi-synthesis of a derivative set that started from the active compounds. The cytotoxic effect of derivatives was tested on six human cancer cell lines and correlated with the inhibition or activation of the NF-κB, STAT3 and Nrf2 pathways. To propose in a preliminary way the mechanism of inhibition of the NF-κB pathway exerted by these compounds, computational docking was performed using the crystal structure of a protein involved in the NF-κB activation.

2. Results and discussion

2.1. Isolation and initial biological screening on well-defined pathways involved in inflammation and carcinogenesis

A total of ten sesquiterpene-type metabolites displaying anti-inflammatory activities[15,16] were obtained from the aerial parts of *H. inuloides* (Fig. 1). 7-Hydroxy-3,4-dihydrocadalene (**1**) and 7-hydroxy-cadalene (**2**) were re-isolated by conventional chromatographic methods (experimental section), and compounds **1–8** were obtained in previous investigations carried out in our laboratory.[16] The isolated compounds were tested in NF-κB, Nrf2 and STAT3-dependent luciferase gene reporter assays, where the amount of the luciferase gene product reflects the extent of the transcription factor activation.

Interestingly, we found that although compounds **1–10** have a high structural similarity, only two of them showed important activity on the evaluated targets, showing their high selectivity (Table 1). 7-Hydroxy-3,4-dihydrocadalene (**1**) and 7-hydroxy-cadalene (**2**) showed anti-NF-κB activities, and 7-hydroxy-3,4-dihydrocadalene was also able to activate antioxidant Nrf2 pathway. All compounds were ineffective as STAT3 inhibitors. These results could explain the use of *H. inuloides* in Mexican folk medicine, since both NF-κB and Nrf2 transcription factors regulate inflammatory processes that are the most common conditions for which this plant is used. Furthermore, because 7-hydroxy-3,4-dihydrocadalene (**1**) is the main constituent in this species, it might significantly contribute to the anti-inflammatory activity observed in its extracts. Our observation agrees with several studies that have demonstrated that inhibition of the NF-κB pathway is an important mechanism exerted by many natural products with therapeutic and preventive effects.[17]

2.2. Semi-synthesis, biological evaluations and molecular docking

Metabolites **1** and **2** showed positive activity on the primary screening and were selected as scaffolds for the preparation of a novel semi synthetic derivative set by simple reactions where the existing functional group could be manipulated to make additional structures. The reactive phenol was transformed to the corresponding benzoates that have electron donating or electron withdrawing substituents in the *meta* and *para* positions (Scheme 1). While generating novel structures, two carbamate derivatives were obtained by the reaction of selected natural products with phenyl isocyanate (Scheme 1).

All semi-synthetic compounds were then subjected to a new biological screening on the selected pathways to analyze how the structural modifications undertaken might have affected their activities. Table 2 summarizes the results of this primary screening along with the cytotoxic effect of derivatives on six human cancer cell lines.

The anti-NF-κB activity previously observed for 7-hydroxy-3,4-dihydrocadalene (**1**) decreased slightly but was retained by the benzoate derivative **11**, indicating that some structural modifications on the phenol moiety of the natural product could be carried out without significantly affecting this activity. However, it was clear that the type and position of the substituent on the benzoyl group is determinant, since compounds **13** and **14** having electron donating groups in the *para*- position showed better anti-NF-κB activities that derivative **11** having not substitution. In contrast, compounds **12**, **15** and **16,** having electron withdrawing substituents in the *para*-position, decreased their activities in comparison with derivative **11**. Benzoate derivatives **17–21** having a substitution in the *meta*-position displayed less anti-NF-κB activity than their corresponding derivatives having *para*-substitution. Although all benzoate derivatives prepared from 7-hydroxy-cadalene (**2**) were less active for NF-κB inhibition than their parent, their activity patterns were generally similar to those of 7-hydroxy-3,4-dihydrocadalene (**1**) derivatives. These patterns indicated a better activity for those compounds containing electron donating groups in the *para*-position.

The Nrf2 activating effect observed for 7-hydroxy-3,4-dihydrocadalene (**1**) was notably improved in the benzoate derivatives **11**, **13** and **16**. Unlike what was observed for the activities of these derivatives on the NF-κB pathway, where the electronic effects of the substituents in the benzoyl moiety seemed to be the determinant, the Nrf2 pathway does not show a clear correlation of these effects with the variation of the potency of compounds. This was because of the presence of electron donating or electron withdrawing groups in compounds **13** and **16**, respectively, does not affect the activity. However, in comparison with derivatives **12**, **14** and **15** having substituents such as chlorine, methoxyl and trifluoromethyl, respectively, com-

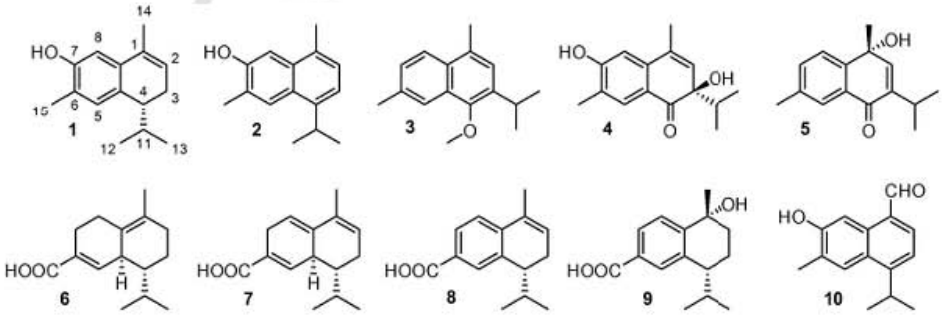

Fig. 1. Structure of cadinane type sesquiterpenoids isolated from *H. inuloides*.

Table 1
Primary screening of some natural cadinane-type sesquiterpenoids on three molecular pathways involved in inflammation and carcinogenesis. All compounds were tested at a concentration of 50 μM. Results are represented as the mean ± standard deviation of at least three different experiments. A minimal value of 50% of inhibition of NF-κB or STAT3 activation and at least two fold inductions in Nrf2 pathway were considered positive results.

Compound	NF-κB inhibition (percentage)	Nrf2 activation (fold induction)	STAT3 inhibition (percentage)
1	50.8 ± 3.6	3.1 ± 0.5	2.1 ± 0.9
2	61.5 ± 3.8	1.7 ± 0.4	3.5 ± 1.1
3	26.5 ± 5.7	1.9 ± 0.4	0.9 ± 0.4
4	28.8 ± 6.6	1.3 ± 0.3	2.2 ± 0.6
5	11.1 ± 3.2	1.7 ± 0.6	2.4 ± 1.6
6	5.9 ± 2.4	1.4 ± 0.4	3.8 ± 0.3
7	12.3 ± 6.2	1.9 ± 0.6	3.6 ± 0.7
8	7.3 ± 4.4	1.8 ± 0.2	2.9 ± 0.5
9	6.7 ± 3.9	1.7 ± 0.6	3.8 ± 1.7
10	40.1 ± 4.1	1.6 ± 0.5	3.5 ± 1.6

pounds **11**, **13** and **16** were notably more potent. This possibly indicates that no substitution in the *para*-position, or substitution with methyl or nitro groups, confers to the molecule a suitable conformation in the pose over one of the receptors involved in the Nrf2 activation pathway.

The potential of compounds showing NF-κB inhibition and Nrf2 activation properties on the primary screening were then compared through dose-response experiments where luciferase activities were measured in cells pre-treated with increasing concentrations of the substances (Fig. 2). The most active compound among those showing anti-NF-κB activity was 7-hydroxy-cadalene (**2**) with an IC_{50} of 16.5 ± 2.2 μM, followed by compound **13** and 7-hydroxy-3,4-dihydrocadalene (**1**) with IC_{50} values of 47.1 ± 2.9 μM and 72.0 ± 3.4 μM, respectively. The decrease on luciferase activity produced by these compounds was not a consequence of its cytotoxicity over the employed cell line. Through kinetic assays, we determined that these compounds are not cytotoxic at the concentrations at which the anti-NF-κB activities were evaluated (Fig. S43, supporting information).

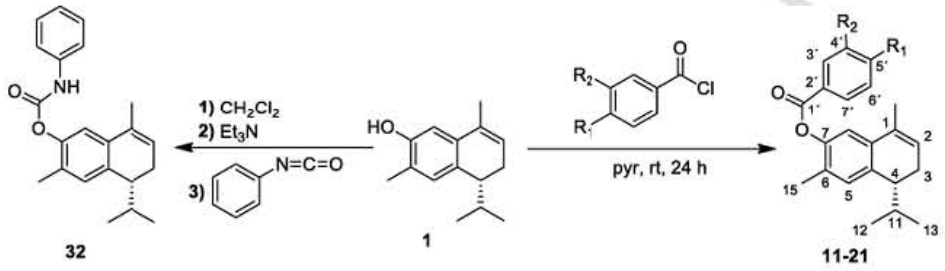

Compound	R_1	R_2
11	H	H
12	Cl	H
13	CH_3	H
14	OCH_3	H
15	CF_3	H
16	NO_2	H
17	H	Cl
18	H	CH_3
19	H	OCH_3
20	H	CF_3
21	H	NO_2

Scheme 1. Semi-synthesis of ester and carbamate derivatives prepared from cadinane-type natural products.

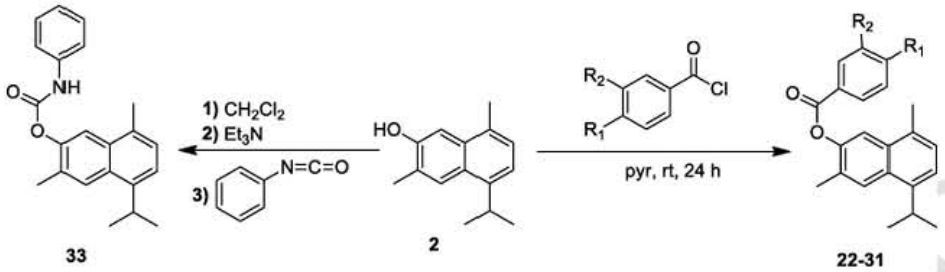

Compound	R_1	R_2
22	H	H
23	Cl	H
24	CH_3	H
25	OCH_3	H
26	CF_3	H
27	NO_2	H
28	H	CH_3
29	H	OCH_3
30	H	CF_3
31	H	Cl

Scheme 1. (*Continued*)

Compound **13** was clearly the best promoter of Nrf2 activation, showing its optimum effect at doses lower than 50 μM because its activity decreases at higher concentrations. As the Nrf2 transcription factor regulates the cellular redox status, some substances that behave as oxidizing agents could indirectly activate the Nrf2 pathway. For this reason, we decided to investigate whether the activating effect on the Nrf2 pathway exerted by compound **13** is a simple consequence of its cellular oxidant effect. Hence, the intracellular accumulation of reactive oxygen species (ROS) was monitored on keratinocytes pre-incubated with increasing concentrations of compound **13**. Fig. 3 shows the fluorometric quantification of ROS using the free radical sensor CM-H2DCFDA (see experimental section for details). The results revealed that compound **13** does not induce the production of ROS. In contrast, it reduces its concentration induced by *tert*-butyl-hydroperoxide (TBHP), which is similar to the antioxidant molecule *N*-acetylcysteine (NAC).

Considering that the signaling pathways involved in the activation of the studied transcription factors represent a focus for pharmacological interventions in situations of chronic inflammation or in cancer, compound **13** showed the best biological profile among ester derivatives by having three important properties. It could activate the Nrf2 pathway, neutralize ROS production and inhibit the NF-κB pathway, which is generally considered as beneficial for cells. For these reasons, we decided to investigate its possible mechanism of action by evaluating its effect on phospho-IκBα, a protein complex involved in the NF-κB activation pathway. In most cells, NF-κB dimers such as p50/RelA are retained in the cytoplasm by interaction with an independent IκB protein (often IκBα). Activation of NF-κB dimers is the result of the phosphorylation, ubiquitination and degradation of the IκB inhibitor that is mediated by the IKK complex, which enables the NF-κB dimers to enter the nucleus and activate specific gene expression targets.[18] Therefore, Western blot analysis was performed to detect levels of endogenous protein expression on cells treated with compound **13**. The results revealed that levels of phospho-IκBα decreased in cells incubated with this semi-synthetic derivative and then treated with TNFα to induce IκBα phosphorylation (Fig. 4). The above observations mean that compound **13** prevents the phosphorylation and degradation of the cytoplasmic IκBα protein. Many substances have been described that inhibit IκB phosphorylation driving to block proteasomal degradation of IκB and allowing it to sequester

Table 2
Cytotoxic effects of semi-synthetic derivatives against six human cancer cell lines and their activities in specific pathways involved in inflammation and carcinogenesis. A minimal value of 50% of inhibition of NF-κB or STAT3 activation and at least two fold inductions in Nrf2 pathway were considered positive results.

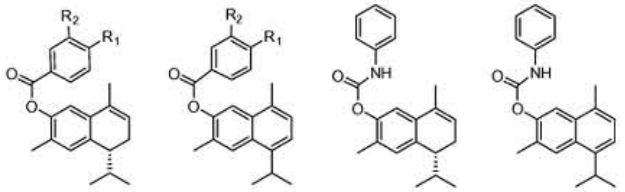

Compound	Substituent		Percentage of inhibition of cell proliferation at a concentration of 50 μM						Activity in transcription factors pathways at a concentration of 50 μM		
			Some IC_{50} values of the most active compounds are included in brackets and represented as the mean ± standard error of at least three different experiments						Results are represented as the mean ± standard deviation of at least three different experiments		
	R_1	R_2	U-251	PC-3	K-562	HCT-15	MCF-7	SK-LU-1	NF-κB inhibition (percentage)	Nrf2 activation (fold induction)	STAT3 inhibition (percentage)
11	H	H	25.8	22.5	NC	49.5	60.7	37.0	47.2 ± 5.3	6.6 ± 0.5	2.4 ± 0.8
12	Cl	H	25.6	34.1	58.9	47.4	79.7	17.4	36.1 ± 3.2	1.3 ± 0.4	2.7 ± 1.0
13	CH_3	H	67.7	49.6	100 [30.94 ± 2.2]	78.9 [40.32 ± 4.1]	65.0	85.4 [33.88 ± 2.2]	76.0 ± 6.6	9.4 ± 0.6	3.1 ± 0.2
14	OCH_3	H	37.0	60.6 [32.17 ± 2.5]	46.5	30.8	80.1	18.6	49.2 ± 4.5	1.9 ± 0.4	1.8 ± 0.7
15	CF_3	H	14.7	12.3	9.0	6.4	40.4	NC	25.4 ± 4.9	1.6 ± 0.4	2.5 ± 0.5
16	NO_2	H	16.8	36.7 [42.47 ± 2.4]	89.0	67.8 [56.33 ± 4.9]	72.9	47.5 [42.89 ± 3.3]	7.2 ± 3.9	8.5 ± 0.7	1.6 ± 0.3
17	H	Cl	0.9	23.4	NC	5.3	40.4	30.6	22.5 ± 5.0	1.4 ± 0.2	1.5 ± 0.6
18	H	CH_3	16.8	38.6	NC	5.3	54.9	NC	44.2 ± 6.7	1.7 ± 0.4	2.3 ± 0.6
19	H	OCH_3	NC	16.3	NC	NC	11.9	24.2	41.2 ± 2.5	1.6 ± 0.5	3.3 ± 0.7
20	H	CF_3	29.3	25.4	45.5	15.0	86.0	18.3	4.4 ± 4.1	1.9 ± 0.2	1.7 ± 0.5
21	H	NO_2	44.0	36.9	15.9	45.9	29.3	60.4	3.5 ± 4.7	1.5 ± 0.4	3.2 ± 0.8
22	H	H	41.5	21.2	44.3	72.0	51.0	63.0	34.5 ± 7.2	1.9 ± 0.7	0.5 ± 0.4
23	Cl	H	92.8 [35.45 ± 0.7]	81.1 [44.01 ± 3.6]	95.4 [19.08 ± 1.8]	82.2 [33.95 ± 1.1]	76.0 [32.13 ± 3.0]	100 [23.85 ± 2.2]	15.5 ± 5.4	1.7 ± 0.5	1.3 ± 0.6
24	CH_3	H	100 [22.79 ± 2.1]	72.3 [23.72 ± 2.0]	100 [8.37 ± 0.6]	86.5 [12.0 ± 0.5]	90.2 [8.20 ± 1.3]	100 [10.23 ± 1.6]	30.3 ± 2.9	1.8 ± 0.3	2.9 ± 0.7
25	OCH_3	H	42.6	10.4	88.6	84.0	93.4	32.8	26.9 ± 4.8	1.3 ± 0.2	2.5 ± 0.8
26	CF_3	H	16.5	100 [34.04 ± 3.5]	45.1	55.6	16.8	28.7	5.2 ± 3.9	1.7 ± 0.5	0.9 ± 0.3
27	NO_2	H	100 [7.75 ± 0.3]	100 [17.57 ± 1.7]	100 [2.28 ± 0.2]	97.6 [7.88 ± 0.7]	100 [7.90 ± 1.7]	100 [9.37 ± 0.9]	18.5 ± 3.0	1.8 ± 0.3	1.6 ± 0.6
28	H	CH_3	5.2	52.4 [47.13 ± 0.7]	17.1	27.6	50.4	NC	4.8 ± 2.7	1.8 ± 0.6	2.0 ± 0.3
29	H	OCH_3	NC	12.5	14.2	35.2	31.8	30.6	2.8 ± 1.9	1.5 ± 0.2	0.8 ± 0.5
30	H	CF_3	NC	26.7	NC	NC	41.5	17.3	4.8 ± 2.0	1.9 ± 0.5	2.7 ± 0.4
31	H	Cl	0.8	4.2	NC	NC	11.4	11.6	25.6 ± 3.7	1.7 ± 0.3	1.8 ± 0.6
32	–		100 [0.46 ± 0.03]	93.2 [7.93 ± 0.6]	92.6 [0.30 ± 0.04]	92.0 [0.03 ± 0.01]	75.1 [4.05 ± 0.1]	100 [0.12 ± 0.01]	4.2 ± 2.1	1.6 ± 0.3	3.3 ± 0.7
33	–		100 [15.78 ± 1.6]	44.7 [8.62 ± 1.1]	100 [13.97 ± 0.4]	84.7 [3.88 ± 0.5]	100	90.4 [10.05 ± 0.8]	13.3 ± 4.1	1.4 ± 0.4	3.0 ± 0.9
Cisplatin	–		3.31 ± 0.6	8.30 ± 0.7	5.34 ± 1.2	10.02 ± 1.0	9.43 ± 1.1	2.03 ± 0.1	–	–	–

U-251 = Central Nervous System (Glia).
PC-3 = Prostate.
K-562 = Leukemia.
HCT-15 = Colon.
MCF-7 = Breast.
SK-LU-1 = Lung.
NC = No cytotoxic.

NF-κB in the cytoplasm in an inactivated state.[17] It is well known that inhibition of NF-κB activation can occur by several mechanisms at different levels of the pathway. One of them is the inhibition of IκB phosphorylation by agents that act directly at the IKK complex.[19] This complex is activated by phosphorylation of its main subunit, IKKβ, in the activation loop at two sites, Ser-177 and Ser-181.[20]

Based on the results showing that compound **13** prevents the phosphorylation and degradation of the IκBα protein, we decided to rationalize the experimental activity at a molecular level. It has been

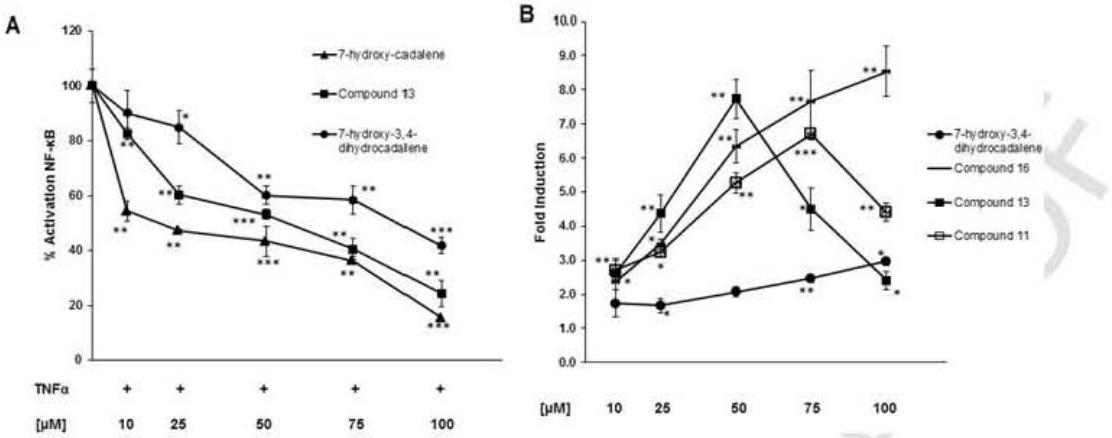

Fig. 2. Effects of *H. inuloides* compounds and some semisynthetic derivatives on NF-κB and Nrf2 activation. (A) NIH-3T3-KBF-Luc cells (fibroblasts) were pre-treated with increasing concentrations of the compounds for 15 min and then stimulated with TNFα (30 ng/mL) for 6 h, after which the luciferase activities were measured in the cell lysates and expressed as percentage of activation considering 100% the value of TNFα-induced NF-κB activation. (B) HaCaT-ARE-Luc cells (keratinocytes) were treated with increasing concentrations of the compounds for 6 h. Luciferase activity was measured in the cell lysates and expressed as fold induction over basal levels. Sample population means were compared against control population means using an unpaired two-tailed Student's *t* test. A p value <0.05 was considered statistically significant ($^{*}p < 0.05$, $^{**}p < 0.01$, $^{***}p < 0.001$). Positive and negative controls are included in the supporting information (Figs. S44, S45 and S46).

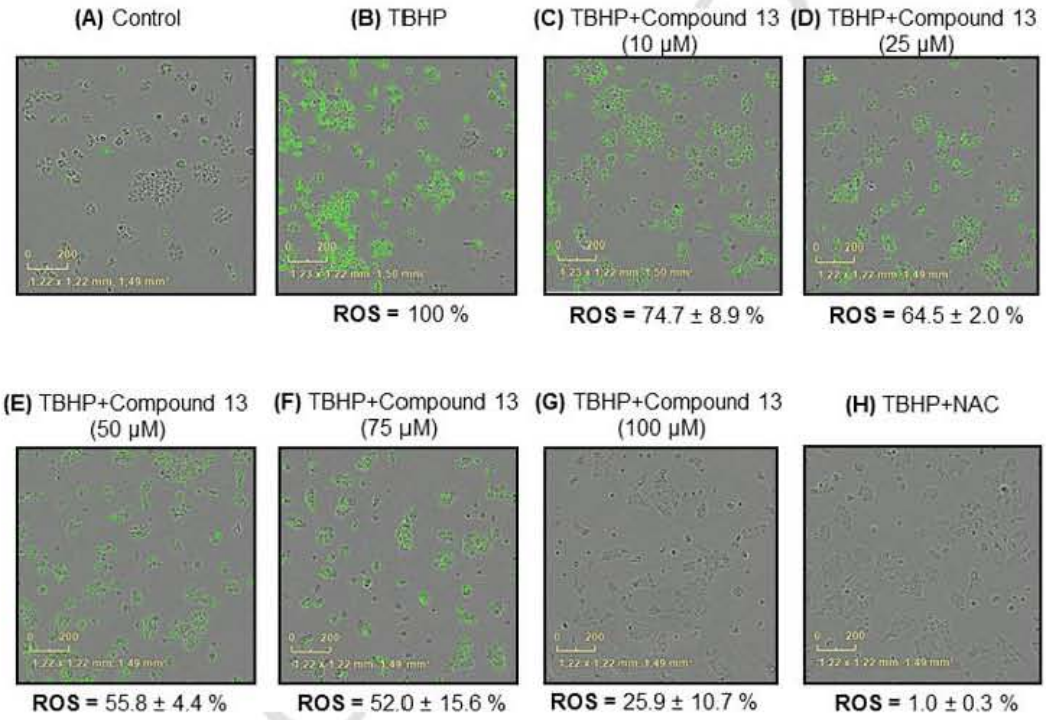

Fig. 3. Fluorometric detection of ROS using the free radical sensor CM-H2DCFDA on HaCaT cell line. (A) Cells over basal conditions. (B) Cells treated with the oxidant compound TBHP (0.4 mM). (C–G) Cells pre-incubated with increasing concentrations of compound **13** and then treated with TBHP (0.4 mM). (H) Cells pre-incubated with the antioxidant NAC (15 mM) and then treated with TBHP (0.4 mM). ROS was measured by changes in fluorescence through imaging analysis of the total green object integrated intensity and expressed as percentage of ROS considering 100% the value of TBHP induction. The results are represented as the mean ± standard deviation of at least three different experiments. Unpaired two-tailed Student's *t* test of the sample population means compared against TBHP population means showed statistically significant differences.

reported that the staurosporine analog K252 is a ligand that interacts with the protomer B of the human IKKβ crystal structure (PDB ID: 4kik).[21] On this basis, molecular docking studies were conducted to evaluate the putative binding modes of compound **13** and staurosporine analog K252 into human IKKβ. The docked structure in Fig. 5 clearly indicated that compound **13** interacts with the ATP-binding pockets by Van der Waals forces (ΔG = −9.43 kcal/mol). A ΔG = −8.67 kcal/mol was calculated for staurosporine analog K252, and the position was similar to that on crystallized structure previous reported (RMSD = 0.074 Å). The value of RMSD indicates good reproducibility and a suitable validation of the docking protocol. Moreover, the protein-ligand interactions between IKKβ and staurosporine analog K252a, found by computational analyses applying our model,

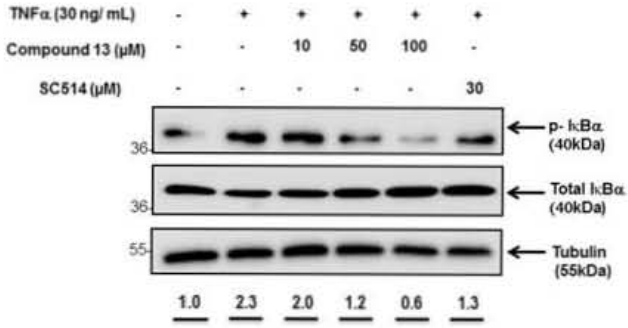

Fig. 4. Compound **13** inhibits phospho-IκBα protein expression. NIH-3T3-KBF-Luc cells were incubated with either increasing concentrations of compound **13** or with the IKKβ inhibitor SC514 during 15 min and then stimulated with TNFα for 20 min. The total cell content was extracted and analyzed to detect the levels of the phospho-IκBα and total IκBα proteins expression using Western blotting.

were similar to those reported for the co-crystallized form (Fig. S47, supporting information).

These results could explain in a preliminary way the inhibitory activity of compound **13**, since it was positioned at the activation loop in the protomer B (residues 166–194), which assumes a conformation characteristic of an active kinase.[21] Those residues are close to the key residues (Ser-177 and Ser-181) for the phosphorylation and subsequent activation of the IKK complex. In this way, the complex protein-compound **13** destabilizes the correct folding of the activation loop. The inactive form IKK complex cannot phosphorylate IκB inhibitor, thus preventing NF-κB release. As previously discussed, the position of the substituent on the benzoyl moiety of the ester derivatives affects their activity on the NF-κB pathway. Considering this observation, the structure of compound **18**, whose structural difference with compound **13** is only the position of the methyl substituent, was also docked at the IKKβ subunit. The results showed that such as occurs with compound **13**, compound **18** also interacts with the ATP-binding pockets of IKKβ by Van der Waals forces (Fig. S48, supporting information) but with a lower energy of union ($\Delta G = -5.02$ kcal/mol), which could explain its minor activity on NF-κB inhibition in comparison with derivative **13**.

Additionally, the molecular structures of 7-hydroxy-cadalene (**2**) and 7-hydroxy-3,4-dihydrocadalene (**1**), both showing in vitro anti-NF-κB activities, were also docked at the IKKβ subunit. The results revealed that compounds **1** and **2** could fit well into the activation pocket through hydrogen bonds with the amino acids Cys-97, Cys-99, Glu-149 and Asn-150 (Fig. 6). The 7-hydroxyl groups make hydrogen bond contact with residue Cys-97 and Cys-99, with a $\Delta G = -7.38$ kcal/mol and $\Delta G = -7.35$ kcal/mol, respectively, indicating that the interaction process is spontaneous and highly favored. Among natural products experimentally tested over the NF-κB pathway (all having the cadinane skeleton), we selected one of the less potent to dock its structure on the IKKβ subunit. Compound **8**, whose structural differences with compound **1** are the substituents on the positions 6 and 7, has a different binding site respect to the ATP-binding pockets (Fig. S49, supporting information). In this way, it could be inferred that the positive activity experimentally observed for the tested compounds depends on its specificity to the ATP-binding pockets of the IKKβ subunit.

Hydrogen bonding and Van der Waals forces probably play a major role in interaction of compound **1** and **2**, while presumably Van der Waals forces are the determinant in the interaction of compound **13** with the ATP-binding pocket.

The primary evaluation of the cytotoxic activities of derivatives over central nervous system, prostate, leukemia, colon, breast and lung cancer cell lines allowed the selection of the most active substances to establish their IC_{50} values (Table 2). These values revealed important activities of the semi-synthetic compounds on leukemia and colon cancer cells. Among the ester derivatives, compounds **24** and **27** were the most potent, with IC_{50} values of 8.37 ± 0.6 μM and

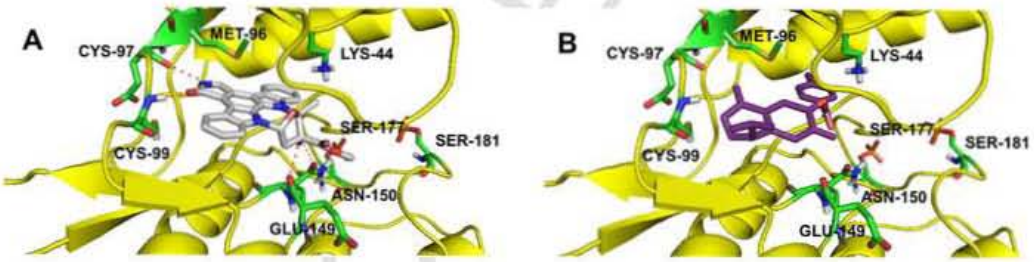

Fig. 5. Docking of staurosporine analog K252 and compound **13** at the protomer B of the human IKKβ crystal structure (PDB ID: 4kik). (A) Staurosporine analog K252 interacts with the ATP-binding pockets through hydrogen bonds with the amino acids Cys-97, Cys-99, Glu-149 and Asn-150 (B) Compound **13** interacts with the ATP-binding pockets by Van der Waals forces ($\Delta G = -9.43$ kcal/mol).

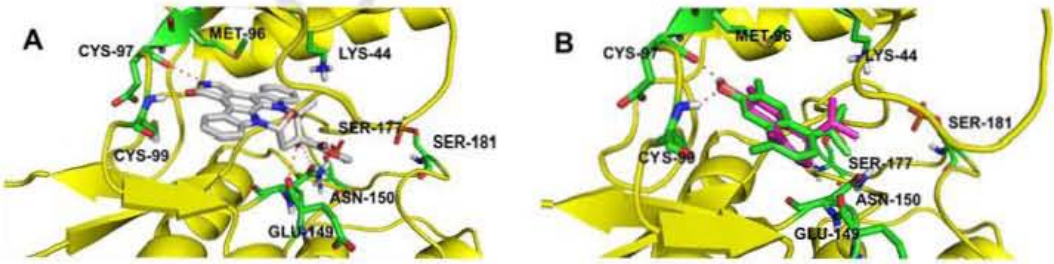

Fig. 6. Docking of staurosporine analog K252, 7-hydroxy-3,4-dihydrocadalene and 7-hydroxy-cadalene at the protomer B of the human IKKβ crystal structure (PDB ID: 4kik). (A) Staurosporine analog K252 interacts with the ATP-binding pockets through hydrogen bonds with the amino acids Cys-97, Cys-99, Glu-149 and Asn-150 (B) 7-hydroxy-3,4-dihydrocadalene (pink) and 7-hydroxy-cadalene (green) interact with the ATP-binding pockets; the 7-hydroxyl group makes hydrogen bond interaction with the residue Cys-97 and Cys-99.

2.28 ± 0.2 μM, respectively, for leukemia cells. Carbamate derivatives **32** and **33** were highly cytotoxic on human colorectal adenocarcinoma with IC_{50} values of 0.03 ± 0.01 μM and 3.88 ± 0.5 μM, respectively. It was clear that the inhibition of cell proliferation over leukemia and colon cancer cells exerted by these four compounds were not a direct consequence of their activity on the evaluated pathways, since they did not show an important effect on NF-κB, Nrf2 or STAT3. This could mean that a different cellular death mechanism could be involved in the effect observed or simply that these compounds are highly toxic on any type of cell. This latter result is undesirable since it is essential that new potential anticancer compounds affect a particular target or pathway involved in the process of malignancy.[17] For this reason, we decided to evaluate its cytotoxicity on a non-tumorigenic primary cell culture from human oral tissue (gingival fibroblast). The results revealed that compounds **24** and **27** showed a 13.37 ± 1.8% and 43.03 ± 1.8%, respectively, of inhibition of cell proliferation at a concentration of 50 μM, indicating low toxicity on healthy cells. Moreover, at this concentration both compounds produce a 100% of inhibition of cell proliferation in leukemia (Table 2). Compound **32** also showed low cytotoxicity in gingival fibroblasts with a 38.24 ± 1.7% of inhibition of cell proliferation at a concentration of 50 μM. Although compound **33** was less potent than **32** for inhibition of human colorectal adenocarcinoma cell proliferation, it was not cytotoxic on gingival fibroblast, which makes it interesting in terms of selectivity. A variety of mechanisms of cell death have been demonstrated for compounds containing the carbamate functionality. For instance, Entinostat, a synthetic benzamide derivative containing a pyridylmethyl carbamate fragment, acts as an antitumor agent through histone deacetylase inhibition.[22] Mitomycin C, a natural chemotherapeutic agent in the treatment of several types of cancer, interacts with ribosomal RNA producing inhibition of protein translation.[23] Recently, the discovery of a potent semi-synthetic phenyl carbamate showing in vitro activity against breast cancer cells through a mechanism involving the receptor tyrosine kinase c-Met has been reported.[24] The ability of carbamates to modulate inter- and intramolecular interactions with the target enzymes or receptors has been widely used in medicinal chemistry.[25]

Although it is known that some anticancer agents that have shown anti-NF-κB activity may exert their effects by lessening proliferation, antiapoptotic or inflammatory activity of NF-κB,[19] we did not find a correlation of the anti-proliferative activity of the compounds in leukemia and colon cancer cells (with their capacity of inhibition of the NF-κB pathway). It is possible that the potency of these compounds for inhibit inflammatory pathways could decrease the optimal conditions for cancer development at an early stage; however, this effect could not be significant enough to cause important inhibition of cancer cell proliferation.

3. Conclusions

The effect of cadinane sesquiterpenoids isolated from *H. inuloides* on two pathways involved in inflammation was observed. The results indicated that 7-hydroxy-3,4-dihydrocadalene (**1**), the main constituent in this species, inhibits the NF-κB pathway and is able to activate the antioxidant Nrf2 pathway, which may correlate with the use of this species in Mexican folk medicine.

A novel semi-synthetic set, including ester and carbamate derivatives, was prepared using the active natural cadinanes as scaffolds. Derivative **13** was more potent for NF-κB inhibition and Nrf2 activation when compared with its parent 7-hydroxy-3,4-dihydrocadalene (**1**). Additionally, compound **13** reduces the intracellular accumulation of ROS induced by TBHP and decreases levels of phospho-IκBα, a protein complex involved in the NF-κB activation pathway. Docking analyses revealed that compound **13** is positioned at the activation loop of the IKKβ subunit, which may explain in a preliminary way, how it prevents IκBα phosphorylation.

Carbamate derivatives **32** and **33** showed potent in vitro cytotoxic activities against human colorectal adenocarcinoma with minimal toxicity on human gingival fibroblast cells. These compounds were ineffective on NF-κB, Nrf2 and STAT3 transcription factors, indicating a cell death mechanism involving different pathways or targets. Thus, further investigations are needed.

Cadinane sesquiterpenoids could now be considered a novel class of natural NF-κB and Nrf2 modulators, which can be useful as templates for the development and optimization of new substances with anti-inflammatory and anticancer activities.

4. Experimental section

4.1. General methods

UV spectra were obtained on a Shimadzu UV–VISIBLE recording Spectrophotometer. IR spectra were recorded on a Bruker Tensor 27 spectrometer. ^{1}H and ^{13}C NMR spectra were measured on a Bruker Avance III, 400 MHz NMR instrument. Chemical shifts are reported in parts per million (δ) relative to TMS, and coupling constants (J) are reported in Hz. The complete assignment of ^{1}H and ^{13}C signals was carried out by an analysis of the correlated homonuclear H,H-COSY, and heteronuclear H,C-HSQC and H,C-HMBC spectra. The HRMS data were taken on a Jeol The AccuTOF JMS T100 LC system with a direct analysis in real time ESI+ ionization mode.

Vacuum liquid chromatography (VLC) was carried out using spherical silica gel with pore size 60 Å and 230–400 mesh particle size. Reactions were monitored by TLC employing Merck silica gel 60 F_{254} plates (0.2 mm) visualized with either an UV lamp (254 and 365 nm) or a charring solution (12 g of ceric ammonium sulfate dihydrate, 22.2 mL of concentrated H_2SO_4, and 350 g of ice). PLCs were conducted using Merck silica gel 60 F_{254} glass plates (2 mm).

4.2. Plant material

H. inuloides (aerial parts) was collected in the region of Ozumba, in Estado de México, Mexico in October 2012. Voucher specimen was authenticated by Edelmira Linares and Robert Bye (collection of E. Linares 2754 and R. Bye) and deposited in the National Herbarium (MEXU), Instituto de Biología de la Universidad Nacional Autónoma de México.

4.3. Extraction and isolation

7-Hydroxy-3,4-dihydrocadalene (**1**) and 7-hydroxy-cadalene (**2**) preparative amounts were obtained by fractionation of an acetonic extract (348.6 g) prepared by maceration (3 times/24 h) of dried and powdered plant material (10 kg). This extract was concentrated under reduced pressure and subjected to separation processes by VLC using a hexanes-EtOAc gradient as mobile phase. From fractions eluted with hexanes-EtOAc 75:25 and 70:30 were obtained 2.7 g of 7-hydroxy-3,4-dihydrocadalene and 331 mg of 7-hydroxy-cadalene, respectively, which were purified through recrystallization from hexanes. Spectroscopic data were compared with authentic samples from our laboratory. Metabolites **1–8** were isolated in previous investigations carried out by our group.[16]

4.4. Semi-synthetic derivatives

*4.4.1. General procedure for esterification of 7-hydroxy-3,4-dihydrocadalene (**1**) and 7-hydroxy-cadalene (**2**)*

A solution of either 7-hydroxy-3,4-dihydrocadalene (1.0 equiv) or 7-hydroxy-cadalene (1.0 equiv) in anhydrous pyridine (1 mL/20 mg of natural product) was flushed with nitrogen gas and then a balloon filled with helium gas was connected to the septum. This solution was treated with the respective benzoyl chloride reagent (2.0 equiv) having electron donating or electron withdrawing substituents in *meta* and *para* positions (Sigma Aldrich). After 24 h stirring the mixture was quenched with ice-cold water and the organic phase was extracted with EtOAc. Excess pyridine was neutralized with HCl (10%), and subsequent addition of a saturated solution of $NaHCO_3$ avoided acidification of the medium. The resulting mixture was treated with a saturated solution of NaCl and the organic phase was passed over Na_2SO_4 to remove remaining water. Purification of each one of the semisynthetic esters was carried out by PLC (hexanes-EtOAc 90:10, two or three elutions). Preparation and structural characterization of derivatives **11** and **22** have been previously described by our research group.[26]

*4.4.1.1. 7-(p-Chloro-benzoyloxy)-3,4-dihydrocadalene (**12**)*

Yellow oil; 34.4 mg 81% yield; UV (MeOH) λ_{max}(log ε) 204 (4.77), 224 (4.52), 239 (4.63) nm; IR ($CHCl_3$) ν_{max} 3536, 2961, 1734, 1594, 1260, 1130, 1093 cm^{-1}; ^1H NMR (400 MHz, $CDCl_3$) 0.84 (3H, d, $J_{13,11}$ 6.8 Hz, CH_3-13), 0.91 (3H, d, $J_{12,11}$ 6.8 Hz, CH_3-12), 1.91 (1H, hept, $J_{11,12;11,13}$ 6.8 Hz, H-11),1.99 (3H, br s, CH_3-14), 2.19 (3H, s, CH_3-15), 2.38 (3H, overlapped, H-3,4), 5.72 (1H, br d, $J_{2,3}$ 1.2 Hz, H-2), 6.96 (1H, s, H-8), 7.00 (1H, s, H-5), 7.50, (2H, br d, $J_{3',4';6',7'}$ 6.8 Hz, H-4′,6′), 8.17, (2H, br d, $J_{3',4';\ 6',7'}$ 6.8 Hz, H-3′,7′); ^{13}C NMR (100 MHz, $CDCl_3$) 16.0 (CH_3-15), 18.9 (CH_3-14), 20.2 (CH_3-12), 21.4 (CH_3-13), 25.5 (CH_2-3), 30.2 (CH-11), 43.8 (CH-4), 116.2 (CH-8), 124.0 (CH-2), 127.3 (C-6), 128.1 (C-5′), 128.9 (CH-4′,6′), 131.1 (CH-5), 131.5 (CH-3′,7′, C-9), 134.8 (C-1), 137.0 (C-10), 140.0 (C-2′), 147.8 (C-7), 164.2 (C-1′); HRESIMS *m/z* 355.14561 $[M+H]^+$ (calcd for $C_{22}H_{24}ClO_2$, 355.14648).

*4.4.1.2. 7-(p-Methyl-benzoyloxy)-3,4-dihydrocadalene (**13**)*

White solid; 32.2 mg 77% yield; UV (MeOH) λ_{max}(log ε) 211 (4.67), 261 (4.57) nm; IR ($CHCl_3$) ν_{max} 3538, 3038, 2961, 1726, 1606, 1256, 1233, 1130 cm^{-1}; ^1H NMR (400 MHz, $CDCl_3$) 0.84 (3H, d, $J_{13,11}$ 6.8 Hz, CH_3-13), 0.91 (3H, d, $J_{12,11}$ 6.8 Hz, CH_3-12), 1.91 (1H, hept, $J_{11,12;11,13}$ 6.8 Hz, H-11),1.99 (3H, br s, CH_3-14), 2.20 (3H, s, CH_3-15), 2.38 (3H, overlapped, H-3,4), 2.46 (3H, s, CH_3-8′), 5.71 (1H, br d, $J_{2,3}$ 1.6 Hz, H-2), 6.98 (1H, s, H-8), 7.0, (1H, s, H-5), 7.32, (2H, d, $J_{4',3';6',7'}$ 9.2 Hz, H-4′,6′), 8.12, (2H, d, $J_{3',4';7',6'}$ 8.12 Hz, H-3′,7′); ^{13}C NMR (100 MHz, $CDCl_3$) 16.0 (CH_3-15), 19.0 (CH_3-14), 20.2 (CH_3-12), 21.4 (CH_3-13), 21.7 (CH_3-8′), 25.5 (CH_2-3), 30.2 (CH-11), 43.8 (CH-4), 116.3 (CH-8), 123.9 (CH-2), 126.9 (C-2′), 127.5 (C-6), 129.3 (CH-4′,6′), 130.2 (CH-3′,7′), 131.0 (CH-5), 131.2 (C-9), 134.7 (C-1), 136.7 (C-10), 144.2 (C-5′), 147.9 (C-7), 165.1 (C-1′); HRESIMS *m/z* 335.20016 $[M+H]^+$ (calcd for $C_{23}H_{27}O_2$, 335.20110).

*4.4.1.3. 7-(p-Methoxy-benzoyloxy)-3,4-dihydrocadalene (**14**)*

White solid; 22.5 mg 69% yield; UV (MeOH) λ_{max}(log ε) 204 (4.80), 239 (4.63) nm; IR ($CHCl_3$) ν_{max} 3533, 3019, 2961, 1730, 1263, 1233, 1131 cm^{-1}; ^1H NMR (400 MHz, $CDCl_3$) 0.84 (3H, d, $J_{13,11}$ 6.8 Hz, CH_3-13), 0.91 (3H, d, $J_{12,11}$ 6.8 Hz, CH_3-12), 1.90 (1H, hept, $J_{11,12;11,13}$ 6.8 Hz, H-11),1.99 (3H, br s, CH_3-14), 2.20 (3H, s, CH_3-15), 2.38 (3H, overlapped, H-3,4), 3.90 (3H, s, CH_3-8′), 5.70 (1H, br d, $J_{2,3}$ 1.6 Hz, H-2), 6.97 (1H, s, H-8), 6.99 (3H, m, H-5,4′,6′), 8.18 (2H, d, $J_{3',4';7',6'}$ 8.8 Hz, H-3′,7′); ^{13}C NMR (100 MHz, $CDCl_3$) 16.0 (CH_3-15), 19.0 (CH_3-14), 20.2 (CH_3-12), 21.4 (CH_3-13), 25.5 (CH_2-3), 30.2 (CH-11), 43.8 (CH-4), 55.5 (CH_3-8′), 113.8 (CH-4′,6′), 116.4 (CH-8), 122.0 (C-2′), 123.8 (CH-2), 127.5 (C-6), 131.0 (CH-5), 131.2 (C-9), 132.2 (CH-3′,7′), 134.7 (C-1), 136.7 (C-10), 148.0 (C-7), 163.8 (C-5′), 164.7 (C-1′); HRESIMS *m/z* 351.19493 $[M+H]^+$ (calcd for $C_{23}H_{27}O_3$, 351.19602).

*4.4.1.4. 7-(p-Trifluoromethyl-benzoyloxy)-3,4-dihydrocadalene (**15**)*

White solid; 22.1 mg 73% yield; UV (MeOH) λ_{max}(log ε) 204 (4.53), 209 (4.51), 229 (4.69), 251 (4.02), 264 (4.03) nm; IR ($CHCl_3$) ν_{max} 2960, 1737, 1325, 1263,1175, 1133 cm^{-1}; ^1H NMR (400 MHz, $CDCl_3$) 0.83 (3H, d, $J_{13,11}$ 6.8 Hz, CH_3-13), 0.91 (3H, d, $J_{12,11}$ 6.8 Hz, CH_3-12), 1.91 (1H, hept, $J_{11,12;11,13}$ 6.8 Hz, H-11), 1.99 (3H, br s, CH_3-14), 2.19 (3H, s, CH_3-15), 2.38 (3H, overlapped, H-3,4), 5.72 (1H, br d, $J_{2,3}$ 1.6 Hz, H-2), 6.97 (1H, s, H-8), 7.01 (1H, s, H-5), 7.79, (2H, br d, $J_{4',3';6',7'}$ 8.8 Hz, H-4′,6′), 8.34, (2H, br d, $J_{3',4';7',6'}$ 8.8 Hz, H-3′,7′); ^{13}C NMR (100 MHz, $CDCl_3$) 16.0 (CH_3-15), 18.9 (CH_3-14), 20.2 (CH_3-12), 21.4 (CH_3-13), 25.5 (CH_2-3), 30.3 (CH-11), 43.8 (CH-4), 116.1 (CH-8), 124.2 (CH-2), 125.6 (CH-4′,6′), 127.2 (C-6), 130.5 (CH-3′,7′), 131.0 (C-9), 131.2 (CH-5), 133.0 (C-5′), 134.9 (C-1, C-2′), 137.2 (C-10), 147.7 (C-7), 163.9 (C-1′); HRESIMS *m/z* 389.17176 $[M+H]^+$ (calcd for $C_{23}H_{24}F_3O_2$, 389.17284).

*4.4.1.5. 7-(p-nitro-Benzoyloxy)-3,4-dihydrocadalene (**16**)*

Yellow oil; 23.1 mg 84% yield; UV (MeOH) λ_{max}(log ε) 205 (3.72), 244 (3.42), 258 (3.46) nm; IR ($CHCl_3$) ν_{max} 3558, 3020, 2960, 1739, 1530, 1262, 1232, 1129 cm^{-1}; ^1H NMR (400 MHz, $CDCl_3$) 0.83 (3H, d, $J_{13,11}$ 6.8 Hz, CH_3-13), 0.91 (3H, d, $J_{12,11}$ 6.8 Hz, CH_3-12), 1.90 (1H, hept, $J_{11,12;11,13}$ 6.8 Hz, H-11), 1.99 (3H, br s, CH_3-14), 2.20 (3H, s, CH_3-15), 2.38 (3H, overlapped, H-3,4), 5.73 (1H, br d, $J_{2,3}$ 1.2 Hz, H-2), 6.97 (1H, s, H-8), 7.01 (1H, s, H-5), 6.97 (4H, m, H-3′,4′,6′,7′); ^{13}C NMR (100 MHz, $CDCl_3$) 16.0 (CH_3-15), 18.9 (CH_3-14), 20.2 (CH_3-12), 21.4 (CH_3-13), 25.4 (CH_2-3), 30.2 (CH-11), 43.8 (CH-4), 115.9 (CH-8), 123.7 (CH-4′,6′), 124.3 (CH-2), 127.0 (C-6), 130.9 (CH-5), 131.2 (CH-3′,7′, C-9), 134.9 (C-1), 135.0 (C-2′), 137.3 (C-10), 147.5 (C-7), 150.8 (C-5′), 163.1 (C-1′); HRESIMS *m/z* 366.16922 $[M+H]^+$ (calcd for $C_{22}H_{24}NO_4$, 366.17053).

*4.4.1.6. 7-(m-Chloro-benzoyloxy)-3,4-dihydrocadalene (**17**)*

Colorless oil; 46.5 mg 77% yield; UV (MeOH) λ_{max}(log ε) 206 (4.55), 225 (4.37), 234 (4.41),), 271 (3.70) nm; IR ($CHCl_3$) ν_{max} 2962, 1711, 1363, 1248, 1131 cm^{-1}; ^1H NMR (400 MHz, $CDCl_3$) 0.83 (3H, d, $J_{13,11}$ 6.8 Hz, CH_3-13), 0.91 (3H, d, $J_{12,11}$ 6.8 Hz, CH_3-12), 1.91 (1H, hept, $J_{11,12;11,13}$ 6.8 Hz, H-11), 1.98 (3H, br s, CH_3-14), 2.19 (3H, s, CH_3-15), 2.38 (3H, overlapped, H-3,4), 5.72 (1H, br d, $J_{2,3}$ 1.6 Hz, H-2), 6.95 (1H, s, H-8), 7.00 (1H, s, H-5), 7.47 (1H, t, $J_{6',5';6',7'}$ 8.0 Hz, H-6′), 7.62 (1H, ddd, $J_{5',6'}$ 8.0 Hz, $J_{5',3'}$ 2.0 Hz, $J_{5'7'}$ 1.2 Hz, H-5′), 8.11 (1H, dt, $J_{7',6'}$ 8.0 Hz, $J_{7',5'}$ 1.2 Hz, H-7′), 8.21 (1H, t, $J_{3',5'}$ 2.0 Hz, H-3′); ^{13}C NMR (100 MHz, $CDCl_3$) 16.0 (CH_3-15), 18.9 (CH_3-14), 20.2 (CH_3-12), 21.4 (CH_3-13), 25.5 (CH_2-3), 30.2 (CH-11), 43.8 (CH-4), 116.1 (CH-8), 124.1 (CH-2), 127.2 (C-6), 128.2 (CH-7′), 129.9 (CH-6′), 130.1 (CH-3′), 131.1 (CH-5), 131.4 (C-1), 133.5 (CH-5′), 133.6 (C-2′), 134.7 (C-4′), 134.8 (C-9), 137.0 (C-10), 147.7 (C-7), 163.8 (C-1′); HRESIMS *m/z* 355.14559 $[M+H]^+$ (calcd for $C_{22}H_{24}ClO_2$, 355.14648).

*4.4.1.7. 7-(m-Methyl-benzoyloxy)-3,4-dihydrocadalene (**18**)*

Yellow oil; 45.1 mg 89% yield; UV (MeOH) λ_{max}(log ε) 205 (4.66), 225 (4.40), 235 (4.45) nm; IR ($CHCl_3$) ν_{max} 3579, 2964, 1732,

1276, 1195, 1129, 1070 cm^{-1}; ^1H NMR (400 MHz, $CDCl_3$) 0.85 (3H, d, $J_{13,11}$ 6.8 Hz, CH_3-13), 0.92 (3H, d, $J_{12,11}$ 6.8 Hz, CH_3-12), 1.92 (1H, hept, $J_{11,12;11,13}$ 6.8 Hz, H-11), 2.00 (3H, br s, CH_3-14), 2.22 (3H, s, CH_3-15), 2.40 (3H, overlapped, H-3,4), 2.47 (3H, s, CH_3-8′), 5.70 (1H, br d, $J_{2,3}$ 0.8 Hz, H-2), 6.99 (1H, s, H-8), 7.01 (1H, s, H-5), 7.44, (2H, m, H-5′,6′), 8.05, (2H, m, H-3′,7′); ^{13}C NMR (100 MHz, $CDCl_3$) 16.0 (CH_3-15), 18.9 (CH_3-14), 20.2 (CH_3-12), 21.3 (CH_3-8′), 21.4 (CH_3-13), 25.5 (CH_2-3), 30.2 (CH-11), 43.8 (CH-4), 116.3 (CH-8), 123.9 (CH-2), 127.3 (CH-7′), 127.4 (C-6), 128.4 (CH-6′), 129.6 (C-2′), 130.6 (CH-3′), 131.0 (CH-5), 131.1 (C-1), 134.2 (CH-5′), 134.7 (C-9), 136.7 (C-10), 138.2 (C-4′), 147.9 (C-7), 165.2 (C-1′); HRESIMS *m/z* 335.20129 $[M+H]^+$ (calcd for $C_{23}H_{27}O_2$, 335.20110).

4.4.1.8. 7-(m-Methoxy-benzoyloxy)-3,4-dihydrocadalene ***(19)***

Yellow oil; 83.0 mg 95% yield; UV (MeOH) λ_{max}(log ε) 214 (4.75), 347 (2.34) nm; IR ($CHCl_3$) ν_{max} 3558, 2962, 1732, 1491, 1277, 1233, 1129 cm^{-1}; ^1H NMR (400 MHz, $CDCl_3$) 0.86 (3H, d, $J_{13,11}$ 6.8 Hz, CH_3-13), 0.93 (3H, d, $J_{12,11}$ 6.8 Hz, CH_3-12), 1.93 (1H, hept, $J_{11,12;11,13}$ 6.8 Hz, H-11), 2.00 (3H, br s, CH_3-14), 2.23 (3H, s, CH_3-15), 2.40 (3H, overlapped, H-3,4), 3.90 (3H, s, CH_3-8′), 5.73 (1H, br d, $J_{2,3}$ 1.2 Hz, H-2), 7.00 (1H, s, H-8), 7.02 (1H, s, H-5), 7.19, (1H, ddd, $J_{5',6'}$ 8.0 Hz, $J_{5',3'}$ 2.8 Hz, $J_{5',7'}$ 1.2 Hz, H-5′), 7.44 (1H, t, $J_{6',5';6',7'}$ 8 Hz, H-6′), 7.76 (1H, t, $J_{3',5'}$ 2.8 Hz, H-3′); 7.86 (1H, dt, $J_{7',6'}$ 8.0 Hz, $J_{7',5'}$ 1.2 Hz, H-7′); ^{13}C NMR (100 MHz, $CDCl_3$) 16.0 (CH_3-15), 18.9 (CH_3-14), 20.2 (CH_3-12), 21.4 (CH_3-13), 25.5 (CH_2-3), 30.2 (CH-11), 43.8 (CH-4), 55.4 (CH_3-8′), 114.5 (CH-3′), 116.2 (CH-8), 120.0 (CH-5′), 122.5 (CH-7′), 123.9 (CH-2), 127.4 (C-6), 129.5 (CH-6′), 130.9 (C-2′), 131.0 (CH-5), 131.1 (C-10), 134.7 (C-1), 136.8 (C-9), 147.9 (C-7), 159.7 (C-4′), 164.8 (C-1′); HRESIMS *m/z* 351.19599 $[M+H]^+$ (calcd for $C_{23}H_{27}O_3$, 351.19602).

4.4.1.9. 7-(m-Trifluoromethyl-benzoyloxy)-3,4-dihydrocadalene ***(20)***

Colorless oil; 22.1 mg 88% yield; UV (MeOH) λ_{max}(log ε) 203 (4.64), 215 (4.55), 226 (4.59) nm; IR ($CHCl_3$) ν_{max} 3576, 2965, 1740, 1336, 1174, 1136, 1073 cm^{-1}; ^1H NMR (400 MHz, $CDCl_3$) 0.84 (3H, d, $J_{13,11}$ 6.8 Hz, CH_3-13), 0.91 (3H, d, $J_{12,11}$ 6.8 Hz, CH_3-12), 1.91 (1H, hept, $J_{11,12;11,13}$ 6.8 Hz, H-11), 1.99 (3H, br s, CH_3-14), 2.21 (3H, s, CH_3-15), 2.39 (3H, overlapped, H-3,4), 5.73 (1H, br d, $J_{2,3}$ 1.2 Hz, H-2), 6.97 (1H, s, H-8), 7.01 (1H, s, H-5), 7.68 (1H, m, H-6′), 7.90, (1H, br d, $J_{5',6'}$ 8.4 Hz, H-5′), 8.41 (1H, d, $J_{7',6'}$ 7.6 Hz, H-7′), 8.50 (1H, s, H-3′); ^{13}C NMR (100 MHz, $CDCl_3$) 16.0 (CH_3-15), 18.9 (CH_3-14), 20.2 (CH_3-12), 21.4 (CH_3-13), 25.5 (CH_2-3), 30.2 (CH-11), 43.8 (CH-4), 116.0 (CH-8), 124.1 (CH-2), 127.0 (CH-3′), 127.2 (C-6), 129.3 (CH-6′), 130.0 (CH-5′), 130.1 (C-2′), 130.5 (C-4′), 131.0 (C-1), 131.1 (CH-5), 133.3 (CH-7′), 135.0 (C-9), 137.1 (C-10), 147.6 (C-7), 163.7 (C-1′); HRESIMS *m/z* 389.17234 $[M+H]^+$ (calcd for $C_{23}H_{24}F_3O_2$, 389.17284).

4.4.1.10. 7-(m-Nitro-benzoyloxy)-3,4-dihydrocadalene ***(21)***

Yellow oil; 32.2 mg 72% yield; UV (MeOH) λ_{max}(log ε) 223 (4.70), 245 (4.19), 260 (4.20) nm; IR ($CHCl_3$) ν_{max} 2959, 1741, 1536, 1353, 1255, 1133 cm^{-1}; ^1H NMR (400 MHz, $CDCl_3$) 0.84 (3H, d, $J_{13,11}$ 6.8 Hz, CH_3-13), 0.91 (3H, d, $J_{12,11}$ 6.8 Hz, CH_3-12), 1.91 (1H, hept, $J_{11,12;11,13}$ 6.8 Hz, H-11), 1.99 (3H, br s, CH_3-14), 2.21 (3H, s, CH_3-15), 2.39 (3H, overlapped, H-3,4), 5.73 (1H, br d, $J_{2,3}$ 1.6 Hz, H-2), 6.98 (1H, s, H-8), 7.02 (1H, s, H-5), 7.74 (1H, t, $J_{6',5';6',7'}$ 8 Hz, H-6′), 8.50, (1H, ddd, $J_{5',6'}$ 8.0 Hz, $J_{5',3'}$ 2.4 Hz, $J_{5',7'}$ 1.2 Hz, H-5′), 8.55 (1H, dt, $J_{7',6'}$ 8.0 Hz, $J_{7',5'}$ 1.2 Hz, H-7′), 9.06 (1H, t, $J_{3',5'}$ 2.4 Hz, H-3′); ^{13}C NMR (100 MHz, $CDCl_3$) 16.0 (CH_3-15), 18.9 (CH_3-14), 20.2 (CH_3-12), 21.4 (CH_3-13), 25.5 (CH_2-3), 30.3 (CH-11), 43.8 (CH-4), 115.9 (CH-8), 124.3 (CH-2), 125.1 (CH-3′), 127.1 (C-6), 127.9 (CH-5′), 129.9 (CH-6′), 131.0 (C-1), 131.2 (CH-5), 131.5 (C-2′), 135.0 (C-9), 135.7 (CH-7′), 137.3 (C-10), 147.6 (C-7), 148.5 (C-4′), 163.0 (C-1′); HRESIMS *m/z* 366.17023 $[M+H]^+$ (calcd for $C_{22}H_{24}NO_4$, 366.17053).

4.4.1.11. 7-(p-Chloro-benzoyloxy)-cadalene ***(23)***

White crystals; 28.2 mg 78% yield; UV (MeOH) λ_{max}(log ε) 208 (4.84), 216 (4.81), 235 (4.91) nm; IR ($CHCl_3$) ν_{max} 2967, 1735, 1267, 1092 cm^{-1}; ^1H NMR (400 MHz, $CDCl_3$) 1.39 (6H, d, $J_{12,11;13,11}$ 6.8 Hz, CH_3-12,13), 2.41 (3H, s, CH_3-15), 2.60 (3H, s, CH_3-14), 3.71 (1H, hept, $J_{11,12;11,13}$ 6.8 Hz, H-11), 7.26 (2H, overlapped, H-2,3), 7.51 (2H, d, $J_{4',3';6',7'}$ 8.8 Hz, H-4′,6′), 7.75 (1H, s, H-8), 8.03 (1H, s, H-5), 8.21 (2H, d, $J_{3',4';7',6'}$ 8.8 Hz, H-3′,7′); ^{13}C NMR (100 MHz, $CDCl_3$) 17.2 (CH_3-15), 19.4 (CH_3-14), 23.6 (CH_3-12,13), 28.5 (CH-11), 116.5 (CH-8), 121.4 (CH-3), 125.8 (CH-5), 126.4 (CH-2), 128.0 (C-5′), 128.5 (C-6), 129.0 (CH-4′,6′), 130.0 (C-10), 131.6 (CH-3′,7′, C-1), 132.5 (C-9), 140.2 (C-2′), 142.2 (C-4), 147.6 (C-7), 164.4 (C-1′); HRESIMS *m/z* 353.12940 $[M+H]^+$ (calcd for $C_{22}H_{22}ClO_2$, 353.13083).

4.4.1.12. 7-(p-Methyl-benzoyloxy)-cadalene ***(24)***

White crystals; 24.7 mg 82% yield; UV (MeOH) λ_{max}(log ε) 208 (7.73), 211 (4.70), 237 (4.87), 281 (4.05) nm; IR ($CHCl_3$) ν_{max} 3693, 2966, 1731, 1611, 1442, 1269, 1129, 1077 cm^{-1}; ^1H NMR (400 MHz, $CDCl_3$) 1.39 (6H, d, $J_{11,12;\ 11,13}$ 6.8 Hz, CH_3-12,13), 2.42 (3H, s, CH_3-15), 2.46 (3H, s, CH_3-8′), 2.60 (3H, s, CH_3-14), 3.71 (1H, hept, $J_{11,12;11,13}$ 6.8 Hz, H-11), 7.25 (2H, overlapped, H-2,3), 7.33 (2H, d, $J_{4',3';6',7'}$ 8.0 Hz, H-4′,6′), 7.75 (1H, s, H-8), 8.02 (1H, s, H-5), 8.17 (2H, d, $J_{3',4';7',6'}$ 8.4 Hz, H-3′,7′); ^{13}C NMR (100 MHz, $CDCl_3$) 17.2 (CH_3-15), 19.4 (CH_3-14), 21.7 (CH_3-8′), 23.6 (CH_3-12,13), 28.4 (CH-11), 116.5 (CH-8), 121.2 (CH-3), 125.7 (CH-5), 126.2 (CH-2), 126.7 (C-2′), 128.8 (C-6), 129.2 (CH-4′,6′), 129.9 (C-10), 130.3 (CH-3′,7′), 131.6 (C-1), 132.5 (C-9), 142.1 (C-4), 144.4 (C-5′), 147.8 (C-7), 165.3 (C-1′); HRESIMS *m/z* 333.18453 $[M+H]^+$ (calcd for $C_{23}H_{25}O_2$, 333.18545).

4.4.1.13. 7-(p-Methoxy-benzoyloxy)-cadalene ***(25)***

Colorless crystals; 24.2 mg 84% yield; UV (MeOH) λ_{max}(log ε) 215 (4.82), 225 (4.76), 231 (4.78), 244 (4.42), 261 (4.59) nm; IR ($CHCl_3$) ν_{max} 3554, 2967, 1728, 1606, 1512, 12,259, 1168, 1129, 1077 cm^{-1}; ^1H NMR (400 MHz, $CDCl_3$) 1.39 (6H, d, $J_{12,11;13,11}$ 6.8 Hz, CH_3-12,13), 2.42 (3H, s, CH_3-15), 2.60 (3H, s, CH_3-14), 3.71 (1H, hept, $J_{11,12;11,13}$ 6.8 Hz, H-11), 3.90 (3H, s, CH_3-8′), 7.01 (2H, d, $J_{4',3';6',7'}$ 8.8 Hz, H-4′,6′), 7.25 (2H, overlapped, H-2,3), 7.75 (1H, s, H-8), 8.02 (1H, s, H-5), 8.23 (2H, d, $J_{3',4';7',6'}$ 8.8 Hz, H-3′,7′); ^{13}C NMR (100 MHz, $CDCl_3$) 17.2 (CH_3-15), 19.4 (CH_3-14), 23.6 (CH_3-12,13), 28.4 (CH-11), 55.5 (CH_3-8′), 113.9 (CH-4′,6′), 116.6 (CH-8), 121.1 (CH-3), 121.8 (C-2′), 125.6 (CH-5), 126.3 (CH-2), 128.9 (C-6), 129.9 (C-10), 131.6 (C-1), 132.2 (CH-3′,7′), 132.5 (C-9), 142.1 (C-4), 147.9 (C-7), 163.9 (C-5′), 164.9 (C-1′); HRESIMS *m/z* 349.17915 $[M+H]^+$ (calcd for $C_{23}H_{25}O_3$, 349.18037).

4.4.1.14. 7-(p-Trifluoromethyl-benzoyloxy)-cadalene ***(26)***

White crystals; 39.6 mg 89% yield; UV (MeOH) λ_{max}(log ε) 235 (4.65), 257 (3.65), 281 (4.76) nm; IR ($CHCl_3$) ν_{max} 3569, 2967, 1738, 1412, 1325, 1269, 1131, 1082 cm^{-1}; ^1H NMR (400 MHz, $CDCl_3$) 1.42 (6H, d, $J_{12,11;13,11}$ 6.8 Hz, CH_3-12,13), 2.45 (3H, s, CH_3-15), 2.63 (3H, s, CH_3-14), 3.73 (1H, hept, $J_{11,12;11,13}$ 6.8 Hz, H-11), 7.30 (2H, overlapped, H-2,3), 7.79 (1H, s, H-8), 7.82 (2H, d, $J_{4',3';6',7'}$ 8.0 Hz, H-4′,6′), 8.07 (1H, s, H-5), 8.42 (2H, d, $J J_{3',4';7',6'}$ 8.0 Hz, H-3′,7′); ^{13}C NMR (100 MHz, $CDCl_3$) 17.1 (CH_3-15), 19.3 (CH_3-14), 23.6 (CH_3-12,13), 28.5 (CH-11), 116.4 (CH-8), 121.5 (CH-3), 122.17 (CH_3-8′), 125.7 (CH-4′,6′), 125.9 (CH-5), 126.5 (CH-2), 128.4 (C-6),

130.1 (C-10), 130.6 (CH-3′,7′), 131.6 (C-1), 132.5 (C-9), 132.7 (C-5′), 135.0 (C-2′), 142.2 (C-4), 147.5 (C-7), 164.1 (C-1′); HRESIMS *m/z* 387.15549 $[M+H]^+$ (calcd for $C_{23}H_{22}F_3O_2$, 387.15719).

*4.4.1.15. 7-(p-Nitro-benzoyloxy)-cadalene (**27**)*

Yellow crystals; 28.2 mg 86% yield; UV (MeOH) λ_{max}(log ε) 233 (5.03), 249 (4.59), 257 (4.60) nm; IR ($CHCl_3$) ν_{max} 3575, 2966, 1741, 1530, 1267, 1233, 1128 cm^{-1}; ^1H NMR (400 MHz, $CDCl_3$) 1.39 (6H, d, $J_{12,11;13,11}$ 6.8 Hz, CH_3-12,13), 2.43 (3H, s, CH_3-15), 2.61 (3H, s, CH_3-14), 3.71 (1H, hept, $J_{11,12;11,13}$ 6.8 Hz, H-11), 7.28 (2H, overlapped, H-2,3), 7.73 (1H, s, H-8), 8.05 (1H, s, H-5), 8.36 (2H, d, $J_{4',3';6',7'}$ 8.4 Hz, H-4′,6′), 8.43 (2H, d, $J_{3',4';7',6'}$ 8.4 Hz, H-3′,7′); ^{13}C NMR (100 MHz, $CDCl_3$) 17.1 (CH_3-15), 19.3 (CH_3-14), 23.6 (CH_3-12,13), 28.5 (CH-11), 116.3 (CH-8), 121.6 (CH-3), 123.7 (CH-4′,6′), 126.0 (CH-5), 126.6 (CH-2), 128.1 (C-6), 130.1 (C-10), 131.3 (CH-3′,7′), 131.6 (C-1), 132.3 (C-9), 134.9 (C-2′), 142.2 (C-4), 147.3 (C-7), 150.9 (C-5′), 163.4 (C-1′); HRESIMS *m/z* 364.15363 $[M+H]^+$ (calcd for $C_{22}H_{22}NO_4$, 364.15488).

*4.4.1.16. 7-(m-Methyl-benzoyloxy)-cadalene (**28**)*

White crystals; 30.0 mg 75% yield; UV (MeOH) λ_{max}(log ε) 205 (4.81), 210 (4.78), 236 (4.90), 264 (4.02), 281 (4.09) nm; IR ($CHCl_3$) ν_{max} 2967, 1732, 1276, 1233, 1197 cm^{-1}; ^1H NMR (400 MHz, $CDCl_3$) 1.39 (6H, d, $J_{11,12;13,11}$ 6.8 Hz, CH_3-12,13), 2.43 (3H, s, CH_3-15), 2.46 (3H, s, CH_3-8′), 2.60 (3H, s, CH_3-14), 3.71 (1H, hept, $J_{11,12;11,13}$ 6.8 Hz, H-11), 7.25 (2H, overlapped, H-2,3), 7.43 (2H, overlapped, H-5′,6′), 7.74 (1H, s, H-8), 8.02 (1H, s, H-5), 8.07 (1H, overlapped, H-7′), 8.09 (1H, s, H-3′); ^{13}C NMR (100 MHz, $CDCl_3$) 17.2 (CH_3-15), 19.4 (CH_3-14), 21.3 (CH_3-8′), 23.6 (CH_3-12,13), 28.4 (CH-11), 116.5 (CH-8), 121.2 (CH-3), 125.7 (CH-5), 126.3 (CH-2), 127.4 (CH-7′), 128.5 (CH-6′), 128.8 (C-6), 129.4 (C-2′), 129.9 (C-10), 130.7 (CH-3′), 131.6 (C-1), 132.5 (C-9), 134.4 (CH-5′), 138.5 (C-4′), 142.1 (C-4), 147.8 (C-7), 165.4 (C-1′); HRESIMS *m/z* 333.18570 $[M+H]^+$ (calcd for $C_{23}H_{25}O_2$, 333.18545).

*4.4.1.17. 7-(m-Methoxy-benzoyloxy)-cadalene (**29**)*

Yellow oil; 9.1 mg 78% yield; UV (MeOH) λ_{max}(log ε) 215 (4.95), 225 (4.91), 233 (4.95), 266 (4.00), 293 (4.16) nm; IR ($CHCl_3$) ν_{max} 3404, 3007, 1711, 1362, 1277, 1237 cm^{-1}; ^1H NMR (400 MHz, $CDCl_3$) 1.39 (6H, d, $J_{12,11;13,11}$ 6.8 Hz, CH_3-12,13), 2.43 (3H, s, CH_3-15), 2.61 (3H, s, CH_3-14), 3.71 (1H, hept, $J_{11,12;11,13}$ 6.8 Hz, H-11), 3.90 (3H, s, CH_3-8′), 7.21 (1H, ddd, $J_{5',6'}$ 8.4 Hz, $J_{5',3'}$ 2.8 Hz, $J_{5',7'}$ 1.2 Hz, H-5′), 7.26 (2H, overlapped, H-2,3), 7.45 (1H, t, $J_{6',5';6',7'}$ 8.0 Hz, H-6′), 7.76 (1H, s, H-8), 7.78 (1H, br t, $J_{3',5'}$ 2.4 Hz, H-3′), 7.89 (1H, dt, $J_{7',6'}$ 8.0 Hz, $J_{7',5'}$ 1.2 Hz, H-7′), 8.03 (1H, s, H-5); ^{13}C NMR (100 MHz, $CDCl_3$) 17.2 (CH_3-15), 19.4 (CH_3-14), 23.6 (CH_3-12,13), 28.5 (CH-11), 55.5 (CH-8′), 114.6 (CH-3′), 116.4 (CH-8), 120.2 (CH-5′), 121.3 (CH-3), 122.6 (CH-7′), 125.8 (CH-5), 126.4 (CH-2), 128.7 (C-6), 129.2 (CH-6′), 130.0 (C-10), 130.1 (C-2′), 131.6 (C-1), 132.5 (C-9), 142.1 (C-4), 147.8 (C-7), 159.8 (C-4′), 165.1 (C-1′); HRESIMS *m/z* 349.18091 $[M+H]^+$ (calcd for $C_{23}H_{25}O_3$, 349.18037).

*4.4.1.18. 7-(m-Trifluoromethyl-benzoyloxy)-cadalene (**30**)*

White crystals; 59.5 mg 94% yield; UV (MeOH) λ_{max}(log ε) 235 (4.89), 258 (3.89), 280 (3.98) nm; IR ($CHCl_3$) ν_{max} 2965, 1740, 1336, 1133 cm^{-1}; ^1H NMR (400 MHz, $CDCl_3$) 1.39 (6H, d, $J_{12,11;12,13}$ 6.8 Hz, CH_3-12,13), 2.43 (3H, s, CH_3-15), 2.61 (3H, s, CH_3-14), 3.71 (1H, hept, $J_{11,12;11,13}$ 6.8 Hz, H-11), 7.27 (2H, overlapped, H-2,3), 7.66 (1H, t, $J_{6',5';6',7'}$ 7.6 Hz, H-6′), 7.77 (1H, s, H-8), 7.90 (1H, d, $J_{5',6'}$ 7.6 Hz, H-5′), 8.05 (1H, s, H-5), 8.45 (1H, d, $J_{7',6'}$ 7.6 Hz, H-7′), 8.56 (1H, s, H-3′); ^{13}C NMR (100 MHz, $CDCl_3$) 17.1 (CH_3-15), 19.4 (CH_3-14), 23.6 (CH_3-12,13), 28.5 (CH-11), 116.4 (CH-8), 121.4 (CH-3), 125.9 (CH-5), 126.5 (CH-2), 127.1 (CH-3′), 128.4 (C-6), 129.3 (CH-6′), 130.1 (CH-5′, C-2′), 130.4 (C-10), 131.2 (C-4′), 131.6 (C-1), 132.5 (C-9), 133.4 (CH-7′), 142.2 (C-4), 147.5 (C-7), 164.0 (C-1′); HRESIMS *m/z* 387.15648 $[M+H]^+$ (calcd for $C_{23}H_{22}F_3O_2$, 387.15719).

*4.4.1.19. 7-(m-Chloro-benzoyloxy)-cadalene (**31**)*

White crystals; 30.8 mg 91% yield; UV (MeOH) λ_{max}(log ε) 208 (4.73), 216 (4.70), 235 (4.86), 261 (3.87), 282 (4.00) nm; IR ($CHCl_3$) ν_{max} 3559, 2963, 1739, 1243, 1130 cm^{-1}; ^1H NMR (400 MHz, $CDCl_3$) 1.39 (6H, d, $J_{12,11;13,11}$ 6.8 Hz, CH_3-12,13), 2.42 (3H, s, CH_3-15), 2.60 (3H, s, CH_3-14), 3.71 (1H, hept, $J_{11,12;11,13}$ 6.8 Hz, H-11), 7.26 (2H, overlapped, H-2,3), 7.48 (1H, t, $J_{6',5';6',7'}$ 7.6 Hz, H-6′), 7.63 (1H, ddd, $J_{5',6'}$ 8.0 Hz, $J_{5',3'}$ 2.0 Hz, $J_{5',7'}$ 0.8 Hz, H-5′), 7.74 (1H, s, H-8), 8.03 (1H, s, H-5), 8.16 (1H, dt, $J_{7',6'}$ 8.0 Hz, $J_{7',5'}$ 0.8 Hz, H-7′), 8.26 (1H, t, $J_{3',5'}$ 2.0 Hz, H-3′); ^{13}C NMR (100 MHz, $CDCl_3$) 17.2 (CH_3-15), 19.4 (CH_3-14), 23.6 (CH_3-12,13), 28.5 (CH-11), 116.4 (CH-8), 121.4 (CH-3), 125.8 (CH-5), 126.5 (CH-2), 128.3(CH-7′), 128.5 (C-6), 129.9 (CH-6′), 130.1 (C-10), 130.2 (CH-3′), 131.3 (C-2′), 131.6 (C-1), 132.5 (C-9), 133.6 (CH-5′), 134.8 (C-4′), 142.2 (C-4), 147.5 (C-7), 164.1 (C-1′); HRESIMS *m/z* 353.13062 $[M+H]^+$ (calcd for $C_{22}H_{22}ClO_2$, 353.13083).

4.4.2. Carbamates

7-Hydroxy-3,4-dihydrocadalene (1.0 equiv, 40 mg) was dissolved in CH_2Cl_2 (1 mL) and a nitrogen atmosphere was generated in the flask containing this solution. Et_3N (3.0 equiv, 76.7 μL) and phenyl isocyanate (3.0 equiv, 60.3 μL) were added and the mixture was stirred at room temperature overnight. Next, the reaction was quenched by adding ice-cold water and the organic phase was extracted with EtOAc and passed over Na_2SO_4. The desired product was purified by PLC (benzene-EtOAc 96:4, two elutions).

The above methodology was applied to obtain the corresponding semisynthetic carbamate from 7-hydroxy-cadalene.

*4.4.2.1. 7-(Phenylcarbamate)-3,4-dihydrocadalene (**32**)*

Yellow oil; 20.5 mg 77% yield; UV (MeOH) λ_{max}(log ε) 204 (4.87), 225 (4.64), 236 (4.68) nm; IR ($CHCl_3$) ν_{max} 3433, 2960, 1746, 1602, 1524, 1442, 1248, 1175, 1131 cm^{-1}; ^1H NMR (400 MHz, $CDCl_3$) 0.82 (3H, d, $J_{13,11}$ 6.8 Hz, CH_3-13), 0.90 (3H, d, $J_{12,11}$ 6.8 Hz, CH_3-12), 1.89 (1H, hept, $J_{11,12;11,13}$ 6.8 Hz, H-11), 1.99 (3H, br s, CH_3-14), 2.24 (3H, s, CH_3-15), 2.36 (3H, overlapped, H-3,4), 5.70 (1H, br d, $J_{2,3}$ 1.2 Hz, H-2), 6.97 (2H, overlapped, H-5,8), 7.03 (1H, br s, NH-2′), 7.10 (1H, d, $J_{6',5';6',7'}$ 7.6 Hz, H-6′), 7.34 (2H, br t, $J_{5',6';7',6'}$ 7.6 Hz, H-5′,7′), 7.46 (2H, d, $J_{4',5';8',7'}$ 8.0 Hz, H-4′,8′); ^{13}C NMR (100 MHz, $CDCl_3$) 15.9 (CH_3-15), 18.9 (CH_3-14), 20.2 (CH_3-12), 21.4 (CH_3-13), 25.4 (CH_2-3), 30.2 (CH-11), 43.8 (CH-4), 116.5 (CH-8), 118.6 (C-1′), 123.7 (CH-6′), 123.9 (CH-2), 127.8 (C-6), 129.1 (CH-5′,7′,4′,8′), 131.0 (CH-5), 131.1 (C-9), 134.7 (C-1), 136.8 (C-10), 137.6 (C-3′), 147.4 (C-7); HRESIMS *m/z* 336.19620 $[M+H]^+$ (calcd for $C_{22}H_{26}NO_2$, 336.19635).

*4.4.2.2. 7-(Phenylcarbamate)-cadalene (**33**)*

White solid; 20.6 mg 79% yield; UV (MeOH) λ_{max}(log ε) 204 (4.80), 209 (4.79), 213 (4.80), 220 (4.79), 238 (4.96), 265 (3.88), 281 (3.99) nm; IR ($CHCl_3$) ν_{max} 3433, 2967, 1754, 1527, 1539, 1130 cm^{-1}; ^1H NMR (400 MHz, $CDCl_3$) 1.38 (6H, d, $J_{12,11;13,11}$ 6.8 Hz, CH_3-12,13), 2.47 (3H, s, CH_3-15), 2.61 (3H, s, CH_3-14), 3.70 (1H, hept, $J_{11,12;11,13}$ 6.8 Hz, H-11), 7.10 (2H, d, $J_{4',5';8',7'}$ 7.2 Hz, H-4′,8′), 7.26 (2H, overlapped, H-2,3), 7.32 (2H, t, $J_{5',4';7',8'}$ 7.6 Hz, H-5′,7′), 7.46 (2H, overlapped, H-6′,NH-2′), 7.75 (1H, s, H-8), 7.99

(1H, s, H-5); ^{13}C NMR (100 MHz, $CDCl_3$) 17.1 (CH_3-15), 19.4 (CH_3-14), 23.6 (CH_3-12,13), 28.4 (CH-11), 116.7 (CH-8), 118.7 (CH-6′), 121.2 (CH-3), 123.9 (CH-4′,8′), 125.7 (CH-5), 126.3 (CH-2), 129.0 (C-6), 129.1 (CH-5′,7′), 129.3 (C-1′), 129.9 (C-10), 131.6 (C-1), 132.5 (C-9), 137.5 (C-3′), 142.1 (C-4), 147.2 (C-7); HRESIMS *m/z* 334.18054 $[M+H]^+$ (calcd for $C_{22}H_{24}NO_2$, 334.18070).

4.5. Biological investigations

4.5.1. Cell cultures

HaCaT cells (human keratinocytes) were obtained from CLS Cell Lines Service GmbH (Germany), HaCaT-ARE-Luc, (human keratinocytes), NIH-3T3-KBF-Luc (mouse fibroblasts), HeLa-STAT3-Luc (human cervix carcinoma) cell lines were constructed in our lab and the characterization of the cells has been previously described.[27] NIH-3T3-NucLight-Red cells were also generated in our lab by infection with a lentivirus encoding a nuclear restricted Red Fluorescent Protein under the EF-1αpromoter and selected with puromycin. All the cell lines were grown in supplemented DMEM medium containing 10% fetal bovine serum and 1% penicillin/streptomycin antibiotics, at 37 °C in a humidified atmosphere of 5% CO_2.

4.5.2. Luciferase assays

For the anti-NF-κB activity NIH-3T3-KBFLuc cells were stimulated with TNFα (30 ng/mL) in the presence or the absence of the compounds for 6 h. For the activation of the antioxidant response element (ARE) that is activated by Nrf2, HaCaTARE-Luc cells were stimulated with the compounds for 6 h. For the anti-STAT3 activity HeLa-STAT-3-Luc cells were stimulated with IFN-γ (25 IU/mL) in the presence or the absence of the compounds for 6 h. After the treatment the cells were washed twice in PBS and lysed in 25 mM Tris-phosphate pH 7.8, 8 mM MgCl2, 1 mM DTT, 1% Triton X-100, and 7% glycerol during 15 min at RT in a horizontal shaker. After centrifugation, luciferase activity in the supernatant was measured using a GloMax 96 microplate luminometer (Promega) following the instructions of the luciferase assay kit (Promega, Madison, WI, USA). For NF-κB inhibition the RLU was calculated and the results were expressed as percentage of inhibition of NF-κB activity induced by TNFα (100% activation). For STAT3 inhibition the RLU were calculated and results were expressed as percentage of inhibition of STAT3 activity induced by IFN-γ (100% activation). The specific Nrf2 activation was expressed as fold induction over basal levels (untreated cells). The experiments for each concentration of the compounds were performed in triplicate wells.

4.5.3. Cellular antioxidant activity

The intracellular accumulation of ROS was detected by fluorometry using the free radical sensor 5-(and-6)-chloromethyl-2′,7′-dichlorosihydrofluorescein diactetate, acetyl ester (CM-H2DCFDA) (Life Technologies). HaCaT cells ($1x10^4$/well) were seeded the day before the assay in a 96-well plate using DMEM supplemented with 10% FBS. After 24 h cells were pre-incubated with the compounds for 30 min and ROS production was induced with 0.4 mM *tert*-butyl-hydroperoxide (TBHP) (Sigma-Aldrich, Saint Louis, USA). After 3 h cells were incubated with CM-H2DCFDA at a concentration of 10 μM during 30 min at 37 °C. ROS production was measured by changes in fluorescence using the Incucyte FLR software; the data were analyzed by the total green object integrated intensity (GCU × μm^2 × Well) of the imaging system IncuCyte HD (Essen BioScience).

4.5.4. Western blots

NIH-3T3-KBF-Luc cells were treated with increasing concentrations of either compound **13** or with SC514, an IKKβ inhibitor, during 15 min at 37 °C and subsequently stimulated with TNFα (30 ng/mL) for 20 min at 37 °C. Total cell content was extracted in 100 μL of lysis buffer (20 mM Hepes pH 8.0, 10 mM KCl, 0.15 mM EGTA, 0.15 mM EDTA, 0.5 mM Na_3VO_4, 5 mM NaF, 1 mM DTT, leupeptin 1 mg/mL, pepstatin 0.5 mg/mL, aprotinin 0.5 mg/mL, and 1 mM PMSF) containing 0.5% NP-40. After incubation of the lysate at 4 °C during 15 min, proteins were obtained by centrifugation at 13,000 rpm (4 °C for 10 min), boiled in Laemmli buffer and electrophoresed in 10% SDS polyacrylamide gels. Separated proteins were transferred to PVDF membranes. Blots were blocked in TBS solution containing 0.1% Tween 20 and 5% nonfat dry milk overnight at 4 °C. Primary antiphospho-IκBα (#9246, Cell Signaling Technology), IκBα (C-21) (Santa Cruz) and anti-αTubulin antibodies (Sigma-Aldrich) were employed to detect specific proteins. Protein levels were quantified using the program Image J.

4.5.5. Cytotoxic assays over human cancer cell lines and gingival fibroblasts

The cytotoxic effects of semi-synthetic derivatives were evaluated on tumor cells provided by the National Cancer Institute (USA) and on human gingival fibroblasts (HGF), applying the protein-binding dye sulforhodamine B (SRB) in a microculture assay to measure cell growth.[28] Colon (HCT-15), breast (MCF-7), leukemia (K-562), central nervous system (U-251, Glia), lung (SK-LU-1), and prostate cancer (PC-3) cells were cultured in RPMI-1640, and HGF were cultured in DMEM, both supplemented with 10% fetal bovine serum, 2 μM L-glutamine, 100 IU/mL penicillin G, 100 μg/mL streptomycin sulfate, and 0.25 μg/mL amphotericin B and were maintained at 37 °C in a 5% CO_2 atmosphere with 95% humidity. For the assay, 100 μL/well of cell suspension containing 5×10^4 cells/mL (K-562, MCF-7), 7.5×10^4 cells/mL (U-251, PC-3, SK-LU-1), 10×10^4 cells/mL (HCT-15, HGF), were seeded in 96-well microtiter plates and incubated to allow cell attachment. After 24 h, 100 μL of each test compound or positive control was added (all test substances were dissolved in DMSO). After 48 h, adherent cell cultures were fixed in situ by adding 50 μL of cold 50% (w/v) aqueous trichloroacetic acid (TCA) and incubated for 60 min at 4 °C. The supernatant was discarded, and the plates were washed three times with water and then dried. Cultures fixed with TCA were stained for 30 min with 100 μL of 0.4% SRB solution. Protein-bound dye was extracted with 10 μM unbuffered Tris base, and optical densities were measured at 515 nm on an Ultra microplate reader (Elx808, Bio-Tek Instruments, Inc.). The results were expressed as percentages of inhibition of cell proliferation at a concentration of 50 μM or as IC_{50} values (μM inhibitory concentration at which 50% of cell proliferation is inhibited), estimated by linear regression equations of dose-response curves, according to the protocol of Monks.[28]

4.5.6. Statistical analysis

Data analysis was performed using at least three independent experiments. For NF-κB, Nrf2 and ROS inhibition reporting results, sample population means were compared against control population means in an unpaired two-tailed Student's *t* test. A p value <0.05 was considered statistically significant. NF-κB IC_{50} calculations were performed using the GraphPad Prism Program (Graph Pad Software, San Diego, CA, USA).

4.6. Molecular docking

7-Hydroxy-3,4-dihydrocadalene, 7-hydroxy-cadalene and compound **13** structures were built using previously reported X-ray crystallography data.[16] Geometries were optimized applying the semi-empirical quantum mechanical method PM3. MGL tools 1.5.4 with AutoDock 4.2[29] were used to set up and perform blinded docking calculations between compounds and IKKβ crystal structure (PDB ID: 4kik).[21,30] Molecules were docked over the entire protein to identify its binding sites. For docking calculations, Lamarckian genetic algorithms (LGA) were implemented in AutoDock 4.2. The final positions of the compounds were ranked by lowest interaction energy values (docking score expressed in kcal/mol). H-bond interactions between the compounds and protein were explored. The output obtained from AutoDock was further analyzed with PyMOL software package. Validation of the employed computational protocol was established through comparison of docking results carried out using data of co-crystallized ligand (staurosporine analog K252a) bound to the IKKβ subunit, with the docking pose of experimental crystal data[21] (Fig. S44, Supporting Information). A docked pose with a RMSD <2 Å is considered acceptable.[31]

Acknowledgments

This work was taken in part from the Ph.D. thesis of V.E. The authors thank Programa de Maestría y Doctorado en Ciencias Químicas and Dirección General de Asuntos del Personal Académico (PAPIIT IG200514), Universidad Nacional Autónoma de México, for support. The authors also acknowledge María Isabel Chávez, Beatriz Quiroz, Alejandra León, Rocío Patiño, Ángeles Peña, Elizabeth Huerta, Lorena K. Calderón-Ortiz, Antonio Nieto, Luis Delgado-Chávez, José Luis Rodríguez-Chávez, Luis Velasco, Javier Pérez (Instituto de Química de la UNAM) and Salvador Matus (Facultad de Química de la UNAM) for technical assistance. V. E. also thanks CONACYT for the graduate scholarship (257805) and Asociación Universitaria Iberoamericana de Postgrado.

A. Supplementary data

Supplementary data associated with this article can be found, in the online version, at http://dx.doi.org/10.1016/j.bmc.2017.03.069.

References

1. L.M. Coussens, Z. Werb, Nature 420 (2002) 860.
2. A. Mantovani, Nature 435 (2005) 752.
3. A. Mantovani, P. Allavena, A. Sica, F. Balkwill, Nature 454 (2008) 436.
4. M. Karin, Nature 441 (2006) 431.
5. E. Pikarsky, R.M. Porat, I. Stein, et al., Nature 431 (2004) 461.
6. H. Yu, H. Lee, A. Herrmann, R. Buettner, R. Jove, Nat Rev Cancer 14 (2014) 736.
7. J.D. Hayes, A.T. Dikova-Kostova, Trends Biochem Sci 39 (2014) 199.
8. M.B. Sporn, K.T. Liby, Nat Rev Cancer 12 (2012) 564.
9. K. Kashfi, Adv Pharmacol 57 (2009) 31.
10. J.T. Thun, S.J. Henley, C. Patrono, J Natl Cancer Inst 94 (2002) 252.
11. P. Bremner, M. Heinrich, J Pharm Pharmacol 54 (2002) 453.
12. B. Orlikova, N. Legran, J. Panning, M. Dicato, M. Diederich, Cancer Treat Res 159 (2014) 123.
13. M.H. Wright, S.A. Sieber, Nat Prod Rep 33 (2016) 681.
14. J.L. Rodríguez-Chávez, V. Egas, E. Linares, et al., J Ethnopharmacol 195 (2017) 39.
15. G. Delgado, M. Olivares, M. Chávez, et al., J Nat Prod 64 (2001) 681.
16. V. Egas, R. Toscano, E. Linares, R. Bye, F. Espinosa-García, G. Delgado, J Nat Prod 78 (2015) 2634.
17. S. Luqman, J.M. Pezzuto, Phytother Res 24 (2010) 949.
18. T.D. Gilmore, Oncogene 25 (2006) 6680.
19. T.D. Gilmore, M. Herscovitch, Oncogene 25 (2006) 6887.
20. F. Mercurio, H. Zhu, B.W. Murray, et al., Science 278 (1997) 860.
21. S. Liu, Y.R. Misquitta, A. Olland, et al., J Biol Chem 288 (2013) 22758.
22. A. Saito, T. Yamashita, Y. Mariko, et al., Proc Natl Acad Sci USA 96 (1999) 4592.
23. R. Snodgrass, A.C. Collier, A.E. Coon, C.A. Pritsos, J Biol Chem 285 (2010) 19068.
24. H.Y. Ebrahim, M.M. Mohyeldin, M.M. Hailat, K.A. El Sayed, Bioorg Med Chem 24 (2016) 5748.
25. A.K. Ghosh, M. Brindisi, J Med Chem 58 (2015) 2895.
26. J.L. Rodríguez-Chávez, Y. Rufino-Gonzáles, M. Ponce-Macotela, G. Delgado, Parasitology 142 (2015) 576.
27. D. Del Prete, E. Millán, F. Pollastro, et al., J Nat Prod 79 (2016) 267.
28. A. Monks, D. Scudiero, P. Skehan, et al., J Natl Cancer Inst 83 (1991) 757.
29. G.M. Morris, D.S. Goodsell, R.S. Halliday, et al., J Comput Chem 19 (1998) 1639.
30. Schrödinger, L. The PyMOL Molecular Graphics System. **2004**.
31. O. Carugo, S. Pongor, Protein Sci 10 (2001) 1470.

CAPÍTULO III

Análisis del contenido metabólico de *Heterotheca inuloides* aplicando cromatografía líquida de alta resolución (CLAR)

Resumen

Los estudios químicos de *H. inuloides* realizados convencionalmente han dado evidencia de su variabilidad metabólica, de acuerdo a diferentes lugares de colecta y estados de madurez de la planta. Con el fin de ponderar esta variabilidad en el contenido metabólico, se diseñó un método que permite la identificación de los sesquiterpenos de tipo cadinano aislados previamente, en extractos de distintas poblaciones de *H. inuloides*, aplicando CLAR. La identificación se basa en la comparación de los tiempos de retención y espectros UV de las sustancias puras con los picos observados en los cromatogramas de los extractos acetónicos. Esta metodología facilita la detección de las diferencias en la composición química de extractos preparados a partir de muestras con características variables, tales como el lugar de colecta, la época del año en la cual el material vegetal fue colectado y la edad o parte de la planta utilizada. De esta manera se estableció un perfil metabólico de la especie, el cual se centra en el análisis de la presencia de sesquiterpenos de tipo cadinano como consituyentes característicos de la planta. El metabolito común en todos los extractos analizados fue el sesquiterpeno 7-hidroxi-3,4-dihidrocadaleno, lo cual posibilita que sea considerado como un marcador metabólico de la especie.

Introducción

Los metabolitos secundarios son ubicuos en las plantas y desempeñan diversos papeles ecológicos. Cada uno de sus constituyentes puede variar en cuanto a su presencia y cantidad, además de que la composición de la mezcla de los productos químicos puede modificarse, de tal manera que la quimiodiversidad puede dividirse dentro y entre individuos. La ontogenia vegetal y la variación ambiental y genética se reconocen como los principales factores que generan la variación química (fenotípica), permitiendo de esta manera una rápida evolución de las especies. El entendimiento de los patrones de diversidad química y la variabilidad en la distribución de los productos naturales tienen repercusiones importantes a nivel ecológico, ya que permiten analizar el papel que cumplen estas sustancias en la naturaleza.[1]

Se ha estimado la existencia de alrededor de 100,000 metabolitos presentes en las plantas, y cada especie puede contener su propio patrón de expresión quimiotípica. Además, se han encontrado variaciones cualitativas y cuantitativas importantes dentro de individuos pertenecientes a la misma especie vegetal. Aunque el conocimiento sobre la regulación de la formación de metabolitos se ha incrementado en los últimos años, sus funciones en la planta, sus vías biosintéticas y la regulación de las mismas aún son desconocidas para algunos de ellos.[2]

Los avances recientes en genómica y en el estudio de perfiles metabólicos han abierto nuevas oportunidades para la investigación de la variación en los rasgos metabólicos de las plantas. Estos avances incluyen el advenimiento de plataformas metabolómicas que permiten la cuantificación de cientos a miles de metabolitos en muchos genotipos diferentes. Dichos estudios proporcionan nuevas perspectivas sobre las estructuras mecanistas y evolutivas, que permiten entender en un contexto más amplio las funciones del metabolismo de las plantas.[3]

Con el objetivo de garantizar la homogeneidad en la calidad de las plantas medicinales, se ha empleado una variedad de técnicas cromatográficas, las cuales permiten llevar a cabo análisis cualitativos y cuantitativos. Estos métodos pueden también ser útiles en el aislamiento e identificación de metabolitos secundarios.

La cromatografía de líquidos de alta resolución (CLAR) es una técnica muy útil para determinaciones cualitativas o cuantitativas de constituyentes específicos en mezclas complejas. Las técnicas de CLAR ofrecen ciertas ventajas al compararlas con la cromatografía de gases (otra técnica frecuentemente empleada en el estudio de extractos de plantas), ya que pueden llevarse a cabo con compuestos termolábiles o de alta polaridad, o con compuestos no volátiles. El acoplamiento de un cromatógrafo con técnicas de detección por arreglo de diodos puede ser especialmente útil en el análisis de compuestos de tipo sesquiterpeno.[4]

El único estudio reportado respecto a la composición química de *H. inuloides* aplicando CLAR, permitió concluir que la edad de la planta es uno de los factores determinantes en la concentración de algunos compuestos en la especie;[5] sin embargo, la cantidad de metabolitos investigados es limitada, lo cual no permite establecer un perfil metabólico claro, al comparar muestras de distintas poblaciones.

Metodología

Con el objetivo de realizar un análisis preliminar del perfil metabólico de la especie, se obtuvieron cromatogramas tridimensionales de dos extractos preparados a partir de las partes aéreas de poblaciones colectadas en la zona de los volcanes, Estado de México. Este tipo de análisis permite dar seguimiento a la absorción a diferentes longitudes de onda durante la corrida cromatográfica, y facilita la identificación de las zonas de mayor contenido metabólico, para que de esta manera la optimización de las condiciones de separación pueda enfocarse en dicha zona (Figura 1).

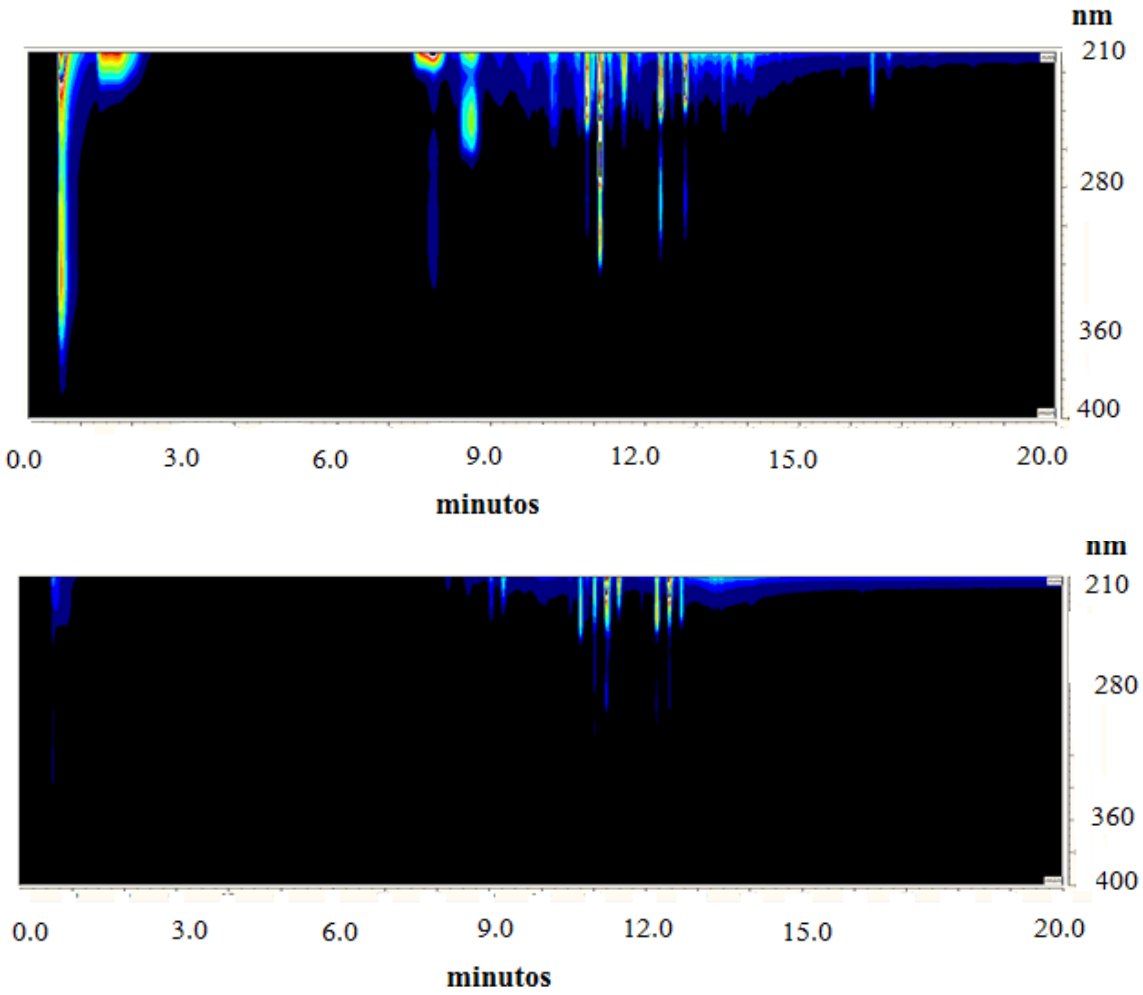

Figura 1. Cromatogramas tridimensionales de dos extractos de *H. inuloides*, en los cuales se puede distinguir los tiempos de retención en los cuales aparecen la mayor cantidad de metabolitos, y las regiones de longitudes de onda de mayor absorción.

En la Figura 1 puede observarse que la zona comprendida entre los tiempos de retención del minuto 7 al 14, es aquella en la cual aparecen la mayor cantidad de compuestos, por lo tanto, se procedió a probar distintas proporciones de eluyentes (metanol, agua), con el objetivo de optimizar la resolución en esta zona del cromatograma.

Condiciones de separación

Los diversos ensayos experimentales realizados permitieron adquirir el conocimiento de las condiciones y procedimientos prácticos a realizar. Derivado de las experiencias adquiridas, se logró establecer que las condiciones cromatográficas con las cuales se consiguió una mejor resolución de los picos fueron las siguientes:

- Se utilizó una columna Agilent Eclipse XDB-C18 RRHT de fase reversa
- Flujo: 1 mL/min
- Tiempo de análisis: 20 minutos
- Temperatura 24 ºC (control de temperatura durante todo el análisis)
- Fase móvil: metanol:agua (gradiente de polaridad, Figura 2).
- El análisis se realizó utilizando un cromatógrafo de líquidos marca Thermo, modelo *Ultimate 3000*, con detector de arreglo de diodos.

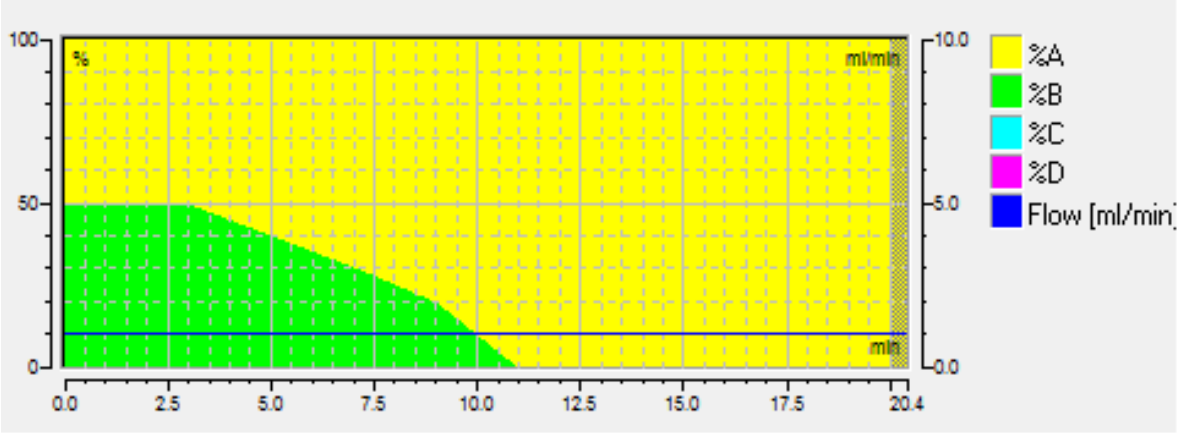

Figura 2. Gradiente de polaridad utilizada en los análisis de los extractos.

A: metanol, B: agua.

Una vez establecidas las condiciones apropiadas para la separación de los picos en la zona de mayor concentración, se procedió a la inyección de las sustancias puras obtenidas previamente, con la finalidad de definir sus tiempos de retención en estas condiciones, y espectros UV, los cuales fueron utilizados en la identificación de estos compuestos en los extractos.

Resultados

En la Figura 3 se muestran los cromatogramas de dos extractos acetónicos de *H. inuloides* obtenidos aplicando la metodología descrita previamente. En dichos cromatogramas se pueden observar diferencias en los perfiles metabólicos de los extractos en cuanto a la presencia y proporción de metabolitos.

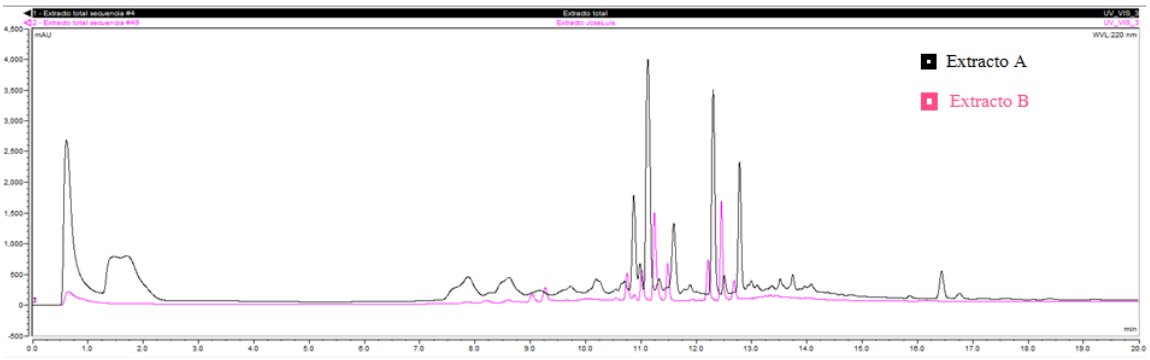

Figura 3. Cromatogramas de dos extractos acetónicos de *H. inuloides*. Extracto A) material vegetal con flor, colectado en Tlacotitlán, Ozumba, Estado de México en Octubre de 2012, número de colecta: E. Linares y Bye 2754. Extracto B) material vegetal con flor, colectado en Cuijingo, Juchitepec, Estado de México en Octubre de 2012.

La obtención de los tiempos de retención de los compuestos en forma pura se hizo a partir de la inyección independiente de cada de una de las sustancias, tal como se muestra en la Figura 4, en la cual se incluye también el cromatograma de uno de los extractos analizados, permitiendo de esta manera la visualización de las regiones donde aparece cada metabolito.

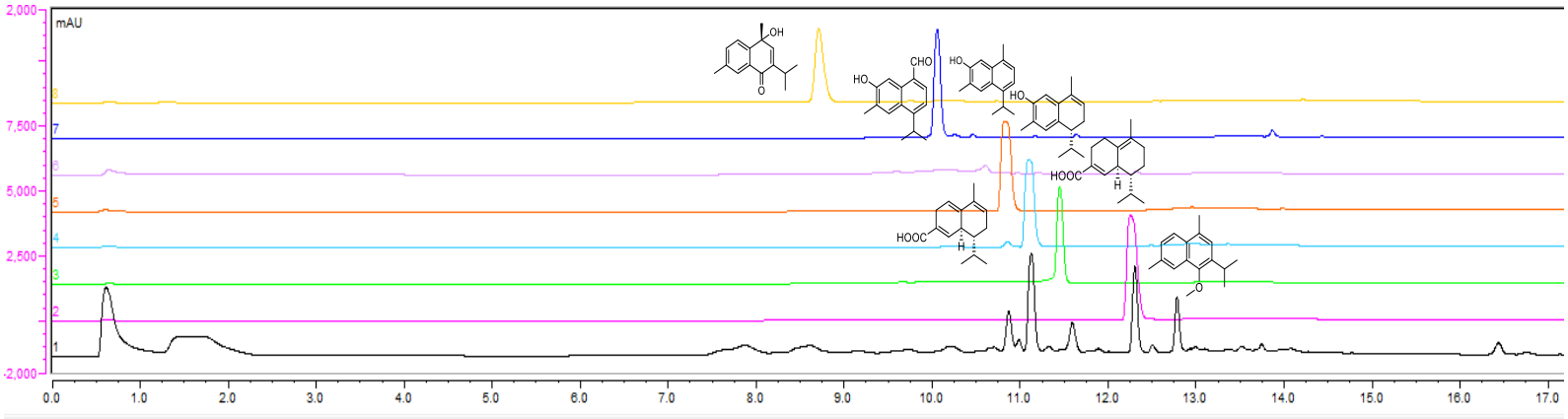

Figura 4. Comparación de los cromatogramas de los compuestos de tipo cadinano aislados de *H. inulolides*, con el cromatograma de un extracto acetónico de las partes aéreas de esta especie. Todos los cromatogramas fueron obtenidos bajo las mismas condiciones de separación.

La identificación de la presencia o ausencia de cada uno de los constituyentes se basó en la comparación de los tiempos de retención y espectros UV de las sustancias puras con los picos observados en los cromatogramas de los extractos acetónicos, como se muestra en la Figura 5, para el caso de los metabolitos mayoritarios 7-hidroxi-3,4-dihidrocadaleno y 7-hidroxicadaleno.

A)

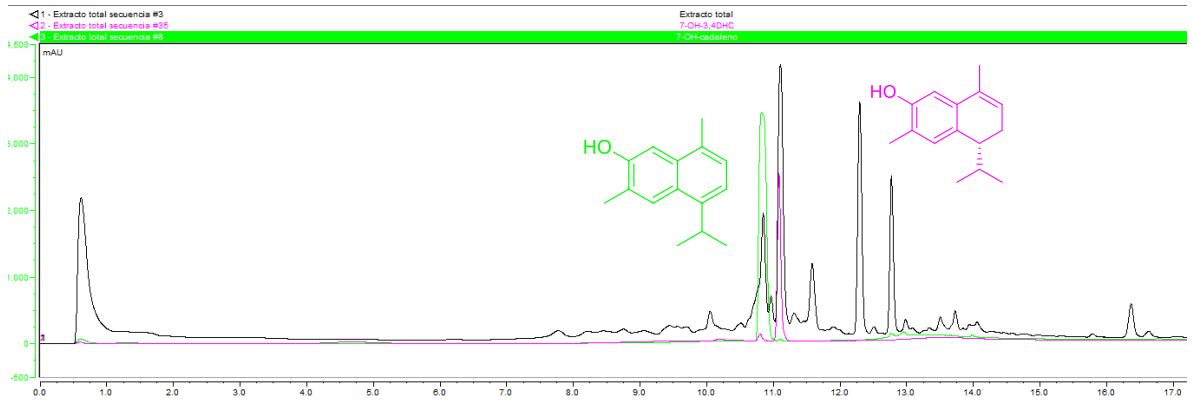

B)

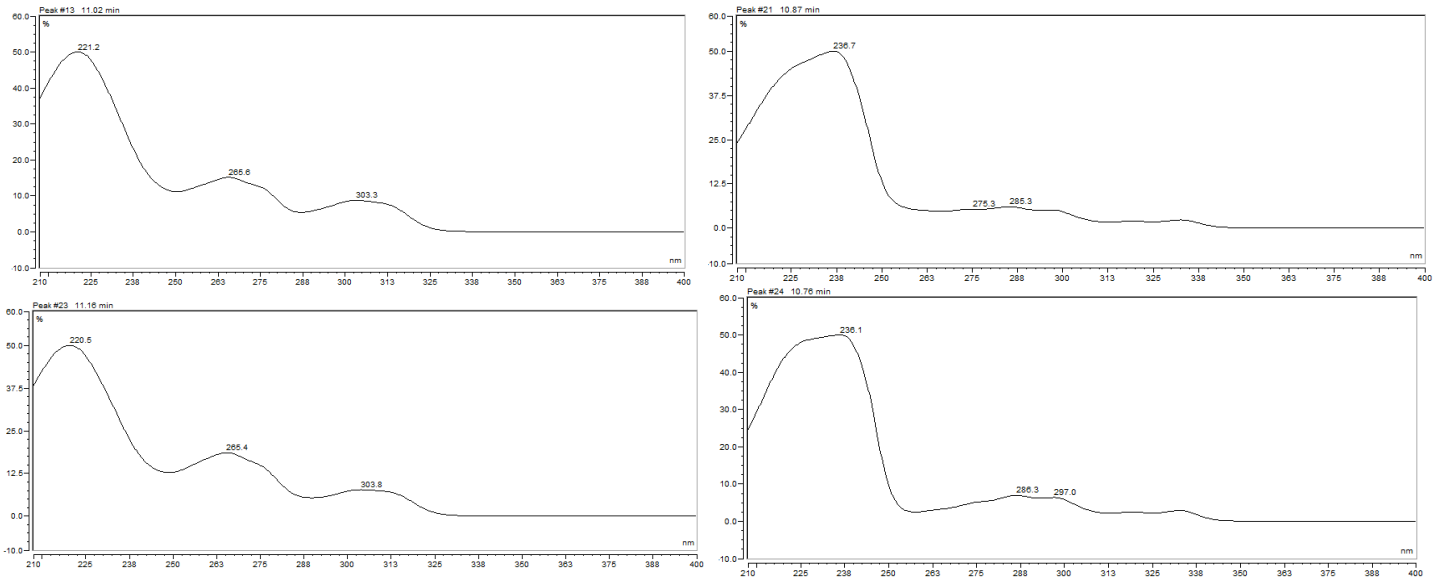

Figura 5. A) Comparación de los cromatogramas de los compuestos mayoritarios 7-hidroxi-3,4-dihidrocadaleno y 7-hidroxicadaleno aislados de *H. inulolides*, con el cromatograma de un extracto acetónico de las partes aéreas de esta especie. **B**) Comparación de los espectros uv para cada uno de los compuestos en forma pura, con los espectros de los picos en el cromatograma del extracto.

De esta manera fue posible la determinación de los tiempos de retención y la obtención de los espectros uv para cada uno de los compuestos de tipo cadinano aislados previamente (Cuadro 1).

Cuadro 1. Tiempos de retención y longitudes de onda de máxima absorción de cada uno de los compuestos de tipo cadinano asilados de *H. inuloides*

Compuesto de tipo cadinano	**Tiempo de retención (min)**	**λ max (nm)**
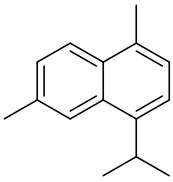	12.667	224.3
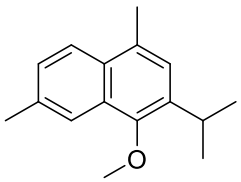	12.257	224.1
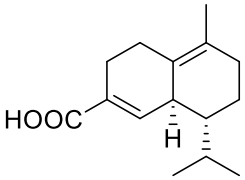	11.450	216.3
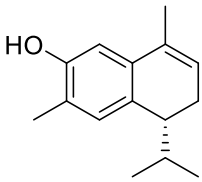	11.163	221.0
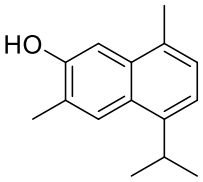	10.713	226.8
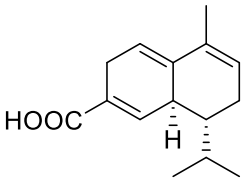	10.607	228.3

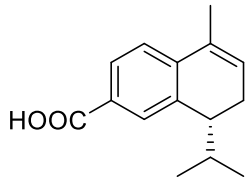	10.467	241.2
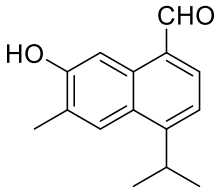	10.013	228.2
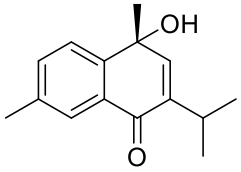	8.713	210.0
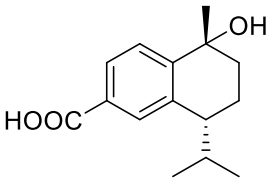	7.603	241.4
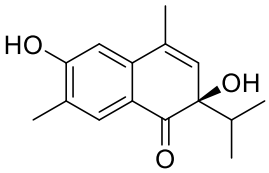	5.653	256.1

Los compuestos identificados, en cada uno de los extractos analizados aplicando el método desarrollado, se muestran en la Figura 6, evidenciando las diferencias en el contenido metabólico de los dos extractos preparados a partir de distintas poblaciones. Considerando que las dos poblaciones investigadas fueron colectados en distintas zonas geográficas, resulta evidente que esta variable puede ser determinante en la composición química de la planta; sin embargo, estudios previos del contenido de algunos metabolitos secundarios de *H. inuloides*, incluyendo sesquiterpenos de tipo cadinano, han evidenciado que la edad de la planta es uno de los factores más importantes que afecta su perfil metabólico.[5]

Otros factores como las condiciones medioambientales (estrés), pueden determinar los niveles de expresión de metabolitos.[6] Por ejemplo, se ha demostrado que la supresión de

genes involucrados en la biosíntesis de cadinanos en la planta del algodón, evita la inducción de la respuesta en defensa a infecciones bacterianas.[7,8]

Ya sea desde un punto de vista ecológico, o de estandarización de extractos para fines terapéuticos, el método cromatográfico desarrollado proporciona de forma preliminar una herramienta para futuras investigaciones en las cuales, a través de un diseño experimental adecuado, sea posible determinar las variables más importantes que generan la presencia o ausencia de determinados metabolitos en esta especie. Además de que su aplicación permite clasificar de mejor manera a los extractos para investigaciones posteriores, facilitando la identificación de muestras que eventualmente posean substancias no aisladas con anterioridad, enfocando las actividaes de aislamiento y purificación sobre estas substancias, con el objetivo de completar el perfil metabólico. La diversidad química y la variación en la abundancia de los metabolitos secundarios, dificulta el desarrollo de un método por CLAR que sea aplicable para la detección de todas las sustancias presentes en la planta; sin embargo, la identificación de los metabolitos característicos y los estudios sobre sus propiedades biológicas (de interés medicinal, ecológico, agronómico, *inter alia*, permiten establecer las correlaciones con otras variables.

Finalmente, se puede concluir que la metodología desarrollada permite la identificación simultánea de sesquiterpenos de tipo cadinano utilizando detección uv o visible, sin la necesidad de derivatización química, y evitando la descomposición de muestras termolábiles, en un tiempo relativamente corto de análisis.

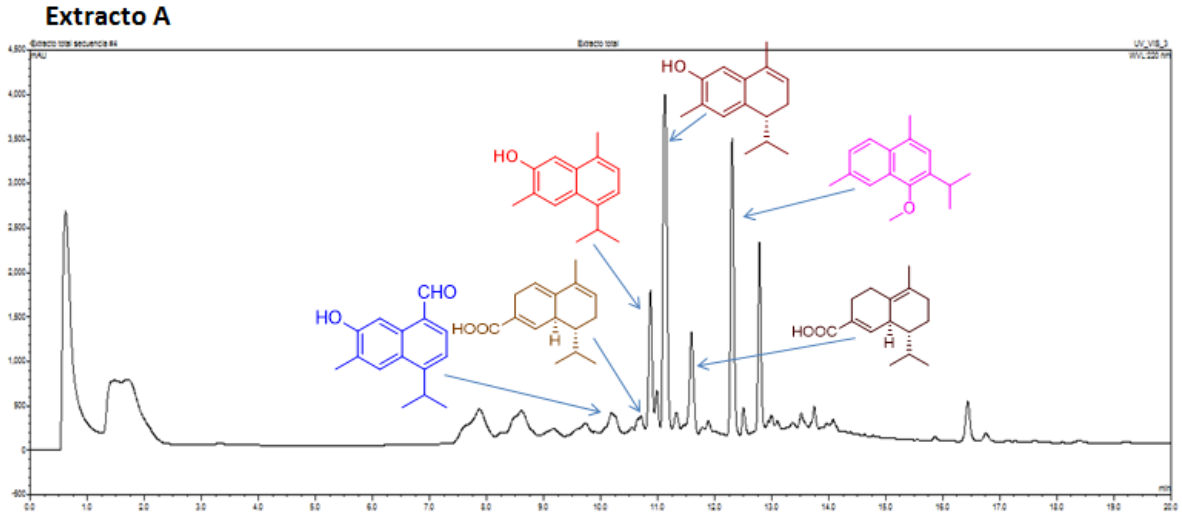

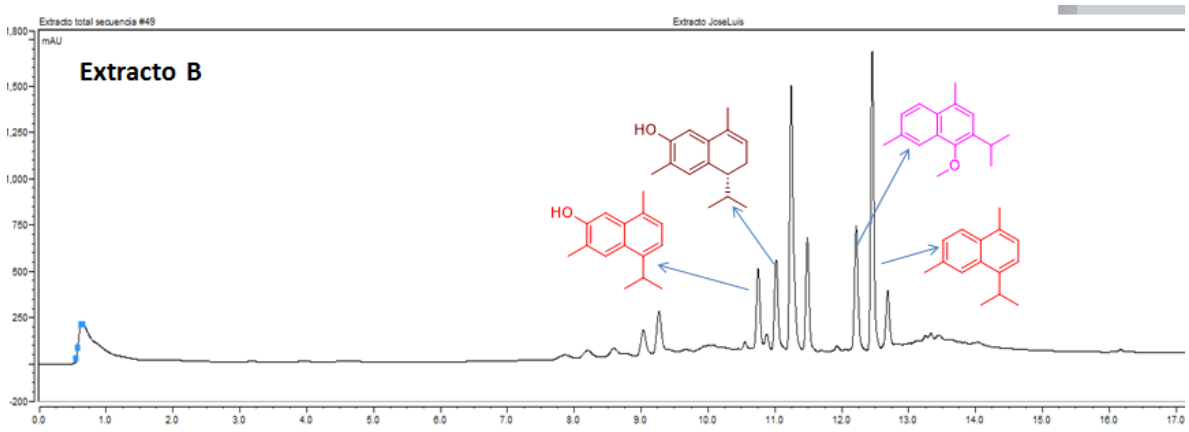

Figura 6. Identificación de compuestos de tipo cadinano en dos extractos de *H. inuloides* mediante la aplicación de CLAR**.** Extracto A) material vegetal con flor, colectado en Tlacotitlán, Ozumba, Estado de México en Octubre de 2012, número de colecta: E. Linares 2754 y Bye. Extracto B) material vegetal con flor, colectado en Cuijingo, Juchitepec, Estado de México en Octubre de 2012.

Referencias

1. a) Moore, B. D.; Andrew, R. L.; Kulheim, C.; Foley, W. J. *New Phytologist* **2014**, 201, 733.
   b) Espinosa-García, F. J.; Delgado, G. *Rev. Latinoam. Quím.* **1998**, 26, 13.
2. Keurentjes, J. J.; Fu, J.; Ric de Vos, C. H.; Lommen, A.; D Hall, R.; Bino, R. J.; van der Plas, H. W.; Jansen, R. C.; Vreugdenhil, D.; Koornneef, M. *Nature Genetics* **2006**, 38, 842.
3. Soltis, N.; Kliebeneistein, D. *Plant Physiology* **2015**, 169, 1456.
4. Merfort, I. *J. Chromatogr*. **2002**, 967, 115.
5. Maldonado-López, Y.; Linares-Mazari, E.; Bye, R.; Delgado, G.; Espinosa-García, F. J. *Economic Botany*, **2008**, 62, 161.
6. Petinatti-Pavarini, D.; Petinatti-Pavarini, S.; Niehues, M.; Peporine-Lopes, N. *Anim feed. sci. tech.* **2012**, 176, 5.
7. Townsend, B. J.; Poole, A.; Blake, C. J.; Llewellyn, D. J. *Plant Physiology* **2005**, 138, 516.
8. Martin, G. S.; Liu, J.; Benedict, C. R.; Stipanovic, R. D.; Magill, C. W. *Phytochemestry*, **2003**, 62, 31.

CAPÍTULO IV

Actividad anti-*Helicobacter pylori*

Resumen

La actividad inhibitoria del crecimiento de *Helicobacter pylori* (*H. pylori*) de los productos naturales mayoritarios aislados de *H. inuloides* fue evaluada a través de un modelo *in vitro*. Los resultados mostraron que los compuestos 7-hidroxi-3,4-dihidrocadaleno y 7-hidroxicadaleno tienen una actividad mayor que la del fármaco de referencia metronidazol y ésta es comparable con la de la claritromicina, uno de los antibióticos de elección en el tratamiento de infecciones causadas por *H. pylori*. Estos resultados motivaron la preparación de una serie de análogos semisintéticos haciendo uso del esqueleto de los cadinanos. A través de reacciones que habían sido exploradas previamente (Capítulo 2), se obtuvo un grupo de sustancias que incluyen derivados benzoilados, los cuales poseen grupos electro atractores y electro donadores en distintas posiciones del anillo aromático incorporado, además de dos compuestos de tipo carbamato. Estos derivados semisintéticos se obtuvieron en las cantidades necesarias para llevar a cabo los bioensayos de inhibición bacteriana. Se identificó que algunos derivados benzoilados preparados a partir del 7-hidroxicadaleno, los cuales tienen sustituyentes en la posición *para* del anillo son más activos que el producto natural.

Introducción

En la actualidad el descubrimiento de nuevas moléculas útiles para el tratamiento de *H. pylori* constituye un reto importante, dada la prevalencia de las infecciones causadas por esta bacteria, y su asociación con el desarrollo de diversas enfermedades del tracto gastrointestinal. La aparición reciente de cepas de *H. pylori* resistentes a antibióticos y los efectos adversos que estos generan, han disminuido la eficacia de las terapias comúnmente empleadas. Generalmente, los antibióticos producen un desequilibrio de la microflora gastrointestinal. Por estas razones, resulta importante la búsqueda de agentes alternativos que reemplacen a los antibióticos con el objetivo de desarrollar una terapia más eficaz y segura. La combinación de estos agentes puede reducir la dosis empleada de antibióticos en las terapias convencionales.[1]

Los productos naturales son fuentes potenciales para el descubrimiento y desarrollo de nuevos agentes eficaces contra infecciones. Existen numerosas publicaciones científicas que describen la actividad antibiótica de productos herbolarios contra *H. pylori*. Estos estudios incluyen investigaciones de plantas, productos naturales y productos procesados. Además del estudio de plantas empleadas en la medicina tradicional, los esfuerzos se han centrado también en el aislamiento biodirigido de productos naturales, así como en la modificación química de estos compuestos con el objetivo de obtener moléculas con mayor actividad. A partir de estos estudios, se han identificado sustancias con actividades anti-*H. pylori* importantes, como es el caso de las catequinas, el plaunotol, el kaempferol y la triptantrina.[2]

Varios estudios han demostrado que los compuestos de tipo flavonoide y las chalconas inhiben la enzima ureasa, la cual es secretada por la bacteria durante la infección para asegurar su supervivencia en el pH ácido del estómago.[3]

Existen reportes del empleo de *H. inuloides* para el tratamiento de desórdenes gastrointestinales.[4] Por esta razón los extractos preparados a partir de esta especie han sido investigados como fuentes potenciales de sustancias con actividad anti-*H. pylori*. Los extractos acuoso y metanólico ha demostrado actividad *in vitro* con concentraciones mínimas inhibitorias de 500 y 31.25 µg/mL, respectivamente.[5] Por esta razón resulta pertinente la investigación de las actividades de sus constituyentes individuales.

Los derivados de tipo cadinano comprenden un grupo interesante de compuestos con un amplio espectro de actividades biológicas. Ha sido demostrado que este tipo de productos naturales poseen propiedades antibacterianas,[6,7] por lo cual pueden resultar útiles en el descubrimiento de agentes anti-*H. pylori*.

Metodología

En el análisis de la actividad anti-*H. pylori* se empleó la cepa ATCC 43504 de la bacteria *H. pylori,* cultivada en agar base Casman (BBL) en placas suplementadas con 5% de sangre de oveja desfibrinada, vancomicina (10 mg/L), trimetoprim (5 mg/L), anfotericina B (2 mg/L), y polimixina B (2,5 mg / L) a 37° C en condiciones microaerofílicas (10% CO_2 y 5% de O_2).[8]

La concentración inhibitoria mínima (MIC) de los compuestos naturales y semisintéticos y de los antibióticos de referencia (amoxicilina, claritromicina y metronidazol) se determinó empleando el método de dilución en caldo nutritivo, de acuerdo con las recomendaciones del Clinical and Laboratory Standards Institute (CLSI)[8], empleando el caldo de Mueller-Hinton (Difco), 0.2 % β- ciclodextrina, 10 mg/L vancomicina, 5 mg/L trimetoprim, 2 mg/L de la anfotericina B, 2,5 mg/L de polimixina B, bajo agitación suave (150 rpm) durante el tiempo de incubación (37° C) bajo condiciones microaerofílicas. Los compuestos se disolvieron en DMSO y se prepararon diluciones seriadas para obtener concentraciones finales en el medio de cultivo de 250, 125, 62.5, 31.2 , 15.6, 7.81 y 3.9 mg/mL. Las pruebas se realizaron en placas de 24 pozos con capacidad de 3 mL. A cada pozo se agregó 1.5 mL de cultivo de *H. pylori* en la fase de crecimiento exponencial (aprox. 108 UFC/ml), más 10 mL de la muestra disuelta de cada una de las concentraciones. Cada ensayo fue realizado por triplicado. Como control negativo se utilizaron 10 mL de DMSO, y como control positivo se emplearon los antibióticos de referencia. Se tomó una alícuota de 750 mL para determinar la absorbancia inicial, posteriormente las placas se colocaron en incubación durante 24 h. Transcurrido este tiempo se midió la lectura final. ΔA se utilizó para calcular el porcentaje de inhibición del crecimiento con respecto al control que se cultivó sólo con DMSO. La MIC definida como la concentración más baja de tratamiento probado que inhibe el crecimiento bacteriano al 100 % se obtuvo mediante la aplicación de las siguientes ecuaciones:

$$\Delta A = A_f - A_i$$

ΔA es la diferencia de absorbancias de cada cultivo, donde A_i = absorbancia inicial, A_f = absorbancia final del cultivo.

El porcentaje de inhibición del crecimiento bacteriano se calculó empleando la siguiente fórmula:

$$\%I = 100 - \left[\frac{\Delta Ae * 100}{\Delta Ac} \right]$$

Resultados

Las actividades anti-*H. pylori* de los productos naturales mayoritarios 7-hidroxi-3,4-dihidrocadaleno y 7-hidroxicadaleno y de algunos derivados de semisíntesis, expresadas como concentración mínima inhibitoria (MIC) se muestran en la Cuadro 1.

Cuadro 1. Actividades anti-*H. pylori* de algunos productos naturales y derivados de semisíntesis obtenidos a partir de *H. inuloides*

COMPUESTO			**MIC (µg/mL)**
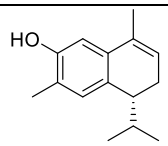			1.95
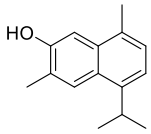			3.91
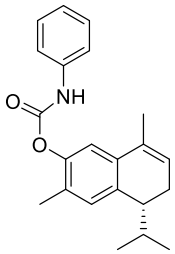			3.91
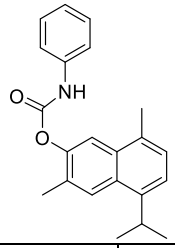			7.81
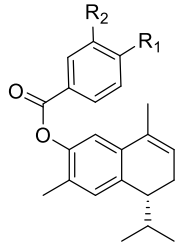	**R_1**	**R_2**	
	H	H	15.62
	CH_3	H	7.81
	OCH_3	H	3.91
	NO_2	H	15.62
	CF_3	H	1.95

	Cl	H	7.81
	H	CH_3	3.91
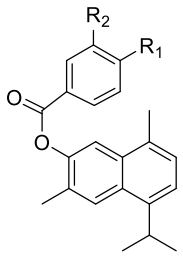	**R_1**	**R_2**	
	H	H	1.95
	CH_3	H	1.95
	OCH_3	H	7.81
	NO_2	H	>15.62
	CF_3	H	>31.25
	Cl	H	1.95
Metronidazol	--	--	300
Amoxicilina	--	--	0.05
Claritromicina	--	--	0.5

Los productos naturales 7-hidroxi-3,4-dihidrocadaleno y 7-hidroxicadaleno poseen actividad inhibitoria del crecimiento de *H. pylori* (Cuadro 1). Esta actividad es mayor que la del fármaco de referencia metronidazol. Este antibiótico es uno de los fármacos de elección en el tratamiento de *H. pylori*, por lo tanto, estos hallazgos resultan importantes considerando que uno de los principales factores que dificultan el tratamiento de las infecciones causadas por esta bacteria, es la aparición de cepas resistentes a estos antibióticos, por lo que el descubrimiento de nuevas sustancias capaces de neutralizar a este microorganismo ofrece una alternativa terapéutica que debe ser considerada después de ampliar el conocimiento acerca de su seguridad y eficacia. Al comparar los valores de la MIC para los compuestos aislados de *H. inuloides* (1.95 y 3.91 µg/mL), con valores reportados en la literatura para sustancias naturales o semisintéticas, se puede observar que son más activos que los derivados de xantonas, un tipo de esqueleto que ha sido utilizado en la búsqueda de sustancias con actividad sobre *H. pylori*. Las MIC para las sustancias más activas que poseen este esqueleto se encuentran en un rango mayor a 20 µg/mL.[9] El 7-

hidroxi-3,4-dihidrocadaleno y 7-hidroxicadaleno, son también más activos que compuestos de tipo sesquiterpeno aislados a través de fraccionamiento biodirigido en búsqueda de sustancias anti- *H. pylori*, a partir de la especie vegetal *Santalum album*. La CIM de la sustancias más activa aislada de esta planta es de 7.8 µg/mL.[10] La actividad de los productos naturales de *H. inuloides* es comparable con la de la corilagina, un producto natural aislado de *Geranium wilfordii* cuya CIM es de 4 µg/mL.[11]

Ninguno de los derivados benzoilados o de tipo carbamato preparados a partir del 7-hidroxi-3,4-dihydrocadaleno, fueron más activos que el producto natural. Sin embargo, se observó una mayor actividad de los derivados benzoilados preparados a partir del 7-hidroxicadaleno, cuando estos tienen sustituyentes metilo o cloro en la posición *para* del anillo.

Dado que ninguno de los derivados semisintéticos evaluados perdió totalmente su actividad, se puede deducir que las modificaciones realizadas sobre el grupo fenólico afectan parcialmente su efecto sobre la bacteria, es decir que la importancia estructural de los productos naturales radica mayormente en una porción distinta de la molécula. Este hallazgo permite proponer que es posible realizar (con mayor libertad) ciertas modificaciones (esterificaciones) del grupo fenólico con el objetivo de mejorar la potencia de los productos naturales o modificar sus características de solubilidad, garantizando un mínimo de actividad bactericida.

Referencias

1. Takeuchi, H.; Trang, Vu.; Morimoto, N.; Nishida, Y.; Matsumura, Y.; Sugiura, T. *World J Gastroenterol* **2014**, 20, 8971.
2. Ayala, G.; Escobedo-Hinojosa, W.; de la Cruz-Herrera, C.; Romero, I. *World J Gastroenterol* **2014**, 20, 1450.
3. Vidal Bonifácio, B.; Aparecido dos Santos Ramos, M.; Bento da Silva, P.; Bauab, T. *Ann Clin Microbiol Antimicrob* **2014**, 13, 54.
4. Cruz, G. Plantas medicinales de nueve comunidades en la frontera entre Chignahuapan, Ixtacamaxtitlan y Aquixtla, Puebla, **2007**. Tesis, Universidad Autónoma de Chapingo, Mexico.
5. Castillo-Juárez, I.; González V.; Jaime-Aguilar H.; Martínez G.; Linares E.; Bye R.; Romero I. *J Ethnopharmacol* **2009**,122, 402.
6. Bunyapaiboonsri, T.; Yoiprommarat, S.; Nopgason R.; Komwijit, S.; Veeranondha S.; Puyngain, P.; Boonpratuang, T. *Phytochemistry* **2014**, 105, 123.
7. Datta, B.; Rahman, M.; Gary, I.; Nahar, L.; Hossein, S.; Auzi, A.; Sarker, S. *J Nat Med* **2007**, 61, 391.
8. Clinical and Laboratory Standars Institute. Performance standars for antimicrobial susceptibility; 17th information supplement (M100-S17). National Committee for clinical laboratory starndars: Wayne. Pa. **2007**.
9. Klesiewicz K.; Karczewska E.; Budak A.; Marona H.; Szkaradek N. *J Antibiot (Tokyo)* **2016**, 69, 825.
10. Ochi T.; Shibata H.; Higuti T.; Kodama KH.; Kusumi T.; Takaishi Y. *J Nat Prod* **2005**, 68, 819.
11. Zhang, X.; Gu, H.; Li, X.; Xu, Z.; Chen, Y.; Li, Y. *J Ethnopharmacol* **2013**, 147, 204.

CONCLUSIONES

1. Considerando el amplio aprecio etnomédico que posee *Heterotheca inuloides* para el tratamiento de diversos padecimientos, su investigación se justifica ampliamente, no sólo por el hallazgo de nuevos productos naturales, sino por las diversas propiedades biológicas (de interés terapéutico, agronómico y ecológico, entre otras) que poseen y la exploración de sus mecanismos de acción.
2. En el presente trabajo de investigación se logró el aislamiento de nuevos productos naturales y la caracterización completa de sustancias reportadas con anterioridad. De las partes aéreas se aislaron cuatro sesquiterpenos de tipo cadinano nuevos y cuatro previamente reportados. La configuración absoluta de los productos naturales nuevos se estableció por comparación de sus espectros de dicroísmo circular electrónico, experimental y calculado, y confirmada a través de difracción de rayos X.
3. El hallazgo de que todos los compuestos que poseen un centro estereogénico en la posición C-4 tengan la misma configuración, concuerda con estudios previos relacionados con la configuración absoluta de los cadinanos que se aislan de *H. inuloides* y permite concluir que esta especie biosintetiza solamente una serie enantiomérica.
4. Los estudios de la capacidad anti-inflamatoria *in vivo* mostraron que varios de los metabolitos de tipo cadinano poseen actividad moderada. Algunos de ellos, tienen un efecto importante sobre factores de transcripción involucrados en los procesos de inflamación y cáncer.
5. Los resultados obtenidos a través de experimentos con líneas celulares muestran que el principal constituyente de esta especie, el 7-hidroxi-3,4-dihidrocadaleno, posee actividad anti- NF-κB y es capaz de activar la vía antioxidante del factor de transcripción Nrf2, lo cual puede correlacionarse con el uso de esta especie en la medicina tradicional como agente antiinflamatorio.
6. Se obtuvo un grupo de compuestos semisintéticos, incluyendo derivados de tipo éster y carbamato, preparados a partir de los cadinanos naturales activos. El derivado 7-(*p*- metilbenzoiloxi)-3,4-dihidrocadaleno, resultó ser un inhibidor de NF-κB y activador de Nrf2 más potente que el producto natural originario. Esta

sustancia reduce la acumulación intracelular de especies reactivas de oxígeno y disminuye los niveles de fosfo-IκBα, un complejo proteico involucrado en la activación del NF-κB. Los análisis de simulación de acoplamiento (reconocimiento) molecular indicaron que este derivado se posiciona en el loop de activación de la subunidad de IKKβ, lo cual explica el mecanismo por el cual evita la fosforilación de IκBα, y concuerda con la evidencia encontrada a través de análisis por western blot. Estos resultados constituyen una contribución importante en la elucidación del mecanismo por el cual los productos naturales de *H. inuloides* ejercen su efecto antiinflamatorio.

7. Los derivados de tipo carbamato tuvieron una actividad citotóxica notable sobre adenocarcinoma colorectal humano con efectos tóxicos mínimos sobre fibroblastos gingivales humanos. Estas sustancias fueron inefectivas sobre los factores de transcripción NF-κB, Nrf2 y STAT3, lo cual indica un mecanismo de citotoxicidad que involucra otros blancos moleculares. Por lo tanto, se requieren investigaciones adicionales.
8. Los compuestos de tipo cadinano pueden considerarse como una nueva clase de moduladores naturales de los factores NF-κB y Nrf2 y ser de utilidad como modelos para el desarrollo y optimización de nuevas sustancias con actividades antiinflamatorias y anticancerígenas.
9. El análisis del contenido metabólico de la especie mediante CLAR proporcionó información importante respecto al perfil químico de la planta, ya que se detectaron diferencias en la composición de extractos de distintas poblaciones, a través de la identificación individual de los constituyentes característicos. Estos resultados pueden ser útiles en la estandarización de extractos y preparados fitofarmacéuticos.
10. Los hallazgos concernientes a la actividad anti-*H. pyori* de los metabolitos y derivados semisintéticos de *H. inuloides* permite proyectar la exploración de su potencial como agentes terapéuticos en el tratamiento de infecciones causadas por esta bacteria, lo cual significa una opción novedosa en el proceso de descubrimiento de sustancias capaces de contrarrestar microorganismos resistentes a los fármacos comúnmente empleados.